JOINT EUROPEAN TORUS JET

JET JOINT UNDERTAKING

PROGRESS REPORT 1983

EUR 9472 EN
EUR-JET-PR1

JET JOINT UNDERTAKING

PROGRESS REPORT 1983

SEPTEMBER 1984

This document is intended for information only
and should not be used as a technical reference.

EUR 9472 EN (EUR-JET-PR1) September 1984
Editorial work on this report was carried out by B.E. Keen and P. Kupschus
The preparation for publication was undertaken by
the Documentation Service Units, Culham Laboratory.

Printed in England

Contents

Foreword

In the preface to the JET Annual Report 1983, published earlier this year, Professor J. Teillac, Chairman of the JET Council, stated that with the start of operations a detailed account of JET's scientific and technical progress would be produced in a separate report prepared by the JET Director. Whilst the issuing of this progress report for 1983 has, for a miscellany of reasons, been delayed, it is our intention in future to publish as soon as possible after the end of the year under review. The progress report for 1984 is already in preparation.

The progress report is intended primarily to meet the particular obligation imposed by the JET Statutes on the Director of the Project to include in an annual report a statement on the performance of the scientific programme. It is anticipated, however, that it will interest a much wider audience than the members of the Joint Undertaking. Its presentation, therefore, is aimed not only at specialists and experts engaged in nuclear fusion and plasma physics, but also at a more general scientific community.

Since this is the first Progress Report, the introductory section provides the general background on the origins, design and objectives of the machine. The body of the report describes the activities of the Operation and Development Department in operating and maintaining the tokamak and in developing equipment to enhance the machine for full performance. It also details the progress of the Scientific Department in the specification, procurement and operation of diagnostic equipment; in executing the experimental programme and interpreting results. The concluding section of the report includes the broad programme plans for JET to 1990.

H-O. Wüster
September 1984

1983 was a year of considerable achievement for the Project. The JET machine was commissioned in its Basic Performance configuration by June 1983. The plasma control system was also commissioned during 1983. Whilst the results achieved in the latter part of the year were well surpassed in 1984 (details of which will be contained in the next progress report), they were nevertheless impressive for the first few months of operation. A peak plasma current of 3MA with a loop voltage as low as 1.4V was achieved in a pulse lasting over 10 seconds. In this pulse, the current was over 1MA for 6.5 seconds. Non-disruptive termination of the current pulse was achieved. In another pulse the current was held constant at 2.3MA for 4 seconds. Electron temperatures in the range $1.5 \rightarrow 2.0$keV were obtained with mean densities in excess of $2 \times 10^{19} m^{-3}$.

My fellow Directors and I are highly gratified to be associated with the JET Project and are proud of its achievements. The successful construction of the device and the encouraging results obtained to date are a tribute to the dedication and skill of all who work on the Project. They also reflect the continuous and growing co-operation and multi-faceted assistance received from the Associated Laboratories and from the Commission of the European Communities. They justify in the most fitting way the confidence and support given to the management of the Project by the JET Council, JET Executive Committee and JET Scientific Council. I have no doubt that with such devotion from all sides, the Project will face the many problems and challenges that will be encountered in the future with faith.

Introduction and Summary

Formally, the Operation Phase of the JET Project started on 1 June 1983, following completion and commissioning of the machine in its basic performance configuration. At that time, the Construction Department was re-named the Operation and Development Department and the JET Project Team was then divided into the three Departments:

(i) Operation and Development Department;

(ii) Scientific Department;

(iii) Administration Department.

JET's experimental programme started on 25 June 1983, when plasmas were successfully produced at the first attempt, and planned experiments have been undertaken since that time. With the start of operation, the Director decided that an Annual Technical Progress Report should be published providing more detailed accounts of JET's scientific and technical activities and progress. This is the first of these Reports, which concentrates mainly on those relevant activities in the Operation and Development Department (ODD) and the Scientific Department.

In order to provide a general background to the Report, Section 2 describes briefly the origins of the JET Project within the EURATOM fusion programme and the objectives and aims of the device. The basic JET design and the overall philosophy of operation is explained and the first six months of operation of the machine is summarised. The Project Team structure adopted for the Operation Phase is set out. Finally, in order to set JET's progress in context, other large tokamaks throughout the world and their achievements are briefly described.

In Section 3, the activities and progress within the Operation and Development Department are set out; particularly, relating to its responsibilities for the operation and maintenance of the tokamak and for developing the necessary engineering equipment to enhance the machine to full performance. Since, the Construction Department was still formally active for the first six months of this reporting period, the Report describes the activities of the relevant Divisions (Magnet Systems, Plasma Systems, and Assembly Divisions) in this configuration and their transition to the present arrangement.

In Section 4, the activities and progress within the Scientific Department are described; particularly, relating to the specification, procurement and operation of diagnostic equipment; definition and execution of the programme; and the interpretation of experimental results.

Finally, Section 5 details JET's programme plans for the immediate future, and gives a broad outline of the JET Development Plan to 1990. The first 5 MW of Neutral Injection (NI) Heating is due for addition to the plasma and up to 3 MW of RF Heating should be due for tests on the machine in 1985. Subsequently, a total of 25 MW of NI and RF Heating should be added by 1988, which will be utilised in heating hydrogen, deuterium and finally tritium plasmas, by 1990.

JET in the Euratom and International Fusion Programme

Euratom Research Programme in the field of Controlled Thermonuclear Fusion
(Euratom Fusion Programme)

Under the Euratom Treaty, the Community research programme in the field of controlled thermonuclear fusion is adopted by the Council of Ministers for periods not exceeding five years, and is part of a long-term co-operative project embracing all the work carried out in nuclear fusion. It is designed to lead in due course to the joint construction of fusion power-producing prototype reactors, with a view to industrial production and marketing. Further details of implementation of the programme are given in the JET Annual Report (EUR-JET-AR6 (1984)).

The strategic assumptions underlying the Euratom fusion programme, which were recommended in 1981 by the "European Fusion Review Panel" and endorsed by the Council of Ministers when adopting the 1982–86 programme, are as follows:-

- The need to pursue a substantial programme following the tokamak route towards a demonstration fusion reactor (DEMO);
- The completion of the first stage of the programme, which is the JET project with its extensions, and carrying out programmes in support of the tokamak confinement systems;
- A reasonable effort within available resources on alternative confinement systems with reactor potential;
- The concept of a single step, NET (Next European Torus), between JET and DEMO and an increased activitiy towards the development of the technology required in this context, guided by conceptual studies.

The Council of Ministers of the European Communities on 30 May 1978 decided to build the Joint European Torus (JET) as the principal experiment of the Euratom fusion programme. To implement the Project, the JET Joint Undertaking was formally established for a duration of twelve years beginning on 1 June 1978 (see Appendices 1 and 2).

The decision states that the JET Joint Undertaking's mandate is to "construct, operate and exploit as part of the Euratom fusion programme and for the benefit of its participants in this programme a large torus facility of tokamak-type and its auxiliary facilities in order to extend the parameter range applicable to controlled thermonuclear fusion experiments up to conditions close to those needed in a thermonuclear reactor".

It was also decided that the device would be built on a site adjacent to the Culham Laboratory, the nuclear fusion research laboratory of the United Kingdom Atomic Energy Authority (UKAEA), and that the UKAEA would act as Host Organisation to the Project.

The members of the JET Joint Undertaking are: Euratom, all its associated partners in the frame of the fusion programme including Sweden and Switzerland; and Greece, Ireland and Luxembourg which have no Contract of Association with Euratom. Greece joined the JET Joint Undertaking on 14 June 1983.

The expenditure of the Joint Undertaking is borne 80 per cent by Euratom and 10 per cent by the United Kingdom Atomic Energy Authority (UKAEA). The remaining 10 per cent is shared between all members having Contracts of Association with Euratom in proportion to the Euratom financial participation in the total costs of the Association. Further details of the financial management of the projects are given in the JET Annual Report (EUR-JET-AR6 (1984)).

Details of the Members and Organisation of the Joint Undertaking are set out in Appendix 3.

Objectives of JET

The essential objective of JET is to obtain and study plasma in conditions and with dimensions approaching those needed in a fusion reactor. These studies will be aimed at:

- The study of plasma processes and scaling laws in regions close to those needed for a fusion reactor;
- The study of the interaction of the plasma with the walls of the torus chamber. This interaction is important because it controls the purity of the plasma which in turn determines the energy lost by radiation;
- The study of methods of heating the plasma to temperatures approaching those required for a reactor;
- The study of the behaviour of the energetic alpha-particles (the nuclei of helium) needed to sustain the

plasma temperature and produced as a result of the fusion between deuterium and tritium.

Two of the key technological issues in the subsequent development of a fusion reactor would be faced for the first time in JET. These were the use of tritium and the application of remote maintenance and repair techniques. The physics basis of the post-JET programme will be greatly strengthened if other fusion experiments currently in progress are successful. The way will then be clear to concentrate on the engineering and technical problems involved in going from an advanced experimental device like JET to a prototype power reactor.

Basic JET Design

As a consequence of these overall aims, the basic JET apparatus was designed as a large tokamak device with overall dimensions of about 15 m in diameter and 12 m in height. A diagram of the apparatus is shown in Fig. 1 and its principal parameters are given in Table 1. At the heart of the machine, there is a toroidal vacuum vessel of major radius 2.96 m having a D-shaped cross-section 2.5 m wide by 4.2 m high. During operation of the machine, a small quantity of gas (hydrogen, deuterium or tritium) is introduced into the vacuum chamber and is heated by passing a large current (up to 3.8 MA during the initial phase, and up to 4.8 MA during the full design phase) through the gas. This current is produced by transformer action using the massive eight-limbed magnetic circuit, which dominates the apparatus (see Fig.1). A set of coils around the centre limb of the magnetic circuit forms the primary winding of the transformer with the hot gas or "plasma" acting as the single turn secondary. Subsequently, additional heating of the plasma will be provided by injecting beams of energetic neutral atoms into the system and by the use of high power radio frequency waves.

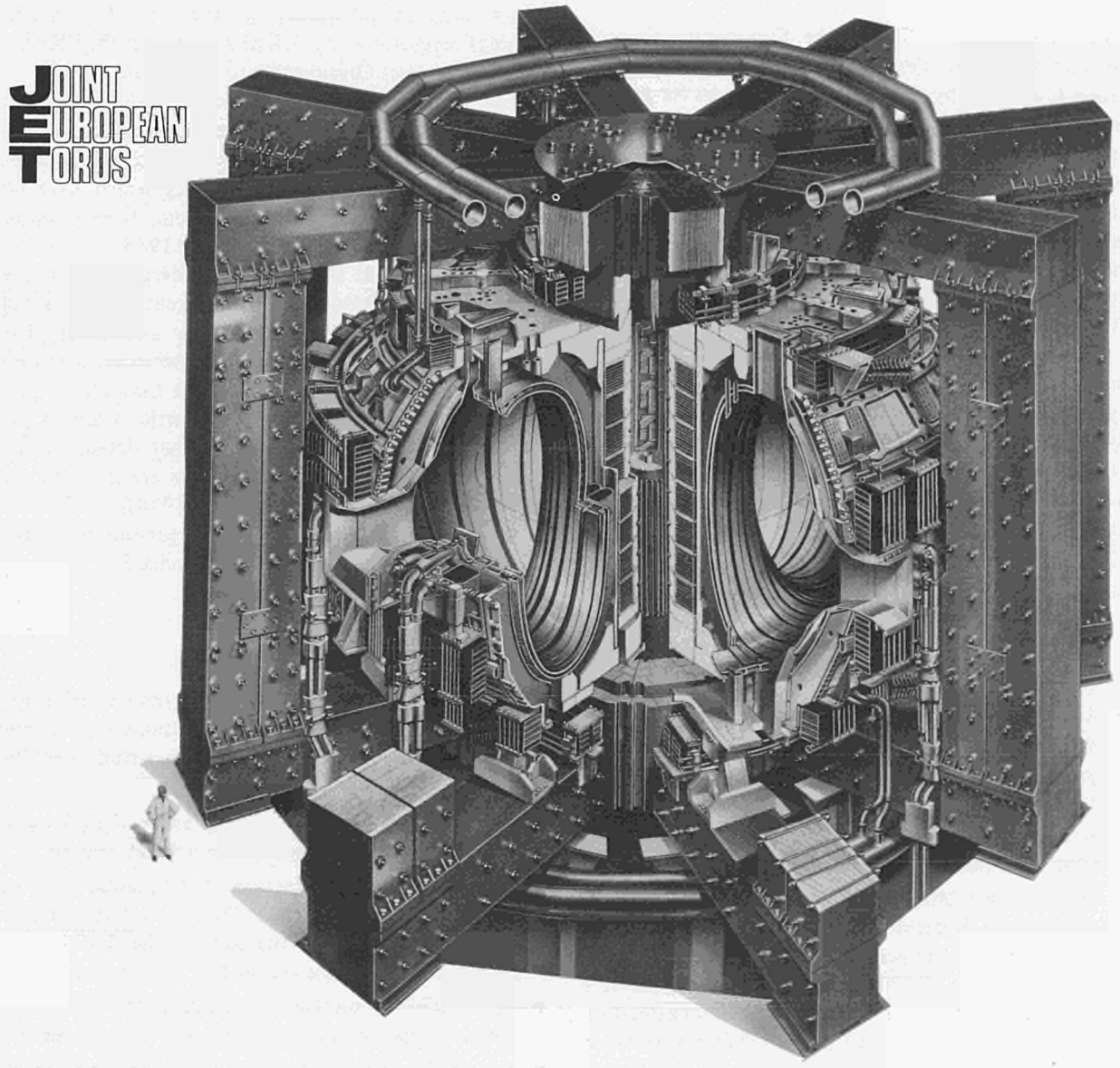

Fig. 1 Diagram of the JET Tokamak.

Table I
Main JET Parameters

Parameter	Value
Plasma minor radius (horizontal), a	1.25m
Plasma minor radius (vertical), b	2.10m
Plasma major radius, R_o	2.96m
Plasma aspect ratio, R_o/a	2.37
Plasma elongation ratio, e=b/a	1.68
Flat top pulse length	10s
Toroidal magnetic field (plasma centre)	3.45T
Plasma current, circular plasma	3.2MA
D shaped plasma	4.8MA
Volt-seconds available	34Vs
Toroidal field peak power	380MW
Poloidal field peak power	300MW
Additional heating power (in plasma)	25MW
Weight of vacuum vessel	108t
Weight of toroidal field coils	384t
Weight of iron core	2800t

The plasma is confined away from the walls of the vacuum vessel by a complex system of magnetic fields, in which the main component, the toroidal field, is provided by 32 D-shaped coils surrounding the vacuum vessel. This field, coupled with that produced by the current flowing through the plasma, forms the basic magnetic field for the tokamak confinement system which provides a field at the centre of 2.8T in the initial phase, rising to 3.45T during the full design phase. The poloidal coils positioned around the outside of the vacuum vessel shape and position the plasma in operation.

Initial experiments are being undertaken using hydrogen plasmas, but in the later stages of the operation, it is planned to operate with deuterium-tritium plasmas so that fusion reactions can occur.

In order to reach conditions close to those relevant to a fusion reactor, a plasma density of $\sim 10^{20}\,m^{-3}$ at a temperature of 10keV would be needed. Even with a current of 4.8MA in JET, this would be inadequate to provide the temperature required using ohmic heating only. Consequently, additional heating would be required and two main systems will be added to JET over the coming years, as follows:

- The injection into the plasma of highly energetic neutral atoms (Neutral Injection heating) and
- The coupling of high power electromagnetic radiation to the plasma (Radio Frequency heating).

The total power into the plasma will increase in discrete steps up to 25MW.

Summary of Initial Experiments

JET's experimental programme started on 25 June 1983, with a discharge current of 19kA at the first attempt to obtain plasma. By the August shutdown, a current of 600kA had been obtained with a loop voltage of 14V. From the high loop voltage, it was clear that the plasma resistivity was high and the temperature correspondingly low, around 50eV. Spectroscopic measurements showed that the discharge was dominated by radiation from the light impurities, carbon and oxygen. In this first campaign, the vertical position control had not been commissioned. As a result, the plasma was vertically unstable and moved to the bottom of the vacuum vessel, terminating the pulse when contact was established.

At the start of the second campaign in October, the bakeout temperature for the torus and ports had been raised to 270° C. It was apparent immediately that the discharge achieved was much cleaner. Spectroscopic measurements showed that metallic impurities, nickel and chromium, were playing a role, since there was now a significant amount of radiation coming from the centre of a much hotter plasma (around 1keV). By the end of October, 1.4MA was achieved with a loop voltage of 4V around the torus.

By November, a more sophisticated feedback system had been implemented to provide tight control of the horizontal and vertical positions of the plasma. The plasma size was then controlled to increase slowly during the current rise, allowing the current to penetrate to the centre of the plasma. The initial rate of current rise was also lowered, and these two changes resulted in much quieter and hotter plasmas. By the end of November, 1.9MA was reached with 1.3V around the torus. The discharge then showed all the attributes of a true tokamak discharge (i.e. low loop voltage and sawtooth oscillations at the plasma centre).

In December, plasma currents in the range 2 to 3MA had been obtained. The pulse length was typically 10s with a flat top of about 4s. Central electron temperatures measured by the newly commissioned electron cyclotron emission (ECE) diagnostic showed values in the region of 1.5 to 2keV. The loop voltage was reduced to about 1V, and the safety factor q at peak current was in the range 2.4 to 5.0. By the end of the second campaign, control had been established over the density behaviour by adjusting the gas feed rate, and density flat tops of 4s were obtained. Average plasma density was approximately $2.5 \times 10^{19}\,m^{-3}$, plasma radius 1.1m, and elongation of 1.2. The highest global energy confinement time was estimated at 0.3s.

Project Team Structure

In the 1982 JET annual Report (EUR-JET-AR5), the main details of the Construction Phase of JET were

described, during which the JET Project Team was divided into three Departments:
(a) Construction Department; (b) Scientific Department; and (c) Administration Department. For the Operation Phase, commencing on 1 June 1983, the Construction Department was re-named the Operation and Development Department (ODD), and the three Departments are now:

(i) Operation and Development Department;

(ii) Scientific Department;

(iii) Administration Department.

This Report describes further the scientific and technical progress made in the Scientific and the Operation and Development Departments during 1983. The responsibilities of these Departments are described below:

Operation and Development Department
The Operation and Development Department is responsible for the operation and maintenance of the tokamak and for developing the necessary engineering equipment to enhance the machine to its full performance. The Department contains six Divisions:

(1) Torus Division, which is responsible for the operation of the Torus, including the creation and training of the operating team and the organisation and execution of maintenance work in the Torus Hall and Basement. The Division also organises major shutdowns for the installation and commissioning of the new equipment and for development work necessary for the improvement of the sub-systems integrated into the JET device (vacuum system, baking and cooling plants, limiters, first wall, etc.).

(2) Power Supply Division, which is responsible for the design, installation, operation, maintenance and modification of all the power supply equipment needed by the Project.

(3) Neutral Beam Heating Division, which is responsible for the construction, installation, commissioning and operation of the neutral injection system, including the development towards full power operation of the device. The Division will participate in the studies of the physics of neutral beam heating.

(4) Radio Frequency Heating Division, which is responsible for the design, construction, commissioning and operating the RF heating system during the different stages of its development to full power. The Division will participate in the studies of the physics of RF heating.

(5) Fusion Technology Division, which is responsible for the design and development of remote handling methods and tools to cope with the requirements of the JET device, and for maintenance, inspection and repairs. Tasks also include design and construction of facilities for the handling of tritium.

(6) Control and Data Acquisition Systems Division (CODAS), which is responsible for the implementation, upgrading and operation of the computer-based control and data acquisition system for JET.

Scientific Department
The Scientific Department is responsible for the definition and execution of the experimental programme, the specification, procurement and operation of the diagnostic equipment and the interpretation of experimental results. The Department contains three Divisions:

(1) Experimental Division 1 (ED1), which is responsible for the specification, procurement and operation of approximately half the JET diagnostic systems. ED1 undertakes electrical measurements, electron temperature measurements, surface and limiter physics and neutron diagnostics.

(2) Experimental Division 2 (ED2), which is responsible for the specification, procurement and operation of the other half of the JET diagnostic systems. ED2 undertakes all spectroscopic diagnostics, bolometers, interferometry, the soft X-ray array and neutral particle analysis.

(3) Theory Division, which is responsible for the prediction by computer simulation of JET performance, the interpretation of JET data and the application of analytic plasma theory to gain an understanding of JET physics.

The Divisions are also involved in:

- The execution of the experimental programme.
- The interpretation of results in collaboration with appropriate Divisions in the Operations and Development Department.
- Making proposals for future experiments.

International Tokamak Research

In order to set the present JET achievements in context and to judge progress made, it is helpful to summarise the present operational state and results achieved on other large tokamaks throughout the world.

Worldwide, there are four large tokamaks operational or under construction: TFTR (USA), JT-60 (Japan), T-15 (USSR) and JET (Europe). TFTR was the first to start operating (December 1982), followed by JET (June 1983). JT-60 is expected to be operating by the end of 1984 and T-15 in 1985. Although each of the experiments has a different scientific objective, they all represent a major and logical step towards the development of a fusion reactor. JET and TFTR are designed to operate with deuterium and tritium plasmas. T-15 will have super-conducting toroidal field coils and powerful heating at the electron cyclotron frequency. JT-60 has a form of divertor and will use a wide range of heating techniques.

Results reported from the ohmic heating operation of the TFTR tokamak at Princeton (USA) during 1983 have been of considerable interest to JET. Shortly after the end of the year, a maximum current of 1.5 MA with a flat-top duration time of one second was reached. Normalised tokamak parameters (on the Hugill diagram) show JET and TFTR to be working in essentially similar ranges. As in JET, the central electron temperature reached values in the range 1.5 to 2 keV. The maximum global energy confinement time was about 270 ms, which within the measurement accuracies, was essentially the same as that found on JET. Experiments on TFTR have shown only a very weak dependence of confinement time on the minor radius of the discharge. Comparison with data from other tokamaks shows that the principal advantage of increased size results from the increase in the major radius.

During the year, experiments continued worldwide on a number of medium sized tokamaks with powerful additional heating. An important result for JET has been the observation on the ISX-B limiter tokamak at Oak Ridge National Laboratory (USA) of good confinement with additional heating when the discharge was ungettered or when neon gas was puffed into the plasma. Although not completely understood these results show that confinement degradation is not the inevitable result of applying additional heating in a tokamak such as JET, where the plasma is bounded by a limiter.

Since the major additional heating method on JET will be ion cyclotron resonance heating (ICRH), the experiments worldwide in that field were especially significant. Work on the TFR tokamak in France, partly in response to JET requests, has shown that the generation of impurities at the plasma boundary by this heating method remains a critical problem. For the same power input, the production of metallic impurities was about three times higher for ICRH than for ohmic or neutral beam injection heating. The RF input increased the plasma density at the boundary by a factor of ten and the electron temperature by a factor of two to about 10 eV. This effect was independent of whether the input RF power direction was aligned with the toroidal field or with that of the local magnetic field. Investigating these effects and possible solutions will be an important part of the first experiments on JET with the prototype antennae, early in 1985. By contrast, heating of tokamaks and stellarators at the electron cyclotron resonance (ECR) frequency has shown further notable success with no problems of coupling the energy into the plasma, localising the power absorption or of impurity generation. The major difficulty and the main reason why it is not yet planned to apply this technique to JET is the lack of suitable high power sources (gyrotrons) at the required frequencies around 100 GHz.

On the theoretical front, the Lausanne group have derived a 'universal' relationship between the maximum β_{max} ~3% for the extended JET performance current of 4.8 MA at full field and aperture. To obtain plasma ignition at this β would require the unlikely confinement time of about 4 seconds. However, by increasing the current above 4.8 MA both β and the energy confinement time should increase linearly according to present ideas and significant alpha-particle production should be obtainable at the ~ 7 MA level, at least.

Theoretical efforts worldwide have so far been unsuccessful in providing a convincing and definitive explanation for the high energy transport observed in ohmic-heated discharges. Some work at UKAEA, Culham Laboratory has attempted to explain the further increase in energy transport observed when additional heating is applied. This work has developed the notion that the critical plasma pressure gradient for ideal ballooning modes is reached for a progressively larger proportion of the minor radius as the additional input power is increased. This model applied to JET would severely limit its performance. However, it should be emphasised that there are many potential reasons why such speculation may prove to be incorrect. Plasma stability might be improved by the presence of high energy particles produced by neutral injection and thermonuclear reactions. In addition, the non-linear consequences of violating stability criteria might be less than anticipated. Definitive answers will come only from the on-going programme of worldwide tokamak research.

JET – Operations and Development

Introduction

The Operation and Development Department was formally brought into existence at the start of the Operations Phase in June 1983, following completion of the Construction Phase. At this time, the Department was made responsible for the operation and maintenance of the machine and for developing the necessary engineering equipment to enhance the machine to its full performance. In undertaking these tasks the Department is now subdivided into six Divisions:

(1) Torus Division;
(2) Power Supply Division;
(3) Neutral Beam Heating Division;
(4) Radio Frequency Heating Division;
(5) Fusion Technology Division;
(6) Control and Data Acquisition Systems (CODAS) Division.

The present structure to Group Leader level is shown in Fig. 2 and the list of Divisional Staff at 31st December 1983 is shown in Fig. 3.

Since the Construction Department existed for the first six months of this reporting period, the activities of the relevant Divisions (Magnet Systems, Plasma Systems and Assembly Divisions) are described. The structure, at the 1st January 1983 to Group Leader level and the list of Divisional staff are shown in Figs. 4 and 5 respectively.

Summary of Progress

During the year, Torus (formerly Magnet and part of Plasma Systems), Assembly, Power Supplies and CODAS Divisions were deeply involved in completing the installation, commissioning and operating the JET machine. This assisted in achieving the first plasma on time, and, with subsequent improvement in equipment performance, a plasma current of 3 MA was obtained by December 1983.

The toroidal field coils, assembled with the machine octants, were positioned and shimmed inside the mechanical (shell) structure. The upper poloidal field coils were accurately positioned and the magnetic circuit closed by mounting the upper transformer limbs. Installation was completed on the busbar systems which feed the coils; and on the upper part of the cooling pipework to the poloidal and toroidal loops. Extensive cabling for electrical heating and for data acquisition and control was also carried out.

Welds on the lip seals joining the vacuum vessel octants were undertaken to close the vessel, and its interior was carefully cleaned by hot water/high pressure scouring. After installation of the limiters and the mounting of the pumping chambers to octants 1 and 5, commissioning of the vacuum system was undertaken.

The two large flywheel generators and the first static unit to supply power directly from the grid were brought into operation. The ohmic heating circuit (including fast current rise) and the radial and vertical field amplifiers, though not commissioned to their maximum performance in 1983 – permitted initial operations. From the first plasma, a stepwise commissioning took place.

The CODAS system of 13 on-line subsystem computers (and a total of 25 computers) including their peripherals were operating for the first plasma operation and data acquisition services were immediately available. The entire system (continually being upgraded) has shown a high degree of operational reliability. The software is constantly being expanded.

Some effort was also devoted to enhance the future performance of the machine. A belt limiter concept, compatible with the RF-antennae system, was developed and the use of beryllium as a limiter (and wall) material was considered.

Good progress was made on the first neutral beam heating (NBH) system, for which some major components have been delivered and pre-assembly has started. Eight PINI beam sources have been delivered and three of them fully tested. In tests at the Culham Laboratory, 80kV/60A pulses have been reached for 5 s duration.

Problems with incorrect steering of beamlets and lower than expected proton yield of the plasma source were encountered and are presently being tackled. The Neutral Injection Testbed commenced operation. All but a few major components have been ordered for the second NBH system. For later injection with deuterium, tests at CEA, Fontenay-aux-Roses, have successfully shown PINI operation at 160kV. Three of the first five outdoor high voltage supplies (serving two PINIs each) for the NI Testbed and the first NBH system have been delivered: three have already completed their acceptance tests.

The first high voltage protection unit has been delivered as well as the first auxiliary power supply and integrated tests are to start on the NI Testbed. Two further protection units have passed their factory tests. Three high

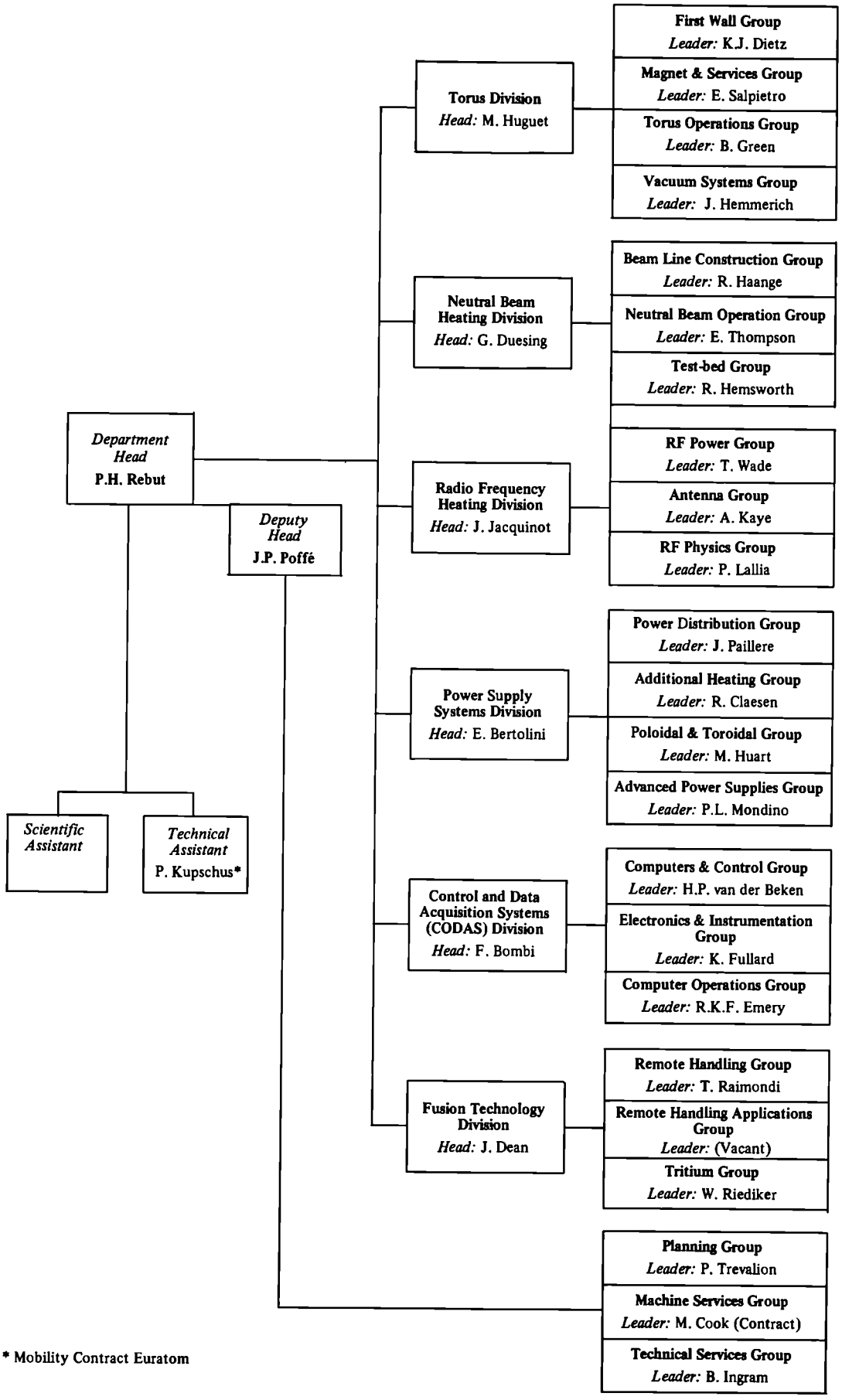

Fig. 2 Operation and Development Deparmment: Group structure (December 1983).

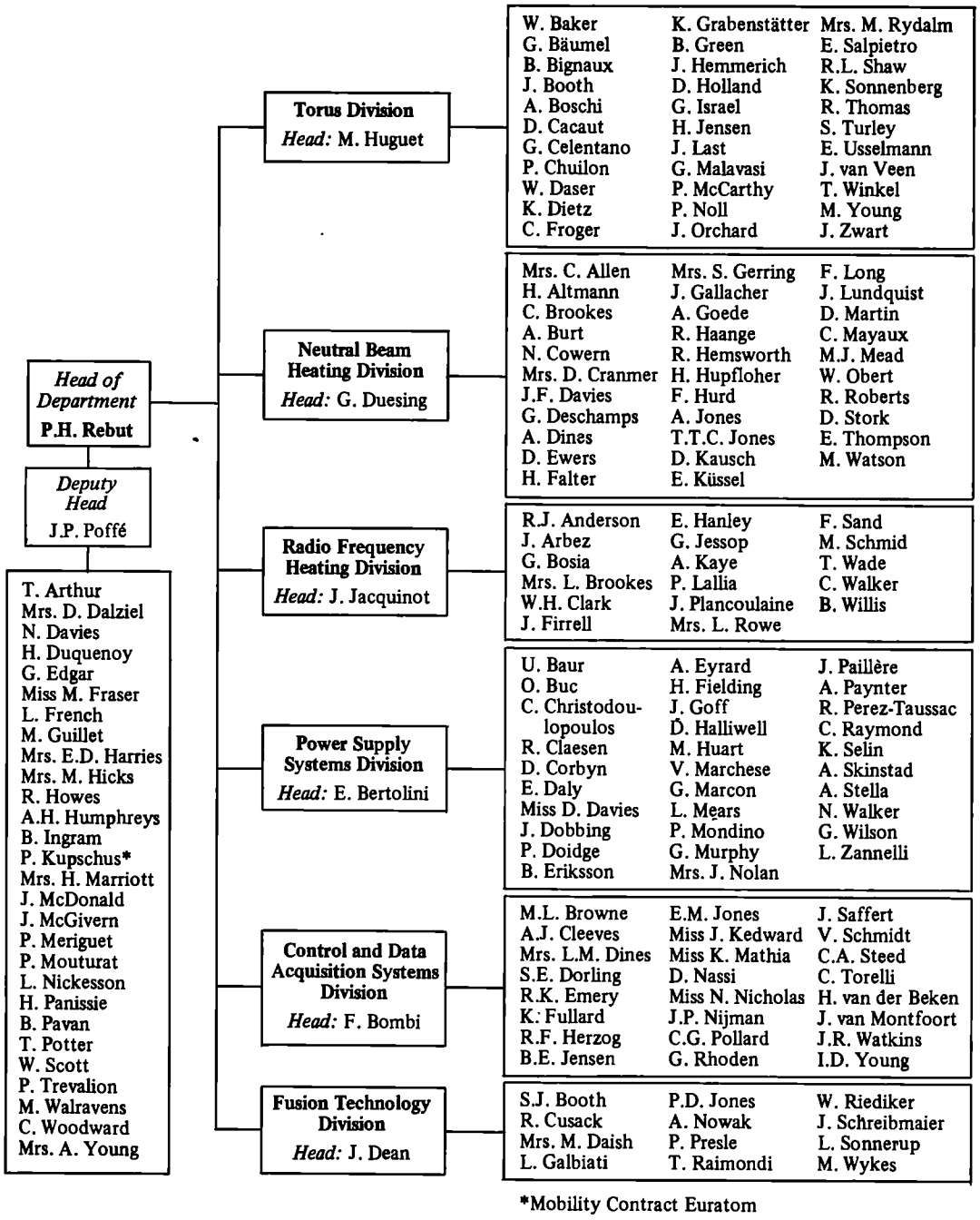

Fig. 3 Project team staff in the Operation and Development Department (December 1983).

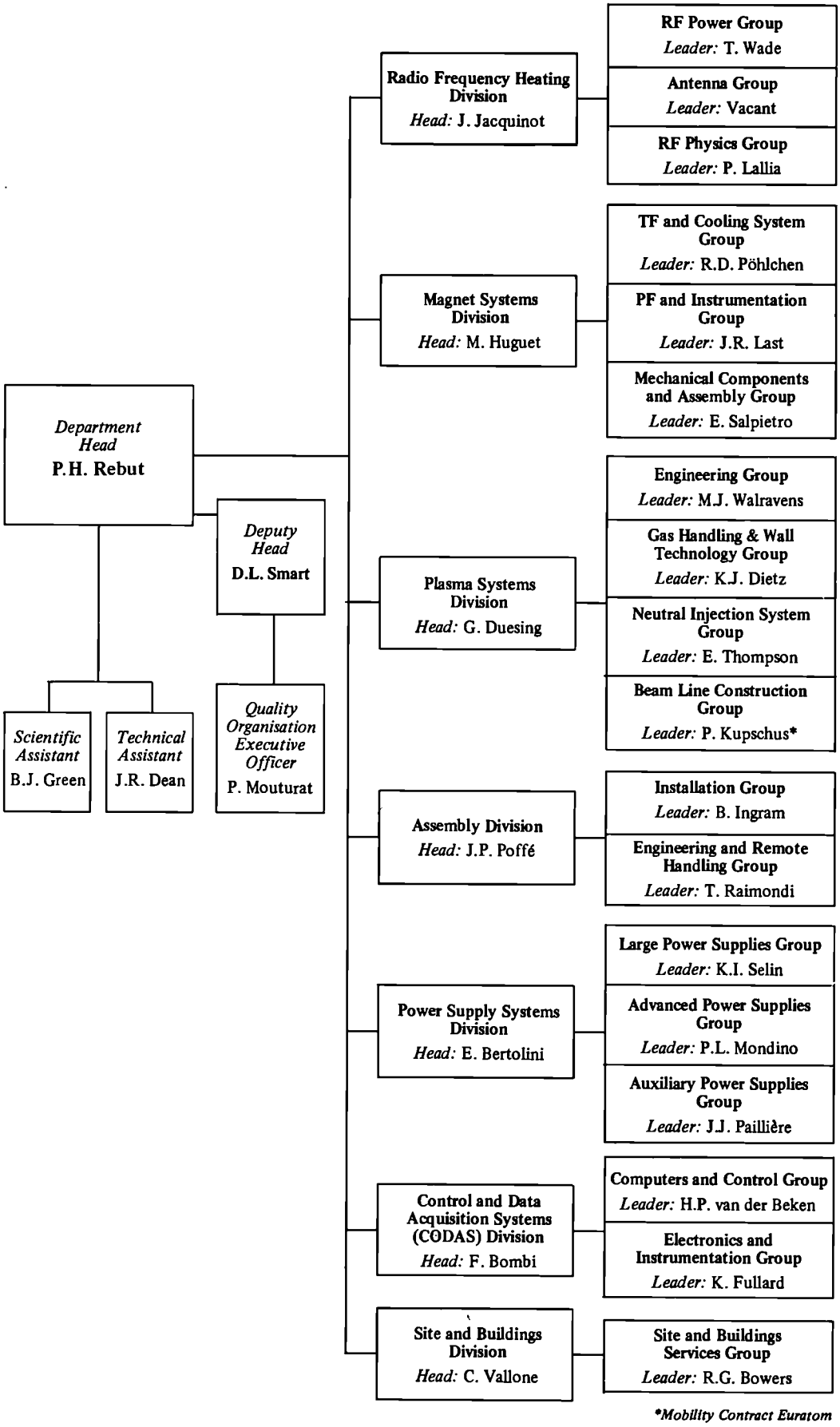

Fig. 4 Construction Department: group structure (January 1983).

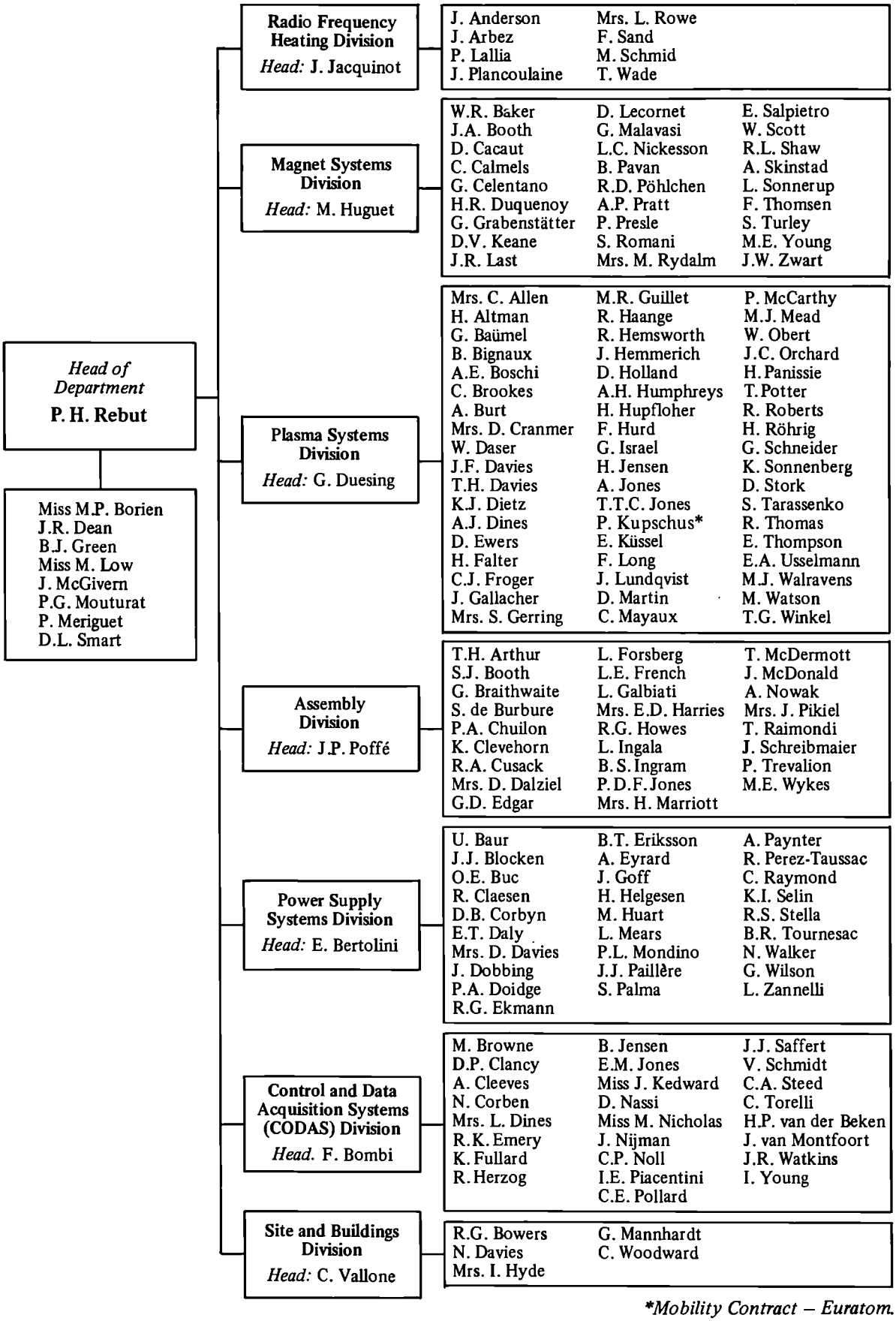

*Mobility Contract – Euratom.

Fig. 5 Project team staff in the Construction Department (January 1983).

voltage transmission lines have been delivered and parts for the SF_6 tower are under manufacture. Power supplies for the second NBH system are well advanced and three outdoor units are already on site.

Ion cyclotron resonance RF Heating has concentrated on the detailed design of antennae and on the manufacture of RF generators and of the main transmission lines. By August, the RF Testbed at Fontenay-aux-Roses was brought into operation. Contracts for the DC power supplies to the RF generators have been awarded for the main power supplies, and for the design of the auxiliary supplies are well advanced.

Preliminary work for the active phase involving remote handling has included development of an in-vessel-inspection system which has now been delivered and is being incorporated into the machine. An in-vessel articulated boom has also been ordered. A preliminary design of the tritium handling plant was presented to the Scientific Council in October and this concept is now being pursued.

Operations & Development Department Directorate

(Division Head: J.P. Poffé)

For the Operations Phase of JET, the Operation and Development Department (ODD) provides various services to the whole project at the Directorate level. The services are distributed between five operational units as described below.

Planning Group
(P. Trevalion, G. Edgar, L. French, E. Harries)
This unit is responsible for long term technical planning and detailed preparation and monitoring of new assembly work. Planning of assembly work is an essential part of its responsibilities, particularly that occurring during major shutdowns, when the Torus Hall becomes accessible.

Technical Service Group
(B. Ingram, T. Arthur, N. Davis, R. Howes, J. McDonald, C. Woodward)
This unit provides:

- Mechanical support services for the JET device, auxiliary equipment, and diagnostics.
  (A new support contract similar to the previous Main Assembly Contract (MAC) was awarded which provided for a maximum workforce of 30 (doubled during major shutdowns) and its five professional staff);
- Availability of mechanical services in the buildings. Four long-term maintenance contracts for specialised equipment were awarded;
- Supply of civil works support. (This work was still carried out up to December by the former Site and Buildings Division).

Machine Service Group
(D. Lecornet, L. Nickerson, W. Scott)
This Unit is responsible for all piping services to the Torus: it coordinates the routing of all pipes and cables and is responsible for all intrusions through the biological shielding. The main work has been devoted to establishment of drawing records, the preparation of maintenance schedules and the settlement of conflicts between installation and design principles.

Drawing Office
(H. Duquenoy, D. Dalziel, M. Guillet, A.H. Humphreys, B. Pavan, T. Potter)
Over 40 designers and draughtsmen together provide design support to the Project. A configuration control section inspects geometrical interfaces and two models (1/10 scale of the Torus, 1/25 scale of the basement) are kept updated as essential design tools.

Quality Control
(P. Meriguet, J. McGivern)
This unit defines requirements of JET policy on quality control and assists Divisions in its implementation. A "JET Quality Library" has been organised, where all quality documents generated during the life of important manufacturing contracts and assembly procedures are stored.

Assembly Division

(Division Head: J.P. Poffé)
The Assembly Division existed during the Construction Phase, and following successful completion of its work, the Division was disbanded in June 1983, and, for the Operations Phase, its remaining activities were embraced within the responsibilities of newly formed Divisions. During 1983, the Division's main efforts were dedicated to piping, cabling and electrical activities as well as to the provision of logistic services for torus assembly and commissioning. Also, the Division managed the Main Assembly Contract (MAC), from which effort was mainly devoted to completion of the Torus Assembly and whose manpower was technically supervised by members of other Divisions.

The Remote Handling Group left the Division early in 1983 to join the newly formed Fusion Technology Division, and its activities are reported within that section of the Report. Divisional staff and Contractors were involved in a considerable amount of extra day and night work to meet the scheduled starting date of operation.

Piping Activities
(P. Chuilon)
During 1983, eleven prefabricated piping systems were installed, and nine were tested and commissioned. These concerned the distribution of demineralised cooling water (to the various components: such as coils, pumps, limiters, etc.), compressed air (3 pressures), nitrogen venting gas, liquid helium and nitrogen (these were not commissioned) as well as the gas introduction system (into the Torus

and neutral injectors). From eight sets of cubicles installed in the basement, water, air, and nitrogen gas were distributed through stainless multitube pipes along the eight vertical limbs to limb junction boxes. From there, flexible connections (equipped with remote handling connectors) carry the fluids to the relevant equipment.

Cabling and Electrical Activities
(S. Booth, G. Braithwaite, K. Clevehorn, B. Ingram)
A broad spectrum of cabling and electrical services were provided for many Divisions, using a main electrical contractor (MEC) who carried out the work to meet the tight schedules. Up to forty-five electricians and cable pullers worked extended shifts in the Torus Hall, hot cell, basement and diagnostic wing:

(a) to install 40 limb junction boxes (5 per vertical limb), 100 air tight penetrations (through the biological shield), 40 termination and signal conditioning cubicles;
(b) to lay, terminate and test 150km of multiwire cables between equipment on the Torus and these cubicles in the basement or diagnostic hall. These transmission cables were dedicated to the operation and control of the Torus and list A diagnostics.

The final connections from the limb junction boxes to the instruments and components installed on the Torus itself were made by short connecting jumper cables equipped at both ends with specific remote handling plugs. 1500 of these cables were manufactured and more than half installed, during the period.

Logistics
(G. Edgar, L. Forsberg, L. French, R. Howes,
T. McDermott, J. McDonald, P. Trevalion)
A comprehensive range of services was consistently provided by the Division using the main assembly contractor, the Host Laboratory and outside Contractors. These services were:

- Short and long term planning;
- Duty Officer (rota, instruction, supervision);
- Storage facilities, mechanical handling (including Statutory inspections);
- Drawing office, configuration control (1/10 scale model of the Torus and auxiliary equipment, 1/25 model of the basement);
- Mechanical workshop, procurement of technical equipment;
- Maintenance of mechanical and electrical building services;
- Quality control related to assembly work;
- Alignment, photogrammetry;
- Clean condition facilities.

Plasma Systems Division

(Division Head: G. Duesing)
Plasma Systems Division existed during the Construction Phase, and at that time, the Division's work was divided between the construction and commissioning of the vacuum systems, and neutral injection (NI) heating. The work on Neutral Injection continues in the Operation Phase within the newly formed Neutral Beam Heating Division and is described separately in that section of the Report. The vacuum systems were completed during the Construction Phase, and, following the first operational period of JET, were handed over to other Divisions. A summary description of these systems, with an emphasis on progress in 1983, is given in the following sections.

Contributing Staff (Vacuum Systems)
G. Duesing (Division Head)

J. Dean, K.J. Dietz, J. Hemmerich, P. Kupschus, W. Walravens (Group Leaders).

J. Arbez, A. Boschi, S. Baumel, C. Froger, M. Mead, R. Roberts, H.D. Rohrig, S. Skellett, K. Sonnenberg, S. Stober, S. Tarassenko, U. Usselmann, K. Walter, T. Winkel, D. Barnes, B. Bignaux, W. Daser, J. Davies, T. Davies, J. Gallagher, K. Grabenstatter, M. Guillet, D. Holland, G. Israel, H. Jensen, A. Jones, G. Lundquist, P. McCarthy, J.P. Moussy, J. Orchard, H. Panissie, R. Sandstrom, G. Schneider, R. Thomas.

Vacuum Vessel System
The vacuum vessel system consists of the vacuum vessel and internal and external components. The vessel is a gas-heated toroidal structure with electrically heated ports. Internal components include the limiters for which the cooling is provided by the Draining and Refilling System. External components are the Pumping Chambers, the Middle Port Adaptors and the Rotary High Vacuum Valves.

Vacuum Vessel

Design
The toroidal vacuum vessel (Torus) is an all metallic all-welded structure. It has a D-shaped minor cross-section of 4.3m vertically and a 2.7m horizontal inner diameter.
It has a double wall structure for the following reasons:

- With stiffening ribs between the inner and outer skin, it provides high rigidity for minimum weight;
- The interspace is an independent vacuum chamber with its own pumping system. This provides high system availability, and with certain restrictions, operation can continue with a vacuum leak in the inner wall;
- By circulation of gas through the interspace, the inner vessel can be baked for outgassing or cooled as required;
- During D-T plasma operation, the double wall, together with a suitable heat transport medium and close-up system, reduces the tritium permeation to the outside by several orders of magnitude;
- The interspace also facilitated leak detection during the manufacture of vessel octants. A full leak test was possible without evacuating the main volume.

The vessel was manufactured in octants, which at a later stage in machine assembly, were joined by renewable lip welds. Each octant consists of five rigid sectors and four bellows assemblies. The rigid sectors were made of vacuum melted Nicrofer 7216 LC (equivalent to Inconel 600), and the bellows of Inconel 625. The materials were chosen for good mechanical properties at elevated temperature, good weldability and low magnetic permeability. High electrical resistivity for the bellows material was important in order to have a high overall vessel resistance (0.6mΩ).

Matching materials for sectors and bellows were selected for welding and thermal expansion purposes. Modular restraint rings encircled the vessel, 1m above and below the horizontal mid-plane, consisting of up to 90mm thick outer skins of the rigid sectors and electrically insulated bridges across the bellows. These restraint rings provided increased rigidity in the toroidal direction.

Manufacture

Manufacture of the vacuum vessel octants was performed in three parts; rigid sectors (three different types), bellows assemblies (inner and outer bellows and two flanges) and assembly of an octant. The rigid sectors were produced under clean working conditions. Plates were plasma-cut and rolled to the correct curvature, and the inner wall plates were electropolished. About 1km of UHV quality welding per octant was undertaken. The butt-welds were x-rayed where possible, and further x-ray and other weld tests were performed on coupons. A radial tolerance of ± 3mm was achieved for the rigid sectors, to allow the correct fitting of the bellows assemblies. The close dimensions of the TF coils also required this tolerance. The final sizing of the various port apertures was carried out on a boring machine, and the sector faces were machined to the correct angles. A vacuum leak test was performed on each sector.

Bellows were fabricated from Inconel 625 sheets of 2mm thickness with bellows convolutions of 120mm and 10mm width of convolution. Bellows assemblies were produced by welding two perforated flanges made of 4mm thick Nicrofer 7216 LC plates to an inner and an outer bellows.

Preparation on site

After delivery, each vessel octant was baked in an oven at 520° C to outgas the vessel walls and to test its suitability for normal service operation at 500° C. Global leak tests were carried out at 350° C. Leaks as small as 3×10^{-9} mbar $1\ s^{-1}$ were found and repaired. At ambient temperature, 10^{-11} mbar $1\ s^{-1}\ cm^{-2}$ hydrogen outgassing rates were normally reached.

Further octant preparation consisted of fitting magnetic flux loops, electrical heaters and thermocouples outside the octant and of covering it by Microtherm thermal insulation, as this material has low thermal transmission and does not deteriorate at 500° C. Precisely fitting insulation panels were applied in two overlapping layers.

Limiters

A modular limiter was chosen for the initial phases of JET operation. Each unit is of area $0.32\,m^2$, located in the horizontal vacuum vessel mid-plane at the outside wall and adjustable in the radial direction. The limiters are shaped in order to keep the thermal power density approximately constant across the surface.

For long pulse operation, the nickel-surface limiters are actively cooled and designed to carry thermal loads up to $10^7\,Wm^{-2}$ in stationary conditions. They consist of a precipitation hardened copper-chromium structure with fins standing across cooling water channels. The two-phase cooling operates at 6 bars pressure. The limiter surface is clad with a 1.5mm thick layer of nickel, which was chosen for its high thermal conductivity and for compatibility with the vacuum vessel material. Uncooled graphite limiters of identical geometry were also built. For the beginning of operation, four graphite limiters and eight nickel surface limiters were installed.

Draining and refilling system

Depending on the plasma operation mode, internal structures such as limiters, beam scrapers and glow discharge electrodes are either water cooled, gas cooled or drained. A system is being installed, which provides appropriate cooling for each operational mode and the transitions between different cooling conditions. For the draining and refilling system, there are three main operational modes of the Torus:

- main discharge: Limiters, beam scrapers, glow discharge electrodes etc. are water cooled;
- glow discharge cleaning at 250° C: only the glow discharge electrodes are waterr cooled, the other systems are drained.
- baking the Torus at 500° C: Limiters and beam scrapers are water cooled with a reduced flow rate, all other systems are drained. During cool-down the limiters and scrapers are also drained below 300° C, to avoid cold traps.

During glow discharge cleaning, the limiters, beam scrapers and internal cooling panels reach temperatures that are too high to refill immediately with water. These components are first cooled by nitrogen gas. Each unit can be shut-off within 0.2s from the gas loop and from the water supply, in case a water leak develops inside the Torus. This system (with about 125 valves) is controlled by a programmable controller, which transforms the CODAS control commands into operational signals to solenoid valves, provides interlocks and keeps the system in a safe state.

Pumping chambers, port adaptors, flanges

Pumping Chambers are mounted at two main horizontal ports (Octants 1 and 5) and these vacuum chambers serve several purposes:

- Two turbomolecular pumps are attached at the base of each. The chamber dimensions are determined by the required conductance and by the need to install the turbo pumps where the magnetic

field perpendicular to the vertical pump axis is less than 0.03 T;

- The residual gas analyser system and the primary vacuum by-pass lines are attached to other flanges;
- Opposite the Torus port, each pumping chamber has a 1200 mm i.d. door, which gives personnel access to the Torus and, at later stages, for a remotely controlled articulated boom, which will carry telemanipulated tools for in-vessel operations.

The chambers are welded structures made from SS 304L sheet and the flanges from forged material. The renewable vacuum sealing weld to the Torus is an Inconel to Inconel lip weld.

After delivery to the JET site, the chambers were vacuum baked at 400° C and leak-tested. Electrical heaters (Fig. 6) (for baking to 400° C during operation), thermocouples and thermal insulation were installed, and the pre-assembly completed by mounting the gate valves and turbomolecular pumps (Fig. 7). Middle Port Adaptors are mounted to the main horizontal ports of Octant 4 and 8 through which Neutral Injection beams will enter the Torus. Each adaptor incorporates actively water-cooled beam scrapers to protect the narrow entrance duct of the Torus port from the beam fringes and from reionised particles. Though much smaller, the adaptors are in design principles and manufacturing procedures quite similar to the Pumping Chambers. A Rotary Valve will be attached to the outside of each port adaptor. The vacuum seals between Rotary Valve, Middle Port Adaptor and Torus are lip welds.

All other vacuum seals in the system are Helicoflex seals. The flange is designed for remotely controlled demounting and re-assembly. For small diameter connections, single Helicoflex seals are used. For inner diameters from 225 mm to 1200 mm a balanced design with two Helicoflex seals has been selected in order to avoid bending stresses in the flanges and to minimise flange sizes. The seal clad material is normally aluminium, but for higher baking temperatures, silver is used. Tests have successfully been carried out at 300° C with aluminium cladding and at 400° C with silver cladding.

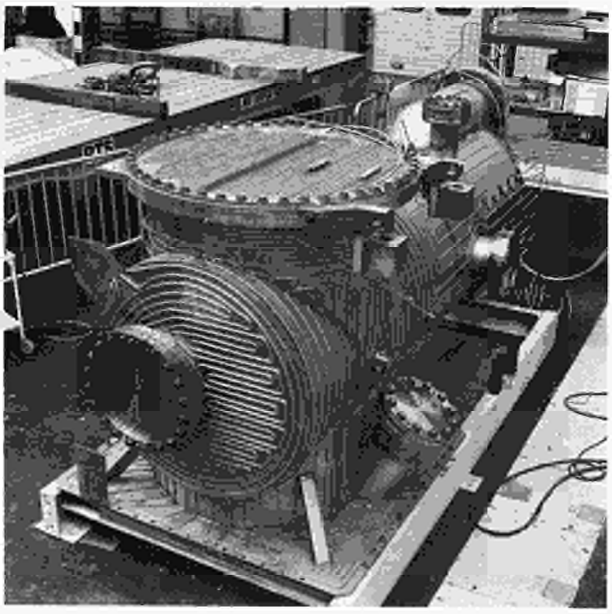

Fig. 6 Installation of electrical heaters onto the Pumping Chamber.

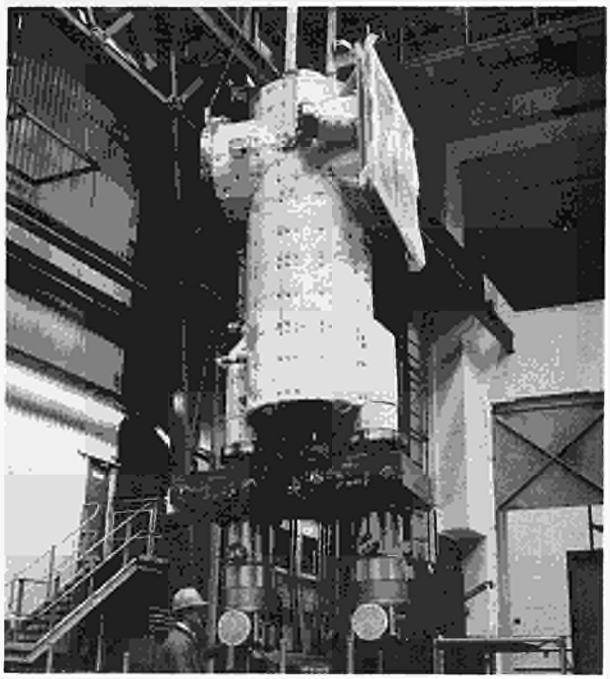

Fig. 7 Pumping Chamber with all-metallic gate valves and turbomolecular pumps.

Rotary high vacuum gate valve

The valve that isolates the Torus from the neutral beam injector vacuum system is the Rotary Valve (Fig. 8). Beams enter the plasma through a race-track shape opening of 0.5 m horizontally and 1.1 m full width vertically. The design is based on a cylindrical rotor with vertical axis, which carries two Helicoflex seals to seal the rotor when the valve entrance is closed against both the valve entrance and exit side. The seal interspace is pumped. The rotor opens the valve by a 90° rotation.

The valve is fully vacuum welded and is bakeable to 400° C (when opened) by electrical heating of the body and the rotor. The inside of the valve is protected against the thermal load from partial re-ionisation of the neutral beams by a water-cooled nickel tube heat exchanger. Two valves have successfully passed functional tests. The measured helium leak-rate was better than 10^{-9} mbar l s^{-1} through the valve.

Gas blower baking and cooling plant

A gas can be blown through the double wall interspace of the vacuum vessel, for heating or cooling. Each octant has two gas inlets and two outlets for this purpose. Baffles in the interspace provide an adequate gas flow distribution. The gas blower plant consists of a gas storage and pressure

Fig. 8 The rotor of a rotary valve is lowered into the valve body. The race-track shaped sealing surface on one of the pressure plates is visible.

holding system, heat exchanger and the blower. The heat exchanger is of the tube bundle type with air cooling, and contains radiant electrical heaters with a total power of 1 MW.

The plant can heat the vacuum vessel to 500°C. Originally CO_2 was selected as the process gas, as the volume flow rates required to reach turbulent flow were relatively low, and therefore, this would lead to an economical blower. For this performance, a CO_2 flow rate of $14.5\,m^3\,s^{-1}$ would be required at 500°C and 1.3 bar pressure (which is the maximum for safe operation of the vessel bellows). However, the final decision has settled on a single stage radial turbo-compressor that provides a particularly high compression and thereby provides scope for the use of other gases. Helium requires a volume flow rate of $25\,m^3\,s^{-1}$ and is attractive for various reasons. With its lower Z_{eff}, an order of magnitude larger leak rate between the Torus main volume and interspace can be accepted in tokamak operation, than with CO_2. Further, helium can be cleaned continuously from any contamination, (such as tritium), by a cryogenic trap in a by-pass loop. Finally, helium would not be activated, as would CO_2.

Electrical baking

Effective cleaning during baking is only achieved if no surfaces on the vacuum side of the Torus remain cold. Since ports, port adaptors, pumping chambers, valves and attached diagnostic equipment (altogether 150 units) cannot be heated by the gas flowing through the Torus interspace, additional electrical heating systems were required. Each unit is equipped with two heaters, two thermocouples and thermal insulation. Heaters and insulation are designed so that the units reach their maximum temperature within about 10 h and cool down with a time constant of about 15 h. The power input to each unit follows the time-temperature profile of the Torus, which is determined by the gas heating. Controlled power input is also important to keep thermal stresses small. The system is controlled by CODAS generating analogue signals proportional to the required power, which operate about 80 individual thyristor units.

Vacuum pumping and gas handling

Vacuum pumping

Vacuum pumping is provided by turbo-molecular pump units for the Torus main volume (4 units at the Pumping Chambers and 2 units at the Rotary Valves), the interspace in the Torus shell (2 units), the Neutral Injection vacuum boxes (1 unit each) and the Neutral Injection testbed (2 units). The pump units (speed $2600\,l\,s^{-1}$ for H_2) can be isolated from their vacuum chamber by 400 mm i.d. all-metallic gate valves. The pumps have been made suitable for pumping tritium by using all-metallic gate valves and life-time oil reservoirs, and are equipped with venting valves and pressure gauges.

The Torus main volume pumping system consists of turbomolecular pumps at each Pumping Chamber for first operation, and, subsequently, a turbomolecular pump at each Rotary Valve will contribute to the Torus pumping, when the valves are open.

The system is based on the following design parameters:

Vessel volume $200\,m^3$;

Vessel inner surface $800\,m^2$;

Conductance through port, Pumping Chamber and gate valve:

for impurities: $6{,}300\,l\,s^{-1}$;

for hydrogen: $24{,}100\,l\,s^{-1}$;

Conductance through port, Rotary Valve and gate valve:

for impurities: $3{,}100\,l\,s^{-1}$;

for hydrogen: $11{,}900\,l\,s^{-1}$;

Effective pumping speed for impurities: $6{,}040\,l\,s^{-1}$;

Effective pumping speed for hydrogen: $8{,}550\,l\,s^{-1}$.

Between plasma discharges, the Torus must be pumped down in a reasonably short time from typically 10^{-2} mbar to 10^{-8} mbar. With six turbomolecular pumps, this pump-down time is five minutes.

Each turbomolecular pump unit or roughing/backing station has a built-in Programmable Logic Controller to control its internal running sequences including the operation of valves and pressure gauges. The controllers perform all necessary interlocks and check the availability of services like water, compressed air and venting nitrogen gas. In case of faults, the systems automatically attain a

safe state. The units can be controlled locally or by CODAS.

Vacuum measurements

Pressure is measured from 1 bar to 10^{-10} mbar by Pirani, Penning and ionisation gauges. The gauge heads give pressure readings as analogue signals, and provide digital output for pressure indication relative to a set point and for heat fault indication. The system control is based on local programmable controllers. Logical operational sequences for the gauge control are resident there and only status signals are given to CODAS and system/stop signals received from there. The control of the main isolating valves is also performed locally, which ensures a fast response and maintains the operation when CODAS is not operational.

Gas introduction

The gas introduction system fulfils the following requirements:

- transfer of the high-purity gases required for the different operational modes, from high-pressure bottles to the low pressure gas handling unit;
- quality and purity check and control (volumes, pressures, temperatures and flow rates) of the different gases (for Torus discharges, Neutral Injectors, or RF Heating admixtures);
- transfer of the prepared gases to the Torus and the Neutral Injectors;
- timed fast introduction of the required quantities or flow rates into the Torus and Neutral Injectors.

The gas filling requirements to feed the plasma discharges are:

initial filling density: 10^{19}–20^{20} m^{-3}

initial filling time: 0.1–0.2 s

reproducibility: ±5%

additional filling rate: 1 to 300 mbar 1 s^{-1}.

The gas introduction into the Torus is performed by four manifolded flanges, fitted with a set of special valves, which are symmetrically distributed around the Torus. On each module, a gas transfer line and a vacuum pumping line can be isolated from the final gas introduction valves, which directly face the Torus. A calibrated volume reservoir can be filled with the required quantity of gas, preselected by the gas handling unit, which is released by opening the fast valve. Additional filling is provided by the dosing valve. Both valves are specially designed: full metal construction, bakeable at 250° C, radiation resistant, suitable for tritium operation and compatible with high stray magnetic fields. The dosing valve is of the needle type, magnetically driven by two electromagnetic coils interacting with an intermediate aluminium disc fixed to the valve shaft. The response time of this valve is about 20 ms.

Venting Gas

When the Torus is returned to atmospheric pressure, it is vented with nitrogen. This gas is taken from the exhaust of the liquid nitrogen system for which an evaporator provides the gas quantities required.

Assembly and Commissioning

After the machine octants assembly, the Torus octants were completed by fitting several types of penetrations through the double-wall structure, such as the limiter guide tubes, intermediate ports and gas feed pipes. These items were leak-tight welded to the Torus interspace and main volume. Most of these welds were made at the inside octant as they were inaccessible from the outside. Vacuum testing was carried out by purpose-built pumping boxes with specially moulded silicon rubber seals, which were placed across the welds to create a local vacuum.

For easy installation of the machine octants into the tokamak assembly, the vacuum vessel octants were slightly reduced in width by evacuating the interspace volumes. The excellent dimensional accuracy achieved became apparent, when, after installation, the half-convolution bellows at the edges of the vacuum vessel octants showed even gaps between each other in this state.

The vacuum seal between octants was a U-joint lip-weld, performed (Fig. 9) by using a remotely controlled welding tool, which had been developed for the active phase of JET operation. The final welds of the U-joint cover plates were tested by evacuating the interspace between U-joints and cover plates. In all cases, leak rates better than 10^{-9} mbar 1 s^{-1} were measured. After leak testing, the various types of internal protection plates were individually fitted, and the nickel surface limiters as well as Pumping Chambers (Fig. 10) and Port Adaptors were installed. The installation of various service subsystems, pipework, cable ducts and cable junction boxes

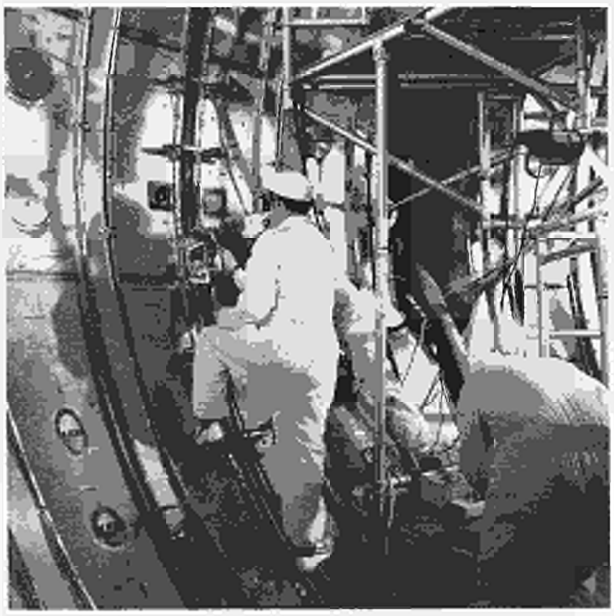

Fig. 9 Welding of the Torus U-joints, the vacuum seals between octants.

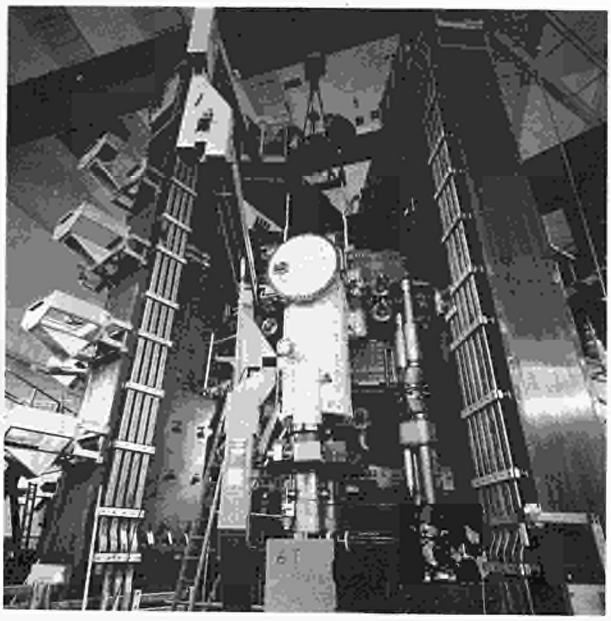

Fig. 10 Installation of a Pumping Chamber to a Torus main port. The circular door at the front of the Pumping Chamber gives access to the Torus inside. At the bottom of the chamber two gate valves and turbomolecular pumps are installed.

and the pulling and termination of power and instrumentation cables (Fig. 11) took the first half of 1983 and determined the commissioning schedule and the machine availability for system tests.

The final mechanical cleaning of the Torus was undertaken using automatic high pressure scouring with hot water and detergent (Fig. 12). After cleaning, the Torus was pumped down. Only two leaks on external welds needed repair, after which a Torus pressure of several times 10^{-6} mbar was achieved, determined by outgassing only.

By baking the Torus, Torus Ports and external attachments at approximately 250° C, and subsequent glow discharge cleaning at 200° C, a total impurity base pressure of 3×10^{-9} mbar (measured at a Torus temperature of 100° C) was achieved. The total outgassing rate for impurities was 1×10^{-12} mbar $1\ s^{-1}\ cm^{-2}$ (measured at 100° C wall temperature). These values might be a factor of 10 lower at room temperature.

With these conditions the first plasma discharges were performed.

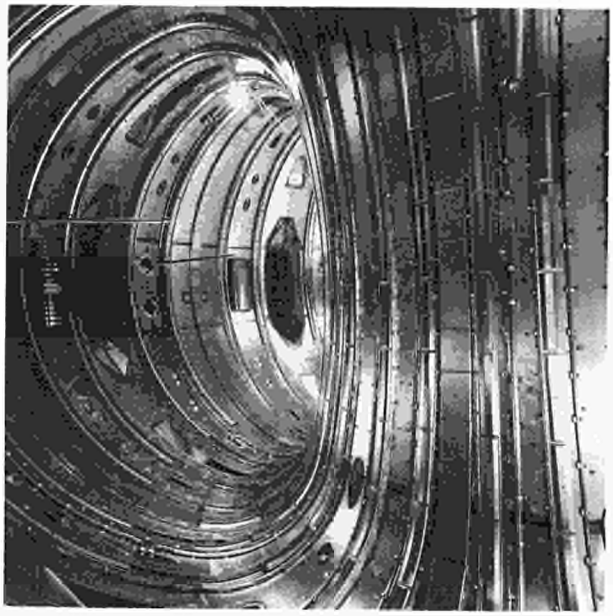

Fig. 12 Inside the Torus with limiters and with water spray heads. The U-joint and bellows protection plates are partly installed.

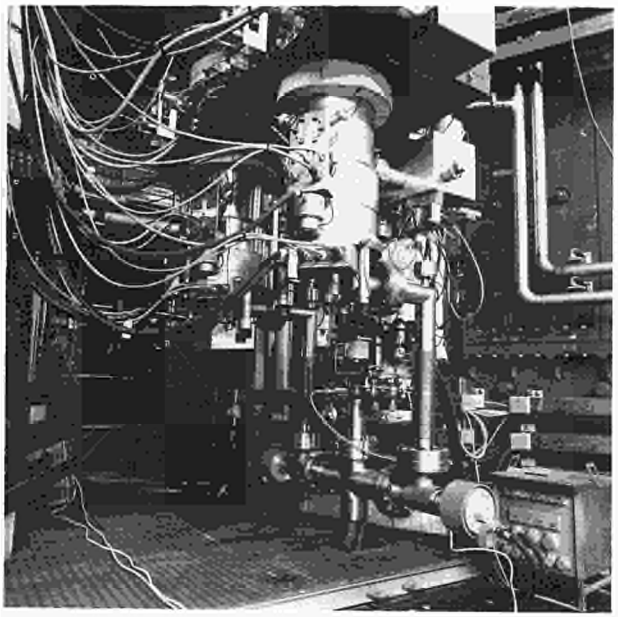

Fig. 11 Turbomolecular pumps installed at the tokamak.

Magnet Systems Division

(Division Head: M. Huguet)

During 1983, the Magnet Systems Division's main efforts were devoted to completion of assembly work and the commissioning of the Toroidal Field and Poloidal Field systems. In May and June 1983, the Division was heavily involved in the first JET operation. At the end of the JET Construction Phase, the Division had completed its mission and it ceased to exist in the organisation for the Operational Phase.

The mechanical assembly of the JET machine was completed in January 1983 with the erection of the upper poloidal coils and the upper limbs of the magnetic circuit. The busbar systems for both the toroidal and poloidal field coil systems were also erected during the first months of 1983.

The preparation of commissioning procedures, already started at the end of 1982, became the main activity of the Division by the beginning of 1983. High voltage and

water pressure tests had been partially carried out throughout the assembly phase, but tests at power started at the end of March. This advanced preparation permitted rapid progress, leading to a first plasma discharge by the end of June 1983.

During the last two months of its existence, the Division devoted all its resources to JET operation. This involved: supervision of work in the Torus Hall; inspection and preparation of the machine before operational runs; search and access control procedures in experimental areas; monitoring and recording of instrumentation signals; and the running of water cooling systems required for operation.

Toroidal Field (TF) System

(J.A. Booth, R.D. Pöhlchen, W. Scott, A. Skinstadt)

Assembly Work

The busbars for assembly in the basement and on the limbs of the magnetic circuit were delivered in January 1983, and erection was completed by mid-March 1983. A metallic protective cage was then constructed along the busbars in the basement and protective rubber sheaths were installed on the bars along the magnetic limbs in the Torus Hall. Rubber covers were also fitted around the TF coil water terminals to avoid water spillages inside the machine.

The final step of the TF magnet assembly was the positioning and shimming of the coils inside the mechanical structure. The straight part of each TF coil fitted into a cylindrical groove machined on the inner cylinder, so that the coil was located and supported against lateral forces. The coils were pressed radially against the inner cylinder with a force of 10 tonnes per coil by means of mechanical jacks provided on the mechanical structure. At this later stage, gaps between the mechanical shell and the lateral surfaces of the coils were measured all along the outer contour of each coil by means of a special gauge. The shims, which located and supported the coils, were machined to the measured dimensions and inserted. Due to the large number of these shims (608 in total), a detailed procedure was prepared and special procedures were set up for the measurement, machining, checking and final insertion of the shims. Unreliable operation of the measuring gauge made the whole operation lengthier than anticipated. It was realised later that some measurements were out of tolerance and parts of this work were repeated in August during machine shut-down.

Following this initial shimming, the coils were pressed magnetically against the inner cylinder, using coil currents up to 15kA. In this way, centripetal forces up to 100 tonnes per coil were produced, which ensured that all coils were fully engaged in the inner cylinder grooves. At this stage, the collar and ring teeth were tightened up and the ring shims were inserted to provide full lateral support to the coils.

The accuracy of positioning of the TF coils was believed to be about 0.4mm for the straight part and 1 mm for the outer contour. This accuracy was dictated not by field perturbations or associated forces, but by assembly requirements.

Commissioning

The busbars were tested relative to earth at high voltages up to 20kV DC and the coils were tested up to 10kV DC. For the first power test, the coils were short-circuited and a current of 67kA was passed in the busbars alone. No abnormal deflection was observed during this test.

The coils were commissioned initially at currents up to 25kA using the TF static unit alone as a power supply. For those early tests, the coils were not water cooled because the pipework in the Torus Hall had not been completed. In June, when the pipework was ready, the coils were pressure tested initially with air, then filled with water and pressure tested again. Relatively few leaks occurred, in spite of the TF cooling circuit including about 1650 quick release water couplings. Initial flow tests indicated that the circulation of water was not properly established in some coils. This was found to be due to air locks in the lower water manifolds and was cured by providing necessary vents. In June, the flywheel generator was used to provide a current of 40kA in the coils. Finally, in November, the generator and the static unit in combined operation delivered a current of 53kA with a flat top for 10s. The maximum energy delivered per pulse at this current level was 3100MJ, compared with the maximum design value of 5100MJ.

The coil's measured expansion in the radial and vertical directions was in agreement with calculated values, which confirmed that bending stresses had been eliminated by the D-shape. The cooling water temperature peaked about 30s after the pulse and, after some slight oscillations due to the recirculation of hot water around the loop, returned to its average level within 5 minutes (see Fig. 13).

Poloidal Field (PF) System

(D. Cacaut, C. Calmels, J.R. Last, D. Lecornet, A.P. Pratt, S. Turley, M.E. Young)

Assembly Work

In January 1983, the upper poloidal field coils No. 3 and No. 4 and the upper limbs of the magnetic circuit were installed on the machine. By February, most busbars and accessories (i.e. clamps and supports) had been delivered and the PF busbar system was rapidly assembled. Work progressed in parallel on assembly of the busbar runs in the basement, on the junctions at the air-tight penetrations between basement and Torus Hall, and on the erection of the busbars on the limbs of the magnetic circuit. At the same time, the design of the busbars was being re-checked, and a few modifications were incorporated to improve insulation resistance and mechanical bar supports. By the end of April, the assembly was completed by the erection of a protective cage all along the busbar runs in the basement (see Fig. 14).

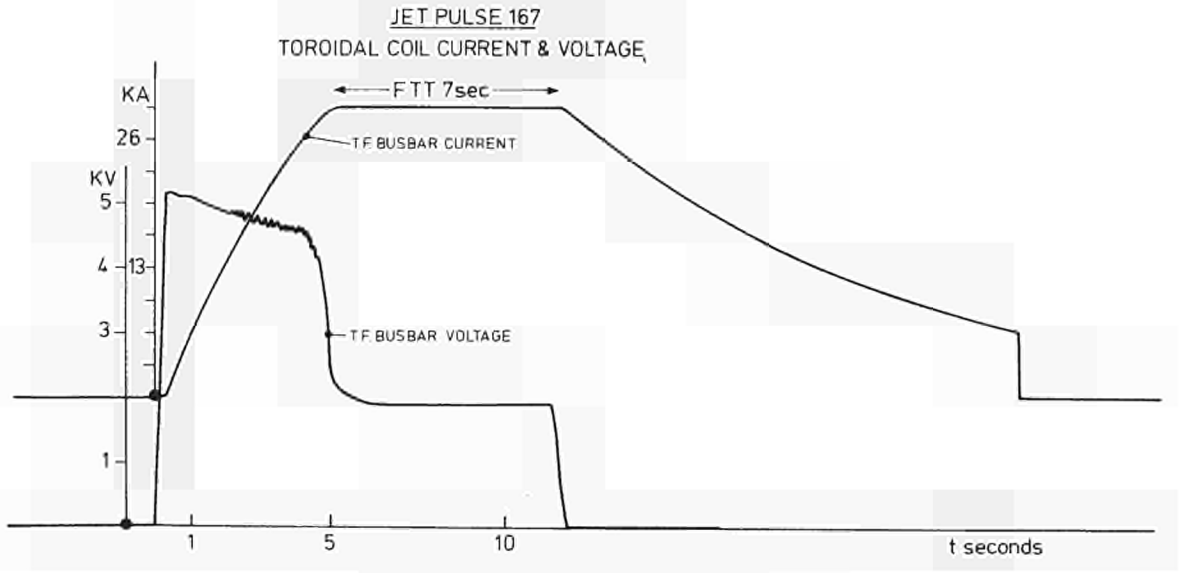

Fig. 13 Toroidal field coil: Pulse at 30kA.

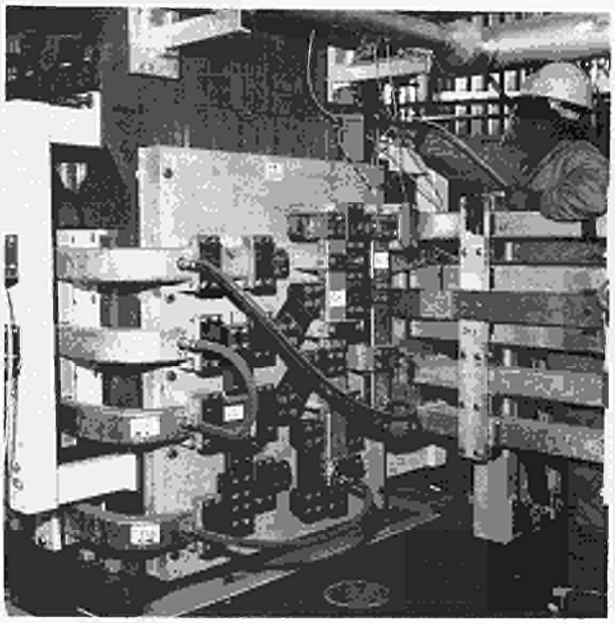

Fig. 14 Poloidal field busbars at floor penetration.

Commissioning

The busbars were tested relative to earth at high voltages of 50kV DC, and 80kV DC was applied between the two main bars of the ohmic circuit. Before filling with water, the coils were tested at high voltage of 45kV relative to earth. Interturn insulation tests were made by discharging a 45μF capacitor into the coil to produce an interturn voltage of 560 volts for the No. 1 coils and 2800 volts for the outer coils Nos. 2, 3 and 4. During this test, a short-circuit was found between two turns in the lower PF coil No. 4. This has not been fully explained, but it was thought that breakdowns to earth during DC ground insulation tests might have generated fast voltage transients puncturing the interturn insulation. The short-circuited turn in this coil, and, for symmetry, the corresponding one in the upper PF No. 4 coil have been excluded from the circuit.

In May, prior to power tests, field and flux measurements were made to check the poloidal field configuration. During the pre-magnetisation phase, the leakage flux from the iron in the area occupied by the plasma was found to be small, in accordance with calculations. The double flux swing in the iron core was measured at about 3.8 volt-second before saturation of the core; as expected, taking into account the magnetic properties of the materials and the steel used for the support rings of the ohmic heating coils. The field maps for the vertical and radial equilibrium field showed excellent agreement with predicted values. In general, the symmetry of the system and, in particular, that of the iron circuit was satisfactory.

In October, only the cooling circuits of the PF coils were filled with water, because of the late delivery of the Torus Hall pipework. The coils and busbars were initially pressure tested with air in order to eliminate major leaks, then the circuits were filled with water and retested at pressure. Very few leaks were detected at quick release water couplings. At this stage, the coils were high-voltage tested to earth, but a DC voltage could not be used because of the low resistance to earth of the circuit when filled with water (i.e. the total resistance was about 15kΩ when the water resistivity was 1MΩ.cm^{-1}). The test was carried out in pulsed mode up to 25kV with the capacitor bank.

The coil system was power tested and used for plasma operation during May–December 1983. The maximum values of the currents reached are indicated in Table II.

Table II
Status of commissioning of the Poloidal Field Coils

Circuit	Mode of Operation	Maximum current reached kA	Maximum design value kA
Ohmic heating	Premagnet-isation	40	80
" "	Slow rise	64	80
Vertical field	Slow rise	20	45
Radial field	–	2	3

Mechanical structure and mechanical components
(W.R. Baker, G. Celentano, G. Malavasi, P. Presle, S. Romi, E. Salpietro, R.L. Shaw, L. Sonnerup)

During early 1983, the Mechanical Group was involved in the completion of the mechanical assembly of the machine, particularly in the final positioning and shimming of the TF coils, and in final dimensional checks and surveys of the machine. Other activities of the Group included the procurement of a spare octant of the mechanical structure and of the interferometer support frame, and on-going stress analysis work.

Spare octant of the mechanical structure

The decision to build a spare octant of the mechanical structure had been taken in late 1982. It was delivered in August 1983 and stored awaiting preparation of a complete machine octant.

Interferometer support frame

The manufacture of the support frame for the infrared interferometer was completed smoothly and speedily, and was delivered on schedule in September 1983. All assembly procedures for the erection on site were drafted and approved and, following the delivery at Culham of the first components of the interferometer, assembly started at the end of the year (see Fig. 15).

Stress Analysis

Many mechanical assessments and stress calculations were carried out for Power Supplies Division (generator thrust bearing, SF6 tower vessel), for Plasma Systems Division (cryopumps, hypervapotron dump element, bulkhead of PINI transmission line), for RF Heating Division and Diagnostics. For these calculations the NASTRAN code was used extensively.

The computational model of the JET mechanical structure including the rings, collars and inner cylinder and also the toroidal field coils was created and made ready to be run with load cases.

SF6 tower

Work started on the procurement of the SF6 tower and associated equipment. This work was carried out by Magnet Division staff for Power Supply Division. A description of this work is given in the section for Torus Division.

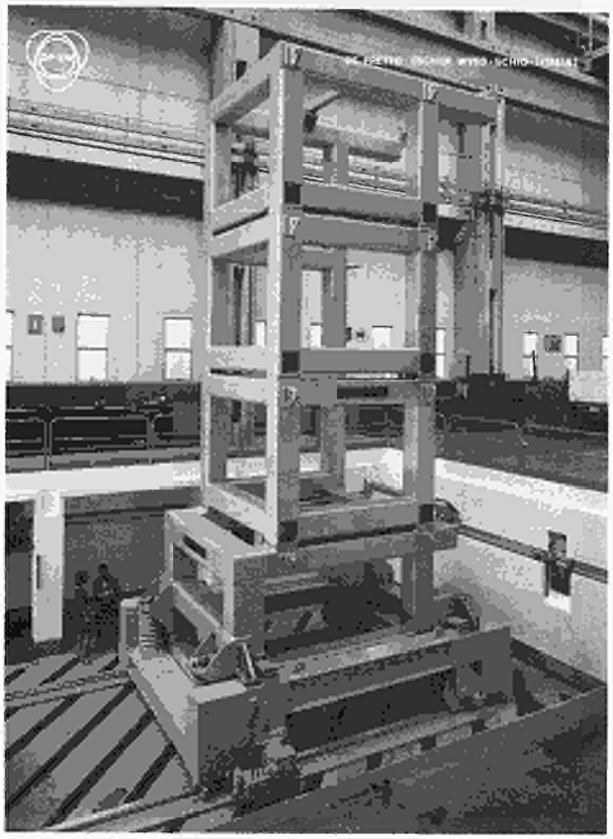

Fig. 15 Interferometer support frame after delivery.

Water Cooling Systems
(G. Grabenstätter, L.C. Nickesson)

Main water cooling system

The main water cooling system including the Site water system, the water treatment plant and the main cooling plant had already been commissioned in 1982.

As soon as the Torus Hall pipework became available, the complete cooling loops were flushed with water in order to remove all debris left inside the pipes. For this, the coils were by-passed by temporary pipe connections and strainers were inserted at the heat exchanger inlets to collect the debris.

The TF coils were first water-cooled in June and the PF coils in November. The plant has been running routinely and reliably for plasma operation as well as during bake-out periods. The electrical resistivity of the water has been maintained between 1 and 2 $M\Omega.cm^{-1}$ which corresponds to a resistance to earth of 10–20 $k\Omega$ for both the TF and PF coil systems. Since the commissioning of the water treatment plant in July 1982, the two mixed bed columns for the TF cooling loop have needed regeneration only once, and the columns for the PF loop were still providing output with a resistivity better than 10 $M\Omega.cm^{-1}$, without regeneration.

Emergency cooling system

The procurement and installation of this system was carried out with great speed, taking only 3 months between the placing of the contract and its commissioning. The plant has been functioning satisfactorily and has been on stand-by during every bake-out period (see Fig. 16).

Cooling plant for the Neutral Beam injection system

The test bed cooling plant was installed and commissioned in September 1983, and operation on a routine basis began in December 1983, together with the initial operation of the test bed equipment (see Fig. 17). The plant at Octant 8 was not fully installed by the end of 1983, because of the low priority accorded this work and due to lack of access in the basement during JET operation. Installation was planned for January 1984. The design of the plant at Octant 4 was completed but installation was not planned before Summer 1984 due to lack of access in the basement.

Draining and refilling system

Installation of pipework and associated hardware was essentially completed by June 1983 (see Fig. 18).

The control cubicles which provide the operation sequences and interlocks were delivered in September and partial commissioning tests were carried out in October and November. Installation of cables and pneumatic pipework for control of the valves progressed slowly and less than 50% was completed by the time the main cabling contractor left the site in September. Some additional cabling work was carried out from October to December but due to the lack of access to the basement,

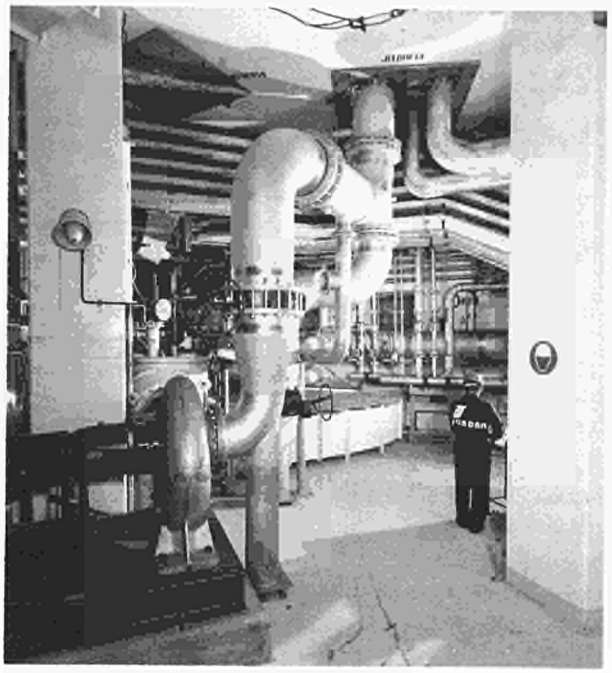

Fig. 17 Cooling plant for the N.I. test bed.

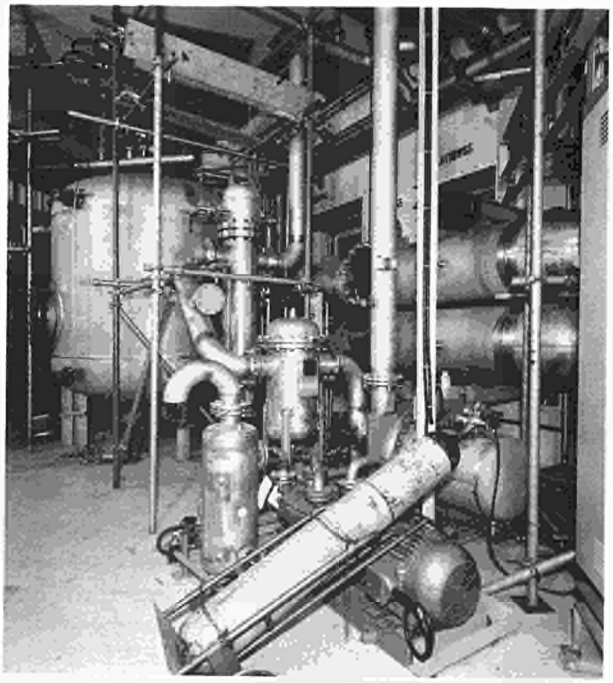

Fig. 18 Equipment at Octant 6 for the drainage and refilling system.

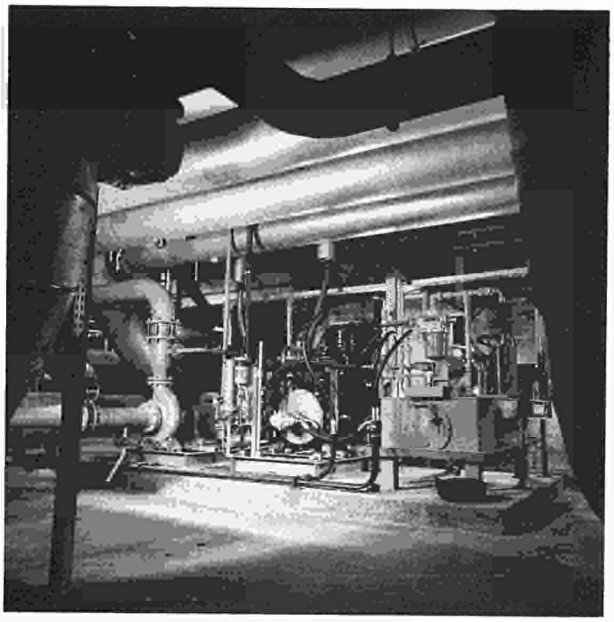

Fig. 16 Diesel engines in the valve pit for the emergency cooling system.

this work was undertaken at night and progress was slow. Completion of installation and commissioning tests were expected early in 1984.

Instrumentation
(D.V. Keane, F. Thomsen, J.W. Zwart)

Installation
Most instrumentation sensors on the coils and structural components had already been fitted in 1982 but some sensors in the Torus Hall and basement could only be installed after the completion of the assembly of the machine and of the busbar runs. Installation progressed slowly and, although the sensors essential for the first plasma operation were available in June, certain sensors (i.e. Rogowski coils on busbars) were fitted only in August.

Jumper cables between sensors on the machine and limb junction boxes were not available in time for the plasma operation and this necessitated the use of temporary cables to record machine signals. In August 1983, the jumper cables were installed and the testing of the complete instrumentation loops started.

Commissioning and operation
For the first commissioning tests and plasma operations from April to July 1983, only a few instrumentation channels were available using temporary cables, and signals were monitored by means of oscilloscopes or recorders.

From October 1983 onwards, most TF and PF instrumentation signals were available in the control room and display software was constantly improved. Display facilities included tables, bar charts and time dependence curves. No attempt was made to create level 2 software to calculate more elaborate functions, or to generate alarms, because of the commitment of CODAS staff to more urgent tasks. The laser diagnostic, which measures the twist of the mechanical structure, was operational from June onwards. The short circuit detection system (DMSS) for the TF magnet was made operational for the first power tests. Initially there were a few erroneous trip signals due to faults within the protection circuit itself but, when these faults were cured, the system operated satisfactorily.

Integrated tests and first plasma operation
Before plasma operation in June, tests were carried out to check the combined operation of the toroidal field and poloidal field systems. A vertical field was generated in order to produce some twisting moment on the toroidal field coils and the mechanical structure. At the low level of the test (2000 tonne-m, i.e. 1/10 of the maximum design value), the rotational deflection of the shell, measured with the laser diagnostics was 0.23 mm, in accordance with calculations.

In June and July 1983, the Division was heavily involved in the first plasma operation. The preparation of the machine before each operation run included the following:

- Inspection to ensure that no tool or equipment was left on the machine;
- Check of water circuits for leaks and check for proper functioning of the water cooling plant;
- High voltage tests or measurements of the resistance to earth of the TF and PF coil systems;
- Evacuation, search procedure and locking up of the basement and Torus Hall.

Conclusion
The main responsibilities of Magnet Systems Division, as defined when the Division was created in June 1983, were the design, procurement, assembly and commissioning of the toroidal field magnet, of the poloidal field coil system and magnetic circuit and of the mechanical structure. In addition, the Division was charged with providing the instrumentation related to the magnets and structural components and with providing the water cooling systems for the whole JET experiment.

Torus Division

(Division Head: M. Huguet)

Torus Division was formally created in August 1983, and is responsible for the operation of the Torus, including the creation and training of the operating team and the organisation and execution of maintenance work in the Torus Hall and Basement. The Division also organises major shutdowns for the installation and commissioning of equipment and for development work necessary for improvement of the sub-systems integrated into the JET device (vacuum system, baking and cooling plants, limiters, first wall, etc.).

The Division undertakes these tasks within the following structure:

- The Division Head is assisted by a senior physicist on general matters such as programme definition and general policies on machine operation, who is also responsible for plasma control and has the special task of liaising with the Scientific Department;
- The Torus Operations Group is responsible for the day-to-day operation and the detailed organisation and planning of the operation and maintenance programme;
- The Magnet Systems Group maintains and operates the coil systems and structural components together with all the machine instrumentation;
- The Vacuum Systems Group is responsible for the integrity and quality of the vacuum, which encompasses the vacuum vessel itself, interfaces with all components connected to the vacuum system, the

pumping system and the gas and electrical bake-out equipment;

- The First Wall Group is charged with the definition, design and procurement of the components for the first wall, (i.e. limiters, protection tiles and wall conditioning techniques), and is responsible for gas handling and gas introduction systems.

At its formation, the Division had 36 staff members coming mainly from the former Plasma Systems and Magnet Systems Divisions. The staff was composed of 19 professional engineers or physicists, 15 technicians and 2 secretaries.

Since its formation, the Division has been heavily involved in JET operation, in which operational duties represented the main task, taking up most of the Division's resources. Design, assembly and commissioning work, not associated directly with machine operation, suffered from the lack of resources, but even so good progress was maintained.

During the August/September shut-down period, the Division's main task was the recommissioning of systems in preparation for plasma operation.

From October to December 1983, considerable resources were devoted to JET operation. In 12 weeks of operation, Torus Division provided the Session Leader for 4 weeks and the Engineer-in-Charge for 8 weeks. Control room staff on duty during operation weeks included an Operations Engineer and an Operator from the Torus Operations Group, one vacuum technician for the monitoring of the vacuum system, gas introduction and residual gas analyser, and another technician for machine instrumentation. More professional or technical staff were on stand-by duty, and were frequently called upon to operate, reset or repair special equipment.

Tasks related to wall conditioning (i.e. bake-out of the vessel and glow discharge cleaning) stretched the resources of the Vacuum Group and First Wall Group. These activities were followed continuously for 3 or 4 days before sessions and every night during operational sessions. This involved a three shift rota system manned by staff from the Vacuum and First Wall Groups and assisted by staff from all other Divisions.

Specific activities of Divisional Staff are described within the Group structure, in the following paragraphs.

Senior Physicist's Activities

(M. Browne, P. Noll, A. Santagiustina)

Plasma Position Control

The important aspect of radial position control of the plasma is based upon the measurement of the poloidal flux difference between the limiter and the desired inboard position of the limiter magnetic surface. The flux error signal is combined with a pre-programmed voltage to control the output voltage of the poloidal vertical field amplifier. At the correct position the flux difference becomes zero.

The feedback signal is obtained from a combination of saddle loop signals and appropriately weighted signals from internal discrete poloidal field pick-up coils as indicated in Fig. 19. An important feature of the control system is the ability to alter the plasma inboard radius during the pulse by means of the preprogrammed function "D_R, Ref" which represents directly the inboard plasma/wall distance. The system also includes an automatic limitation on the plasma vertical dimension. So far, a proportional/derivative controller is used for feedback, in which the loop gain can be altered continuously by the preprogrammed waveform "G_{PVFA}".

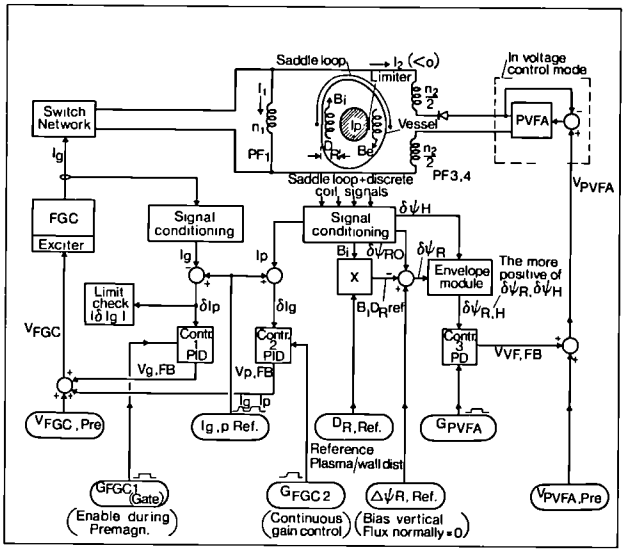

Fig. 19 Block diagram for the control of plasma current, premagnetisation current, and radial plasma position, including automatic limitation of the plasma height.

The stabilisation of the vertical position is achieved in an analogous manner using the measured flux difference between symmetric top and bottom positions for feedback control of the poloidal radial field amplifier. Reference functions are normally set equal to zero because JET is practically symmetric with respect to the midplane. Derivative feedback is essential as the JET plasma is unstable in the vertical direction if the plasma elongation ratio (b/a) is > 1.2.

Fig. 19 also shows the feedback control system for the premagnetisation current and the plasma current. This system has not yet been commissioned and the poloidal flywheel generator convertor has been controlled only by preprogramming the excitation voltage.

In the course of JET operation, the position control system has been enhanced in several steps:

(i) During June to August, only external flux loops were used for radial position control and a passive and partial stabilisation of the vertical position was applied by shorting the radial field coil. The

plasma pulse duration did not exceed 0.25s probably due to vertical position instability;

(ii) In October, feedback stabilisation of the vertical position was included. The pulse duration was then extended to about 2s;

(iii) During November/December, the full position control system was implemented as designed (except for the plasma height limitation). In addition, compensation for erroneous toroidal field pick-up was introduced so that feedback control no longer required a constant toroidal field. Fig. 20 shows typical examples of plasma/wall distances, the reference position and plasma current. The plasma minor radius was increased during the current rise. The vertical position was centred within about 1 cm during most of the pulse;

(iv) From October to December, the turns-ratio of the outer poloidal field coils was not altered. The resulting plasma elongation ratio was 1.2 and the vertical position was marginally stable for the case of a shorted (flux conserving) radial field coil. The performance of the vertical position stabilisation of highly unstable plasmas with elongation ratio (b/a) of 1.5 to 1.7 should be demonstrated in future experiments. Modifications of loop gains and other controller parameters might be necessary.

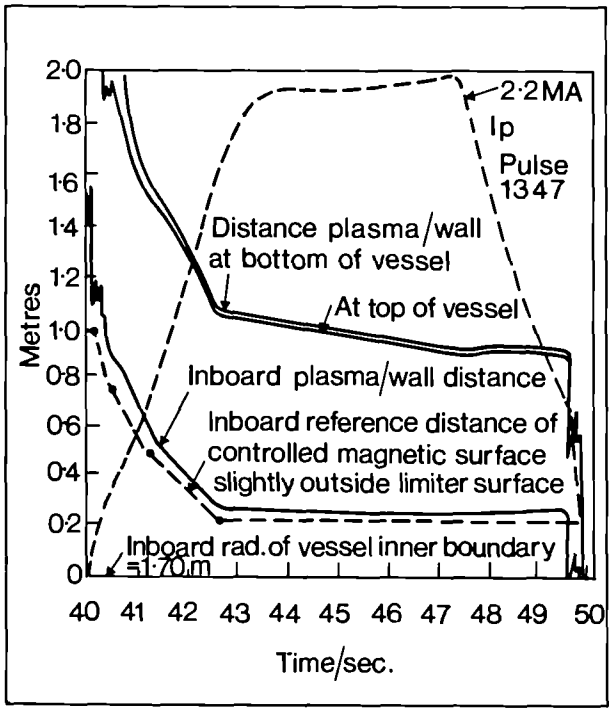

Fig. 20 Example of measured plasma/wall distances (Limiter radius R_L = 4.12m, Pulse # 1347).

Torus Operations Group

(P. Chuilon, F. Erhorn, B.J. Green, G. Kneebone, R. Saunders, R. Thomas).

The Torus Operations Group's responsibility for the operation of the machine includes participation in the establishment of the operation programme and of the machine's operational parameters. Further, the Group organises the operation teams, maintains records of tokamak operation and prepares operation manuals. In addition, the Group is responsible for the design, installation and maintenance of the Personnel Safety and Access Control System and the installation of safety equipment such as fire detectors and alarms.

Operations team

(P. Chuilon, B.J. Green, R. Thomas)

In 1983, the Operations team was composed of only two professionals: the Group Leader (already heavily involved in other duties); and one operator. With such resources, it was not possible to assume all the responsibilities expected from an operations team. Moreover, the staff were fully involved in activities on JET construction up to September and no prior preparation for operational duties had been possible. The October to December period was treated as a learning period during which duties were clarified and the staff became acquainted with requirements.

The Operations team now undertakes the various tasks of an operations session, as described below:

(i) Preparations for a session:
- Search procedure, evacuation of all personnel and securing of all experimental areas;
- removal of earth switch padlocks to permit the opening of switches and energisation of the main circuits.

(ii) Duties during a session:
- Control of personnel access to experimental areas by implementing "Permits to work" and releasing access keys;
- logging of events and recording of pulse schedules;
- setting up machine parameters, including waveforms and timing data for power supplies, plasma position control and gas introduction, which must be edited and loaded in the pulse file.

(iii) Duties at the end of a session:
- Establishment of safe conditions in the experimental area (i.e. padlocking earth switches), inspection and re-opening these areas.

Planning activities

(G. Kneebone, R. Saunders)

Procedures for short term planning and monitoring of all activities in the Torus Hall and basement were established. Experimental and assembly work was discussed at weekly planning meetings and approved programmes were issued. Such programmes included details concerning the status

of the machine and vacuum system, requirements for services such as water cooling, needs for CODAS subsystems computers, restrictions on access to experimental areas and details of experimental and assembly work. Rosters for duty staff or those on-call also formed part of weekly planning sheets.

A "Permit to work" system was established in the Torus Hall and basement to ensure that all assembly work had been properly prepared, approved and was adequately supervised.

Personnel Safety and Access Control Systems (PSACS)
(F. Erhorn, B.J. Green)
The system was designed to prevent personnel access to areas at times that might be hazardous due to operation and to prevent the establishment of hazardous conditions in areas where personnel might be present. Basically three subsystems are included:

(i) a door status and access control system: the status of certain access doors is monitored and interlocked with plant to prevent access to areas containing potential hazards. In particular, this system will not permit machine operation nor a state of pulse readiness to be reached unless the biological shield is sealed.

(ii) a warning system: involving visual and audible warning systems to indicate the status of the machine and to warn of changes when hazards might arise.

(iii) an emergency push button system, which permits the machine to be brought to a state where no further operation is possible until the push button system has been reset.

At the end of the year, the system was well advanced, as follows:

- The door status and access control system hardware was essentially installed together with all door locks,
- key switches and associated cable work. Connections to CODAS and the Central Interlock and Safety System (CISS) had not been made;
- The warning system installation was well advanced;
- The emergency push button system was installed but not yet connected to CISS;
- The CODAS and CISS interfaces had been specified.

It was expected that the basic hardwired system would be operational when machine operation resumed in March 1984. A fire alarm and detection system had been designed for the basement, following smoke tests, and smoke detection tests were being carried out in the Torus Hall.

Magnet Systems Group
(W. Baker, D. Cacaut, G. Celentano, K. Grabenstätter, J.R. Last, D. Le Cornet, G. Malavasi, L. Nickesson, W. Scott, R. Shaw, S.J. Turley, J. van Veen, M.E. Young, J.W. Zwart)
The Magnet Systems Group is responsible for: maintenance and operation of the coil systems and structural components; maintenance and operation of the machine instrumentation and keeping instrumentation records; electromechanical safety of the machine; safety of personnel when machine assembly work is underway; checking and supervising all mechanical machine assembly work. In addition, the Group is cooperating with Power Supplied Division in procurement of equipment for the SF_6 tower.

JET Operation
(D. Cacaut, J.R. Last, S.J. Turley, J. van Veen, M.E. Young, J.W. Zwart)
One Group task included preparation of the machine before operational runs, including checking electrical integrity of the TF and PF circuits and carrying out high voltage tests. Commissioning of the coil systems at higher current levels had taken place gradually during the period from June to September and is described in the Magnet Systems Division Section.

The main operational duty of the Group was in operation of the instrumentation and analysis of the signals. All channels measuring the TF coil movements worked satisfactorily and measured values agreed with predictions. The outer PF coil movements were small at the low operating currents, and no clear conclusion could be drawn from the signals obtained. Cooling water temperatures for both TF and PF coils were monitored and displayed in the control room after each shot.

Strain gauges and crack detectors fitted on the mechanical structure were not operated at this stage due to the low stress level. However, laser measurements of the rotation deflection of the mechanical structure showed tangential rotation in accordance with calculations. A small unexplained vertical rotation was also observed.

The TF-DMSS (short-circuit detection system) was made operational as early as June 1983, but the protection circuit acted only on the generator excitation. The crowbar switch was power tested by Power Supply Division in December, and is expected to form part of the protection circuit, when operations resume in 1984.

The PF-DMSS was partially commissioned. Signals originating from Rogowski coils were monitored and compensated well for the outer PF coils. For the inner PF coils, compensation was not so good suggesting that the sensitivity of fault detection will be lower than planned. The PF-DMSS should be fully operational, early in 1984.

SF_6 Tower
(G. Celentano, W. Baker, R. Shaw)
During 1984, eight Neutral Injection beam sources (PINI's) will be located in a NI box in the Torus Hall, at Octant 8, to produce the first 5MW of injection power.

The Tower is a cylindrical pressure vessel which connects the electrical supplies from the high voltage lines in the Torus hall basement with the NI's. It also supplies the operating gas and the cooling water to the NI's and is fitted with water and gas manifolds and compressed air lines for operation of gas valves. For electrical insulation purposes, the Tower will be filled with sulphur-hexafluoride (SF_6) gas at a pressure of 3.6 bars.

The main components of the assembly are shown in Fig. 21 which include the pressure vessel, the snubbers, the high voltage breaks, the high voltage items and the bulkheads connected to the PINI's.

By March 1983, the general features of the design had been settled, and production of the tower involved various technologies, which required cooperation from organisations operating in different fields of activity and with different background experience. For this reason and in order to shorten production time, it was decided to perform the full detailed design up to the stage of manufacturing drawings and development of all technical problems. This allowed procurement to be split among several contracts, using smaller firms with specific experience and capability. The general manufacturing design was completed by the end of the Summer, but a few components were still under development, which should be finalised early in 1984. Fifteen contracts were placed and set delivery schedules were being maintained. Assembly at JET was expected to start in March 1984, with commissioning following three months later.

Most contracts for procurement of the second SF_6 tower have been placed, with manufacturing work due to start in early 1984. The second tower will provide the supplies for the next 5MW of NI heating and will be positioned at Octant 4.

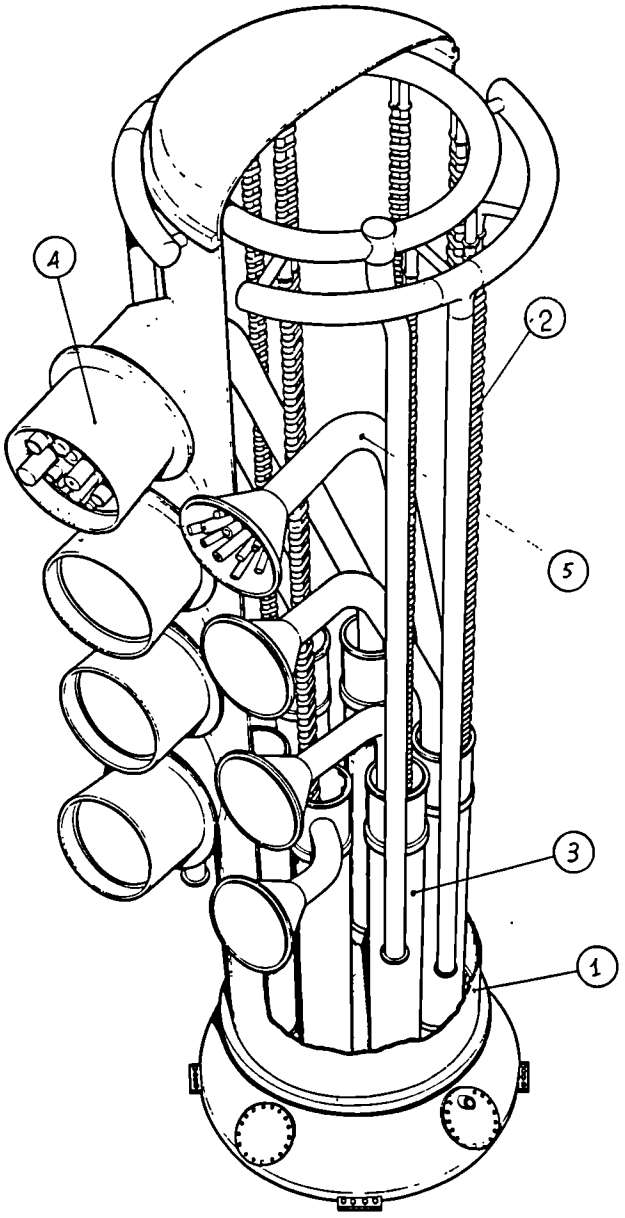

Fig. 21 SF_6 Tower: 1. Vessel; 2. High voltage break; 3. Snubber; 4. Bulkhead; 5. High voltage items.

Vacuum Systems Group

(S. Baumel, B. Bignaux, W. Daser, D. Froger, J. Hemmerich, D. Holland, J. Orchard, E. Usselmann, T. Winkel))

The main responsibility of the Vacuum Systems Group is to produce and maintain a high vacuum within the vessel, which includes the torus proper and the vacuum pumping system, the vacuum interface of components connected to the vessel, and also the gas heating/cooling plant and the electrical baking system. In addition, the Group provides a service to all Divisions for such activities as leak detection, operation and maintenance of vacuum equipment and instrumentation, and the supply of standard vacuum components. To provide this service, the Group is complemented by a vacuum technician pool supervised by the Group, but which is used to undertake work for other Divisions.

Operation of the main vacuum

(W. Daser, D. Holland, J. Orchard, E. Usselmann, T. Winkel)

Achieving and maintaining an ultra-high vacuum in the JET vessel is difficult due to the large number of components, such as limiters, diagnostics and remote handling systems, which are connected to the vacuum, and also due to the on-going assembly work and modifications carried out on these components.

During the operation period from October to December, a significant number of incidents affected the vacuum, such as:

(i) a loss of compressed air which initiated a shut-down of the pumping system;

(ii) a leak between the main vacuum and the cooling circuit of a nickel limiter (up to 3 limiters have developed leaks);

(iii) opening of virtual leaks (probably from the bellows system of some limiters);

(iv) leak at an access door;

(v) a window breakage on the in-vessel inspection system.

However, these incidents caused no major delays in the programme. The last case occurred during a commissioning period and serious consequences were avoided as all main vacuum valves were closed prior to the critical operation of inserting the viewing probe into the vessel.

The other problems were cured quickly without venting the vessel. Even so, the diagnosis and repair of these faults imposed a further heavy work-load on the staff involved, in each case.

Bake-out

(S. Baumel, B. Bignaux, J. Hemmerich)

The bake-out plant was run routinely with a temporary blower, using air instead of CO_2; it provided a temperature ramp and cool-down rate of 15° C per hour, which is slower than originally foreseen but nevertheless adequate. The vessel was maintained for long periods at 300° C but could not be brought to a higher temperature as the nickel limiters were not water cooled. The electrical baking system was also used on a routine basis to heat the ports up to 200° C, for which computer control was established in November.

A rota system was set-up to provide a round-the-clock supervision of the vacuum system when bake-out or glow discharge cleaning were taking place. The three-shift rota was manned by expert staff at professional or technician level from the Vacuum Systems Group and First Wall Group and by an assistant taken from other JET Divisions. This represented a very heavy load in terms of night and weekend work for the staff involved and, as a consequence, reduced the availability of these staff during normal working hours. This problem was recognised by Management and by the end of the year, steps were taken to recruit shift technicians able to take over this kind of supervisory duty.

Design, installation and commissioning

B. Bignaux, S. Baumel, W. Daser, C. Froger, D. Holland, J. Orchard, E. Usselmann, T. Winkel)

The oven in the south wing of the Assembly Hall was used for bake-out and hot leak testing of components, such as diagnostics flanges, prior to their assembly on the torus. Difficulties encountered with the beam scrapers, beam dumps and nickel limiters demonstrated that all components to be attached to or fitted inside the vessel, should undergo baking cycles at the full baking temperature, prior to their assembly on the machine. For this purpose, a vacuum tank to be fitted with electrical heaters, and equipped with ports simulating the JET horizontal and vertical ports was designed and ordered. It will be used for the hot testing of diagnostics and internal components such as limiters.

A number of control systems were at various stages of design and commissioning. The control cublicles of the vacuum system for the A_o antennae was designed. The procurement of these cubicles will be arranged by Torus Division for the RF Heating Division and commissioning will be carried out jointly by staff of both Divisions. The control cubicle for the first rotary valve was also commissioned at the factory, and it is planned for installation at the JET site during the shut-down period in January 1984.

Rotary High Vacuum Valves

(B. Bignaux, C. Froger)

In the first half of the year, some difficulties with the Rotary High Vacuum Valves were successfully overcome by improving the design of the seal unloading spring resulting in a leak tightness better than 10^{-10} mbar l s^{-1} through the closed double sealed valve. The overall global leak tightness was also satisfactory at better than 10^{-10} mbar l s^{-1}. Due to unsatisfactory heating equipment at the manufacturers, it was decided in October to bring the valve for proper bake-out in the JET oven. Vacuum tightness was rechecked during and after bake-out at 350° C and was still found to be fully satisfactory.

Electrical heaters and thermal insulation were fitted and other work continued to prepare the valve for installation on the Torus during the January 1984 shut-down. The completed valve fitted with electrical heaters and without thermal insulation is shown in Fig. 22.

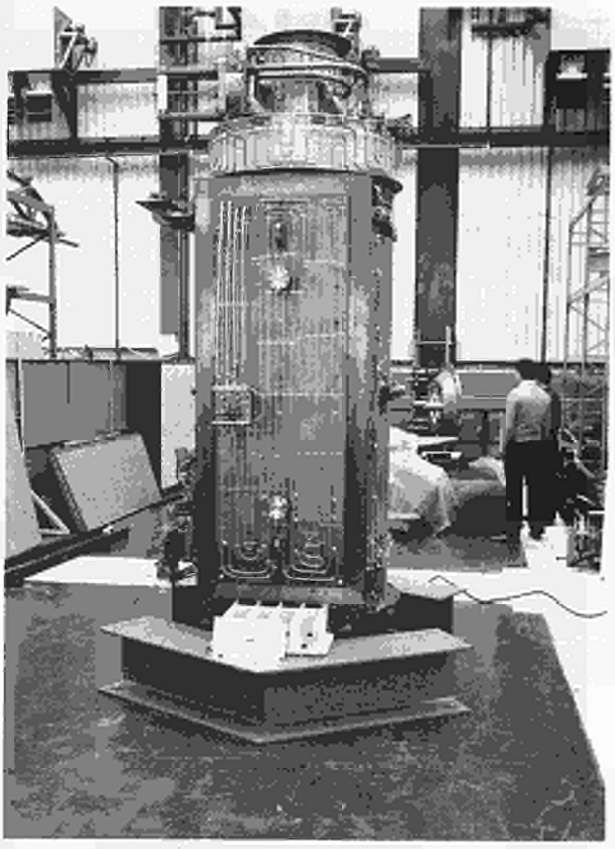

Fig. 22 Completed valve fitted with electrical heaters, but shown without thermal insulation.

Preparation for the active phase

(J. Hemmerich, E. Usselmann, T. Winkel)

Discussions with Fusion Technology Division on the conceptual design of the pumping system for tritium operation are underway. Basic choices on the use of the

existing turbopumps and on the design of the cryo-transfer pumps still need to be settled and will be important tasks for 1984.

First Wall Group

(K.J. Dietz, A. Boschi, J. Booth, K. Sonnenberg, H. Jensen, P. McCarthy, G. Israel)

The First Wall Group is responsible for the definition, design and procurement of the components of the first wall. This includes basic studies related to the use of new low-Z materials, the development of manufacturing technologies and the testing of materials and designs in an environment as close as possible to the environment existing in the JET machine. The Group also defines and implements wall conditioning techniques such as glow discharge cleaning combined with bake-out. In addition, the Group takes responsibility for the gas introduction system which comprises the gas handling system in the west wing of J1 and the introduction modules in the Torus Hall.

Wall conditioning

(A. Boschi, H. Jensen, P. McCarthy)

From October to December, the wall conditioning procedures regularly followed were bake-out assisted by glow discharges. Five days before plasma operation, a bake-out cycle was started by raising the temperature of the ports and the vessel walls to 200° C and 300° C, respectively, in approximately 30 hours. At these temperatures, the pressure took typically 24 hours to settle and then a glow discharge was switched on. Glow discharge was assisted by RF power to allow for a lower pressure during cleaning and therefore a higher removal rate of impurities could be achieved. The typical pressure during glow discharge was 5.10^{-3} mbar. Glow discharge cleaning was maintained for 3 days before plasma operation. This resulted in barely detectable (less than 10^{-9} mbar partial pressure) impurity levels measured with the residual gas analyser, (the only impurities observed were CH_4, H_2O and C_2H_4/CO). The temperatures of the vessel and the ports were reduced to 100° C or 200°, and maintained at this level for the week of plasma operation. Further glow discharges were carried out every night between operational sessions to remove impurities due to leaks or those generated during the discharges.

These procedures have been successful, in that low loop voltage discharges have been achieved, and reasonable reproducibility of discharges have been observed. It has also been demonstrated that these procedures were effective in re-establishing conditions leading to good quality plasma discharges very shortly after opening the vacuum vessel. In November, the vessel was vented due to a window breakage, but after only 3 days of glow discharge cleaning at elevated temperatures, plasma operation was successfully resumed.

During the whole period, the residual gas analyser was operational and proved to be a powerful tool for leak testing, for assessing the effectiveness of wall conditioning procedures and for evaluating the release of impurities after each disruptive shot.

Gas introduction system

(A. Boschi, H. Jensen, P. McCarthy)

The gas introduction system, with two introduction modules at Octants 2 and 6, worked reliably from October to December. The fast valve, which provided a gas pulse by opening a calibrated reservoir, had operated since June 1983 but the dosing valves for preprogrammed filling were commissioned and became computer controlled only by the end of November. This represented an important step in the JET operation, as the gas feed, and as a consequence, the plasma density, could be better controlled. In particular, this helped in achieving a smooth termination of pulses.

Some desirable improvements in the functioning of these dosing valves were identified. In particular, vibrations will need to be damped and the linearity of the response improved.

Operation of the limiters

(G. Israel)

During July to November 1983, four carbon limiters only were used. At that time, the nickel-clad limiters were not water cooled and were retracted 10 cm behind the line of the carbon limiters. During discharges, one of the four carbon limiters was viewed by an infrared camera. There were some indications of arcing especially during the early phases of operation, but later this ceased to be as frequent and some limiter surface heating was observed. The surface temperature never rose above 500° C.

No attempt was made to test the nickel-clad limiters due to the satisfactory behaviour of the carbon limiters and due to lack of time to investigate and compare results of the different types of limiters. In addition, some leaks opened up between the main vacuum and the water cooling circuits of three of the limiters and these circuits have now been blanked off and pumped down. The leaks were probably due to a metallurgical problem and the leaky limiters will be dismantled during the shut-down period in 1984.

Belt limiters

(J. Booth)

A new concept of belt limiters was developed, which consisted of two toroidal rings above and below the equatorial plane, with the RF heating antennae placed between them. Each ring is composed of 16 sections to allow remote replacement, and is made up of water cooling pipes with cooling fins welded to the pipes. The limiter plates are inserted between the fins and thus are radiation cooled. This design is attractive because of the simplicity of the water circuit and the absence of critical thermal stresses. Also the limiter plates can be easily exchanged and replaced with different materials. At the end of the year, the detailed design and technical specifications of the water cooling structure was completed and a call for tender should be sent out, early in 1984.

Use of beryllium
(K.J. Dietz, K. Sonnenberg)
Beryllium promises a number of distinct advantages compared with graphite, and its use is seriously contemplated following encouraging results of preliminary investigations and tests. The health hazard presented by beryllium has been discussed with one of the main beryllium manufacturers and with establishments experienced in processing and machining the material. Safety rules are well established and their application to JET should not represent a major difficulty.

A contract was placed to run a small tokamak at the University of Dusseldorf with beryllium limiters. The results were encouraging as radiatiion due to high-Z metallic impurities was dramatically reduced following introduction of beryllium limiters. A further contract was placed with Oak Ridge National Laboratory (USA) to operate the ISX-B tokamak with beryllium limiters.

A study contract with Euratom-IPP Association, IPP, Garching was placed to find more systematic and reliable data on sputtering and the retention of hydrogen implanted in beryllium. This data is available but mostly for irradiation at room temperature. The aim of the contract is to extend the parameters such as the sample temperature, flux density and fluence of hydrogen to a range more relevant to JET.

Actively cooled limiters
(K. Sonnenberg)
The development of actively cooled limiters using a hypervapotron cooling structure is important as an alternative, in case the radiation cooled belt limiters prove inadequate for the maximum JET heating powers. The development of a hypervapotron structure made of a Cu:Cr:Zr alloy and plated with beryllium tiles has started. Investment casting has been studied for the production of the hypervapotron structure and first test samples exhibited mechanical properties close to the optimum values for Cu:Cr:Zn alloys. For plating with beryllium, the following techniques will be investigated: vacuum brazing; solid state bonding with intermediate silver layer; plasma spraying of beryllium; electroplating of the cooling structure onto the beryllium tiles; and explosive welding. First results of brazing tests show that this technique can be used but the properties of the Cu:Cr:Zr alloy are somewhat degraded. Solid state bonding and explosive welding do not present this disadvantage but are far less developed. Contracts to study these techniques will be placed. Preliminary tests were also performed to investigate plasma spraying and electroplating.

Future Work
In 1984, the operational duties of wall conditioning and plasma operation will continue to take up most of the Division's resources. Three machine shut-downs are planned in 1984 and the two in January and September are major ones, during which significant assembly work will be carried out on the machine and inside the vacuum vessel, in which the Division will be heavily involved. In January, new diagnostics and the rotary valve will be installed on the ports of the vacuum vessel, and the faulty nickel limiters will be dismantled for inspection and repair. In September, the first neutral injection box will be connected at Octant 8 and the two A_0 RF antennae will be fitted.

In addition to operational duties and assembly work, new systems will be designed, procured and commissioned, as follows:

- The plasma current control system will be commissioned;
- The Personnel Safety and Access Control system will be completed and integrated with CODAS and CISS;
- The machine instrumentation and safety systems (DMSS) will be fully commissioned and the associated level 2 and 1 software will be implemented;
- The first SF_6 tower will be delivered and installed;
- Manufacturing contracts for the belt limiters and graphite protection plates will be placed. Contracts for the study of beryllium limiters (ISB-X) and the development of actively cooled limiters will be placed;
- Investigations on a magnetic limiter configuration with a double null using the PF coils No. 3 and No. 2 as dipoles will start;
- The gas introduction system will be improved and completed with the assembly of the last two modules;
- The study of a vacuum pumping system compatible with tritium operation will commence.

Power Supply Division

(Division Head: E. Bertolini)
Power Supply Division is responsible for the design, installation, operation, maintenance and modification of all the power supply equipment needed by the Project. The main JET Power Supplies System, its schematics, principal characteristics and design performance have been described in some detail in previous Annual Reports (EUR-JET-A4 and EUR-JET-A5).

During 1983, the work of the Division comprised four main subjects:

- Commissioning of the JET power supplies ready for generation of the first plasma, and their subsequent operation during the second part of the year.
- Installation of the second set of controlled rectifier power supplies to complete the Phase 1 JET programme during 1984.
- Partial installation and early commissioning of power supplies for the Neutral Injection test bed and the first Neutral Injection System due to provide 5 MW to the JET plasma towards the end of 1984.

- Contract handling for the procurement of equipment to supply the second Neutral Injection System, and of the power supply equipment for the first 9MW of Radio Frequency Heating.

Table III presents the status of contracts on the procurement of the major Power Supply Components at the end of 1983.

Table III
Status of Procurement of Major Power Supply Subsystems

Status			Subsystem
CONTRACTS PLACED	Completed and in Operation	1	Flywheel Generators and AC/DC Convertors.
		2	Toroidal AC/DC (TF1).
		3	Poloidal Vertical Field Amplifiers (PVFA 1,2).
		4	Ohmic Heating Circuit Main Breakers.
		5	Ohmic Heating Circuit Capacitor Banks
		6	Poloidal Radial Field Amplifiers (PRFA 1,2).
		7	Ohmic Heating Circuit.
		8	Glow Discharge Cleaning.
		9	Toroidal and Poloidal Busbars.
		10	Vacuum Vessel Port Heating Power Control.
	Procurement, Installation and Commissioning	11	PINI HV Power Supply and Protection (Mod 1–5).
		12	PINI Auxiliary Power Supplies (Mod 1–5).
		13	PINI HV Transmission Lines (Mod 1–5).
		14	PINI Snubbers (Mod 1–5).
		15	PINI SF_6 Tower (First).
	Installed, and Commissioning	16	11 kV, 33 kV Distribution.
		17	415 V Distribution.
		18	Toroidal AC/DC Convertors (TF2).
		19	Poloidal Vertical Field Amplifiers (PVFA 3, 4).
	Manufactured, and being Installed	20	Third 400 kV/33 kV Transformer.
		21	33 kV Distribution Extension.
		22	Poloidal Radial Field Amplifier (PRFA 3, 4).
		23	PINI HV Power Supply and Protection (Mod 6–9).
	Early Phase of Procurement	24	PINI Auxiliary Power Supplies (Mod 6–9)
		25	PINI Transmission Lines (Mod 6–9).
		26	PINI Snubbers (Mod 6–9).
		27	PINI SF_6 Tower (Second).
		28	RF AC/DC Power Supplies.
		29	RF Preionisation Unit.
Design		30	RF Auxiliary Power Supplies.

During the second part of 1983, the organisational transition from the "Construction Phase" to the "Operation and Development Phase" took place progressively. There are now four Groups in the Division:
(i) Power Distribution; (ii) Toroidal and Poloidal Power Supplies; (iii) Additional Heating Power Supplies; and (iv) Operation and Further Development. The present organisation appears as a natural and rational evolution, leading to a more homogenous task sharing. All AC power supplies and distributions are now the responsibility of Group (i); the pulsed DC magnet power supplies are the responsiblity of Group (ii); Group (iii) looks after all additional heating power supplies; while Group (iv) is a new one and is involved in the Operation of JET and in development required to better match the power supplies to the evolution of JET requirements.

At the end of the Construction Phase, a number of key staff left the Division and returned to their parent organisations. This was unfortunate since it occurred during a year when the workload was very heavy and the replacement of such experienced staff has proved extremely difficult.

Power Distribution
(J. Paillère)

400kV/33kV Substation and Distribution
(J. Paillère, G. Murphy, N. Walker, G. Wilson, D. Halliwell)

To add a third transformer, a new busbar/isolator connection must be installed in the 400kV substation compound. The manufacturing work is underway and the installation should be completed by the beginning of 1985. The third 400kV/33kV transformer has been manufactured and has undergone successful factory tests. Most of the equipment (i.e. 13 breakers, 3 spare cubicles, cables and disconnectors) for the planned extension of the 33kV switchgear, is on site and should be installed by June 1984, subject to the availability of the J5 building extension (see Fig. 23).

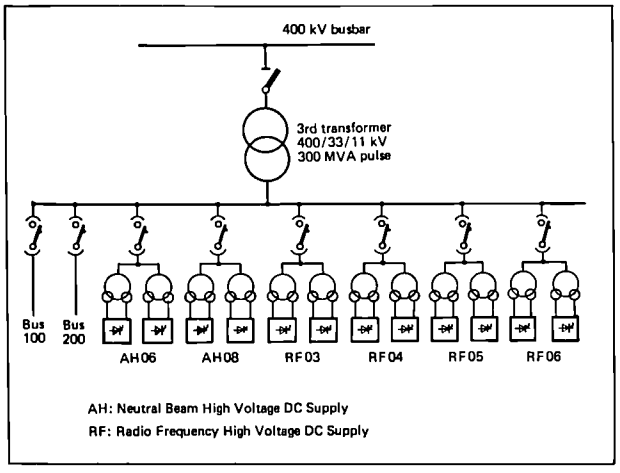

Fig. 23 400/33kV Substation Extension.

This equipment will be used for the pulsed power supplies and is needed for the connection of the additional AC/DC convertors to the grid, required for the implementation of subsequent phases of the JET experimental programme.

11kV and 415V Distributions
(J. Paillère, L. Zannelli, N. Walker, G.P. Marcon)
The 11kV Distribution is now completed and has the capability to meet all foreseen extensions. The previous contract for the 415V Distribution has been extended to cover new section and distribution boards for diagnostics and a 40kW uninterruptible power supply. Further extensions might be required, when and if new diagnostics and/or auxiliary equipment are installed.

Cabling to JET
(J. Paillère, A. Terrington, L. Zannelli)
The second stage of work was started by the main electrical contractor on cabling and cable trunking in the Torus Hall and Basement.

Pulsed Power Supplies for JET Coils

Flywheel Generator Convertor (FGC) Systems
(K. Selin, M. Huart, O. Buc, J. Goff, A. Skinstad)
The period January–May was dedicated to the completion and the commissioning of the two FGC systems ready for operation in June 1983. The commissioning was performed in successive steps to ensure full integration of all auxiliaries and of each FGC system into the Power Supply System. Due to its complexity, each FGC system was subdivided into several sybsystems such as driving, braking, excitation, lubrication, etc.

Following the commissioning of common services (such as 110V DC and 415V AC distribution, 11kV AC distribution, the programmable logic controller and data logger), these subsystems were first tested with only the control power energised. Each subsystem was then tested by checking the system performance against design data. Upon completion of all functional and system tests, the subsystems were then integrated in the first level of co-ordinated control (using the programmable logic controller). This integration was performed in successive phases.

Initially, with the main 11kV power supply disconnected and the generator speed simulated, all programme sequences of control were tested, in order to check the co-ordinated operation of all auxiliaries, switches etc., required for running the complete FGC system. The following phases commissioned and integrated the speed regulation, successively increasing the speed and rotor current regulation up to operational speed.

Following the balancing of the generator rotor, the excitation system, including the voltage regulator, was then integrated and commissioned on open-circuit. In the last phase, the AC/DC convertors were integrated into the FGC system, which was then in turn ready for the main electromechanical tests. These tests were subdivided into two classes depending on whether or not they required the JET load. The tests performed without JET load included: the open-circuit characteristic; the three-phase short-circuit characteristic; the steady line-to-line short-circuit test; the field switching test; the open-circuit core loss and short-circuit load loss tests; and the thermal cycling test.

Finally, the poloidal field FGC was connected to the ohmic-heating circuit for the commissioning on-load of the switching network (the load consisting of a prototype JET ohmic heating coil) and the toroidal field FGC was connected to the JET coils for the commissioning of the voltage and current regulator.

By the end of May 1983, the following performance on load had been achieved:

- Interruption of current up to 40kA in the ohmic heating circuit (dummy load).
- Toroidal field current pulse up to 40kA and energy up to 1200MJ.

The period June–December was dedicated to plasma operation and continuation of the integrated commissioning of the poloidal and toroidal field power supply.

By the end of December 1983, the following performance on the JET load was achieved:

- Peak poloidal field generator current at the end of JET Pulse: 79kA.
- Toroidal field current pulse up to 53kA for 10s flat-top with the series operation of the FGC and one toroidal field static unit.
- Maximum output from the toroidal field generator: 2000MJ.

Consideration of thrust bearing temperature limited the available output energy of the toroidal field FGC system (design 2600MJ) but the thrust bearing will be modified during the winter shutdown to resolve this problem.

AC/DC Thyristor Convertors
(K. Selin, M. Huart, D. Corbyn, L. Mears)
The toroidal controlled rectifier system is made up of two units TF1 and TF2. The first unit was fully commissioned during early 1983, with power tests initially using a resistive dummy load and subsequently with the JET toroidal coils. Load currents up to 53kA (maximum value 67kA) were supplied for several seconds. Short-circuit tests were also performed with currents in excess of 100kA. Voltage or current control were fully tested, together with the fault detection and protection circuits, first locally and then remotely via CODAS.

The poloidal controlled rectifier system comprises the vertical field amplifiers, PVFA, to control the plasma position in the horizontal direction and the radial field amplifiers, PRFA, to control the vertical plasma position. The first stages were commissioned during the Spring, following procedures similar to those for the toroidal unit. In the rectifier bridges of the TF and PVFA units, there are a number of thyristors in each branch and, therefore, the current sharing levels when connected in parallel were checked, and showed deviations less than 10%, which was considered acceptable.

Ohmic Heating (O.H.) circuit

(P.L. Mondino, A. Stella, C. Raymond, T. Eriksson, E. Daly, P. Doidge)

Components of the O.H. circuit were delivered late, so installation on site and site tests were organised within a very tight schedule. Two groups of site tests were performed late in the day after the end of the installation shift. The first, under the Supplier's responsibility consisted mainly of insulation and commissioning tests. The second group (Integrated Tests) was performed under JET responsibility with the manufacturing companies technical staff present. A carefully defined Test Procedure, prepared in advance, proved to be essential for performing the tests in a logical way. The test procedure, with associated safety assessment, was approved jointly in advance.

The integrated tests were arranged in four steps, as described below (see Fig. 24):

- Switching Network Test: The first level of integration was performed within the Switching Network while both busbars were left open at both sides (Generator Convertor and Poloidal Field Coils side). First one and then the other Commutating Capacitors, C2a and C2b (max. 375kJ) were discharged, triggering the relevant Commutating Start Switches 53a and 53b, respectively. Several (19) different circuit configurations were established with the main aim of testing the various components at peak currents (up to 120kA) and at peak voltages (25kV). For the first time, it was possible to apply 20kV across the Nonlinear and Commutating Resistors. Then, both terminals of the Commutating Capacitors were left floating and a peak current was passed through the commutating resistors (35kA) and the nonlinear resistor (3kA).
- OH Circuit Test: In the second stage the OH Circuit was supplied by the PFGC (at reduced speed of 150rpm, available energy 1500MJ, peak power available 200MW). Again several (9) different circuit configurations were connected, with the aim of performing current and temperature rise tests on the various components and busbars. It was shown that the PFGC could deliver 80kA through the busbars and the closed Reversing Make Switches S4 (the Reversing Polarity Arrangement providing a short circuit at the PF coil side). The commutating resistors (with normal configuration: $R_3 = 0.6\Omega$, $R_4 = 0.6\Omega$) were tested up to nominal energy dissipation in 20s every ten minutes for six pulses: steady state conditions were reached during pulses 5 and 6.
- OH Circuit Test with Dummy Load: The prototype coil (L=9.4mH, R=3.2mΩ, I=40kA, V=20kV) of the Magnetising Coils was then connected at the PF Coil side aimed at producing the artificial zero

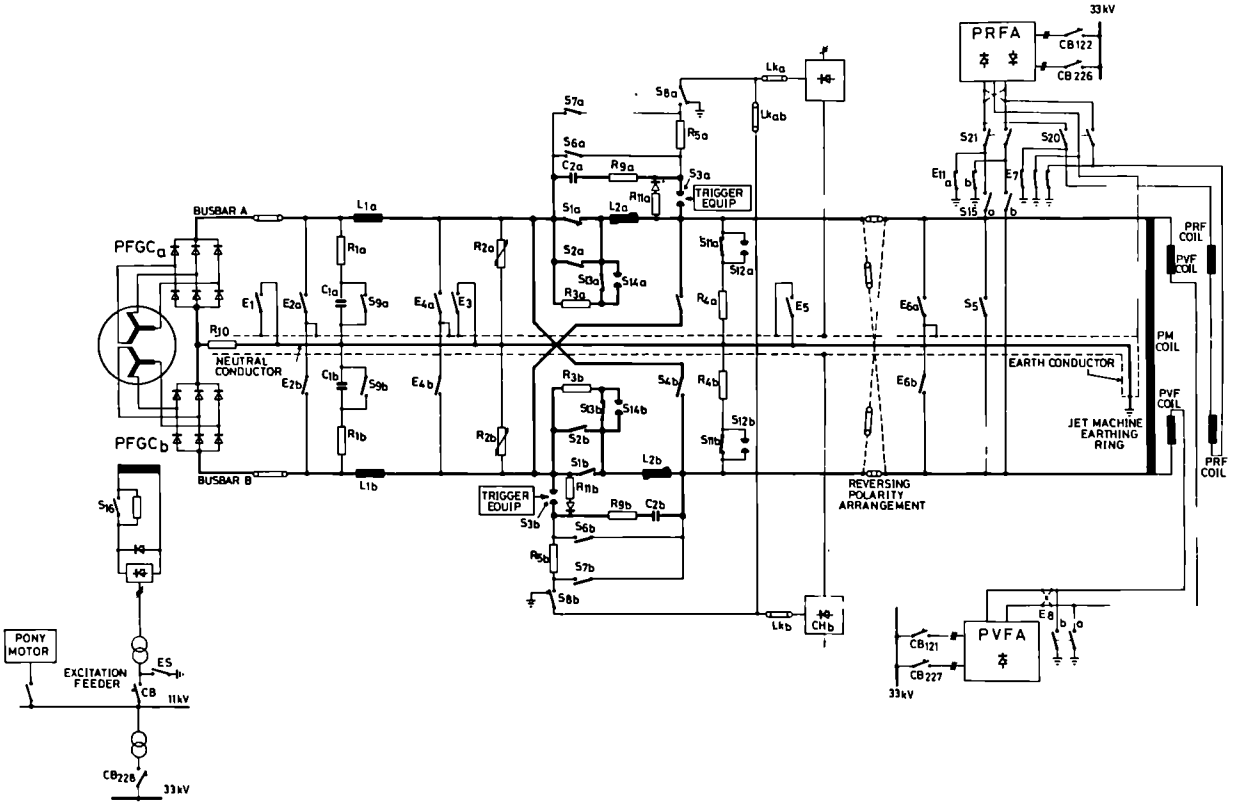

Fig. 24 Ohmic Heating Circuit complete.

of current through the Circuit Breakers S1. At the beginning of this test session, a temporary connection between the prototype coil terminals and the busbars failed mechanically at approximately 20kA. An earth fault developed causing current higher than 5kA to flow in the neutral conductor and the Fast Protective Action de-excited the PFGC. No serious damage occurred, the connection was quickly rebuilt and the tests continued. For different values of Premagnetisation Current (10, 20, 30, 40kA), the most convenient setting of the Saturable Inductors L2 and the corresponding values of the charging voltage of the commutating capacitors C2 were determined. The Circuit Breakers were then tripped synchronously, successfully interrupting the current and causing a peak voltage up to 18kV across the Dummy Load.

- OH Circuit Test with PF Coil: Finally, the PF Coils were connected to the OH Circuit on one side and to the PVFA on the other and the Radial Field Coils were short-circuited. These tests were performed one week before "Day 1". Due to time limitations, the following procedure was adopted: with the circuit configuration of premagnetisation (S1 closed S4 open) the PFGC delivered current pulses (≅ 3s) to the Magnetising Coils. The current was increased in steps to 10kA, then the artificial zero of current was produced in S1 (using the parameters identified during previous test sessions). Finally at the third step, the Circuit Breakers S1 were opened starting the Fast Rise. The same sequence was then repeated increasing the premagnetisation current in steps (15, 20, 30kA), and the peak voltage across the PF Coils increased accordingly.

Comments on the Commissioning

Commissioning of the Power Supplies for Ohmic Heating had to be performed in a time much shorter than planned, due to late delivery of some key power supply components. However, the operation was achieved successfully, allowing JET to start according to plans. Nevertheless, some difficulties were encountered and some technical incidents occurred. A flashover took place on one of the PRFA subsystems during 33kV switching due to the failure of one component (incorrectly specified) of the thyristor protective snubber. A short-circuit occurred between the connections of the dummy load, due to incorrect electromechanical design of the connections themselves. In operation in December (pulse #1179), one of the ohmic heating circuit main protection make switches was damaged in its concrete circuit breaker enclosure due to an internal flashover. Although a fully satisfactory explanation is not yet available, it is most likely that damage to the wall of the switch chamber (made of insulating material) had been caused by the frequent interruptions of the poloidal generator remanence current, which was shown to be much larger (several hundred amperes) than expected from the generator design. Since no additional damage resulted, the make switch was replaced.

A number of difficulties were encountered during installation and commissioning of the two flywheel generators, which led to modifications of the liquid rheostats and correction of insulation breakdown at two locations in the rotor pole field windings. The problem was that the unbalanced magnetic pull on the pony motor was excessive and prevented acceleration of the rotor system. This was resolved by adding crosslinks between two parallel stator windings of the pony motor to reduce the pull. In this way, opposite pole groups took up the same voltage producing identical flux with virtually no unbalance in the magnetic pull.

The power supply commissioning continued during the second half of the year by arranging, according to needs, a sequence of commissioning and operating weeks. The operating performance achieved is compared with the power supply capabilities in Table IV. The voltage needed for breakdown and plasma formation were much lower (6kV, equivalent to a loop voltage of approximately 20V) than the capability of the ohmic heating circuit switching network (40kV).

During 1983, only glow discharge cleaning was used to condition the vacuum vessel. However, the working conditions of the pulse discharge cleaning were defined experimentally, through a series of discharges where the TF unit was used to produce a continuous toroidal magnetic field of less than 0.2T, the PRFA unit was used to produce plasma breakdown and build up the plasma current, with a loop voltage less than 10V and the PVFA unit was for plasma position control.

Power Supplies for Extended Machine Performance

Toroidal Field Enhancement

The extension to full performance required enhancement of the capability of the Power Supplies. Therefore, following approval by the JET Council, the second stage of contracts has been released and some of the equipment needed during the second part of 1984 is ready for commissioning. The first unit to be ready will be TF2, so that toroidal fields up to 3.5T can be obtained.

Table IV
Summary data of performance of Magnet Power Supplies
JET Operation as compared with design performance
(in brackets)

Subsystem	DC Voltage (kV)	DC Current (kA)	Pulse Length (s)
FGC_T	5 (9)	40 (67)	10 (20)
TF_1	2 (2)	25 (67)	10 (20)
$FGC_T + TF_1$	7 (11)	53 (67)	5 (20)
FGC_p	5	40 (67)	5 (20)
OHC	18 (40)	40 (80)	5 (20)
$PVFA_1$	±2 (±2.3)	2.5 (25)	5 (20)
$PRFA_1$	±0.5 (±2.3)	±1.0 (±2.0)	5 (20)

The FGC_p can give 100kA for 5s.

Additional Heating Power Supplies

The procurement of the power supplies for the two additional heating methods are at different stages of development. Commissioning on site has started of the Neutral Injector Power Supplies for the Neutral Injection Test-Bed, whereas the Radio Frequency AC/DC Power Supplies are in the early stages of manufacture.

Neutral Injection (NI) Power Supplies

(P.L. Mondino, R. Claesen, T. Dobbing, U. Baur, A. Eyrard, R. Perez-Taussac, A. Paynter, H. Fielding)

Phase 1 of NI heating requires installation of five complete power supply modules – to serve two beam sources (PINI's) each – one of them being used for PINI testing purposes at the test-bed in the Hot Cell.

The complete PINI supply is made up of several components, for which different contracts were awarded during previous years. The overall structure of the PINI power supplies was described in the 1981 Annual Report (EUR-JET-AR4). The main components for the accelerating grid supply are: the Outdoor Power Supply rectifying the 33kV AC voltage into 95kV DC; the Protection System stabilising the 95kV DC into ripple free 80kV DC, giving fast turn-on, and providing the fast turn-off of this 80kV DC in case of breakdown in the PINI's themselves; the Transmission Lines for transporting the 80kV to the PINI's; and the snubbers to dump the capacitive energy of the transmission line in the event of a PINI breakdown.

The Auxiliary Power Supplies contain the arc supply and the filament supply for the PINI plasma source, the grid 2 and grid 3 supplies, and the bias supply for the snubbers. The supply for the bending magnet inside the NI box completed the total of the supplies necessary for the Neutral Injection System.

A set of transmission lines insulated in SF_6 carry the power from the J1 North Wing where the indoor power supplies are installed (HV modulators and auxiliary power supplies) to the Neutral Injector box in the Torus Hall. The interface between the injectors and the transmission lines is the SF_6 Tower, which will house the snubbers, provide the isolation for the cooling of the PINI's and will contain different HV components to activate the PINI's.

During 1983, the components for the 8 outdoor power supplies were delivered to site. The installation of the first five power supplies was completed, while numbers 6, 7 and 8 should be finished during the first half of 1984. The site acceptance tests of the first 3 power supplies were successfully completed and tests of the next two have started. The installation of the first protection system in the hot cell was completed and acceptance tests are in progress. The first unit of the auxiliary power supplies was installed. Tests with the dummy load have been undertaken and filament and arc tests with the PINI arc load are in progress. The integrated tests involving the power supply, the protection system in the hot cell and the first auxiliary power supply have started and are due for completion during January 1984. During 1983, modules 2 and 3 of the protection system were successfully tested in the factory. Installation on site of module 2 is completed and testing has started.

Figs. 25, 26(a) and 26(b) show a cross-section and two different views of a transmission line, of which the length of each is approximately 85 m. Since a voltage of 160kV DC will be required at a later stage for Deuterium operation, it was imperative for the line to have a capacitance as low as possible in order to minimise the size of the snubber required to dump the capacitive energy contained in the line in case of PINI breakdown. On the other hand, restrictions were placed on the maximum dimensions of the line due to lack of space. For these reasons, a co-axial line pressurised with SF_6 was chosen to withstand the maximum voltage of 160kV between inner and outer conductor. the outer conductor of the transmission lines is connected to the SF_6 tower which is completely isolated from local earth and is connected to the JET machine. This necessitates an insulated installation of the lines over the total length. The inner conductor encloses all the feed cables linking the PINI's with the filament, the arc and the Grid 2 supply, as well as the bias supply cable for the snubber.

All these supplies were referenced to the Grid 1 supply voltage of the inner conductor in this way limiting the requirements on their insulation level and the stray capacitance to earth to a minimum. Manufacture of eight lines is almost complete and factory acceptance tests are in progress, while the first four lines have been delivered on site.

The detailed design of the snubber was completed in early 1983. An active (biased) snubber was chosen as this minimised the space required because of the larger available flux swing. The construction of all the cores and other components was finished and tested successfully in the factory. The assembly of snubbers will start in January 1984, in time for the acceptance tests and installation of the SF_6 Tower.

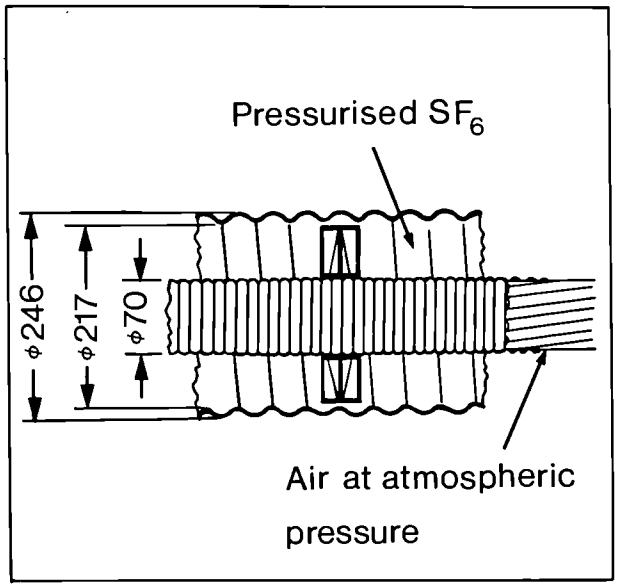

Fig. 25 Cross-section schematic of transmission line (PINI).

Fig. 26(a) Photograph of transmission line (PINI).

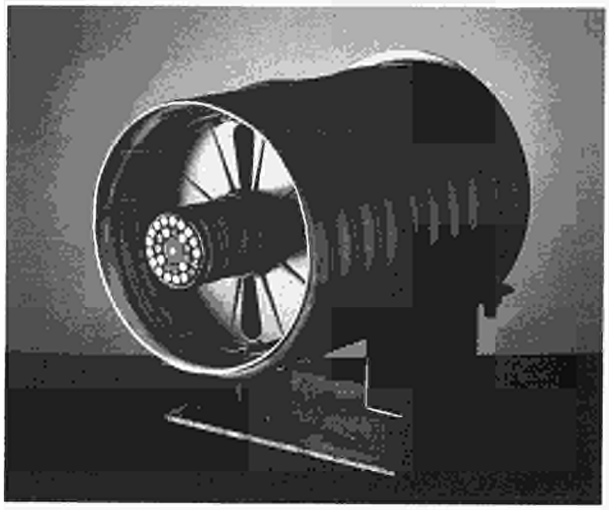

Fig. 26(b) Photograph of transmission line (PINI).

The first SF_6 tower is in the late stage of manufacture and related work on the mechanical aspects is being performed in cooperation with the Torus Division and Neutral Beam Heating Division.

Radio Frequency Heating Power Supplies
(R. Claesen, C. Christodoulopoulos)

The power supplies for RF heating can be divided into three parts: the power supply for the preionisation generator, the auxiliary and the main power supplies for the RF generators.

The call for tender for the preionisation generator power supply was issued in May, and the contract was placed in August 1983. This power supply has a fixed DC voltage of approximately 10kV and a current capability of 60A. The manufacture of the main components is finished and some of them have been factory tested. Final acceptance tests, delivery and installation are foreseen for early 1984.

The call for tender for the main power supplies for the RF generators was issued at the end of 1982. The offers were received in early 1983 and the contracts awarded in March 1983. The contract covers different stages in line with the RF generators. Released are four power supplies providing the DC power for eight RF generator units.

Fig. 27 shows how each power supply is connected to the 33kV AC distribution system and to the RF generators. Each power supply provides the DC power for the RF generators connected to one octant of the JET machine. It is fed from the 33kV busbar through one circuit breaker and two disconnectors. This provides the possibility of isolating each rectifier and filter circuit independently. At the DC output, each rectifier and filter circuit provides power through individual DC isolators and earth switches to two RF amplification chains.

Each of these chains needs a common-zero and a nominal 11kV for the driver tube and a nominal 22kV for the end tube.

One of the main features of the DC power supply is that the output voltage must be variable between 14–26.4kV for the 22kV nominal output and between 7–13.2kV for the 11kV nominal output, even under full-load conditions, in order to minimise the power dissipated in the RF generator tetrode over the full operating range while maximising the RF output power of the generator.

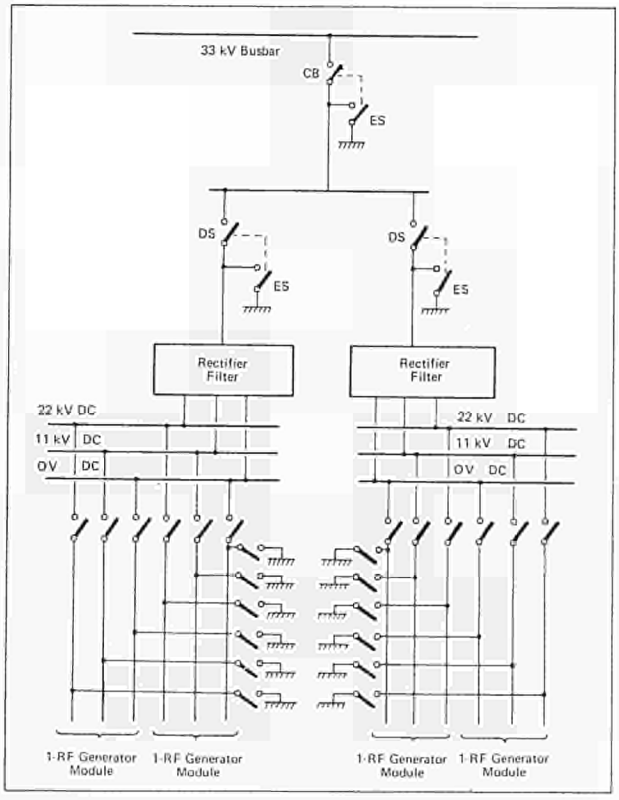

Fig. 27 Schematic of RF Power Supplies (1).

Each rectifier and filter circuit of Fig. 27 consists of two circuits, as shown in Fig. 28, which are connected in series on the DC side. This circuit was selected both for its performance and cost. The output voltage is variable between 7kV and 13.2kV. The 33kV is transformed down to approximately 1kV by means of the matching transformer.

At this level, the output DC voltage is regulated on the AC side by means of the thyristor bridge in the star point of the rectifier transformer. The inductance on the DC side of this bridge provides part of the filtering, while the precharging circuits serve the purpose of pre-loading this inductance every time the RF generator is taking power at the beginning of the JET pulse. The rectifier transformer brings the voltage to the required nominal level for the DC voltage. The filtering circuit is completed with the R and C elements in the DC output.

The reference design for the auxiliary power supplies for the RF generator is in progress. The call for tender will be issued and the contract will be placed in 1984. Installation and commissioning is foreseen for early 1985. Since a temporary supply is available, the first RF generators can be operated at any time.

Future Work and New Tasks

The Division's activities during 1984 will be devoted to the following main five tasks:

- The Operation of power supplies, both during plasma sessions and commissioning sessions, when the JET machine is used as a load. A main concern will be to improve power supply operation by completing, with CODAS, the commissioning to include alarm handling and "automatic" operation in preparing for the pulse.

  In addition, the commissioning of the two flywheel generators at full rotational speed should be completed and the new AC braking system will be fitted in order to allow a braking time of around 20 minutes from idling speed (half of the maximum speed).
- The follow-up of contracts for the extension to full performance, including factory tests, installation, testing and commissioning on the JET site. Most of this work will be related to additional heating and, during 1984, the first neutral injection box with its power supplies should be fitted to the JET machine. This should be a demanding task, in terms of technical and human resources.
- New designs on modifications suggested by the first months of JET operation. Among these are a modified ohmic heating circuit which should include features already included in the plans for extension to full performance, such as the energy recovery system, as well as a number of filters at the output of the toroidal and poloidal AC/DC power supplies in order to reduce the voltage ripple level seen by the JET coils.
- A new service for the Project, in the procurement and installation of all types of cables required for power, diagnostics, instrumentation, etc.
- A reassessment of the operating conditions of the 400kV high voltage line. During 1983, the pulse power taken directly from the mains did not exceed 120MW. In 1984, the 300MW level is likely to be reached, and, therefore, the data collected on voltage drop, reactive power demands and harmonic level should allow JET and CEGB to better define the pulse capability of the grid, when the upper limit of about 600MW is approached. This should permit detailed design of such equipment as harmonic filters and reactive power compensators, if required.

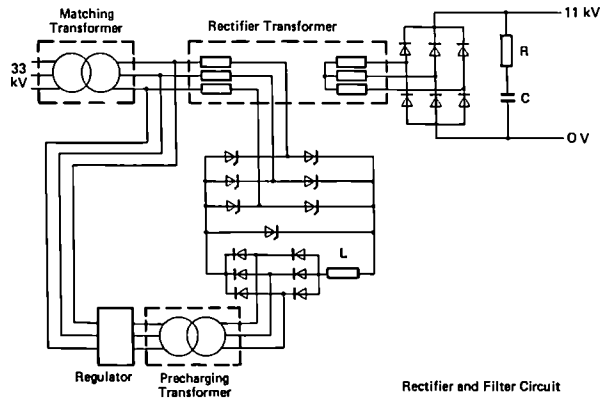

Fig. 28 Schematic of RF Power Supplies (2).

Control & Data Acquisition System (CODAS) Division

(Division Head: F. Bombi)

The Control and Data Acquisition System (CODAS) Division is responsible for the implementation, upgrading and operation of the computer based control and data acquisition system for JET. During 1983, the Division underwent a major reorganisation following completion of the Construction Phase and start of the Operations Phase.

The Division is now structured in four groups as follows:

(i) The Computer Operations Group, which is responsible for the procurement and operation of the computer network.

(ii) The Computers and Control Group, which is responsible for the control subsystems and of overall software development coordination.

(iii) Diagnostic Data Acquisition Group which is responsible for diagnostic subsystems and for the acquisition software.

(iv) The Electronics and Instrumentation Group, which is responsible for the Division's electronics and for a number of auxiliary systems.

The first half of the year was devoted to completion start-up and to integration of the major software and hardware components required for the centralised operation of the JET device and its diagnostics. Although integration was compressed into a short period of time, CODAS was ready to provide a comprehensive data acquisition service and essential control functions from the first experimental pulse.

The June–July operation campaign highlighted some deficiencies in the control system and some minor faults in the software. Most of these were remedied during the August–September shutdown and, in parallel with operation, during the subsequent October–December operation period. During this phase, an impressive number of new services and systems were progressively brought into operation using a demanding two-week cycle in which commissioning of new equipment or modes of operation were interspersed with experimental periods.

In the second half of 1983, the start of operation caused a considerable increase in the divisional work load, without a corresponding increase in professional staff. New demands, related to operation and caused by a shift of responsibilities from other Divisions disbanded at the end of the Construction Phase, have been combined with steady procurement and installation work required by the extension to the full performance programme. At the end of the year, 64 CODAS staff were present on site; of which 33 were employed as permanent staff or as contractors blocking a staff post; 9 in the electronic maintenance pool; 9 computer and system operators, 11 in the software development teams; and 2 visiting scientists.

Computer Operations Group

(P.J. Card, G.P. Davis, R.K.F. Emery, D.I. Hardwick)

The Group was formed at the beginning of the year, with responsibility for operating the CODAS computer system, its supporting terminal and communication system, and quality assurance of operational software.

The CODAS computer system has been extended to 25 computers (see Table V and Fig. 29, which shows 22 computers linked together), which have been commissioned and integrated into the system network. These machines are installed in the J2 Control Building with the exceptions of one in the Electronics Laboratory for type approval and acceptance tests of CAMAC modules, and one in the computer room at UKAEA, Harwell to support the transport of experimental data to the Harwell IBM and CRAY computers.

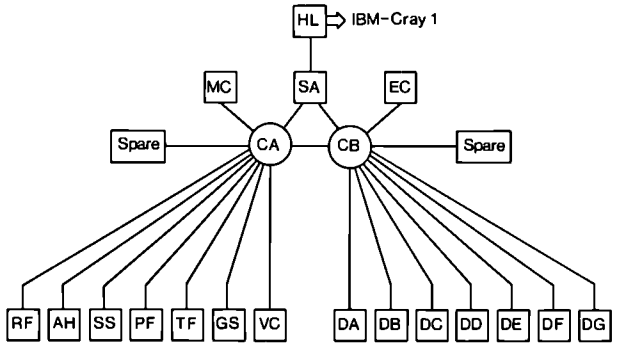

Fig. 29 JET CODAS Network.

Table V
CODAS Computers Configuration – End 1983

Subsystem	Model	Memory MByte	Disc MByte	Use
CB	100	.37	1 x 10	On-line
DA	520	1.25	2 x 75	On-line
DD	520	1.25	2 x 75	On-line
DC	520	1.25	2 x 75	On-line
EC	520	1.25	2 x 75	On-line
GS	100	.5	1 x 75	On-line
HL	100	.5	1 x 10	On-line
MC	100	.5	1 x 75	On-line
PF	100	.5	1 x 75	On-line
SA	560	1.25	2 x 288	On-line
SS	100	.5	1 x 75	On-line
TB	100	.5	1 x 75	On-line
TF	100	.5	1 x 75	On-line
VC	100	1.0	1 x 75	On-line
CA	100	.37	1 x 10	On-line spare
DB	520	1.25	2 x 75	GAP development
DF	520	1.25	1 x 288	Program development (diagnostics)
DG	520	1.25	2 x 75	Program development (diagnostics)
EL	100	.62	1 x 75	Electronic workshop
RH	100	.5	2 x 10	Program development (remote handling)
SB	100	.75	2 x 75	Stand-by (back-up and software)
			2 x 10 1 x 288	(integration)
TS	100	.75	1 x 75	Program development (CODAS)
YC	100	.5	1 x 75	CAMAC U-port testing
YD	100	.5	1 x 75	Program development (CODAS)
YE	100	.62	1 x 75	Drivers development

Note: YC and YD computers will be redeployed for Radio Frequency on-line and testbed subsystems.

Eight of these computers are 32-bit ND-500 series computers equipped with 1.25 M-bytes of main memory to support data acquisition and analysis of the diagnostic subsystems and fast presentation of results after each pulse. Following the start of operation, 14 computers have been placed "on-line" to their subsystems and form the basis for control and data acquisition for JET operation. This on-line network of machines has operated consistently and reliably, providing availability in excess of 99%. This high figure has been achieved by using a standby computer system which provided redundancy in case of faults on operational machines. The overall availability of the total computer system has been better than 98%, with the average availability of each individual computer system being better than the target 95%. A programme of work is continuing, in conjunction with Norsk Data, to further improve this availability.

The number of terminals attached to the computer system has been increased by the purchase of 66 Westward graphic terminals, including 13 with colour graphics and 13 high-resolution models. To provide better utilisation of terminals, a Gandalf terminal multiplexer has been installed to replace the former manual patching system. By dialogue with the terminal, a user can select any particular computer system required. It also facilitates control of access to "on-line" subsystems with the use of passwords. A line concentrator has been installed to merge messages produced by the error device of each computer into few streams of data to be routed to a single terminal and/or to a printer. This arrangement will permit monitoring of the complete network performance from a single point and the permanent logging of system errors and alarm messages. The pressure on terminal resources, particularly graphic terminals, has increased further, and additional graphics terminal will be purchased in 1984. Five Versatec hardcopy units were obtained to provide hardcopy of graphical results. However, operational experience has shown that these facilities were insufficient and, at the end of 1983, a laser printer/plotter was ordered to meet this demand.

A wide range of operational services have also been provided, such as routine archiving, file and manual library, software and system update and installation, system status monitoring, terminal and mobile console movement and installation, design provision of special communications cables, installation of modules and procurement of consumables.

In the early Operations Phase, insufficient effort was devoted to quality assurance and configuration control in relation to new software components. This is of paramount importance due to the need to introduce new services on short timescales and usually with limited integration time. A professional quality assurance specialist was recruited recently, who is now designing and adopting procedures and methods which should have an increasing impact, early in 1984.

Computer and Control Group

(M.L. Browne, T. Budd, J.L.G. Eveleigh, O.N. Hemming, R.F. Herzog, S.R. James, P.A. McCullen, G.D. Rhoden, C. Torelli, H. van der Beken, B.A. Wallender, F. Youhanaie, I.D. Young)

The main activites of 1983 were:

(a) Commissioning of subsystems required for the first operation of JET.

(b) Implementation and testing of the Level 2 software, permitting subsystem operation as a whole, as opposed to the operation of individual components, already provided by the Level 3 software.

(c) From June 1983, the control system was exposed to real life, and an important part of the Group's activities were devoted to operational support.

By the end of 1983, 15 computers were on-line, 14 computers controlling the JET device plus one on-line to the neutral injection test-bed, as shown in Fig. 29. The computers were as follows:

- The Machine Console subsystem (MC) supports countdown of the JET pulse, issues orders to the other subsystems and checks their readiness at each phase of countdown.
- The Experimental Console subsystem (EC) gathers a subset of the experimental data from the other subsystems and presents a synopsis of the results shortly after the pulse.
- The Poloidal Field subsystem (PF) controls the Central Timing System (CTS), the PF flywheel generator and convertor, the ohmic heating circuit, the poloidal vertical and radial field amplifiers, the plasma position and current feedback control circuitry and some of the torus instrumentation.
- The Toroidal Field subsystem (TF) controls the TF flywheel generator convertor, the static unit SU1, a large part of the torus instrumentation and the toroidal coils safety system.
- The Vacuum subystem (VC) controls gas handling, the gas introduction, all the torus pumping, the baking of the vessel and its attachments, the glow discharge cleaning and the torus vacuum instrumentation.
- The General Service subsystem (GS) controls all the pulsed power distribution (440 kV and 33 kV), the auxiliary power distribution (11 kV and 415 V), the cooling system (site water and demineralised water [Fig. 30]) and some auxiliary services.
- The Safety and Access subsystem (SS) at present covers only the radiological protection system.
- Three diagnostic subsystems (DA, DD, DC) cover the on-line diagnostic control and data acquisition.
- The Storage and Analysis subsystem (SA) archives all the JET pulse files, allows data analysis for large programs running on the 500 CPU and drives one end of the link to Harwell, where JET pulse files (JPF's) are processed on the IBM and CRAY computers.
- The Harwell subsystem (HL) is located near the IBM at Harwell (through a 14 km line) and handles the data transfer protocols through an IBM 2701

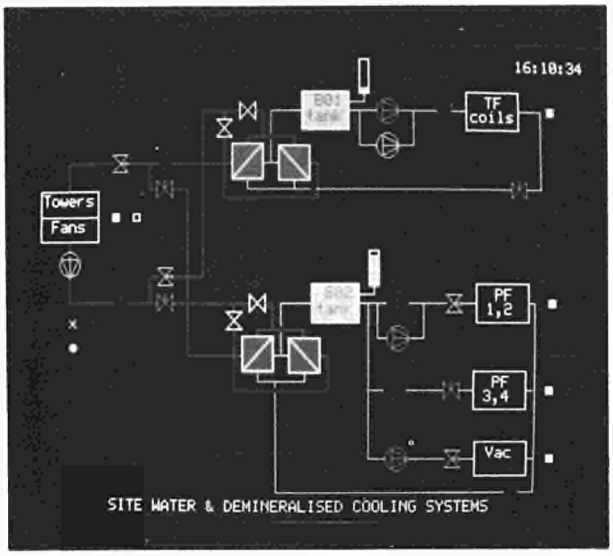

Fig. 30 Mimic of Site Water and Demineralised Cooling Systems.

control unit.

- One Communication computer (CB) handles the computer to computer communication for all on-line subsystems.
- One computer on-line with the Test Bed (TB) provides control and data acquisition to the neutral injector test facility.

The computer network was split during operation into two sections, to provide better protection of the on-line subsystems. The off-line network covers all computers used for program development and for commissioning of subsystems not yet fully operational.

JET operation, steered entirely from the J2 control rooms (Figs. 31, 32), is based on two classes of software: the pulse related package, mainly the general acquisition program (GAP) and specific application software in charge of local units, like the ohmic heating circuit or the gas introduction. GAP is used to preset all parameters of the machine, including the central timing system (CTS) and the reference waveform generators. Then, the pulse itself is driven only by the timers. After the pulse, GAP proceeds to the collection and archiving of the engineering and diagnostic data. The specific application software is in charge of all operations requiring sequencing and testing. Examples of this are the positioning of the ohmic heating switches, their presetting for opening or closure and the sequence of operation of the gas introduction valves system providing gas in the Torus for plasma breakdown.

The console software, which supports the 2 main consoles (EC and MC) and the subsystem consoles, is now complete. In order to use a console, a log-in process is required which implies positive vetting from Duty Officers. This vetting covers also all terminals attempting to log-in to an on-line subsystem through the terminal multiplexer.

Fig. 31 JET Machine Control Room Console with Synoptic view above.

Fig. 32 Machine Subsystems consoles in machine control room.

At the end of the year, the integration of major software components achieved is summarised below:

- The Plasma Fault Protection System (PFPS) is based on a program residing in a CAMAC auxiliary crate controller which checks the plasma quality and issues a soft termination request if a disruption is predicted.
- The Direct Magnet Safety System (DMSS) has been fully integrated in the TF and commissioned on the PF systems.
- The software to drive the Pulse Discharge Cleaning (PDC) has been commissioned and allowed to define the operating parameters.
- Alarm handling and reporting is now available and will be integrated early in 1984.
- Most of the CODAS "drivers" have been written, consisting of a set of re-entrant shared subroutines which mask from the user the idiosyncrasies of the CAMAC modules and permit him to concentrate on accessing process variables (input or output) by name.
- The electrical-baking software has been integrated to control about 70 electrical heaters regulating the temperature of the vessel and its various attachments during the baking phase;
- Various applications of the CAMAC auxiliary crate controller (CAC) have been integrated. These cover the control of three types of low-level multiplexer, control the data link to the flywheel generator convertors, control the data link to the high voltage power supplies for the neutral injector and its test-bed, control real-time waveform generators, and control the cameras for the in-vessel inspection system.

A basic problem in the communication software has prevented extensive usage of the computer-to-computer communication, but the problem has now been identified. A corrected version has been tested successfully and will be installed early in 1984.

Diagnostic Data Acquisition Group

(H.E. Clarke, E.M. Jones, E. Mathia, J. Saffert, C.A. Steed)

During the first half of the year, most effort was concentrated on integrating the data-acquisition software on the diagnostic subsystem computers, and in operation of the host link to the Harwell computers ready to start-up in June 1983.

Subsequently, work has continued in consolidating the reliable operation of the host link, in enhancing the data acquisition software to cover all subsystem computers and in extending the range of CODAS standard CAMAC modules which can be handled by the GAP software. In addition, during the latter half of the year, a substantial effort was devoted to supporting the Scientific Department in commissioning and testing various diagnostics, which were due for operation early in 1984.

Progress made during the year included graphic software and hardware support, leading to the selection and purchase of a laser printer/plotter for fast hardcopy output. Improved software support for the NORD 500

computers included provision for accessing JPF and IPF data direct from this computer.

Electronics and Instrumentation Group

(B.J. Brewerton, A.N. Cleaves, S.E. Dorling, K. Fullard, D.S. Nassi, J.P. Nijman, C.G. Pollard, V. Schmidt, J.E. van Montfoort, J.R. Watkins)

At the end of 1983, 65 CODAS interface cubicles had been installed, compared with only 25 installed (of which 8 had been commissioned), at the start of the year. This was achieved due to an intense period of cubicle specification, manufacture, installation and commissioning in the first half of the year, and ensured the availability of control and monitoring services from the control computers for JET operation.

Interface cubicles use a large complement of electronic modules, which vary in complexity from simple filters to powerful, compact microcomputers. The procurement and testing of these items has been a major task, but the value of the testing work was evident by the rapid commissioning time of the assembled cubicles' electronics prior to connection to the plant. Much of the testing work was carried out using computers. A program was written for each type of module, which exercised each module function many times. The tests were run at elevated temperatures or at high speed to reveal incipient faults.

Prior to commissioning of each cubicle, a connection was established to the centrally located computers. In CODAS, fibre-optic connections have been used and have proved particularly successful. Their high performance was of especial value during cubicle commissioning as all cubicles related to one computer (typically 6) were connected in a chain to form a large loop. At any one time, with many cubicles not yet commissioned, the loop was required to operate with many temporary joints and without the benefit of the optical repeaters in the cubicle.

When JET became operational in mid-year, emphasis shifted towards keeping the commissioned systems working and to making adjustments to the control and monitoring services in order to keep them in line with increasing knowledge of JET performance and its auxiliaries. The number of hardware failures were small, considering the large amount of untried equipment. Most problems occurred at the interface with the controlled equipment, reflecting the difficulty of communicating detailed information between design organisations.

An electronics maintenance team was established in April, sufficiently early for its members to be involved in the commissioning work, which provided a good opportunity to acquire knowledge of the plant and its modules. The number of types of modules delivered to JET are listed in Table VI. Most of these have been installed and are tended by the maintenance team, both in a scheduled way and by intervention in case of suspected failures.

In the second half of the year, further consoles were added in the control rooms. This expansion reflected the difficulty of releasing mobile consoles from plant commissioning work for use in their planned secondary role in the control rooms. There was also an increased use of computer terminals in control console functions. A large uniform console framework was built in each control room but flexibility was retained by using a design which could house a full console function or a simple computer terminal.

Table VI
Summary of Interface Electronic Components

	Delivered at	
	14.12.83	14.12.82
CAMAC crates	146	74
CAMAC system modules (controllers, LAM graders, etc.)	511	207
CAMAC auxiliary crate controllers	51	26
U-port adaptors	116	17
CAMAC digital input and output modules	502	203
CAMAC analogue input and output modules	461	138
CAMAC display modules	237	85
Timing system modules	283	132
Digital signal conditioning (Eurocard)	1,914	1,110
Analogue signal conditioning (Eurocard)	1,273	39
Cubicle frames	105	87
Eurocard subracks	489	203
Console devices (TV screens, touch panels, etc.)	218	66
Fibre-optic lightguide	35km	25km

The Central Interlock and Safety System's (CISS) controllers were installed by the start of the year, so that the main remaining task was to connect these to the plant and to program their logic functions. The connections are now complete, but the programs are still subject to change, reflecting the increasing operational experience being obtained by JET's plant designers.

Future Work

In 1984, Divisional activities should follow the lines developed in the second half of 1983, in two main areas: support of Tokamak operation; and implementation of new services in accordance with the extension to full performance.

In the computer operations area, special efforts should be devoted to a more comprehensive quality-assurance scheme, which should improve availability of the overall system towards that of its components. Following experience gained during the first six months of operation, it is planned to concentrate on the following activities:

- Correction of some component weaknesses which are not sufficiently resilient to errors, and the

correction of known "bugs". This includes the installation of the new communications software.

- Improvement of the performance of those components which are used most often during operation.
- Improvement of the user image to permit a more convenient operation and to make it less prone to operator errors.
- Installation of more and improved level 2 software to make operations more "automatic" and to reduce the staff required for operations.
- Expansion of the level 1 software to cover various modes of machine operation and to provide a more automated countdown sequence.
- Addition of more machine subsystems.
- Enhancement of the data acquisition programs to support handling of large data files on local subsystems and to improve facilities for commissioning and testing. In addition, diagnostics support, both in software and hardware, will need to be greatly enhanced to match the substantial increase in the number of JET diagnostics becoming operational throughout the coming year.
- In the electronics area, interface cubicle development is expected to continue at a rate between 1 and 2 per week, depending upon the progress of the diagnostic and additional heating systems. Most of the electronics and communications required will exploit techniques already in use but there will be a modest programme of module development.
- Hardware quality assurance, effort will be contrated on improving test programs to detect problems revealed by operational experience and to provide easy-to-use tests for the maintenance team. The Division will continue to equip consoles as new JET subsystems become operational. CISS interlocks will be refined and the public address, intercom and closed circuit television systems will be fully commissioned.

Neutral Beam Heating Division

(Division Head: G. Duesing)

Neutral Beam Heating Division is responsible for the construction, installation, commissioning and operation of the neutral injection system (see Figs. 33 and 34), including the development towards full power operation. The Division also investigates the physics of neutral beam heating. These topics are undertaken by three Groups: the Beam Line Construction Group, the Neutral Beam Operation Group, and the Test-Bed Group.

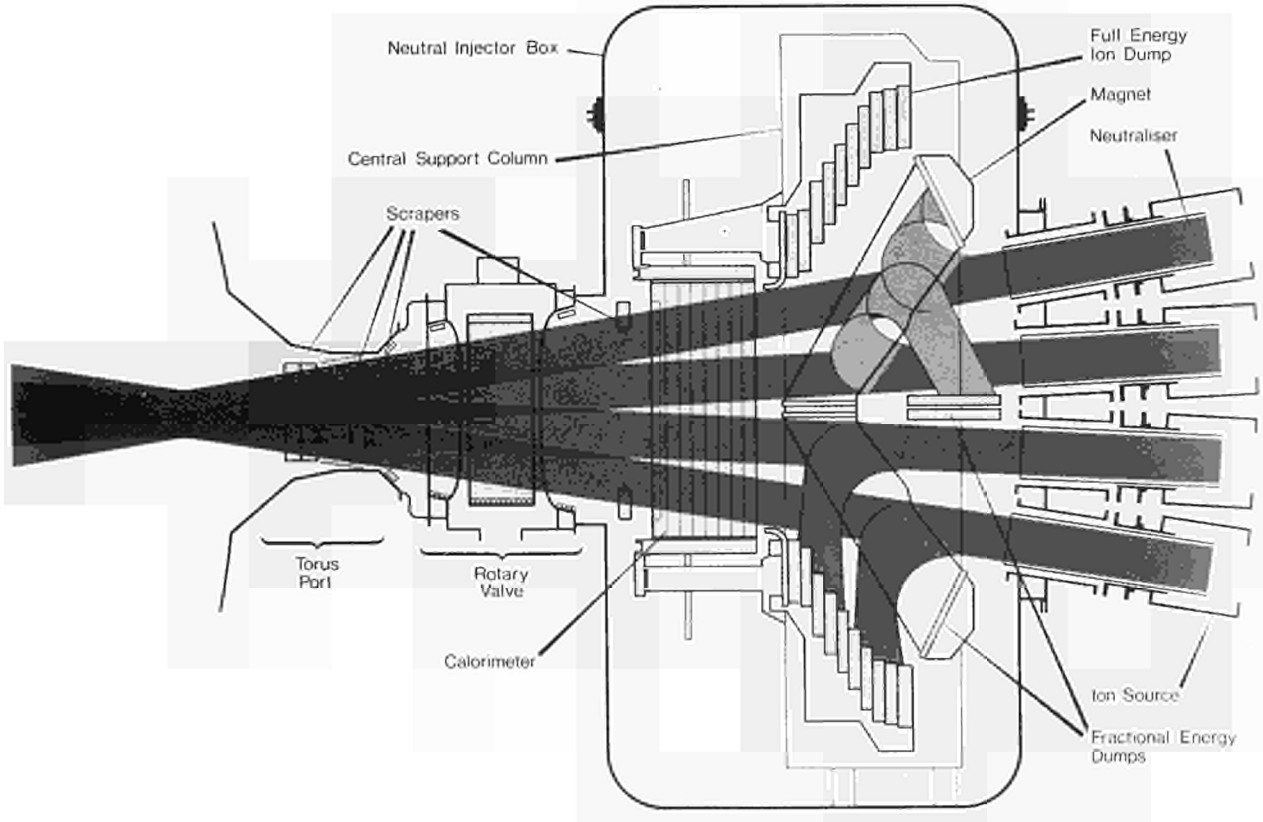

Fig. 33 Neutral Injection system, in elevation.

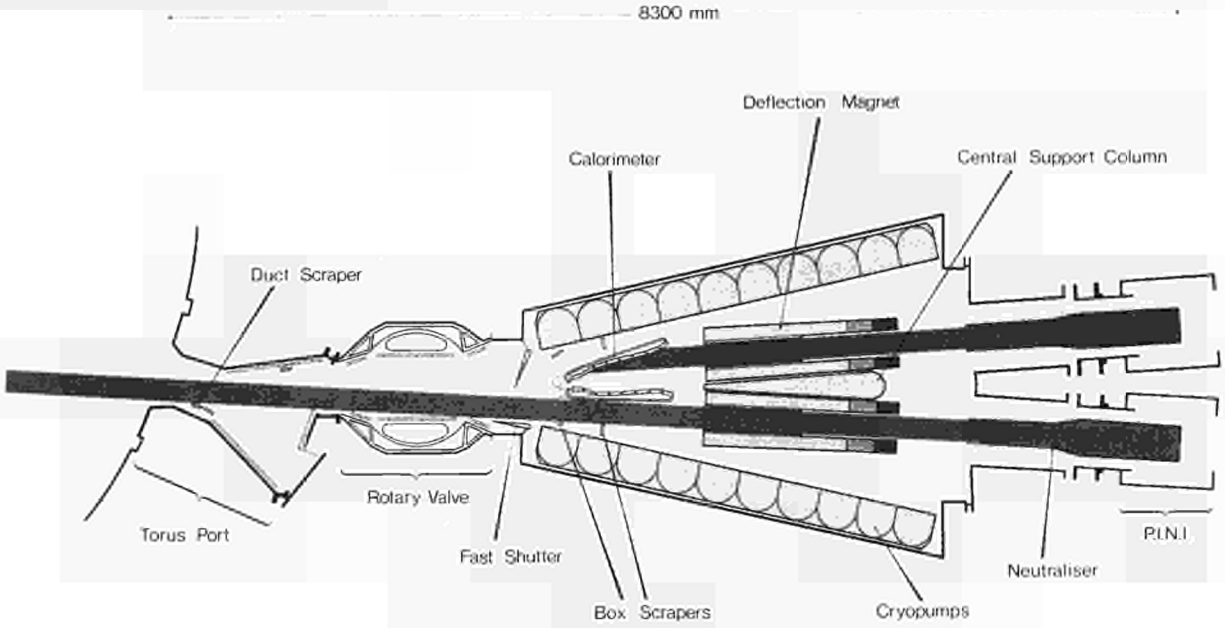

Fig. 34 Neutral Injection system – plan view.

The main 1983 achievements are summarised below:

(i) The JET neutral injection test bed has been installed and commissioned, together with a PINI beam source, neutraliser, duct simulation scrapers, beam dump, cryopumps, turbomolecular pumps and related instrumentation; it will be ready for PINI commissioning, as soon as the power supplies become available in January 1984.

(ii) Component manufacture and assembly preparation have progressed satisfactorily on the first injection system. A pre-assembly of duct scraper, injector vacuum box, turbomolecular pump, cooling water piping and magnet shielding has been carried out at JET.

(iii) The rotary valve (the main valve between the injector system and the Torus), fast shutter, central support column and deflection magnets (Fig. 35) have been delivered to Site and are being prepared for installation.

(iv) During 1983, it was decided to undertake pre-operational tests of thermal cycling on all beam stopping or scraping components. The first full energy ion dumps, duct scraper and box scrapers have passed these tests and are now ready for delivery.

(v) The manufacture of the neutralisers, the magnet liners and several other types of cooled screens (and also the extraction grids for the second series of beam sources) uses the electro-deposition of copper for the forming of cooling water channels. During 1983, several unexpected problems have had to be resolved to establish the details of the component production procedures. Production is now underway, but the first components were delivered only at the end of the year.

(vi) The cryopump is ready for delivery. A 1/10 mode pump (pumping speed $8 \times 10^5\ 1s^{-1}$) has been operated in the test bed and has fully confirmed the design parameters. The cryo-liquid transfer-lines have been successfully tested and installed.

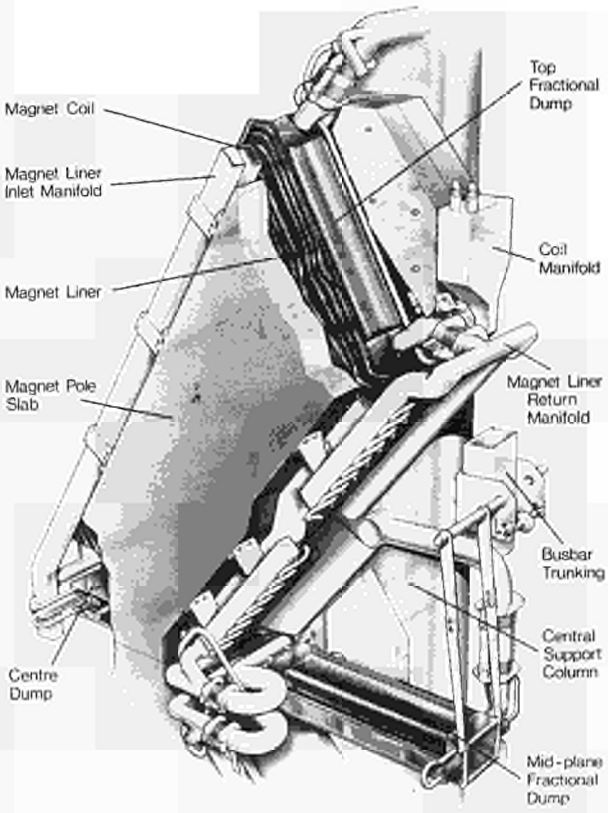

Fig. 35 Deflection magnet, liners and fractional energy dumps.

(vii) Eight PINI beam sources have been delivered, and 3 have been tested. Beams have been extracted at the nominal 80kV and 60A with beam durations of 5s, and the PINI has proved to be a very robust structure and easy to condition.

(viii) The focussing of the beams appears to be stronger than expected. this is an important factor with respect to power loadings on beam wing scrapers and ion beam dumps, and is being further investigated. It may lead to a slight change in the aperture positions in one of the four grids of the PINI, which can be remedied on the existing grids.

(ix) The species yield of the bucket ion sources is being improved (in cooperation with EURATOM-UKAEA Association, Culham Laboratory) by superimposing a super-cusp field on the normal magnetic field configuration. Preliminary tests lead to the expectation that the proton yield can be increased into the 80% range without deteriorating the specified plasma uniformity of ±5%.

(x) Rapid progress has been made on the PINI development for deuterium injection (in co-operation with the EURATOM-CEA Association, Fontenay-aux-Roses Laboratory). Hydrogen beams at 160kV and 35A and with good beam optics have been produced by a three-electrode extraction system.

Neutral Injection Test Bed

(R. Hemsworth, H. Falter, E. Thompson, A. Burt, N. Cowern, J. Davies, G.H. Deschamps, D.T. Ewers, H. Hupfloher, T.T.C. Jones, D. Kausch, F. Long, D. Martin, P. Massmann, M. Mead, D. Raisbeck, D. Stork)

All the outstanding major components for the neutral injection Test Bed were delivered and installed during 1983. The Test Bed Ion Dump (Fig. 36) is an arrangement of three sections, which are adjustable so that the angle between the sections and the ion and neutral beam may be varied. Each section is made from horizontally mounted hypervapotron elements (0.11m wide x1.00m long) with their long dimensions orthogonal to the beam axis. A total of 36 elements are used in the dump. An advantage of this type of dump is the low pressure drop (0.5bar) in the cooling channels.

The Test Bed Box Scrapers, which scrape the beam as it leaves the Neutral Injector Box (NIB) have been installed. The scrapers (Fig. 37) simulating the duct between the NIB and the Torus have been installed in the Target Tank. Two modules of the open structure cryopumps have been attached in the test bed NIB and a PINI (Fig. 38) installed on the rear of the NIB. All the power supplies necessary for the operation of the PINI have now been connected. The supplies for the operation of the arc discharge have been commissioned and are fully operational under computer control. More details are given in the Power Supply Division's section of this report.

Fig. 36 Testbed Beam Dump.

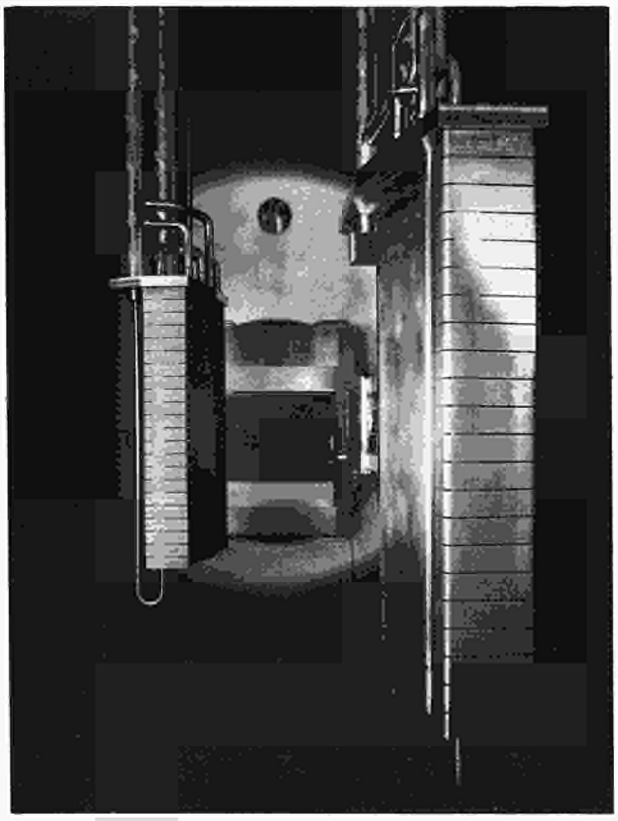

Fig. 37 Torus entrance duct simulation in the Testbed.

The majority of the hardware for the control and data acquisition and the control cables and data links between the test bed and the data acquisition cubicles in the control room have been installed in the test bed control room. Commissioning of the control and data acquisition system is at an advanced state: the fast multiplexing system necessary for recording data from the

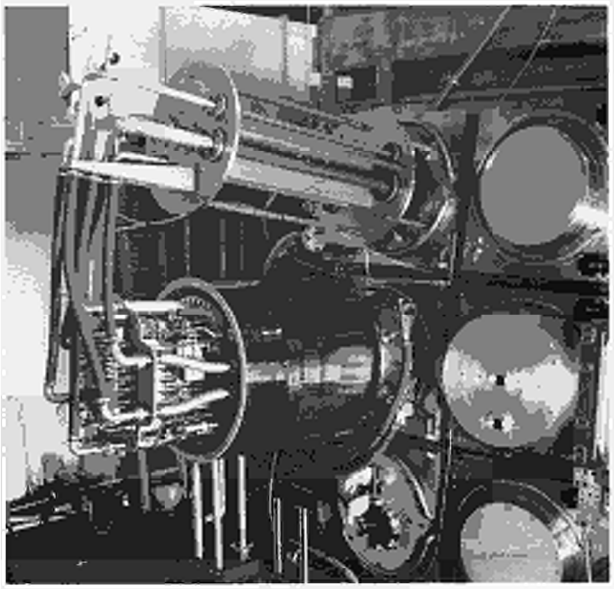

Fig. 38 PINI beam source on the Testbed.

large number of thermocouples (~ 300) has recently been commissioned, and the control of the optical beam scanners has been demonstrated.The large turbomolecular pumps and the associated vacuum systems operate under automatic control.

Initial operation of the PINI plasma source on the test bed was achieved in November, and arc currents up to 900A were obtained (compared with the maximum, which will be ~ 1200A ultimately). This operation has revealed some minor problems with the arc supplies that are presently being resolved. The arc current in the 'bucket' source was observed previously to "run-away" due to arc current heating of the emission (i.e. temperature) limited filaments. This run-away is not now observed, even without feedback stabilisation. A second feature of the filament feedback system is that it is designed to allow for arc current control (i.e. the filament heater current is adjusted to give a pre-set value of the arc current). This was successfully demonstrated by deliberately starting the filament supplies so that the initial arc current was either below or above the pre-set level.

Beam Line Systems

(R. Haange, P. Kupschus, C. Brookes, A. Dines, J. Gallacher, A. Goede, F. Hurd, A. Ingersoll, G. Lundqvist, R. Tivey, M. Watson)

Component Procurement

The Neutral Injection Box (NIB), Central Support Column (CSC) and box stand and magnetic shielding for the first system were delivered by early 1983.

The delivery of dumps, calorimeter and scrapers, which are heat load components using hypervapotron elements, suffered delays following manufacturing problems with cracks in vacuum brazes near electron-beam welds and leaks in components already installed in the Torus. Joint designs have been modified and manufacturing processes altered slightly. To improve the testing of the reliability of the joints in beam stopping elements, it was decided to subject the components to thermal cycling from ambient to 300° C in a vacuum furnace during acceptance testing.

The redesign for the reversal of the calorimeter was completed early in 1983 and the manufacturing contract was re-started. Endurance testing of compensators undergoing large deflections during operation have been completed successfully. The first calorimeter assembly is due for delivery by May 1984.

The Full Energy Ion Dumps and the Box Scrapers are scheduled for delivery in January 1984. Fractional Energy Dumps will be delivered during January and February.

The design of the magnet liners and calorimeter back panels is based on copper sheets on which cooling channels are formed by electro-deposition onto wax profiles, which are coated with a conductive layer and are melted out afterwards. The liners and panels are now in various stages of manufacture. The first sets are due for leak testing and thermal cycling from ambient to 150° C in January 1984.

The deflection magnets and their power supplies for the first beam line were delivered early in 1983. The manufacture and testing of the sets for the second beam line including spare coils have also been completed. The magnets show a high degree of reproducibility: the field strength values for all eight magnets agree within a factor of 3×10^{-3}. The busbars and current and signal vacuum-feedthrough assemblies have been designed and the procurement contracts have been placed. Delivery of the first system is scheduled for February 1984.

The Fast Shutter, including pneumatic actuators, was tested at the contractors and was accepted with a closing time of approximately 0.5 s. A faster system (with about 0.2s closing time) using hydraulic actuators has been designed and the manufacturing contract for this system, including electronic control and hydraulic power pack will be placed early in 1984. After full life-cycle endurance testing at JET, this system will be retro-fitted to the two beam line systems.

Components for the second beam line system, including some spare components, have been ordered. Some have already been delivered during 1983 (stand and shielding) and others should be delivered in January 1984 (NIB and CSC).

Assembly and Tests on Site

During 1983, the central support column (CSC) was aligned in the NIB. The stand and magnetic shielding for the NIB were pre-assembled and aligned with respect to the injection Torus port (see Fig. 39). The operation of the heavy duty roller bearings was demonstrated which allows the NIB to move some 50mm away from the Torus when the latter expands due to baking. The main coolant piping and vacuum pumping systems were installed and subjected to the same movement.

The duct scrapers (Fig.40) were installed in January

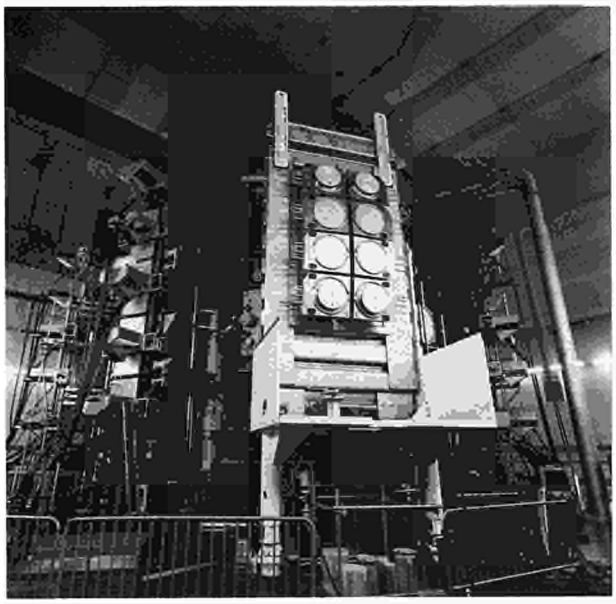

Fig. 39 Neutral Injection Box (NIB) at the Tokamak.

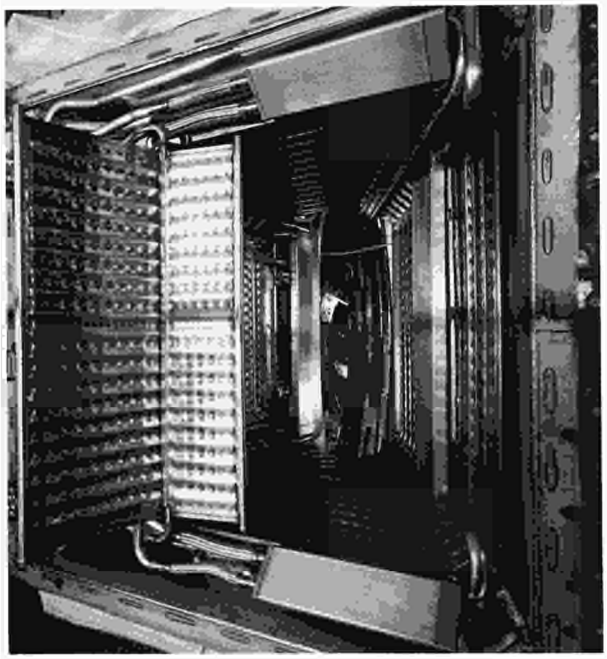

Fig. 40 Torus port with neutral beam duct scrapers.

1983 but had to be withdrawn in August, following development of a leak in a repaired beam stopping element. The repair procedure was agreed, the duct scrapers have been modified and are due for re-installation in January 1984. The deflection magnets were pre-assembled and successfully operated at JET for electrical power and CODAS interface tests, after minor modifications to the iron yokes. Assembly of the magnets on the CSC is shown in Fig. 41. The fast shutter assembly is under installation and due for preliminary tests during January 1984.

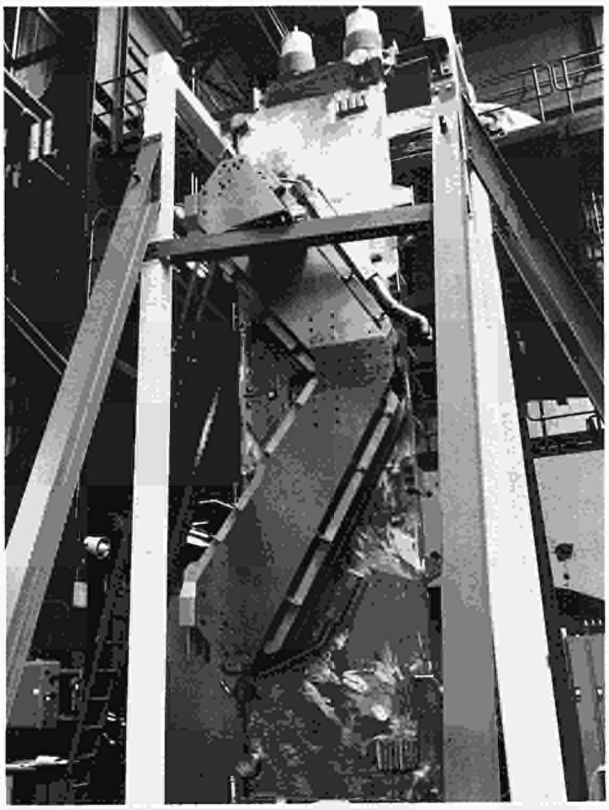

Fig. 41 Ion beam deflection magnet in a pre-assembly on the support and cooling water supply column.

Cryogenic System

(P. Kupschus, W. Obert, A. Jones, E. Kussel, C. Mayeux, M. Mead, R. Roberts, H. Santos, F. Spath)

The 20 modules for the first cryopump system have been completed and extensively tested (50 bar pressure test, thermal cycling from +100 C to −200 C, He leak test). The modules have been incorporated into the cryopump system which was pretested at the manufacturer's premises and is ready for delivery. All cryopanels for the second cryosystem have been machined, surface finished, equipped with aluminium-stainless steel transitions and delivered to the pump manufacturer.

An assembly of two full-size cryopump modules (Fig. 42) representing one-tenth of the pump has been installed in the test bed and successfully tested. The obtained pumping speed of 8.5×10^5 $1s^{-1}$ and heat load of 5W for 3.6K helium were within the design specification. The semi-flexible cryotransfer-lines for liquid nitrogen and liquid helium have been installed at Octant 8 and the test bed (Fig. 43), after successful tests of the JET design helium lines at CEA-Saclay.

The liquid nitrogen supply system is fully operational and in use for the test bed cryosupply. The system is also used extensively for the provision of dry nitrogen gas for torus venting and for vacuum pump gas ballast. The manufacture of the liquid helium refrigerator (350W at 3.5K) is well advanced, and the first components (the 500kW compressor – Fig. 44 – and platform structure) have been installed on site.

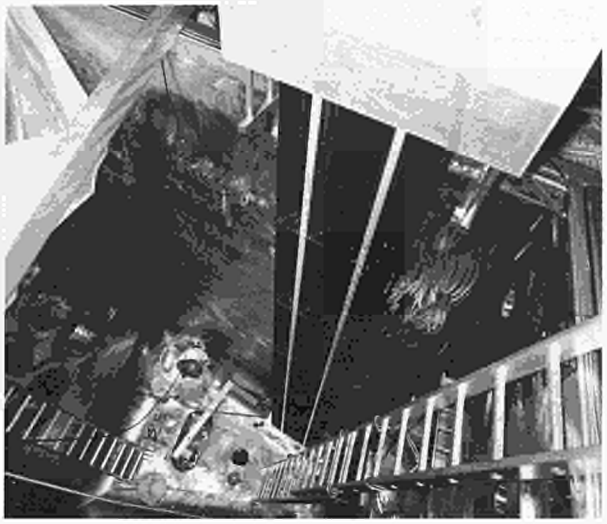

Fig. 42 Two 6m cryopump modules in the Testbed, representing 1/10th of the full-size cryopump.

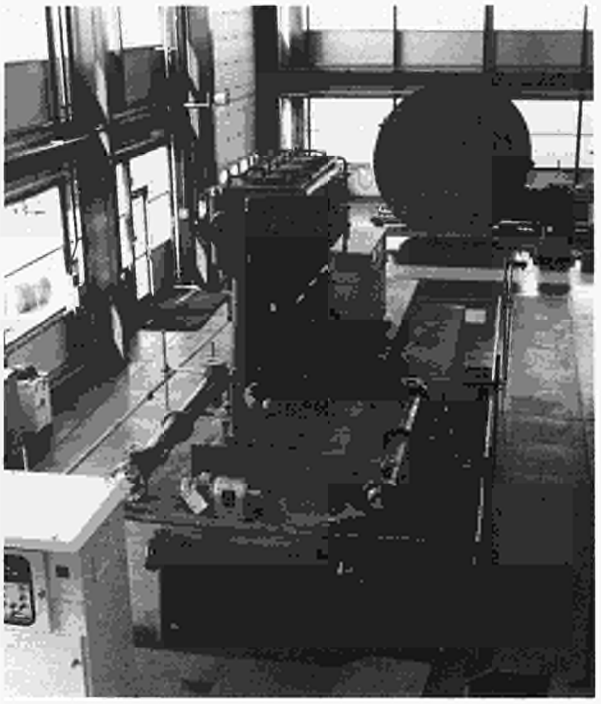

Fig. 44 He line refrigerator compressor during installation.

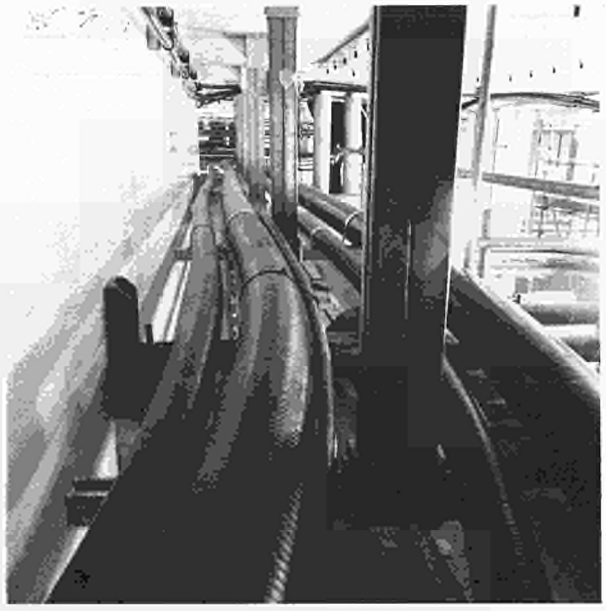

Fig. 43 Cryogenic transfer lines (80m long) to the Testbed: Gaseous N_2 for venting: liquid He outward and return; liquid N_2 outward, cold N_2 return.

PINI Beam Sources

(H. Altmann, R. Haange, R. Hemsworth, F. Hurd, T.T.C. Jones, E. Thompson)

Procurement

Eight PINI beam sources for the first injection system have been delivered to JET. The remaining two beam sources have been disassembled at the contractor's works for remachining of grid No. 3, and should be completed in January 1984. The contract for the beam sources for the second injection system has been placed and production has started, with delivery scheduled for late 1984. Two neutralisers for the test bed have been delivered. The eight neutralisers for the first injection system are in various stages of manufacture and should be delivered by May 1984.

The design of the neutralisers is based on copper electro-deposition onto a perspex mandrel. At positions of high heat load, narrow cooling channels are formed in the copper by filling machined grooves with aluminium tubes. After completion of the electro-deposition process, the aluminium is removed by etching. Problems have been encountered during manufacture leading to several months' delay. The difficulties were mainly concerned with obtaining the drawing tolerances, etching out the aluminium tubes, and with electric field distribution in the electro-deposition baths. Small modifications in the design have now been made and manufacturing processes have been improved and proven by pre-tests. The order for the second system neutralisers has now been placed.

A design has been completed using a grid holder box as a liquid nitrogen cooled first stage neutraliser, to reduce the neutraliser gas flow into the NIB. This design will be tested in the test bed and could be included in the design of the triode grid stacks for operation at 160keV.

Testing

Eight series PINI's have been delivered for testing at EURATOM-UKAEA Association, Culham Laboratory and have undergone pre-tests of their vacuum and electrical integrity. Two PINI's have completed the full set of tests on the Megawatt Beam Line. The final tests

of the PINI reliability were carried out at only 75kV due to limitations of the beam line. Results from PINI 3 are shown in Fig. 45 which gives the extracted energy on each of 80 consecutive shots at 5s, 75kV, 58A expressed as a percentage of a breakdown-free pulse. The majority of shots had less than two breakdowns, and the maximum number was eight. Several shots at 80kV, 60A, 5s have been extracted from each PINI so far tested. The waveforms recorded from one such pulse are shown in Fig. 46.

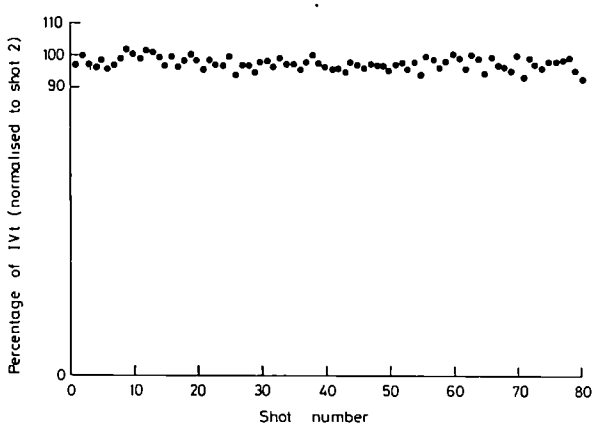

Fig. 45 Extracted beam energy for a series of PINI pulses at nominal 5s, 75kV and 58A.

Species Enhancement

Experiments on both the prototype and series PINI's have revealed that the proton fraction of the extracted ion beam is ~ 65%. This is unacceptably low for the JET injector, and remedial work is currently underway at Culham Laboratory. In early 1983, enhancement to the proton yield was demonstrated by modifying arrangements of the external permanent magnets on the bucket source, so that internal filter magnetic fields were created. Initial results showed that up to 88% protons could be obtained, but with magnet configurations that resulted in non-uniform plasmas across the extraction system. The present understanding is that a filter field can prevent high energy primary electrons from the filaments reaching the region in front of the extraction system, which prevents H_2^+ creation in that region. This reduces the H_2^+ and H_3^+ fraction in the beam, thus enhancing the proton fraction. (H_3^+ is produced from H_2^+, and both may be broken up by electrons on their way to the grid if not created close to the grid). The presence of these primary electrons close to the extracting grid is manifested through a high negative floating potential for that grid (i.e. the potential taken up by the grid with respect to the plasma potential, which is close to the anode potential).

Work is presently underway to find magnet configurations that simultaneously give a low floating potential and a uniform plasma density across the extraction (if

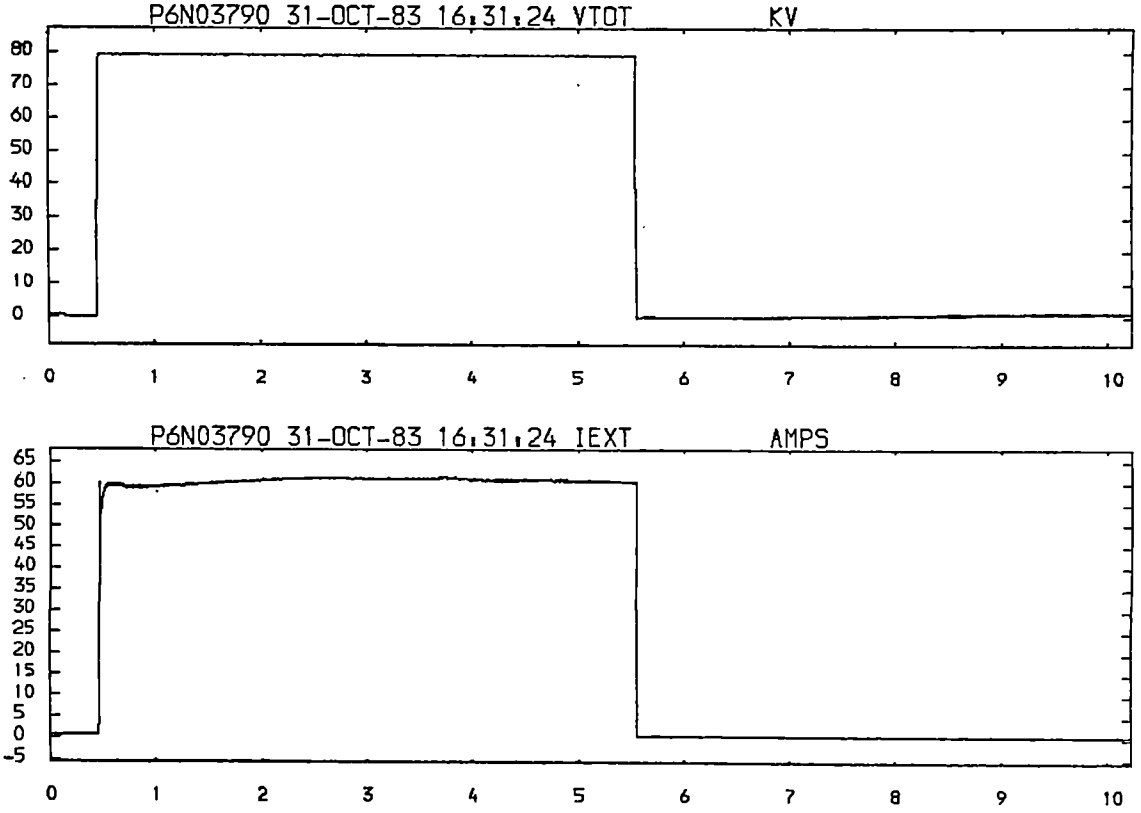

Fig. 46 Voltage and current in a breakdown-free 5s PINI beam at nominal 80kV and 60A.

possible, without significant decrease in the electrical efficiency of the source). So far three configurations have been identified that give floating potentials of ~ 3–4V (compared to the 40V of the present source), with adequate plasma uniformity. One such configuration is shown in Fig.47. The species ratios will be measured early in 1984.

Beam Steering

The JET beam line design requires that the beam extracted from the ion source should be focussed at 10m in the horizontal plane and at 14m in the vertical plane. In the vertical plane, the focussing is achieved by aiming the upper and lower half grids at 14m (each electrode of the extraction system is formed from two halves stacked vertically), and by offsetting the apertures in grid No. 3 (the negative, or deceleration grid) in order to cause each beamlet to be steered to 14m. The focussing in the horizontal plane is achieved purely by offsetting the apertures in grid No. 3.

The PINI's beam steering has been examined experimentally at Culham Laboratory. Two basic techniques have been used: the calorimetric measurement of beam power profiles at 3m and ~ 9m from the extraction system, and the measurement of Doppler shifted H_α light profiles from the beam at various locations along the beam line. (The H_α light arises from the collision of beam particles with background H_2 and the Doppler shifted light comes only from beam particles). The profiles measured at long distances are determined

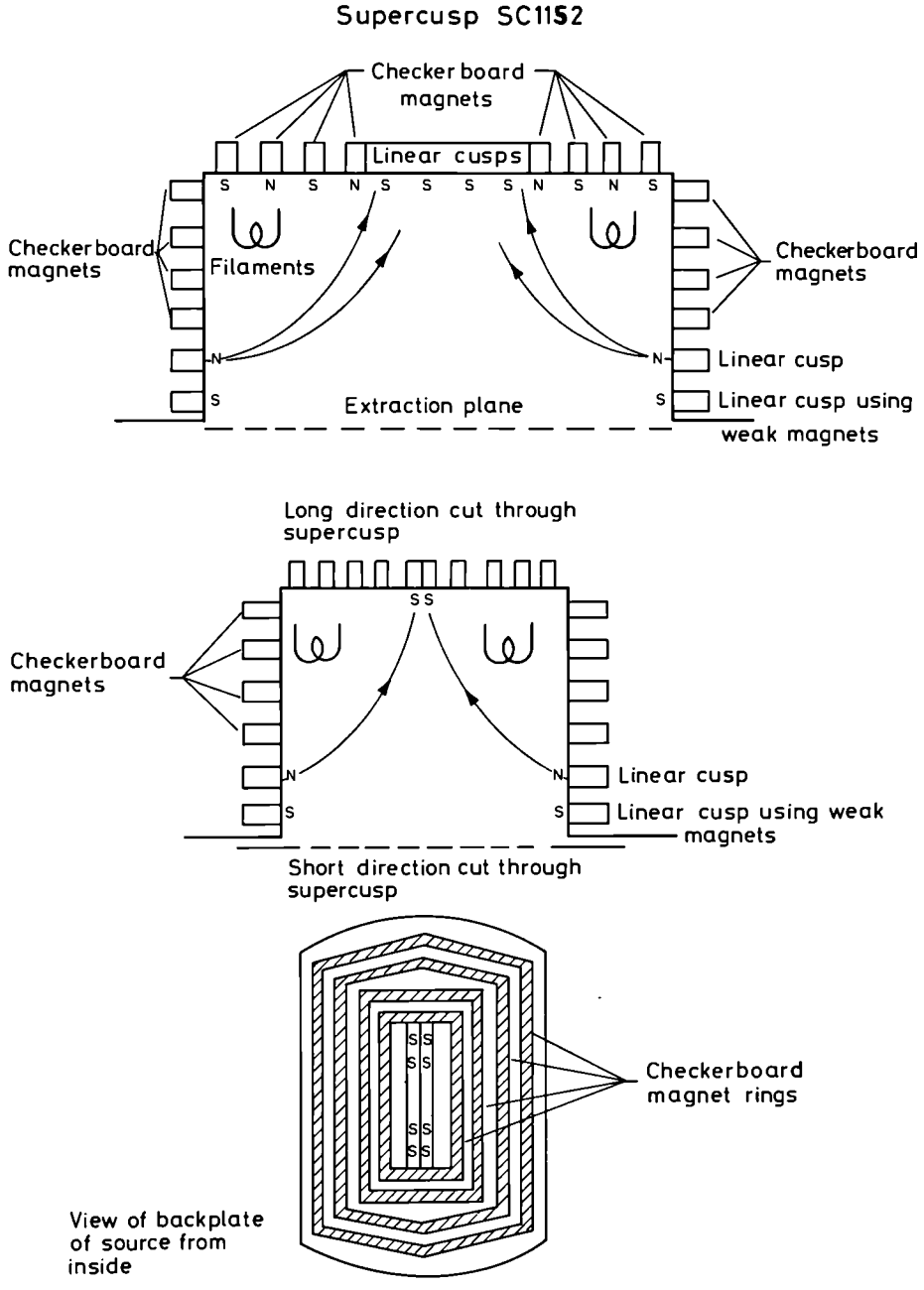

Fig.47 Checkerboard plus supercusp magnet configuration of the PINI ion source (development work at Culham Laboratory).

essentially by the beamlet divergence, whereas those measured close to the source are determined by the beam focussing. Both techniques reveal that the beam profiles measured at short distances (< 4m) are not as predicted.

The first-order interpretation of the measured profiles is that the beamlet steering by offsetting the apertures in grid No. 3 is nearly twice as strong as predicted. This was borne out by examining the beam from the prototype PINI when it was equipped with different grids at No. 3 positions, with various offsets. The main consequence of the resultant short focal lengths is a very high power density on the ion dumps. The reason for the over-steering is not known and an investigation of this phenomenon is continuing.

160kV Development

PINI development for deuterium extraction at 160kV has been carried out at the EURATOM-CEA Association, Fontenay-aux-Roses Laboratory where a PINI was changed over to a three grid system (Fig. 48). It was encouraging that within two months the system was operating in H_2 at 160kV, and 35A beams were extracted (Fig. 49), although only for short pulses as the first grid was uncooled. Since then, operation has concentrated on characterising the beam extracted from this system. Beam profiles measured at 4.8m and 7.4m from the extraction system are those predicted.

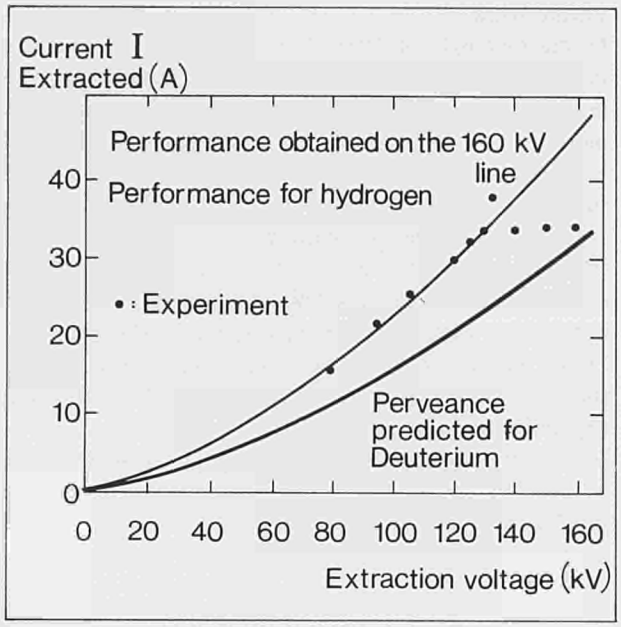

Fig.49 PINI operation with hydrogen at 160kV (development work at Fontenay-aux-Roses Laboratory).

Control and Data Acquisition

(E. Thompson, N. Cowern, T.T.C. Jones, D. Stork)

Effort has concentrated on the development of the applications software. The overall structure of the system is defined using the standard JET data acquisition programme (GAP). Several programmes for analysis and display of electrical and thermocouple data have been checked using dummy data.

The timing programme is also operational. This enables the setting up and checking of all timing requirements for logical sequences. In addition, it ensures that, when a single timing parameter is changed, all other necessary changes are automatically carried out. Using these programmes, various modes of operation are being assembled using the "task scheduler" concept developed by Lawrence-Berkeley Laboratory. Several software packages were transferred to JET and operated on the NORD system.

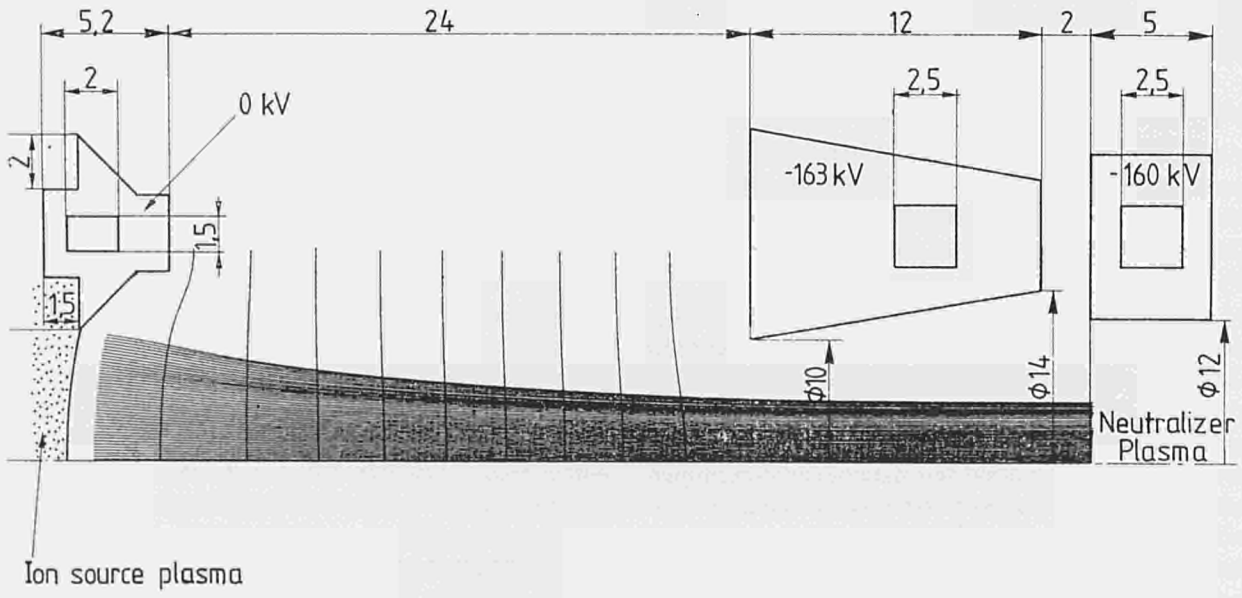

Fig.48 Three electrode system for 160kV (development work at Fontenay-aux-Roses Laboratory).

Future Work

In the first part of 1984, it is planned to assemble the first injection system. This includes: the assembly of liners and fractional energy dumps onto the deflection magnets and the installation of these units; the full energy ion dumps and the calorimeter onto the central support column as well as the commissioning of the cryopump and the fast shutter in the vacuum box and the installation of the box, the rotary valve and the duct scraper at the machine. In parallel, the second injection system assembly will start. In the test bed, PINI's will be operated with power supplies similar to the final ones, and beam transmission and beam power deposition will be investigated.

In early Summer, the first beam line system should be installed in the test bed and commissioned with the simultaneous operation of two PINI's and long beam duration.

Radio Frequency (RF) Heating Division

(Division Head: J. Jacquinot)

Radio Frequency Heating Division is responsible for the design, construction, commissioning and operation of the RF heating system during the different stages of its development to full power. The Division also participates in studies of the physics of RF heating.

It was decided only in 1981 to use waves in the ion cyclotron range of frequency (ICRF) as a heating method to provide a further 15MW of power to the JET plasma. Design work was started immediately, with assistance from the EURATOM-CEA Association, Fontenay-aux-Roses Laboratory; creation of the Division followed in 1982 and most professional staff were recruited during the latter part of 1982 and during 1983. The Division will be completed in 1985, with the arrival of a second complement of technicians.

The Division's tasks can be divided into three main areas reflecting the Group organisation as follows:

(i) The RF Power Group is charged with the construction and operation of the generator system (up to 33MW output), and of the matching and transmission networks (up to 1.5km of coaxial lines).

(ii) The RF Antenna System Group is responsible for the construction and operation of the launching structures. The construction is organised in three phases (Table VII) matching the modes of JET operation. Prototype antennae (A_0 generation) will provide critical test data of coupling properties and will allow a choice of the optimum configuration (monopole versus quadrupole). This will be followed by the introduction of toroidal limiters (A_1 generation) and the preparation for the active phase of JET (A_2 generation).

(iii) The RF Physics Group is in charge of conceptual aspects of heating scenarios and of the physics of the experimental programme.

Table VII
Plan for antenna development and installation in JET

2 prototype antennae A_0 End of 1984	• 2 versions 1 quadrupole, 1 monopole • Antennae equipped with radiation cooled graphite limiters and nickel screen • Short pulse operation (1s)
6 antennae (A_1) Early 1986	• Water cooling of screen and protection frame, integrated with toroidal limiters
Up to 10 antennae (A_2) Mid 1987	• Optimised coupling and cooling

RF Power Group

(T. Wade, R. Anderson, G. Bosia, G. Jessop)

The work of the Group is concerned with placing contracts, installation, commissioning and operation of the complete ICRF heating plant. The plant consists of the RF generators in the north wing of the JET building (see Fig. 50) and the coaxial transmission lines which feed RF power through the basement and up to the antenna vacuum transmission lines on JET. During the year, the major contract for the supply of the high-power RF generators progressed from initial to detailed design. Manufacturing permission was granted later in the year, followed by delivery of the main supporting framework and its installation in the North Wing ready to receive the first RF unit.

At the same time, prototype RF amplifier equipment reached the assembly stage at the manufacturers. Transmission line specification was also completed and, after competitive tendering, the contract was placed with the selected manufacturer. Much effort was devoted to progressing these contracts. In addition, an examination was undertaken of the performance limits imposed on the RF generators by the operating parameters of commercially available RF power tetrode valves and ensuring that the transmission line insulators would withstand the high RF voltages specified. Ensuring compatibility with the high-voltage DC power supplies was also a major priority, as flexibility will be an important factor in maximising the RF generator's performance.

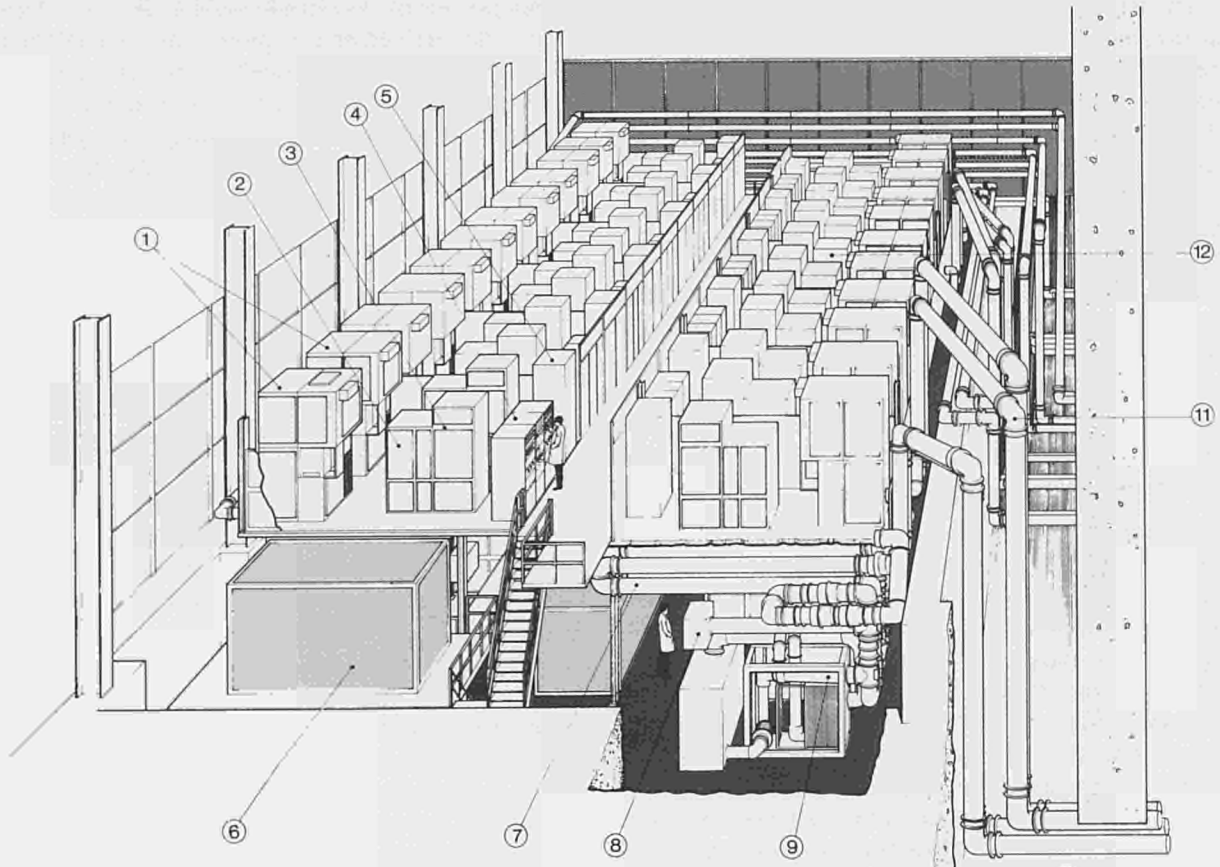

1. *1·5MW end stages.*
2. *Driver stage.*
3. *Crowbar cubicle.*
4. *Local control equipment.*
5. *CODAS remote control cubicle.*
6. *De-ionised water heat exchanger.*
7. *Transmission line equalising length.*
8. *Motorised tuning stub.*
9. *Soda water test load.*
10. *RF power to torus.*
11. *Coaxial transmission line.*
12. *Area for possible additional units.*

Fig. 50 Conceptual view of JET ICRF heating system.

Design Philosophy of Generators

The design was based on requirements for heating plasmas with a range of ion species, plasma parameters and magnetic fields, which dictated an operating frequency range of 25–55 MHz. In this range, RF high-power tetrodes are commercially available and the recent interest in ion cyclotron heating for tokamaks and their use for other high-energy physics experiments has encouraged manufacturers to improve specifications. The JET requirement to use proven technology dictated the choice of the Eimac 8973 for the high power stages. However, the RF generators have been designed to allow adaptation to other power tetrode models should suitable designs appear during JET's life-time. The selected model can deliver 1.5 MW of RF power into load mismatches of up to 50% (SWR = 1.5) for periods of 20 s.

The space available for routing RF transmission lines and siting launching antennae is limited. Operating experience should dictate the maximum power capabilities of transmission lines and antennae delivering the RF power. However, it is important to drive each part of the delivery system close to its maximum capacity. As the lines and antennae are intended to handle 3 MW, the RF generators are designed for optional tandem operation. This requires a combining device with a high power handling capacity, which has been included in the design and specification. A start has been made on the design of SF_6 pressurisation plant which will further improve the power handling capacity of the RF transmission lines and impedance matching components.

Radio Frequency Generator Unit Design

The low power stages (including the amplitude, phase and frequency control circuits) feed wideband transistor power amplifiers providing up to 600 W each to the two power amplifier vacuum tube chains. Each chain consists of 3 RF tetrodes producing 20 kW, 100 kW and 1.5 MW respectively. Coupling between stages is provided by wideband impedance transformers. However, some tuning is required primarily to compensate internal tetrode capacitances. All tuning adjustments are motorised to provide automatic setting of the generator operating frequency within the 25–55 MHZ operating range. The tuned bandwidth is designed sufficiently broad to allow 'instantaneous' frequency shifts (within ± 2 MHz) from the mechanically tuned setting. This facility is important for rapidly matching the generator to load variations caused by changes within the plasma.

The RF power from the final stage tetrode is coupled to the transmission line (30Ω impedance) through a specially developed high-power matching network which provides bandwidth, impedance transformation and filtering for the harmonics generated in the Class B operating regime.

The 100kW and 1.5MW stages are water cooled and the lower power stages are air cooled. Due to the high DC power supply voltages used (up to 30kV), the generators and, in particular, the high power tetrodes are protected against flashovers by ignitrons which short circuit the DC supplies, causing them to shut-down rapidly. An emphasis on unattended and fail-safe operation has been applied to the design of the control system for the generators. During normal operation, the generators will be computer controlled using CODAS.

Simulation of the Final Stage Power Capability

The central design problem of the RF generators has been to deliver the required energy into a plasma whose parameters might vary widely during a pulse, causing an ever-changing fraction of the power to be reflected back down the transmission lines towards the generators. Compensation for this reflected power can be made partly by 'electrically' adjusting the transmission line length by shifting the generator frequency ±2MHz during the pulse. However, a proportion of the reflected power may still reach the RF generators, which they must withstand.

Depending on the reflected power phase angle, any of a number of normal tetrode operating parameters might be exceeded, including anode dissipation, screen grid current and anode voltage. The HVDC power supply to the tetrode is designed to change the voltage dynamically during the course of the 20s discharge in order to set the maximum safety margin before exceeding the various parameters. Eventually, with increasing reflected power, the RF generator protection circuits should reduce the RF power generated to protect the tetrode. Calculations have been made to investigate the available power from a tetrode valve, depending on the phase and magnitude of RF power reflected back to the valve anode.

ICRF Transmission Line System

The Transmission Line System not only transfers power from the generators to the antennae, but is also part of a matching system which must ensure that the load presented to the generators is optimal, for efficient operation and maximum output power. Matching is achieved by placing a stub at the correct position and slightly varying the frequency, which effectively varies the electrical length of the long line (approximately 75m) between antenna and variable stub (see Fig. 51).

Since the frequency can be varied instantaneously, the best compromise working load during 20s RF pulses can be selected for varying antenna admittance parameters. One drawback of this system is that the major part of the transmission line can be exposed to high reactive power levels (high voltage standing wave ratios), and, therefore, to high voltages, high currents and higher losses. To improve this, a second fixed stub close to the antenna is proposed.

The line parameters are as follows:

Outer Conductor:	
Aluminium Alloy,	ID = 230mm
Inner Conductor: Copper,	OD = 140mm
Characteristic Impedance:	Z_0 = 30 Ω
Losses at 55MHz:	$\alpha < 1.4.10^{-3}$ dBm
Specified Maximum Voltage	u = 50kV

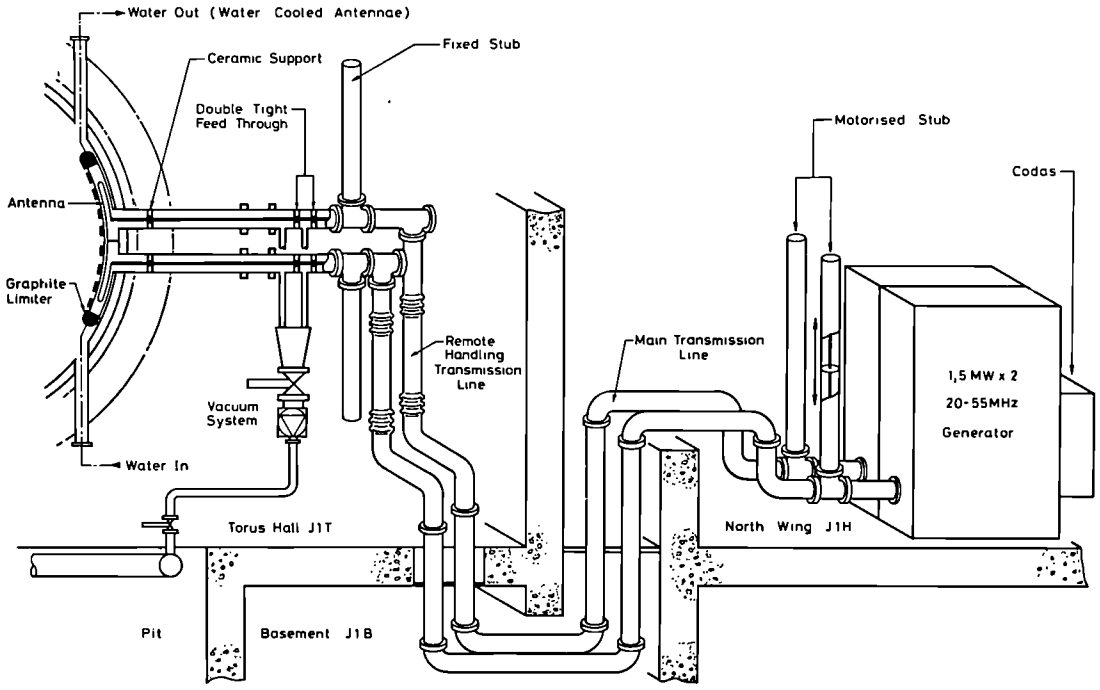

Fig. 51 Model view of transmission lines.

30Ω is a non standard line impedance and all components are a special design for JET. A number of components are novel as follows:

(i) Directional bridge for the RL 230–140 line.

(ii) DC break/switch: This permits isolation of the line outer conductor, allowing complete DC-isolation of the generators from the machine, and enabling safe test load operation while the machine is running.

(iii) Phase-shifter in the RL 230–140 line: a huge trombone structure, with a composite stroke of 3m, used to test the generators and the stub under varying reactive/resistance loads.

(iv) Soda test load for testing the generators: capable of dissipating 3.0MW during 20s, and equipped with calorimetric power measurement facilities for accurate power measurements.

All line components (except the loads) can be pressurised to 4 bars relative pressure with dry air or with SF_6. Ceramic support design for the inner line conductor was carefully monitored to achieve the required voltage stand-off. The first four lines should be constructed in 1984 and the system expanded up to 20 lines in 1985/86, eventually coupling up to 30MW to the ICRF antennae.

Interface of the RF Plant with the CODAS System

Each of the 10 RF units can be independently and remotely controlled, using two ND Nord 100 computers and CODAS computer links. Each RF unit can be rapidly connected to either serial highway loop, to cope with conflicting operational requirements on different units (JET operation, cold tests, test load commissioning, test bed operation, etc). Interface is provided by a dedicated CODAS cubicle per unit plus one bulkhead cubicle (where the highway switching is performed). One further CODAS cubicle is dedicated to instrumentation interface and one for the test bed interface. Production of interface cubicles started in September 1983 and will continue throughout 1984.

The ordered RF units will be delivered in 1984 at monthly intervals and, therefore, plant commissioning will extend well over one year. To minimise the commissioning time on JET, and to maximise the availability of commissioning of RF units during 1984, individual commissioning of the interface between the plant and CODAS cubicles is being performed at the manufacturers, where each CODAS cubicle is sent after construction. A small system has been set up on an Apple microcomputer to simulate every CODAS function.

Automatic Transmitter Matching

Optimised RF plant operation requires that each transmitter is properly impedance matched to the time varying antenna load. The accessible parameters are:

(i) The RF instantaneous frequency, which may be varied ±2MHz with respect to any operating frequency.

(ii) The transmitter output impedance, which may be changed about 20% around its nominal value (30Ω) by varying the generators HVDC voltage at constant anode current.

(iii) The stub piston length (λ/4 at minimum frequency) located at the transmitter end.

In view of the large number of transmitters (24), it is preferable that matching should be performed automatically as much as possible, and slight mismatches due to plasma position or profile variations should be compensated in real time. A theoretical and experimental analysis has been carried out and various control mechanisms have been identified. Some have been tested at low power and further tests at high power are underway to select the most suitable for JET operation.

RF Antennae Systems Group

(A. Kaye, J. Arbez, E. Hanley, J. Plancoulaine, C.Walker)

Design, Construction and Testing of ICRF Antenna

Installation of two prototype ICRF antennae (A_0) is planned for September 1984. The A_0 antennae are designed for short pulse operation to investigate such areas as coupling efficiency to the plasma, impurity production mechanisms and RF current and voltage limitations on the antenna and transmission line components. The results will be used to optimise subsequent antenna design. The A_0 antennae have been fully designed and construction is nearing completion.

The first long pulse RF heating of JET will be initiated with the installation of six A_1 antennae in early 1986. The design of these antennae, rated for full power operation (9MW in total) at full pulse duration, is well advanced. Subsequently, ten A_2 antennae will be installed in late 1987, with optimised design taking into account operational results from the prototype antenna.

Severe constraints are imposed on component design by pre-existing torus features. The antennae must be located in a space 150mm wide, between the plasma scrape-off layer and the wall. The input transmission lines must enter the torus through the limiter guide-tubes, originally provided for mounting the poloidal limiters, which are 153mm ID and of 560mm pitch between centres. The former places a major constraint on the voltage stand-off and current carrying capacity of the coaxial line, severly complicating the assembly procedure, limiting the vacuum conductance within the torus, and necessitating the provision of additional pumping capacity on the vacuum transmission line. In turn, the transmission line pitch is not well suited for feeding the antenna central conductor at the inner or the outer end, and a somewhat unconventional trombone central conductor is required. Further constraints on the transmission line are imposed by requirements to clear various diagnostics, which has necessitated the development of a compact double vacuum-tight window.

In the tritium phase, the antennae must be installed and maintained remotely. In order to gain experience with this procedure, all antennae have been designed for compatability with remote installation and maintenance.

In addition, the antennae are subject to the usual design constraints of ICRF antennae, that they must be located close (~ 30mm) to the plasma edge to achieve

efficient coupling. Consequently, the structure's sides are subject to bombardment by high energy particles, causing both high thermal loads and substantial sputtering. Therefore a low-Z side protection resembling a poloidal limiter will be provided. The antenna conductors also need protection from the plasma to obtain the necessary voltage stand-off, and this was provided by a toroidally slotted metal screen assembly between the conductor and the plasma. This screen is transparent to the poloidally polarised wave component, and also reduces impurity production by suppressing surface mode excitation. Each screen assembly is subjected to substantial RF losses (~ 10%) and to plasma radiation. The screen material must have low Z and high RF conductivity to minimise the effect of sputtered impurities and RF losses.

Design Features of the A_0 Antennae

The A_0 antennae are designed to operate at 1.5 MW power into the plasma for a 1 s pulse, every 10 minutes. They are not actively cooled, and rely on radiation cooling only between pulses. The design, completed in 1983, has the following features:

Side Protection

High purity graphite tiles, typically 0.2 m x 0.2 m frontal area, provide side protection. They are flexibly mounted on Inconel 600 carriers, which can be installed remotely onto rails on the antennae housing, and are profiled to maintain nearly constant power density on the surface for a scrape-off layer of about 15 mm e-folding thickness, with an initial slope of about 10%. The front tile face is typically 20 mm behind the poloidal limiter. 46 tiles are used to surround completely the antenna housing. They are vacuum baked and ultrasonically cleaned before installation, and are radiation cooled only.

Electrostatic Screen

The A_0 screen elements are tilted 15° to the horizontal to be parallel to the magnetic field lines. The screen is not actively cooled, which limits the pulse length used. The screen elements are made of pure nickel alternating T profiles typically 18 x 18 mm in section, mounted 10–15 mm behind the graphite tiles arranged with no line-of-sight through the screen. The screen is electrically isolated from the antenna housing, to limit forces induced during a disruption. The A_0 screen is mounted on the housing.

Antenna Housing and Central Conductor

The housing is a shallow Inconel 600 box (typically 2 m x 0.8 m x 0.2 m) located on two conical spigots in the torus wall at the transmission lines, and bolted to the torus at each corner for additional mechanical support during a disruption.

Two types of interchangeable central conductor have been produced: one is a monopole conductor (Fig. 52), typically 1.8 m x 0.4 m with a central short circuit; and the second is a quadrupole conductor (Fig. 53). Both are fabricated in Inconel 600, and designed to accommodate differential thermal expansion during operation. All current-carrying surfaces of the housing and conductor are electropolished and silver plated.

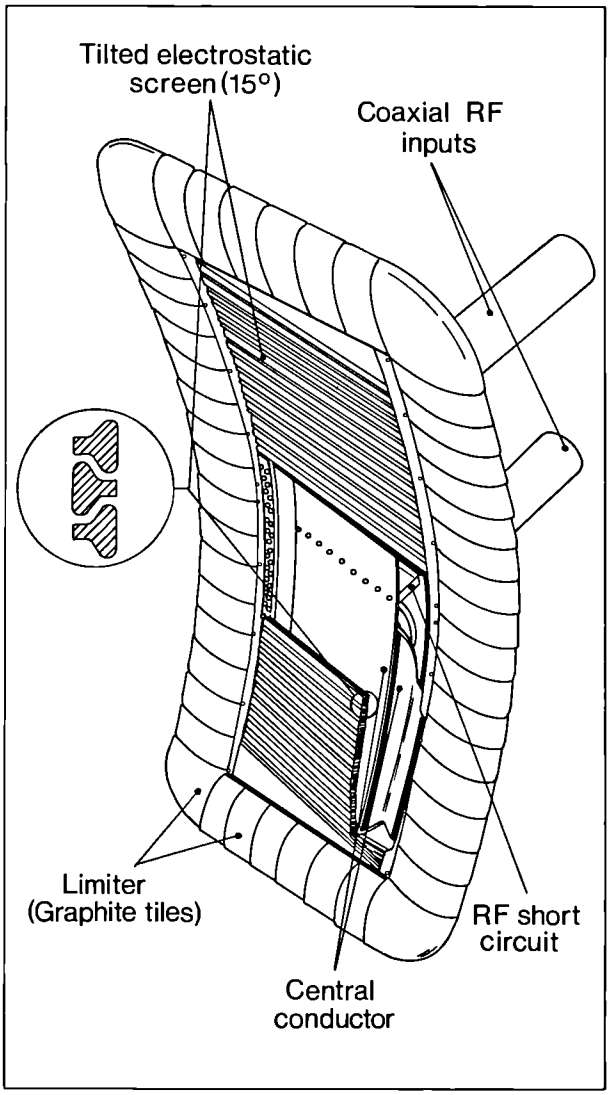

Fig. 52 JET ICRF Monopole Antenna (A_{01}).

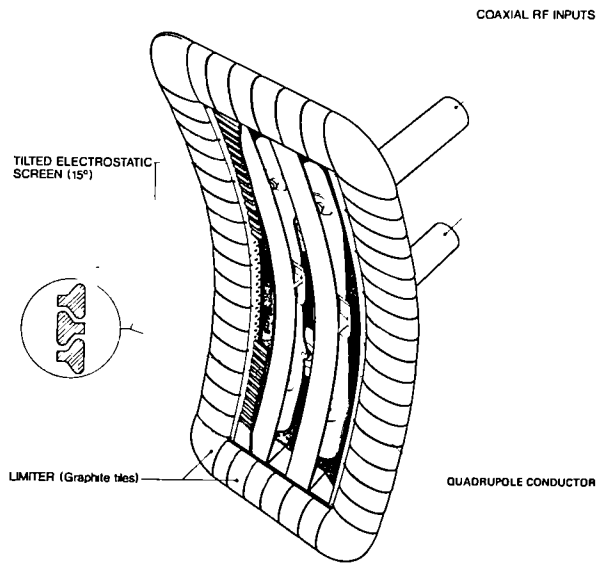

Fig. 53 JET ICRF Quadrupole Antenna (A_{02}).

Vacuum Transmission Line

Two vacuum transmission lines (VTL) connect each antenna to the main pressurised transmission line via ceramic vacuum windows. The VTL is a coaxial 30Ω line which varies in diameter from 104mm to 230mm and is rated at 1500A, 50kV at some 50MHz. Components are made in Inconel 600 or pure nickel, with silver plated surfaces, carefully profiled to minimise equipotential compression, near the surface. At the antenna, the inner conductor is supported on a conical ceramic co-incident with a line diameter change, giving minimal increase in electrical stress. This ceramic has been tested to 21 tonnes axial load and 50kV RF voltage. The central conductor incorporates a bellows (to accommodate differential expansion), which has been tested to full rated current.

Vacuum Window

The vacuum window is a vacuum brazed alumina ceramic assembly which comprises two ceramic annuli in a brazed assembly typically 230mm diameter x 200mm long. The interspace can be evacuated or pressurised. This window represents a major technological achievement. Prototype units have been successfully tested to maximum voltage and current; the pressurised side is the most difficult and pressurisation at 3 bars of dry air or SF_6 is required to achieve the required rating. The corona ring and ceramic profiles are the most critical areas for achieving electrical performance.

VTL Vacuum System

Due to low conductance to the torus, the VTL must be pumped externally. On the A_0 antenna lines, a $500ls^{-1}$ turbomolecular pump mounted close to the transmission lines pumps the pair of lines for each antenna, and also pumps the window interspace via a bakeable T-valve utilising Helicoflex seals.

Antenna Pressurised Transmission Line

The VTL inner conductor is located in the conical ceramic by a 2 tonnes axial load applied internally through the bellows section of the inner conductor from a spring assembly on the pressurised side of the window. This pressurised line uses mainly standard 230mm RF line components and also supports the local tuning stub, if required.

Status of Construction of the A_0 Antenna

The major A_0 antenna contracts are nearing completion and final preparations are underway for testing integrated assemblies and for installation in the torus. The major contracts are summarised in Table VIII.

Many contractors have worked near the limit of existing technology on material specifications, dimensional tolerances, immunity to large temperature excursions and integrity of the UHV systems. Initial deliveries of all components have been received, which are now undergoing RF and assembly testing. In addition, the tools for remote assembly in the torus are mainly completed and are being tested.

Table VIII
Major contracts on A_0 Antenna

Item	Country
Graphite Tiles	France
A_0 Antenna	France
VTL	Eire
Ceramics	France
Vacuum System	UK/Germany
Pressurised Line	Germany
Electropolishing	UK
Silver Plating	Switzerland
'T' Valves	UK
Forgings	UK
Test Beds	France

RF Tests on A_0 Antenna Components

(In conjunction with B. Beaumont, EURATOM-CEA Association, Fontenay-aux-Roses)

The JET RF test-bed comprises a bakeable high-vacuum vessel with two side tubes to simulate the restrictive guide-tubes of the JET torus. It is presently installed at the Fontenay-aux-Roses Laboratory, using the TFR RF generators, and is operated under contract by CEA, with substantial direct JET involvement. A complete antenna and matching transmission lines may be assembled in the test-bed. The RF tests are carried out using a high-Q resonant load assembly. This set-up is particularly sensitive to defects in the test assembly, which rapidly lead to detuning of the high-Q circuit. In addition, this feature minimises component damage as little energy is deposited in the event of electrical breakdown.

Defects on the vacuum side can exhibit several different symptoms. At its mildest, a slight increase in pressure is observed. A barely visible glow may also appear but have no detectable effect on the circuit Q. With increasing severity, a detuning of the circuit occurs associated with substantial pressure fluctuation, which is typical of a multipactor discharge. The most intense breakdown produces an audible click and violent fluctuations.

Initial tests proved time consuming. Key features of the test assemblies were identified: it was crucial to avoid all trapped or poorly pumped volumes close to the current path. Considerable difficulty was experienced under vacuum with components used in the pressurised lines, apparently associated with labyrinths in the inner conductor surface. The surface material was also important; aluminium appeared to provide poor resistance to multipactor arcs, a result which might have been expected from the high secondary electron emission coefficient of aluminium oxide. Much higher resistance was found on silver plated aluminium components. There was some evidence that copper might give a further improvement.

The appearance of breakdown over a range of low voltages was characteristic of multipactor currents. The extent of this forbidden band depended on the rate of

voltage rise; a rapid voltage rise suppressed the onset of arcs. In addition, the effect was suppressed in regions of high RF current. The significance of these effects to JET performance was marginal, in general corresponding to low power levels (~15kW). Difficulties might occur close to voltage minima in the line, if these coincide with critical items; however, these are also regions of high current which might suppress the effect.

A_1 Design

The A_1 antenna outline design has been largely completed, and differs from the A_0 in several respects. A water cooled screen assembly is utilised; fabrication of which provides a technological challenge in maintaining the UHV integrity close to the plasma, whilst dissipating typically 400kW per screen. In addition, the housing width is substantially increased to improve the coupling efficiency of the quadrupole antenna. The side protection may be either graphite or beryllium, and an enhanced radiation cooled design similar to the toroidal limiter is utilised. The pitch of the tiles is the same as the screen elements, to give enhanced RF coupling. The VTL is cooled by recirculated flow of pressurised gas in the inner conductor, and an improved design of the ceramic window is being developed. Major contracts are expected to be placed during Summer 1984.

RF Physics Group

(P.P. Lallia, W.H.M. Clark, F. Sand)

During 1983, the RF Physics Group undertook studies on the following aspects of ICRF heating:

Antenna Coupling

The RF properties of the JET prototype antennae, A_0, are being assessed by the following two lines of studies:

- An experimental investigation without plasma of full scale models, constructed of aluminium with a slightly simplified geometry.
- A theoretical calculation of the coupling properties with and without plasma (work undertaken within article 14 contracts by EURATOM-CEA and EURATOM-EB Associations).

Full Scale Model Studies

Three different flat models were studied. FM-TI was a flexible "trombone type" antenna which allowed adjustment of various dimensions. It had junctions parallel to the z axis and the screen blades could be tilted by up to 15°. Experience gained in the modelling fixed the electrical design of the prototype A_{01} (see Fig. 52). The RF properties were checked by the model FM-T2, which had both junctions and screen blades tilted 15° to the z axis. FM-Q1 was the model used to study the multipole antenna, which fixed the electrical design of the prototype A_{02} (see Fig. 53).

Experiments indicated the importance of the coupling for interpreting measurements. The behaviour could be accurately simulated by an equivalent circuit of lumped elements (see Fig. 54). In this domain (< 60MHz), local field measurements showed that transmission line propagation effects did not play a dominant role; the inductance was determined by the upper conductor and the capacitance determined largely by the lower plate.

The coupling of the trombone antenna could be greatly reduced by placing a short circuit (nicknamed "moustache") at the junction of the two antenna halves (between the conductor and the screen). The main electrical parameters (L, C, Z and Q) could be deduced from the resonance curve, which confirmed that there was a good match between the antenna ($Z_0 \sim 25\Omega$) and the line ($Z_0 = 30\Omega$), required to enhance the bandwidth of the system.

Measurements of the input impedance of FM-T2 (with and without the screen) compared favourably with the calculated values. Flux measurements with and without the screen have also been performed on FM-T1 at low frequencies, where propagation effects remained negligible. These results, confirmed at higher frequencies by local measurements, showed that the transparency was as high as 90% and tilting the screen by 15° decreased this transparency by no more than 3%.

Simulation Codes

A 3D model, including connections and based on a variational principle providing self-consistent currents in the antenna, has been developed to calculate both the fields

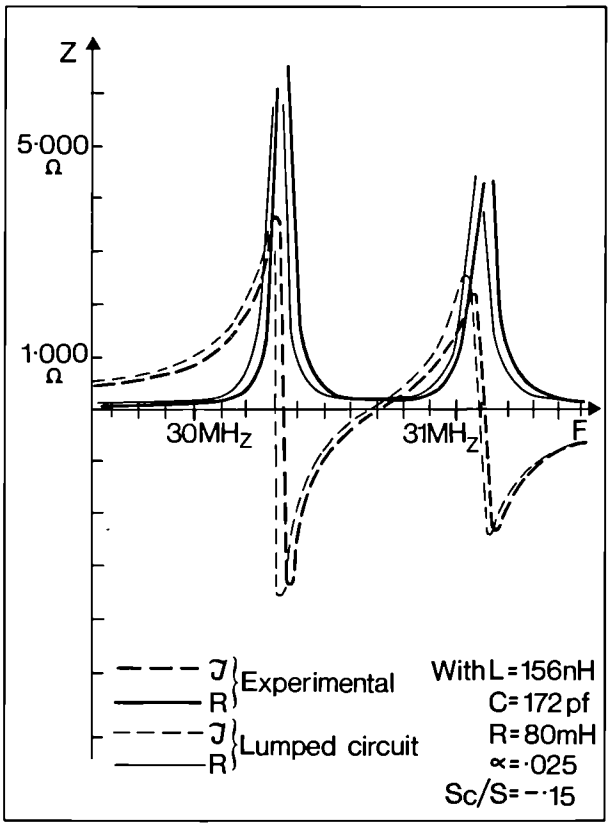

Fig. 54 Experimental and numerical approximately of FM-T2 impedance.

excited in the plasma close to the antenna and the antenna impedance. This was expanded to include a description of the folded conductor. The results obtained in vacuum were in agreement with the measurements on FM-T1.

ICRF Heating Power Deposition Profiles and Modes of Operation

The JET ICRF heating system design has been optimised for operation in deuterium or deuterium-tritium plasmas. However, the first ICRF experimental tests are likely to be performed in a neutron-free hydrogen plasma. Within the bandwidth of the generator (25–55 MHz), the following three scenarios are possible:

- ^{3}He minority heating in a wide range of magnetic fields.
- D minority heating with $n_D/n_H \cong 3\%$, if $B > 3T$.
- Second harmonic ICRF ($2f_{CH}$) heating in a pure H plasma, if $B < 2T$.

Core Absorption

The technical convenience of placing the antennae on the low field side of the tokamak is paid for by the penalty of prohibiting the successful scenarios tested on TFR, namely that of the so-called "wave conversion heating" at the ion-ion hybrid layer, which permits the presence of a relatively high proportion of the minority constituent. With the low field side excitation planned for JET, the minority concentration must be kept low enough so that the correct electric field (E) polarisation occurs close to the minority cyclotron layer. An approximate limit can be found by calculating that the Doppler broadening of the minority cyclotron resonance must exceed the distance between the L cut-off and the cyclotron resonance.

Table IX gives the maximum concentration for different minorities calculated for a typical JET plasma.

Since the core absorption is proportional to the number of resonant particles, this suggests that excitation of waves with large vector components parallel to the magnetic field are preferable. This poses a conflict of interest between strong core absorption and efficient tuning of the antennae to the plasma. Indeed, good coupling necessarily requires that the compressional wave can propagate in the plasma from the edge of the tokamak discharge.

Calculations have been made of the minority temperature versus the total RF power coupled to the JET plasma. This is shown in Fig. 55 for the (D)H scenario which is well suited to produce fast deuterons. The absorption quality factor, η, (defined as the ratio of the power absorbed in the plasma core to the coupled power) is plotted in Fig. 56 versus the input power. While first increasing with the input power, it saturates above 1.5MW. In addition to 5–10% of the coupled power being directly absorbed by electrons (via TTMP or Landau damping), most of the RF power will be transferred eventually, via collisions, when the input power exceeds 5MW in this relatively low temperature, low density plasma.

In the "minority" schemes, the absorption was not found to be significantly sensitive to the bulk plasma temperature, but the relative power directly transferred to electrons increased with temperature.

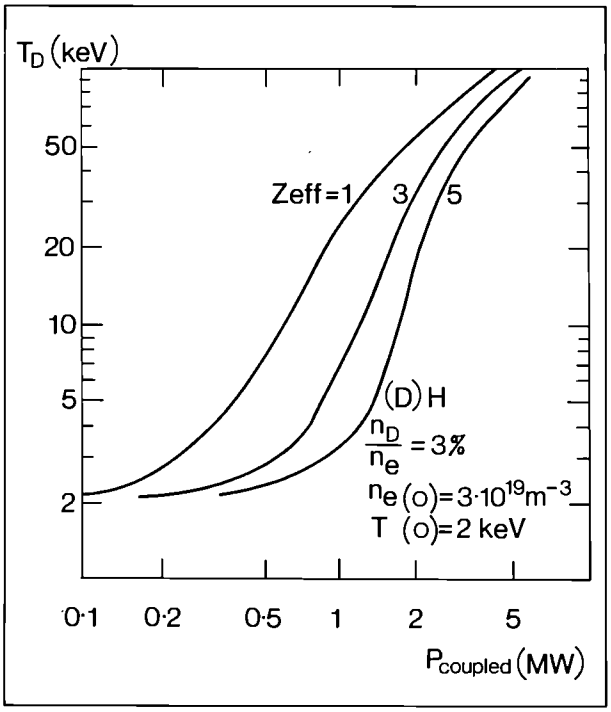

Fig. 55 The minority (D) temperature versus the total RF power coupled to the plasma (n_D/n_e = 3%; n_e - 3.10^{19} m^{-3}; T(o) = 2keV).

Table IX

Scenario	(H) D	(D) H	(^{3}He) H	(C^6) H	(^{3}He) ^{4}He	(^{3}He) D	(D) T	(T) D
Maximum Concentration (%)	10	3.5	3.0	0.25	11.5	6.0	11.0	6.0

(The minority species is indicated in brackets)

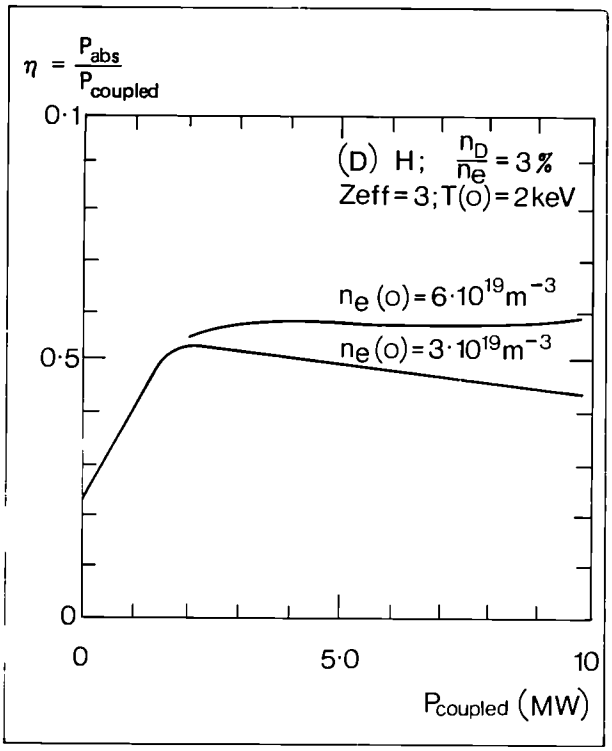

Fig. 56 The absorption quality factor (η) versus the input power (n_D/n_e = 3%; Z_{eff} = 3; $T_i(0)$ = 2keV).

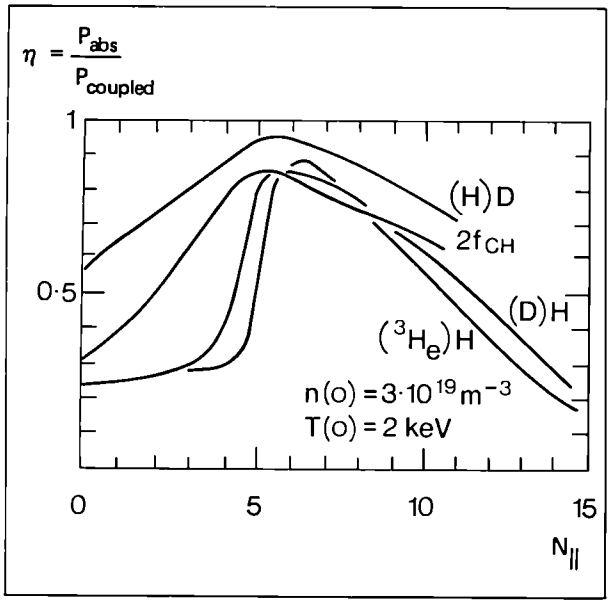

Fig. 57 The absorption quality factor (η) as a function of the wave index component parallel to the static magnetic field ($N_{||}$).

Optimisation of the Wave Spectrum

Fig. 57 shows the absorption quality factor, η, as a function of the wave vector component parallel to the magnetic field, $N_{||}$, for various scenarios in the basic JET plasma. The general trend to optimise core absorption seemed to favour a radiation spectrum centred around $N_{||} = 5$. The purpose of the "quadrupole" antenna is to test the validity of this prediction.

Conclusion

Part of the initial operational RF programme on JET will be devoted to identifying the optimum scenario for eventual full power operations, as well as the validity of the above considerations regarding the shaping of the N spectrum. "Heavy" minority schemes and second harmonic ion cyclotron ($2f_{ci}$) heating, while calculated to be less efficiently damped than "light" minority schemes, have been shown to approach an absorption efficiency of 50%.

Fokker-Planck Calculations for JET

ICRF Heating Scenarios

(In conjunction with J. Scharer, University of Wisconsin-Madison, Madison, Wisconsin 53706)

The magnetic flux surface averaged ICRF heating of JET has been considered utilising an anisotropic, time dependent Fokker-Planck code, including a quasilinear ICRF term. This formulation assumes that the plasma is sufficiently collisional, so that particles lose their phase relationship with the wave in two successive passages into the resonance zones: in particular, all particles are supposed to be circulating. This should be a good approximation for the central core of JET, if the power absorption is concentrated there as expected from ray tracing calculations.

A study has been performed of the time dependent nature of an isotropic non-Maxwellian ion distribution for several mixes of D-T ions, with up to 15MW ICRF power absorbed and energy confinement times τ_E from 0.5 to 1.5s.

2-D Ray focussing and 1-D single pass absorption considerations

Single pass absorption for the fundamental minority deuterium case has been examined, using the ray tracing FEMIR code and a 1-D fast wave local absorption code. The single pass absorption for a wide range of parallel wave vector ($N_{||}$) values has shown that strong single pass absorption (> 50%) is obtained for a major portion of the launched $N_{||}$ spectrum ($0.03 cm^{-1}$). A corresponding study of the second harmonic tritium case with 10% tritium (T_T = 30keV, T_D = 2keV), for $N_{||} = 0.06 cm^{-1}$, yields only 9.2% single pass absorption.

ICRF Tokamak Heating Physics Model

The perpendicular wave vector $N_\perp$ and the wave polarisation have been deduced from the unbounded wave equation (full hot plasma dispersion tensor). The RF power absorbed by the plasma is used as input data to find the electric field amplitude. Mode conversion processes were neglected in the cases of interest. To model radial conduction and convection, finite energy confinement times were introduced for the different species. The code also included ohmic heating through a Spitzer resistivity, D-T and D-D fusions and alpha-particle production in the overall energy balance and

particle source terms. The initial conditions for the RF turn-on were taken to be $n_e = n_i = 5 \times 10^{19}\,m^{-3}$ and $T_i = T_e = 1.7$keV ($E_j = 2.55$keV) so that the local ohmic heating was weak compared to the RF power for the cases studied and decreased further as the electrons were heated. For fusion reactions in D-T, the Hybrid II code computed the fusion energy. To simulate wave focussing in the central plasma region, it was assumed that the absorbed power density was four times that for uniform power absorption.

Deuterium/Tritium Heating Scenarios with Alpha Production

Second Harmonic Tritium

A tritium concentration of 50/50 D-T at an electron density of $n_e = 5 \times 10^{19}\,m^{-3}$ was first considered. An energy confinement time $\tau_E = 0.5$s was imposed for all species. The input power level for a 1s RF pulse was 1.5MW at a 5cm flux average. The tritium energy rose rapidly to about 3.8keV with a thermal anisotropy $E_\perp/E_\parallel = 1.4$ at the end of the RF pulse, and then decayed. The electron power absorption competed slightly at early times with the tritium absorption and after the tritium was heated, it totally dominated the flux average power absorption. The fusion Q = 0.02 was reached at the end of RF pulse.

Fundamental Minority Deuterium

A case was considered of a 10% deuterium concentration operating at 25MHz with a 3.29T field on axis and 3MW of power absorbed. The flux average was obtained at r = 10cm with $\tau_E = 0.5$s. The deuterium heated rapidly and peaked at 6.9keV with an anisotropy $E_\perp/E_\parallel = 1.3$ at 1.0s, when the ICRF power was turned off. The electrons and tritium reached 4.8 and 5.2keV respectively and decayed at the end of the pulse. The alpha particle density reached $10^{16}\,m^{-3}$ with average energies decreasing throughout the pulse and a maximum Q(1s) = 0.04.

At a lower initial deuterium concentration of 5% with an ICRF absorbed power level of 11.25MW, an ohmic current of 4.8MA, a flux average at r = 10cm and $\tau_E \to \infty$, the system energy rose to within 10% of the input power for the 1s RF pulse with a peak energy of 95keV and a thermal anisotropy of $E_\perp/E_\parallel = 3.5$. The electron and tritium energies continued to rise after the ICRF pulse to 30.8keV and 28.1keV respectively at 1.5s. The fusion Q was 1.1 (90% higher than energy equivalent Maxwellians) at the end of the one second ICRF pulse, and the average alpha energy, after an initial decay, rose towards the end of the pulse to 2.2MeV and an alpha particle density of $1.8 \times 10^{17}\,m^{-3}$. At these lower alpha particle densities (< 0.3%), the power absorption resulting from Doppler shift was negligible compared to the deuterium absorption. Since $\tau_E \to \infty$, the system energy continued to rise after the RF pulse was turned off. If the energy confinement times for all species was reduced to 1.5s (with the rest of the plasma and ICRF parameters remaining the same), the deuterium energy rose to 63keV at the end of the RF pulse with a fusion Q = 0.88. The system did not ignite due to the substantial energy losses for all species.

Discussion

This work indicates that an efficiently coupled 1s ICRF power pulse of around 15MW can heat the core of the JET plasma to the Q = 1 regime, if the energy confinement time stays above 1s. The deuterium energy is then in excess of 60keV.

Tests in TFR of a JET Antenna Model

The aim of these tests was to study the behaviour of a specially made antenna (Low Field Side Antenna – LFSA), where the following special JET design features were included:

(i) Low field side excitation.
(ii) Thick screen elements.
(iii) Side protection limiters allowing the outermost closed magnetic surface to be close to the antenna.
(iv) Wider central conductor for improved plasma coupling.

This work performed by EURATOM-CEA Association was supported partly by JET contract and involved active participation by JET team members. The results of this work are summarised below, and some comparison is made with the usual TFR High Field Side Antenna (HFSA).

Design of the LFSA

Figure 58 shows a schematic diagram of the LFSA. In each of the two sections of the antenna, the central conductor (20cm in the toroidal and 20cm in the poloidal directions) was enclosed by a metal box preventing direct RF radiation in the toroidal direction. On both sides of this box, carbon limiters prevented plasma flowing along the magnetic field in the scrape-off layer, from reaching the shield, which was made of 14 Inconel T-shaped rails (1cm thick in the radial direction).

At 60MHz, the electrical length of each of the 2 sections was 30° in the poloidal direction. RF current was maximum in the equatorial plane but remained essentially constant along the antenna, reaching 800A for a supply RF voltage of 20kV. The LFSA load resistance was 2.0–2.5Ω with plasma present. These values were comparable to those computed assuming a model with an ideal Faraday shield of zero thickness in the radial direction (i.e. 1.5Ω for 3cm separation between the central conductor and the plasma edge). This indicated that a thick Faraday shield has excellent transparency to the RF field and that such equipment, required for long duration pulses, should not be an obstacle for efficient RF coupling in the future large machines. Maximum power achieved was 600kW, corresponding to a supply voltage of 17–20kV.

Power Losses Associated with the Impurities

The level of plasma contamination by the limiter, antennae and torus wall metals was determined by spectroscopic analysis of Ni, Fe, Cr and Ti lines.

The following observations were made:

(i) Replacing the Inconel by a carbon limiter reduced the Ni XVIII radiance by a factor > 2.5.

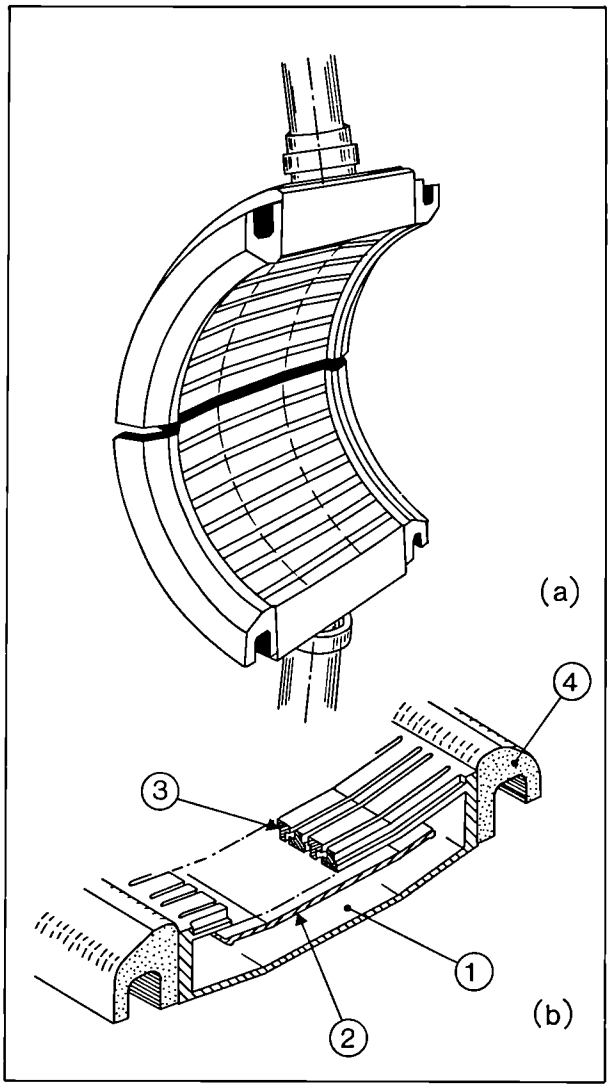

Fig. 58 Schematic diagram of the Low Field Side Antenna (LFSA).

(ii) To a significant extent, the antennae were responsible for the level of metallic impurity release. However, other parts of the machine (in particular the torus wall itself) could not be eliminated as sources.

(iii) The antennae contribution to contamination was due, in some part, to interaction with the lateral sides of the Faraday shield rather than with the shield facing the plasma: changing the front shield from stainless steel to Inconel did not lead to significant changes in Fe XVI radiation. On the other hand, protecting the lateral parts of the Ti HFSA shield by C resulted in a significant Ti reduction.

(iv) The metallic impurity radiation level increased linearly with the RF power and with pulse length (up to 0.1s). Longer pulses indicated a signal saturation, but no data were available on the radiation evolution by higher ionisation states from the central plasma.

(v) The low metal level observed with the HFSA fitted with a Ti shield could not be achieved using the LFSA.

(vi) Even in best conditions, the metal impurity levels were higher than those observed at the same power level during ohmic or neutral injection heating.

(vii) No relationship was found between the metal density and the presence of a high energy tail in the ion distribution function, during RF heating. While varying the ratio n_H/n_D led to different degrees of distortion of the distribution function, this had no detectable effect on the rate of metallic impurity production.

(viii) At constant n_H/n_D ($\cong 0.05$) ratio, metallic impurity production was a minimum when the proton cyclotron resonance was located near the centre of the discharge (i.e. when the heating efficiency was maximised).

Plasma Heating using the LFSA

Most experiments using the LFSA were carried out under the following conditions appropriate to minority heating:

Toroidal field	4.0T
Peak electron density	$1.10^{20}\,m^{-3}$
H to D density ratio	0.05
T_e (on axis)	1.3keV
T_i (on axis)	0.8–0.85keV
V_L	1.5 to 2V

In these conditions, the RF power could be increased up to 600kW, and was limited by a maximum 20kV RF voltage on the transmission line. At this level, the central D temperature rise, evaluated from the increase of the neutron rate, reached 300eV, corresponding to a heating rate of 0.5eV/kW. However, charge exchange measurements of T_D led to larger heating effects, the peak temperature growing from 800 to 1250eV for 580kW RF power (Fig. 59). Such a difference could be attributed to an overestimate of the actual D density in the evaluation of T_D from the neutron rate: an increase of Z_{eff} from 2.5 to 3.5 (as frequently observed in these experiments), corresponded to an increase of the low Z impurities and hence to a decay of the D density, not taken into account in the interpretation of the neutron rate in terms of temperature. Up to the maximum power level, no significant T_e increase was detected. This was confirmed by the loop voltage evolution following a curve similar to the one, in the absence of RF.

Conclusions

The principal characteristics of the antennae were tested, including the main features: thick Faraday shield; limiter protections; and low field side excitation (with the important exception of length: 1/4 the JET design):

(i) The thick Faraday shield did not limit the transparency of the TE mode and the radiation resistance (with plasma) was close to the predicted value.

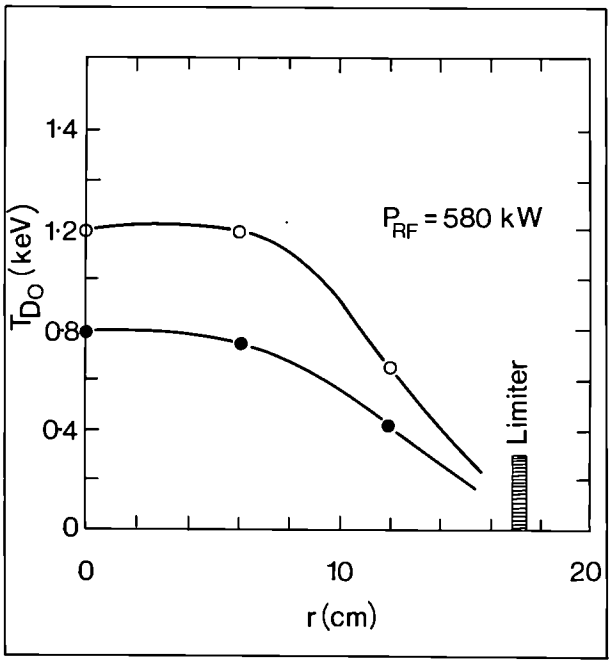

Fig. 59 Deuterium (D) temperature (T_D) as a function of radial position, before and after introduction P_{RF} = 580kW.

(ii) Coupling to 300kW RF power in a high density deuterium plasma ($n_e \sim 1.10^{20}\,m^{-3}$) containing about 5% hydrogen (with $f \cong f_{ch}$ in the centre of the plasma) led to a T_D increase of 0.7eV/kW after 30–50ms, generally followed by a gradual decay of T_D. At higher RF power (600kW), the heating efficiency was reduced to 0.5 eV/kW. As expected, a large increase of the minority species average energy was observed, corresponding to a significant distortion of the velocity distribution function. In all experiments, no significant increase in electron temperature was seen.

No appreciable heating of ions or electrons was observed in the mode conversion regime ($n_H/n_D \sim 0.2$). This was in agreement with the models predicting low efficiency of ion cyclotron damping. However, resonant modes expected on a simple slab model were not observed. In this case, important wave power absorption was likely in the peripheral regions of the plasmas.

A large influx of metallic impurities was observed in all experimental conditions, the level being roughly proportional to the RF power and to the duration of the pulse, at least up to 100ms. On the basis of spectroscopic data and a numerical transport code, the total metal density in the plasma core was estimated at $4–8 \times 10^{16}\,m^{-3}$ at the end of a 100ms 300kW RF pulse, corresponding to 75–150kW radiated power. This level is higher than that observed in the HFSA experiments, particularly when the antenna was protected by C or Ti limiters.

Although no clear conclusion was derived on the mechanisms responsible, various observations tend to indicate that these effects should be related to the absorption of some fraction of the wave power in the scrape-off layer rather than to the damping mechanisms in the plasma core.

Ion Cyclotron Emission Studies

The possibility of measuring the ion cyclotron emission (ICE) spectrum from JET, using one half of a heating antenna as a receiver, is being studied. The theory for ICE can be developed by analogy with the electron cyclotron emission (ECE) case. For JET, with ion temperatures ~5keV and density in excess of $10^{19}\,m^{-3}$, the emission at twice the ion cyclotron frequency ($2f_{ci}$) should be near black-body at the plasma centre. The radiation coupling to the antenna is well understood from studies carried out for the heating programme, suggesting that ion temperatures in the plasma centre can be deduced from ICE spectrum measurements.

To test this proposal, TFR measurements have been made using both low (LFSA) and high field (HFSA) side antennae to detect the ICE spectra from both ohmic and ICRH discharges, using a narrow band filter to reject the heating frequency. Fig. 60 shows spectra detected by the LFSA during ohmic discharges for different values of the toroidal magnetic field (similar spectra were observed with the HFSA). When the frequencies of the characteristic peaks were transformed to major radius geometry, these appeared to be emitted from the plasma periphery. However, the emitted power (at $2f_{ci}$ from the plasma centre was 1/3 of the estimated black-body level, which is consistent with the fact that the TFR plasma was not optically thick for ICE.

During ICRH at the proton cyclotron frequency in a deuterium plasma with a hydrogen minority, the overall

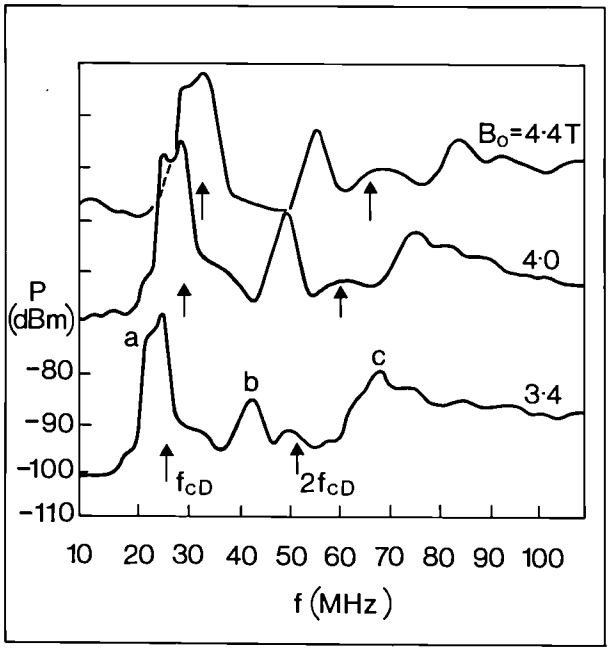

Fig. 60 RF Spectra detected by the LFSA during TFR ohmic heating discharges for different values of magnetic field.

signal level increased by a factor x100 and the spectra exhibited peaks centred at 1/2, 3/2, and 5/2 of the RF heating frequency. When heating with the LFSA and a low minority concentration, η (i.e. the minority heating regime), these peaks had a relatively broad bandwidth and were only present when the proton resonance was within the plasma (Fig. 61(a)). When heating with the HFSA and the proton resonance occurred near the outside plasma edge (i.e. the wave conversion regime), the peaks narrowed and their amplitudes increased as η was increased (Fig. 61(b)).

Although non-thermal levels of emission from RF heated discharges are not fully understood, the emission measurements look encouraging for use as an ion temperature diagnostic in JET. Such tests will take place in JET at the beginning of RF operations.

Fusion Technology Division

(Division Head: J.R.Dean).

Fusion Technology Division is responsible for the design and development of remote handling methods and tools to cope with the requirements of the JET device for maintenance, inspection and repairs. The Division also undertakes design and construction of facilities for the handling of tritium. These tasks are carried out within three Groups: the Remote Handling Group; Remote Handling Applications Group; and the Tritium Group.

The Remote Handling Group is responsible for the development, acquisition and commissioning of the general purpose remote-handling machines and the viewing and sensing equipment, based largely on robotics practices. This includes general purpose manipulators, transporters to carry and place the manipulators, JET components and special tools. Also included are special purpose, automatic, self-propelling cutting and welding machines for the standard JET lip-joints. The Group has also developed and now specifies, procures and tests all of the demountable water and vacuum connections for JET.

The Remote Handling Applications Group is responsible for applying remote handling equipment and techniques to tasks on JET by ensuring compatability of design and access of subsystems and components, by developing local tools to meet all needs and by preparing remote handling schedules based on procedures provided

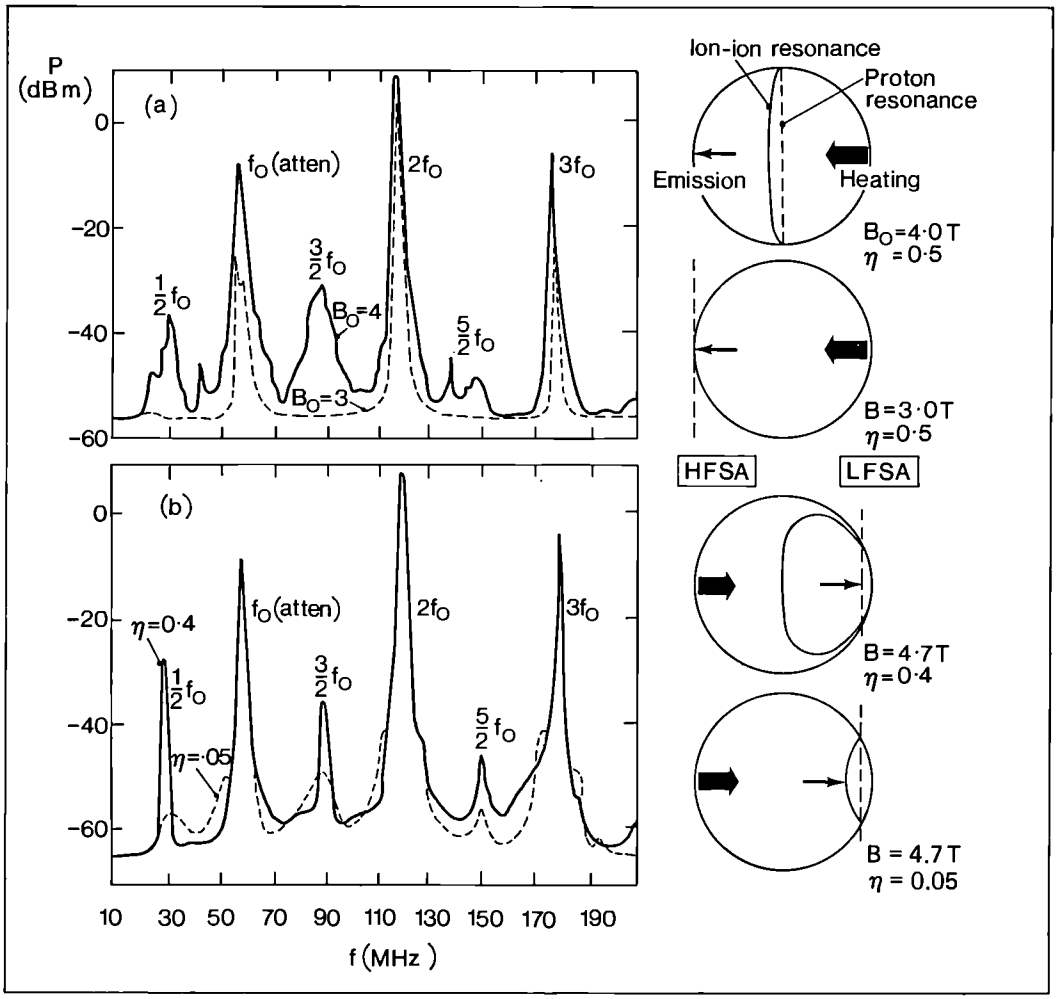

Fig. 61 RF Spectra detected (a) during heating with the LFSA; and (b) during heating with the HFSA.

by the designers. This Group will also provide the means and techniques to carry out work on the machine when it is contaminated with beryllium and when the components are radioactive.

The Tritium Group is responsible for the design and construction of facilities for the handling of tritium on the JET site.

Remote Handling Group

Articulated Boom and End Effectors

(P.D.F. Jones)

Boom

After full tendering, the contract to manufacture the articulated boom was placed in July 1983. It is nearing completion and will be delivered for testing and commissioning in August 1984. The articulated boom will be the only means for carrying components, machines, tools and equipment into and out of the JET torus when it has become radioactive. Its four straight sections and four motorised horizontal joints will enable it to reach any point in the equatorial plane round one half of the inside of the torus, entering through the main horizontal port in either Octant No. 1 or the diametrically opposite Octant No. 5 (Fig. 62).

The boom is designed to carry 1 tonne when fully extended to 9m as a cantilever, which will cope with the weight of the proposed radio-frequency (RF) antenna. The limb has been optimally chosen in respect of strength and weight, from those materials acceptable within the vessel, and is aluminium for the end section and stainless steel for the others. The aluminium fabrication weighs 350kg, the stainless steel about 1500kg and the mild steel about 14000kg (giving a total of about 16 tonnes).

The boom will be carried on a mild steel trolley running beneath a mild steel beam supported between the wall of the torus hall and a support spanning two of the JET magnetic limbs. This boom trolley and beam assembly will be placed in position and removed remotely by the 150 tonne crane, when JET has been irradiated. Fig. 63 shows a model of the assembly in its working position.

All motions are driven by DC motors. It is intended

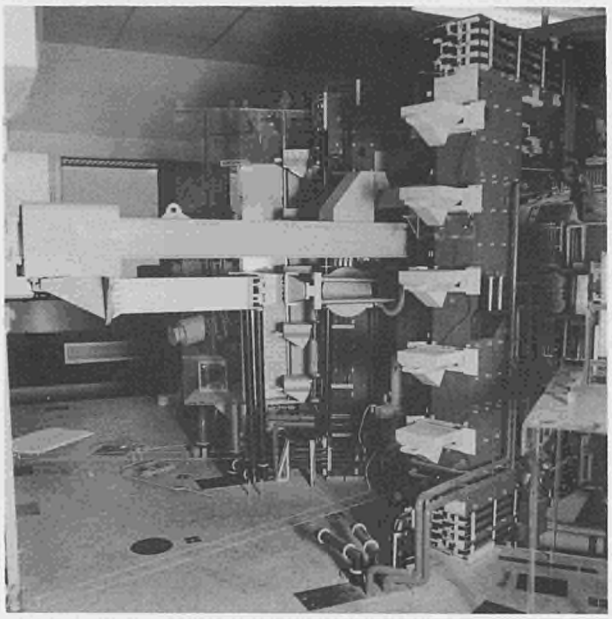

Fig. 63 Model of boom in working position.

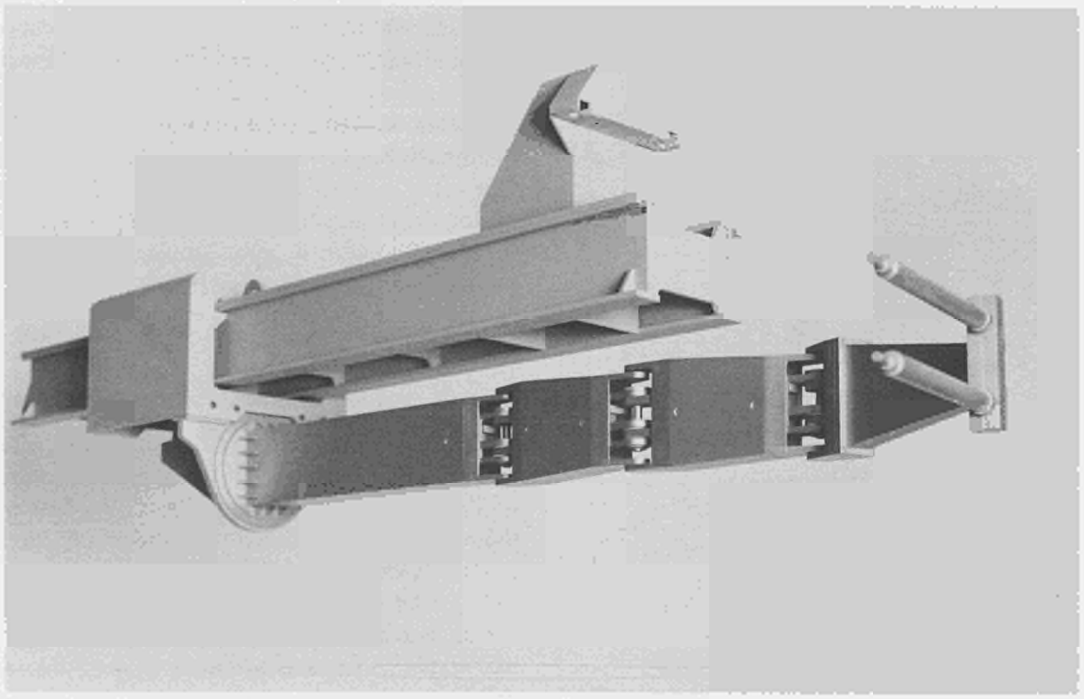

Fig. 62 Model of articulated boom carrying a limiter.

that the four horizontal joints will eventually be under closed-loop servo control. Initially, they will be operated manually, from position transducer readings, one at a time. A single control panel for this is nearly completed by the boom manufacturer.

Originally, the principal task of the boom was to carry the JET limiters of initial design or a force-feedback manipulator. Consequently, a "grabber" fitting on the end of the boom and attaching under remote control to a limiter was included in the manufacturing contract which is nearing completion. This provides extra motions such as linear vertical motion, tilt and operation of the clasping jaws. In all, there are seven motions of the boom-grabber combination, in addition to the vertical joint rotations, and these will be manually operated from transducer readings.

It is now also recognised that the boom should be used to replace the projected belt limiters and RF antennae. More devices are needed to attach these to the boom, which are in the process of design and construction. The boom will be connected to the pumping box door by a flexible detachable sleeve which prevents egress of contaminated material from the vacuum vessel into the torus hall.

RF Antenna (A_0) Grabber

The design study has been completed of a simple hands-on tool that can be attached to the end of the boom flange for lifting a 700kg A_0 antenna, without the tiles attached. This device was designed to engage the antenna with 4 bolts, and to rotate it about a horizontal and a vertical axis to bring the long side of the antenna alongside the grabber, in order to pass it through the horizontal part of the vessel (see Fig. 64). The design caters for a hands-on assembly/dismantling operation, but is flexible in that the grabber can readily be converted to a remote handling tool with the minimum of expense. The design of this conversion is at an advanced stage. This tool is suitable for extension to full remote handling capability and the design caters for tight clearances (of about 8mm) around the main port during entry and withdrawal. Drawings and specifications were prepared for tender action. Included in this contract is a special remote handling lifting frame for transferral of the A_0 antenna from the assembly hall to the articulated boom trolley beam situated near the torus.

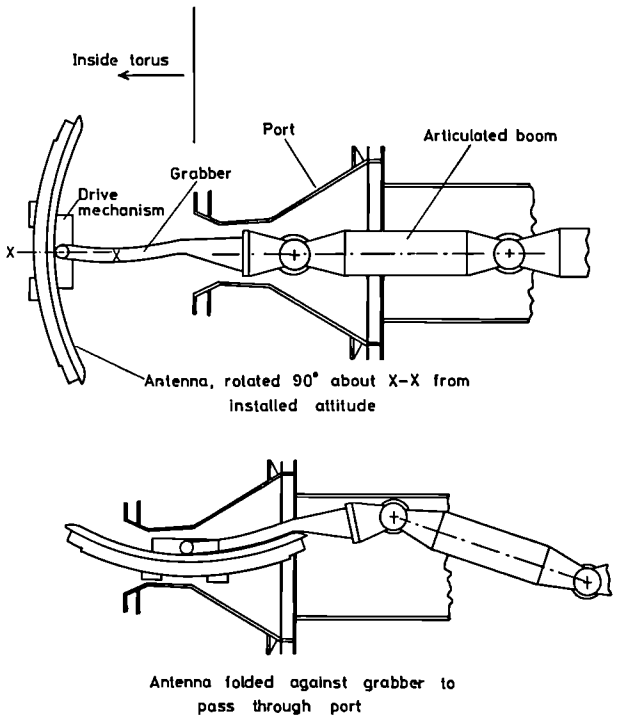

Fig. 64 Boom passing RF antenna through port.

RF Antenna (A_1) Grabber

A study of the handling of the A_1 RF antenna was undertaken. This component will be installed in two different parts and special lifting pins have been developed for fail-safe transferral of load from grabber to torus wall. These features have been incorporated in the design of the A_1 antenna.

Toroidal (Belt) Limiter Gripper

A design was initiated on a device to handle the 26 belt limiters weighing approximately 150kg, plus the facing tiles. It consists of a gripper mounted on an extension fixture flanged to the articulated boom. The gripper is provided with an adjustable tilt motion and the extension fixture includes pan-tilt-twist motion, so that it is possible to reach the limiters at about 700mm above and below the equatorial plane, to bring them to the equatorial plane and to rotate them to pass through the port.

There is need for close control of the trajectory and attitude of the limiter along segments of arcs to pass behind adjacent limiter piping and with vertical strokes for the final insertion of the cooling pipes, which will then have to be welded. The components and design initiated in the A_0 antenna's grabber have been utilised as far as possible although several extra features are required.

Boom Extension

A boom extension has been designed which allows for three further motorised degrees of freedom at the boom end. This multi-purpose extension will position the servo-manipulator in the torus and also the belt limiter gripper. The same type of compact high-torque gearboxes and motor drives are used to drive the pan and tilt mechanisms. A space is also provided for cable reeling mechanisms used for in-vessel work.

Special Tools for handling, cutting and welding

RF Transmission line R.H. Tools

(P.D.F. Jones)

Tools are required for handling, lifting and assembly of various components of the horizontal transmission line of the RF heating system using the A_0 antenna. While the tools were required for the hands-on assembly operation, they will also be used during the test phase by EURATOM-CEA Association, Fontenay-aux-Roses, and future remote handling dismantling/assembly. A comprehensive set of tools, shown in Fig. 65, has now been delivered.

A preliminary design study for tools for lifting and

Fig. 65 Set of tools for handling RF transmission line components.

assembly of the vertical (down) lines of the RF heating system was necessary to enable the down-line itself to be optimally designed. This task is important, since the transmission lines must be removed, before the antenna can be extracted.

Cutting of welds on water-cooled limiters

(M. Wykes, J. Schreibmaier)

Water cooled limiters were removed from the torus during the December 1983 shutdown. Prior to withdrawing the limiters from the vacuum vessel, the seal welds between the two limiter pipes and their abutting guide tubes had to be cut. The cutting system had to meet the following criteria:

- Use a conventional cutting action.
- Produce a guide-tube surface finish suitable for rewelding without subsequent rework.
- Produce material offcuts which would be verifiably capturable.
- Release no organic materials to the working environment.
- Easily operable by a skilled fitter after a short training period.

A survey or proprietary pipe cutting machines revealed that a split-bodied orbital pipe lathe was available, which would fit into the available access and cut at the required diameter. As supplied, this machine was clamped to the outside of the pipe by four feet equispaced around the machine bore (two fixed and the remaining two being radially adjustable). A special adapter was made to mount the machine to the limiter, as with the limiter drive worm assembly removed the only mounting surface available was the lead screw and its mating driving nut. Fig. 66 shows an elevation of the mounting arrangements. The special adaptor consisted of two end flanges with screwed bores to engage with the limiter lead screws and connected by a machined pipe section welded to the flange outside diameters. The space between the flanges and the pipe section bore was designed to accommodate the captured limiter drive nut. The special adaptor was split on the centreline for assembly purposes and held in position by countersunk capscrews.

To prevent contamination of the torus environment the exhaust air of the drive motor was ducted out of the Torus Hall. To ensure offcut capture, the cutting area was surrounded in a polythene tent. Fig. 67 shows a cutting machine in operation on a limiter. It was found in practice that a cutting speed in the region of $10\,cm\,s^{-1}$ produced the best cuts, in terms of surface finish and smoothness of operation. A tendency to chatter was eliminated by intermittently applying small amounts of demineralised cooling water. The axial weld length cut was approximately three times greater than the cutting tool width and since the machine had no axial feed, it was unclamped and reset three times to complete the cutting of each weld. The cycle time for the set-up and cutting of each weld was approximately 2½ hours.

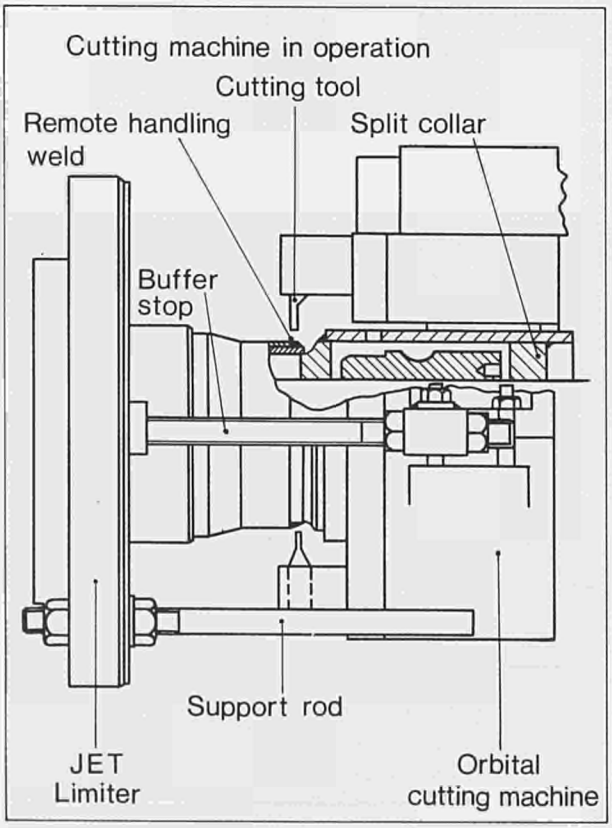

Fig. 66 Mounting of limiter pipe cutter.

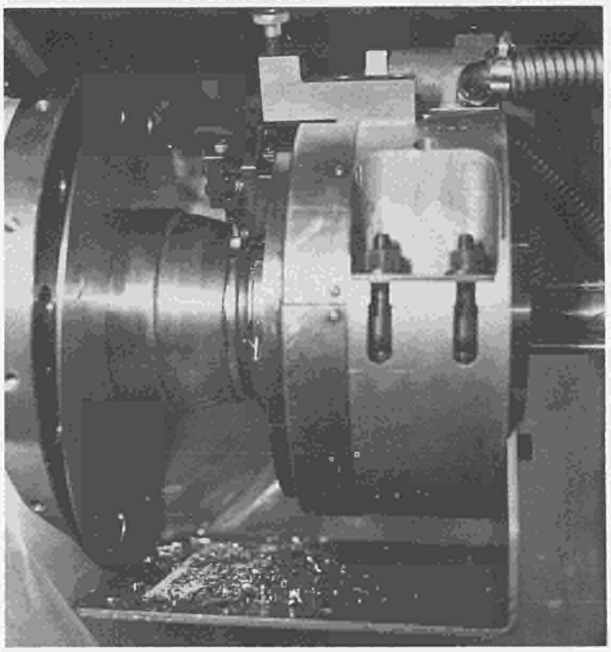

Fig. 67 Cutting limiter seal welds with modified orbital lathe.

Connectors

Remote Handling Pipe Clamps for the Toroidal Cooling System

(M. Wykes)

Cooling water for the toroidal coils is supplied through crown rings above and below the torus. The crown rings are connected to the distribution manifolds on the mechanical structure by 150 flow and return pipes, which incorporate hinged and gimballed bellows units to accommodate thermal expansion. A fault analysis of the pipe system indicated that in-service failure of the bellows hinge bearing would result in bending moments large enough to separate the JET standard "V-band" pipe clamps used in other water pipe systems. An additional "heavy duty" special pipe clamp was designed to meet the following criteria:

(a) Sufficiently compact to fit around all required flanges without fouling adjacent machine elements.

(b) A bending moment capability so that the adjacent pipe-line would yield before the flanged connection leaked.

(c) Meet the requirements for Remote Handling Class 2.

Fig. 68 shows the special pipe clamp. It consists of identical half pieces with internal profiles to match the mating flanges. The halves are connected by two cap screws with replaceable nuts. To minimise fatigue loading, the cap screws load the clamp halves through disc springs which attenuate the cyclic thermal dilation of the clamp halves. The clearance between cap screws and their passing holes in the clamp halves is such that the connection can be made by sequentially running in each cap screw twice with a suitable wrench. The clamp sets are designed for two-handed servomanipulator handling. One servomanipulator jaw supports and manoeuvres the clamp set by gripping the side faces of one of the clamp halves, while the other servomanipulator jaw wields a wrench to run in the cap screws.

Fig. 68 Remote handling pipe clamp.

Anti-seizure coating for screw threads

(A. Nowak)

To prevent metals seizing together in the absence of oxygen (particularly identical metals, especially at high temperatures), titanium nitride has been identified and tested as a surface treatment for nuts and bolts. It can withstand 500° C and will not contaminate the plasma. It is applied by "sputter ion plating" to a thickness of $1.5–2 \times 10^{-6}$ m. Smooth rolled threads are best, with the oxide layers removed before treatment by blasting with fine glass beads. Spring loaded nut and bolt pairs have been thermally cycled up to 500° C in vacuum (10^{-5} mbar). No significant deterioration was noticed after one 24h cycle, but testing continues. The alternative molybdenum disulphide coating reacts with the silver gaskets of high vacuum flanges.

Remote Handling Applications Group

In Vessel Inspection System

(R. Cusack, L. Galbiati, P. Presle)

In the system now fitted to JET, four identical television cameras can be inserted into the torus through symmetrically disposed top ports.

The three main subsystems, delivered in mid 1983, are as follows:

- Vacuum and guide units: Incorporated into each guide unit is a viewing tube with a glass window attached (Fig. 69). Due to the narrowness of the available port, the tube size was limited to 54mm diameter. Long bellows form the barrier between the air and the vacuum, permitting the cameras to be retracted from the torus and parked behind vacuum valves. In order that the torus vacuum is

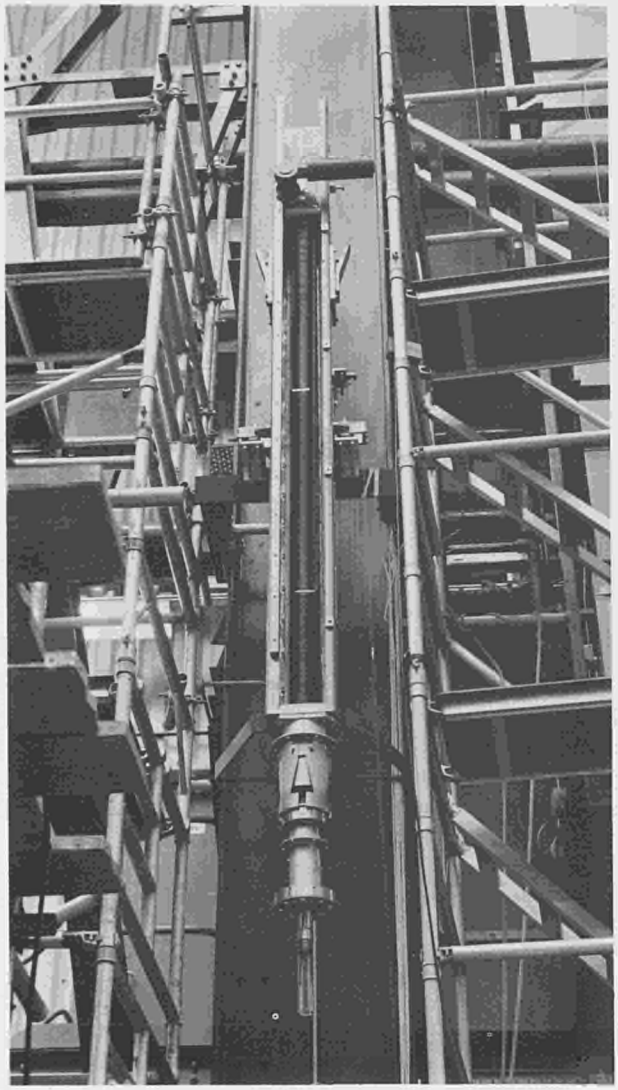

Fig. 69 Camera drive and bellows assembly.

not degraded, vacuum is always maintained between the valves and the bellows, by a secondary pumped manifold. Vacuum and guide units were installed during September 1983. Cold and hot leak testing of the guide units should take place during January 1984.

- Viewing Assembly: In the latter part of 1983, the viewing assemblies were tested and should be inserted into the viewing tubes in January 1984. Each assembly comprises a television camera with a specially designed telescopic zoom lens operating over a range of 35mm to 120mm, a rotable prism and a flash light with a reflector. Motorised adjustment is provided for: focussing; iris opening; changing a prism angle to vary the vertical viewing angle; rotation of the viewing tube to vary the horizontal viewing angle; and rotation of the flash light reflector. Flash-light is used to overcome the severe heating problems of a continuous intense light in a confined space. The four viewing assemblies were driven into the torus, when the torus was at atmospheric pressure (Fig. 70) and pictures recorded (Fig. 71). During this operation, one assembly scanned, while an adjacent one provided illumination.
- Control System: Control system software provides for local control at present but, by May 1984, the system will be controlled from the JET control room. A digital frame store is provided to capture a still picture during the flash. The image can later be enhanced, analysed and compared with previous records. In future, sequences of viewing fields will be programmed and repeated under computer control.

Some mapping of the torus has been undertaken, storing in the computer a set of adjustment parameters corresponding to specific named positions on the torus wall. During this operation, an optical resolution was achieved at the viewing screen of 1mm at 5m distance. The maximum tolerable temperature of the air-cooled cameras is 60° C, so these can operate only in a relatively cool torus. They will remain in their retracted positions while the torus is baked at 300° C and the ports are at 170° C.

Work on JET during Operations with Beryllium
(S.J. Booth)

Beryllium has an attractive combination of physical properties which have led to its consideration as a facing material for JET vacuum vessel components, such as the limiters and first wall tiles. Its low Z, high resistance to thermal shock and reasonable thermal conductivity make it an alternative material to such contenders as graphite and nickel.

However, there are a number of problems associated with the handling of beryllium and its compounds. In particular, when in a finely divided form, beryllium is

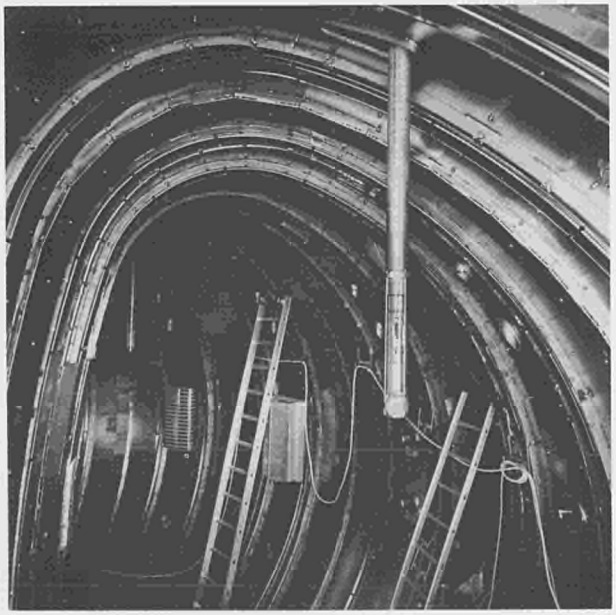

Fig. 70 In vessel inspection camera in viewing position.

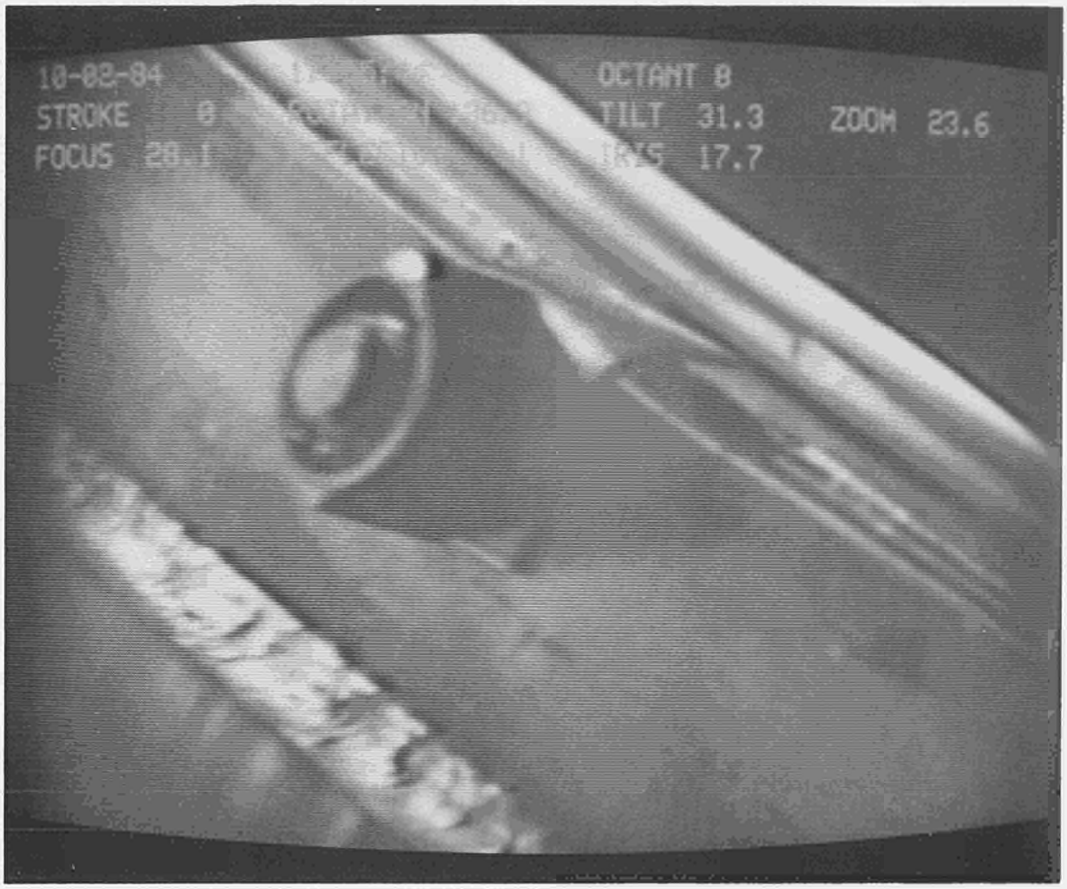

Fig. 71 View of protection plate rail taken with in-vessel inspection camera.

recognised as an injurious dust and comes under the general provisions of the Health and Safety at Work Act. Accordingly, operations with beryllium should be carried out in a controlled area and the approved upper limits for concentrations are shown in Table X.

Beryllium associated handling operations on JET would be conducted in accordance with accepted codes of practice, and, as far as possible would be confined to the high integrity double walled vacuum vessel. The Torus Hall would act as a closed secondary containment.

For maintenance work inside the vessel, a portable cabin (illustrated in Fig. 72) has been designed, which can be sealed onto the pumping chamber to allow access into the vessel for personnel wearing suitable protective clothing and respiratory protection. The cabin would include a change area and the services necessary for maintenance work and could also be operated away from the machine for waste packaging, equipment maintenance and decontamination.

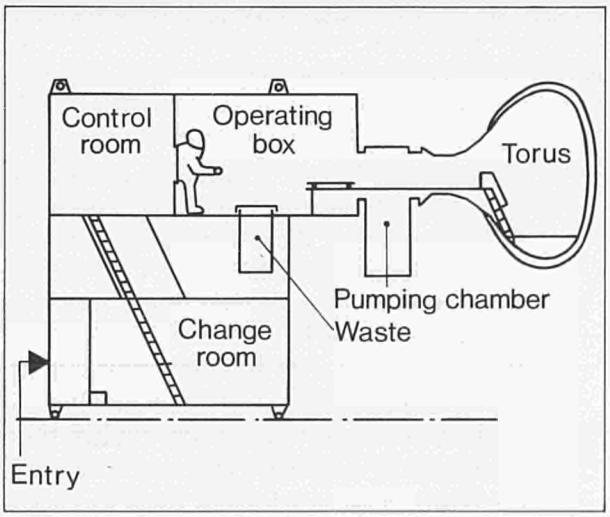

Fig. 72 Entry cabin for work in contaminated areas.

Table X

	Concentration in air $\mu g/m^3$	Surface contamination $\mu g/m^2$
Controlled area	2	100
Uncontrolled area	0,01	10

Less frequent maintenance on peripheral equipment outside the vessel would be conducted in temporary enclosures, designed to fit the requirements at the time.

During all the operations, monitoring and analysis of samples would be conducted by the Joint Health Physics and Safety Section, who would also organise the training of staff in the appropriate safety requirements.

The risk of a spread of beryllium dust from the machine would be minimised during maintenance, by holding the vessel at a pressure slightly below atmospheric, and eliminating ventilation air flows which could induce dust migration. This could be achieved by employing pressure regulating devices, such as Vortex amplifiers, in the cabin ventilation circuit. Man access during such operations would be in pressurised PVC suits fed with a breathing air line. These would be entered via a double lidded port, either at the neck opening or in the rear of the suit.

In addition to enabling the safe handling of beryllium, the intervention cabin will provide a clean conditions access system and be compatible with handling operations in the active phase.

Tritium Group

Tritium Plant

(W. Riediker)

If the machine performs as planned with hydrogen and deuterium, tritium will be introduced into the plasma in mid-1988. Thereafter, the planned 10,000 pulses at full performance, with approximately equal particle mixtures of deuterium and tritium, are expected to use about 2kg of tritium. If this was passed through the machine and discarded it would cost more than $40M for purchase and disposal. Consequently, a recovery plant is projected which will chemically purify the exhaust gases from the torus and from the cryopanels of the neutral injection boxes, and separate the hydrogen isotopes for re-use.

The anticipated loss is less than $14M. The tritium inventory of the plant is expected to be about 10g, which is much less than would need to be kept on site if the once-through principle was used.

Based on proposals in a preliminary study of suitable processes by the EURATOM-CEA Association, France, gas chromatography has been chosen for isotope separation. In the last few months, an engineering concept has been developed using cryogenic pumping techniques and enclosing the primary circuit components in vacuum vessels which serve as the secondary containment. The more difficult access is offset by not requiring the complex clean-up systems and operating teams necessary with classical glove-box containment.

JET–Scientific

Introduction

The Scientific Department is responsible for the definition and execution of the experimental programme, the specification, procurement and operation of the diagnostic equipment and the interpretation of experimental results. The Department is now in its Operations Phase configuration with one Theory and two Experimental Divisions. The structure down to Group Leader level is shown in Fig. 73 and the list of Divisional Staff at December 1983 is shown in Fig. 74.

Summary of Progress

During early 1983, considerable activity was devoted to installing those diagnostics needed for the first operation of JET, and the following systems were made operational for the first plasma discharge in June:

- Single channel interferometer.
- Flux loops.
- Internal poloidal field pick-up coils.
- One bolometer.
- Limiter surface temperature diagnostic.

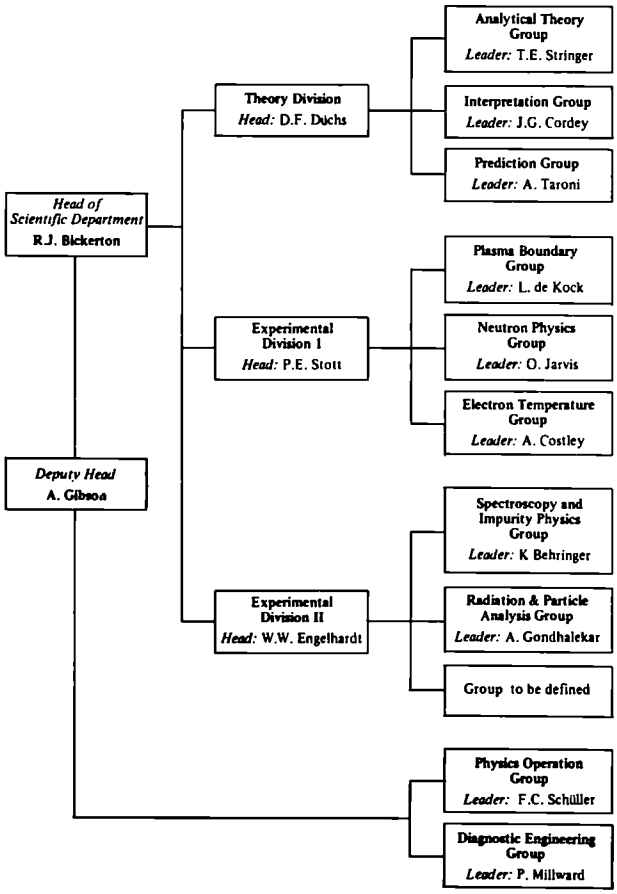

Fig. 73 Scientific Department, Group Structure (December 1983).

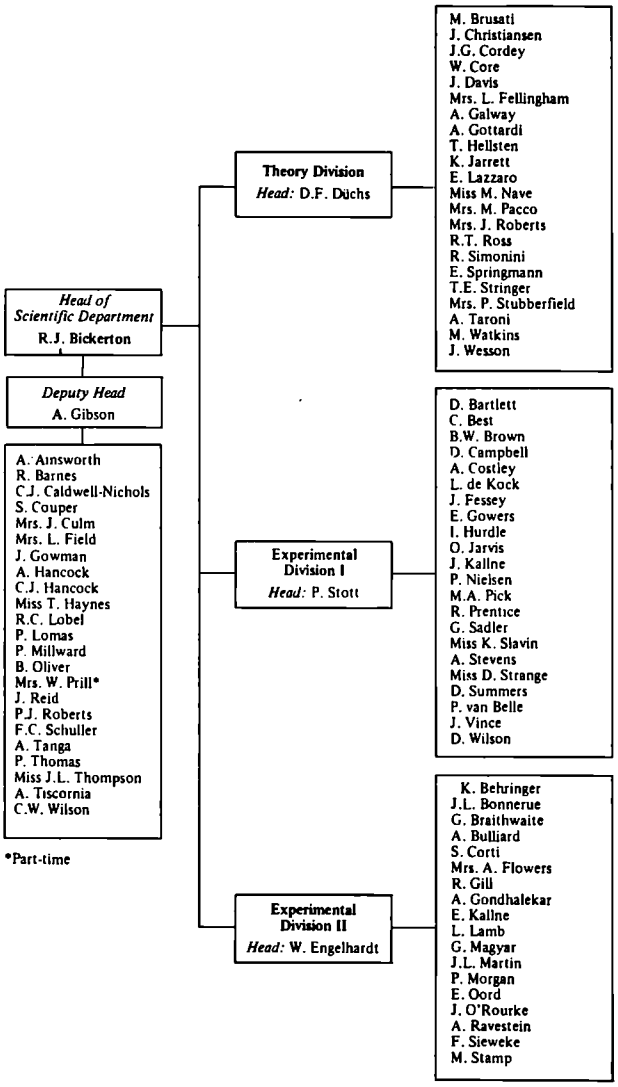

Fig. 74 Project team staff in the Scientific Department (December 1983).

Table XI
Status of the JET Diagnostics Systems

Diagnostic System No.	*Diagnostic*	*Purpose*	*Association*	*Status Dec. 1983*	*Expected Date for operation in JET*
KB1	Bolometer Scan	Time and space resolved total radiated power	IPP Garching	Operational	Mid 1983 partly Early 1984 fully
KC1	Magnetic Diagnostics	Plasma current, loop volts, plasma position, shape of flux surfaces	JET	Operational	Mid 1983
KE1	Single Point Thomson Scattering	T_e and n_e at one point several times	Risø	Being installed	Early 1984
KG1	Multichannel Far Infrared Interferometer	$\int n_e$ (r) ds on 7 vertical and 3 horizontal chords	CEA Fontenay-aux-Roses	Under construction	Early 1984
KG2	Single Channel 2mm Interferometer	$\int n_e$ (r) ds on 1 vertical chord in low density plasmas ($< 10^{14}$ cm^{-3})	JET and FOM Rijnhuizen JET	Operational Extension to 1 mm	Mid 1983 Mid 1984
KH1	Hard X-ray Monitors	Runaway electrons and disruptions	JET	Operational	Mid 1983
KH2	X-ray Pulse Height Spectrometer	Plasma purity monitor and T_e profile	JET	Under construction	Mid 1984
KJ1	Soft X-ray Diode Arrays	MHD instabilities and location of rational surfaces	IPP Garching	Provisional system operational. Full system under construction	End 1984
KK1	Electron Cyclotron Emission Spatial Scan	T_e (r,t) with scan time of a few ms	NPL, Culham and JET	Partly operational	Late 1983
KK2	Electron Cyclotron Emission Fast System	T_e (r,t) on μs time scale	FOM, Rijnhuizen	Under construction	Mid 1984
KL1	Limiter Surface Temperature	(i) Temperature of wall and limiter surfaces (ii) Monitor of hot spots on limiter	JET and KFA, Julich	Partly operational	Mid 1984
KM1	2.4 MeV Neutron Spectrometer	Neutron spectra in D-D discharges, ion temperatures and energy distributions	UKAEA, Harwell	Construction proceeding	Early 1985
KM3	2.4 MeV Time-of-Flight Neutron Spectrometer		NEBESD, Studsvik	Construction proceeding	Mid 1984
KN1	Time Resolved Neutron Yield Monitor	Time resolved neutron flux	UKAEA, Harwell	Operational	Mid 1983
KN2	Neutron Activation	Absolute fluxes of neutrons	UKAEA, Harwell	Construction proceeding	Early 1985
KN3	Neutron Yield Profile Measuring System	Space and time resolved profile of neutron flux	UKAEA, Harwell	Construction proceeding	Early 1985
KR1	Neutral Particle Analyser Array	Profiles of ion temperature	ENEA Frascati	Being installed	Early 1984
KS1	Active Phase Spectroscopy	Impurity behaviour in active conditions	IPP Garching	Being designed	Mid 1985
KS2	Spatial Scan X-ray Crystal Spectroscopy	Space and time resolved impurity density profiles	IPP Garching	Being designed	Mid 1985
KS3	H_α and Visible Light Monitors	Ionisation rate, Z_{eff}, Impurity fluxes	JET	Operational	Early 1983 Early 1985 Full System
KT1	VUV Spectroscopy Spatial Span	Time and space resolved impurity densities	CEA Fontenay-aux-Roses	Under construction	Mid 1984
KT2	VUV Broadband Spectroscopy	Impurity survey	UKAEA, Culham	Being installed	Early 1984
KT3	Visible Spectroscopy	Impurity fluxes from wall and limiters	JET	Operational	Mid 1983
KX1	High Resolution X-ray Crystal Spectroscopy	Ion temperature by line broadening	ENEA Frascati	Under construction	Early 1985
KY1	Surface Analysis Station	Plasma-wall and limiter interactions including release and hydrogen isotope recycling	IPP Garching	Construction proceeding	Early 1985
KY2	Surface Probe Fast Transfer System		UKAEA, Culham	Construction proceeding	Late 1984
KY3	Plasma Boundary Probe	Simplified probe system for monitoring progress of discharge cleaning and preliminary plasma-wall interaction experiments	JET UKAEA, Culham and IPP, Garching	One unit ready for installation. Second unit being constructed	Mid 1984
KZ1	Pellet Injector	Particle transport, fuelling	IPP, Garching	Under construction	Mid 1985

- Hard X-ray monitors.
- Neutron yield counters.
- Health physics monitors.
- Visible spectrometers using fibre optics.
- H-alpha monitors.

Further diagnostic systems were made operational before the end of 1983. These included a fourteen channel bolometer array, four X-ray diodes, a quartz UV spectrometer, an optical multichannel analyser and part of the electron cyclotron emission system. In addition, the single point Thomson scattering, neutral particle analyser array and the VUV broadband spectroscopy apparatus are being installed and should be operational early in 1984. The status of JET's diagnostic systems at the end of 1983, is summarised in Table XI and their general layout in the machine is shown in Fig. 75. The bulk of the systems not already installed should be operational by mid-1985. As well, feasibility studies on potential new diagnostics and upgrades of existing ones have proceeded, particularly on a microwave reflectometer, a 1mm microwave interferometer, a LIDAR (Light Detection and Ranging) Thomson scattering system and 14MeV neutron spectrometers. During the year, staff in the Experimental Divisions, the Diagnostic Engineering Group and the Operations and Development Department, were still heavily involved in completing specifications and checking interfaces and remote handling capability for diagnostics being constructed in the Associations.

In addition to the requirements of assisting with machine operation and maintaining the diagnostics systems following start-up, experimental planning, control room duties and interpretation of results have become an important part of the work of the Department. Considerable effort has been devoted to optimising breakdown conditions and understanding current-rise phenomena and disruptions occurring in the plasma. Impurities played a major role in the plasmas obtained during first operation, producing radiation losses and influencing stability. The sources, time evolution and transport phenomena were studied using spectroscopic diagnostics and methods of reducing the effects are being investigated.

Theoretical analysis, interpretation and prediction are powerful tools in providing a description of plasma behaviour and improving understanding of plasma phenomena as plasma parameters approach those necessary for a fusion reactor. Following an increase in staff numbers, activity in theoretical studies increased during 1983,

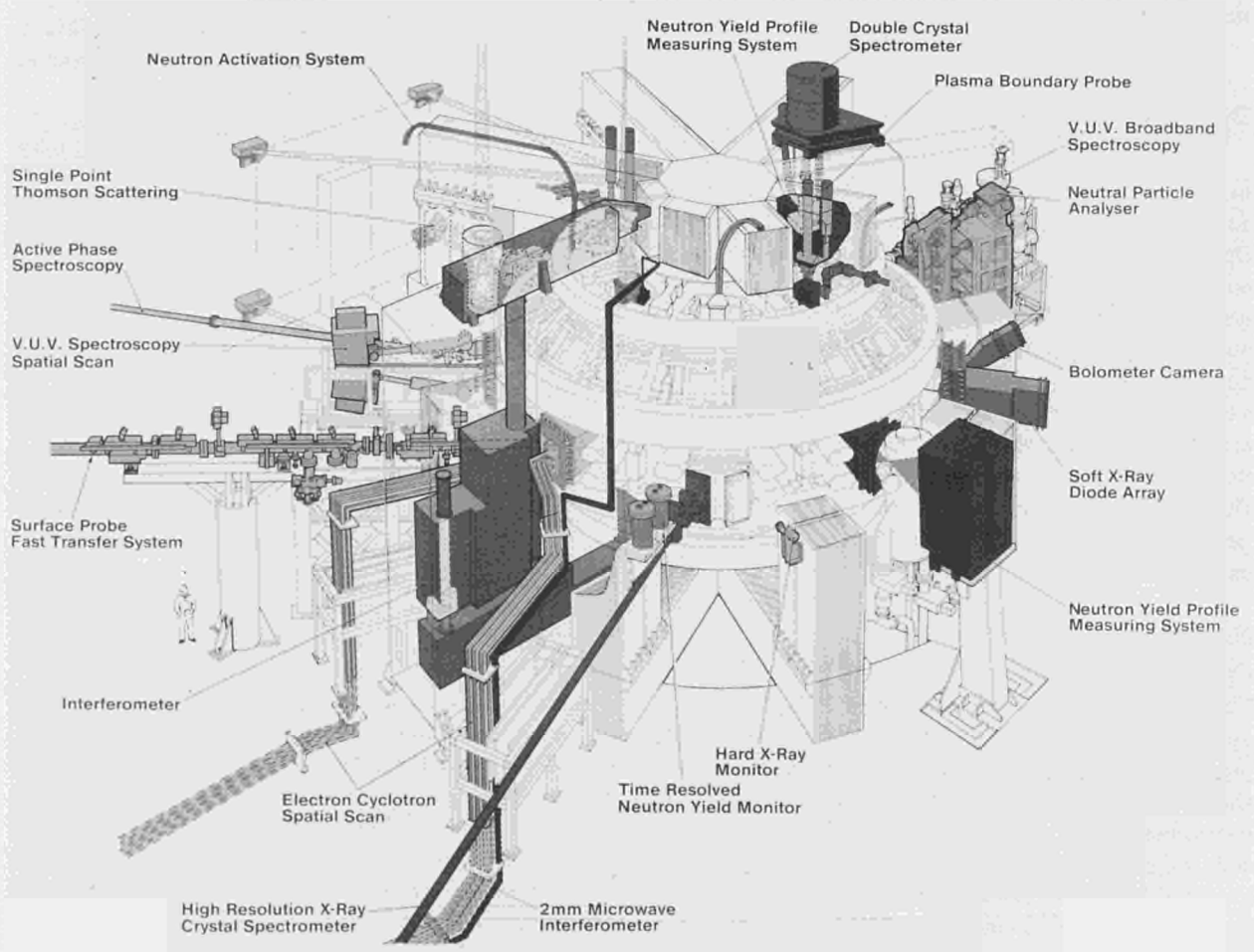

Fig. 75 Layout of Diagnostics, in the machine.

particularly in MHD stability studies and optimisation of RF and neutral injection heating schemes. During the early part of the year, interpretation codes were developed and installed on the relevant computers and a general display package was produced. Since start-up, analysis of data, both during machine operation and subsequently, has been a priority activity. Prediction work has been important in studies of future JET plasmas, especially those involving different limiter materials, changed geometry and various heating scenarios.

The system for the attachment to the Scientific Department of staff from the Associations came into operation during 1983. Task Agreements centred around specific fields of research have permitted close collaboration with Association Laboratories, in which these laboratories have accepted responsibility to play a significant (but not exclusive) role in particular investigations. In many cases, the agreements are closely connected to diagnostic instruments built in the Associations, but they are also based on existing special expertise, and include such topics as: installation, commissioning and operation of diagnostics; physics investigations; and interpretation of results in collaboration with the JET team. Further details are included in the following Sections. For smaller laboratories, the simple assignment of individual staff is more appropriate. A few staff members only have been attached under these latter arrangements, but numbers should grow now that experiments are underway.

Physics Operations Group

In 1983, experimental planning and control room duties became an important part of the work of the Physics Operations Group; these included commissioning tests on pulse discharge cleaning, plasma fault protection system and measurements of the poloidal field distribution. Operation related physics subjects such as breakdown conditions, current-rise phenomena and disruptions were studied. Software tools, such as interpulse display programmes, were refined and tested under real operational conditions. Two working groups, overseen by the Physics Operations Group were established to study the possibilities of using magnetic limiters and pumping panels in JET.

Planning of Experiments

Organisation of Operations

Following start-up of JET in Summer 1983, a system of operation was established, in which Programme Leaders proposed an outline experimental plan for one month ahead. This was discussed and approved in detail by an Experiments Committee, which met weekly to determine and progress programme aims. Daily operations were executed by a team headed by a Session Leader assisted by an Engineer-in-Charge, a Physicist-in-Charge and a member of the Physics Operations Group. This daily team defined a pulse schedule for the day, involving the following parameters:

- time sequence scenario.
- toroidal field flat-top value.
- voltage waveform on the primary coil.
- waveforms for radial and vertical position control.
- initial filling pressure and subsequent gas injection waveform.

During the session, deviations from the pulse schedule were agreed regularly on the basis of the observed data. On good days, about twenty pulses were achieved; this modest number was determined partly by necessary discussions on the course of action; partly by software optimisation; and partly by hardware failures. It became clear that improvements would be necessary to increase this rate, during 1984.

After sessions, a discussion meeting on the day results was held to provide guidance for the next day's pulse schedule. In addition to these small meetings, larger bi-weekly meetings were organised where staff presented preliminary analyses of the measurements for the teams general information.

Proposals for Experiments

The experimental plan, endorsed by the Experiments Committee, was proposal driven (i.e. papers proposing certain conditions to study particular topics were submitted to the meeting). The Physics Operations Group was especially involved in two main topics:

- general plasma optimisation: breakdown conditions, current rise-rates and exploration of the accessible q and $\bar{n}R/B$ parameter space.
- disruption-studies.

Commissioning Tests

Before and during operational periods in 1983, the Physics Operations Group was involved in the following commissioning tests:

- Pulse Discharge Cleaning (PDC).
- Plasma Fault Protection System (PFPS).
- Poloidal Field Distribution without plasma

Pulse Discharge Cleaning (PDC)

(F.C. Schüller, A. Tanga, P. Noll)

For PDC, the poloidal radial field amplifier was connected to the terminals of the primary transformer coil P1, which limited the maximum breakdown voltage to 8V. It was not known, whether this would be sufficient to achieve breakdown with the low value of steady state toroidal field used. Commissioning was carried out using simplified preliminary software, with the intention of creating more sophisticated control software once operating conditions were established. It turned out that breakdown conditions were more critical than for normal discharges, but once conditions were established, cycling operation with pulse intervals of 15s was achieved. Peak currents between 100 and 330kA were obtained with a plasma duration up to 400ms. In Fig. 76 a set of voltage, current and density traces during typical PDC operations are shown.

Although commissioning operation was carried out

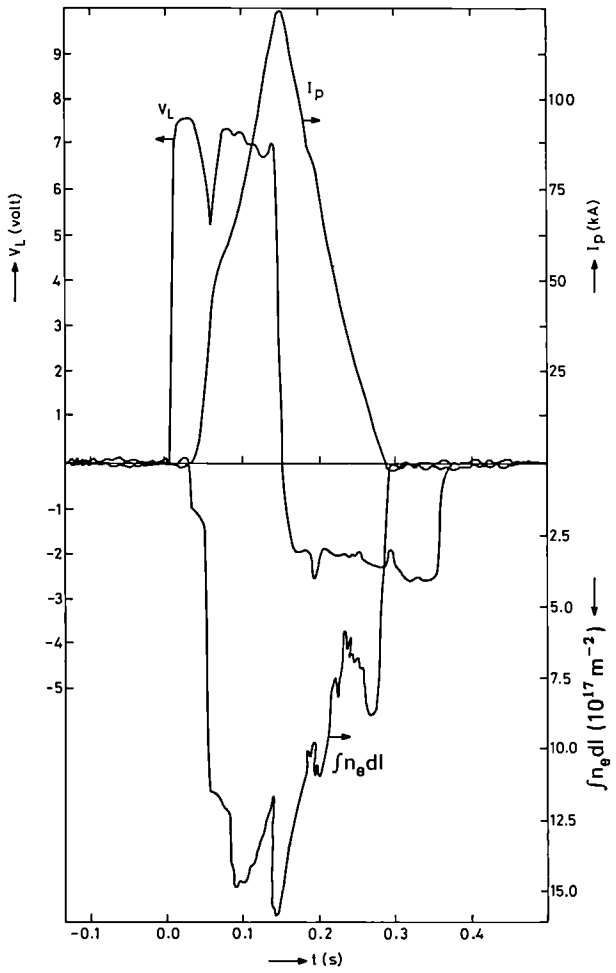

Fig. 76 Voltage, current and density traces during typical Pulse Discharge Cleaning (PDC) operations.

with cycling continuing for less than 1 hour, the pump-out of H_2O and CH_4 increased by more than an order of magnitude over the background rate. Longer periods of cycling operation for real cleaning purposes will be attempted at the start of the next operational period. Two modes of operation are envisaged for this period:

- low current, low temperature PDC optimised for maximum production of atomic hydrogen
- high current PDC with a maximum limiter heating capability.

Permanent software aimed at reducing the number of operating staff is being studied and should be available in Autumn 1984.

The Plasma Fault Protection System (PFPS)

(P. Lomas, A. Gondhalekar)

The Plasma Fault Protection System (PFPS) is designed to help safeguard JET against plasma behaviour which might cause damage to the installation. At present, it is intended to terminate the pulse when a plasma fault is detected. In the long run, it is desirable to respond to actual and potential plasma faults before these become irreversible, and this will require active control of the discharge. PFPS could also be used to terminate unproductive discharges which fail to meet some preset criteria and thereby save "undue operation",and improve overall efficiency.

PFPS consists of a programmable logic element (ACC) which samples diagnostic information regularly during the pulse, assesses whether these signals indicate a plasma fault, and if so issues appropriate instructions to relevant controls. The diagnostic information consists of plasma current, loop voltage, plasma density, total plasma light and hard X-ray flux. Using these signals, a number of fault conditions have already been detected (e.g. faltering breakdown, excessive hard X-rays, excessive plasma light and disruptions).

In the second half of 1983, the system was commissioned in open loop mode (i.e. without actually interfering with the machine operation). Fig. 77 shows pulse #1349, where PFPS correctly identified an abrupt change in current and simultaneous reversal of loop voltage as a major disruption. In this case, the indicated response was for soft termination (end the pulse in an orderly manner). Now that PFPS has been successfully demonstrated, the links from PFPS to the plant will be installed before the next period of operation so that such responses can be executed.

Experience in operation indicated a number of ways in which PFPS could be improved to detect other fault

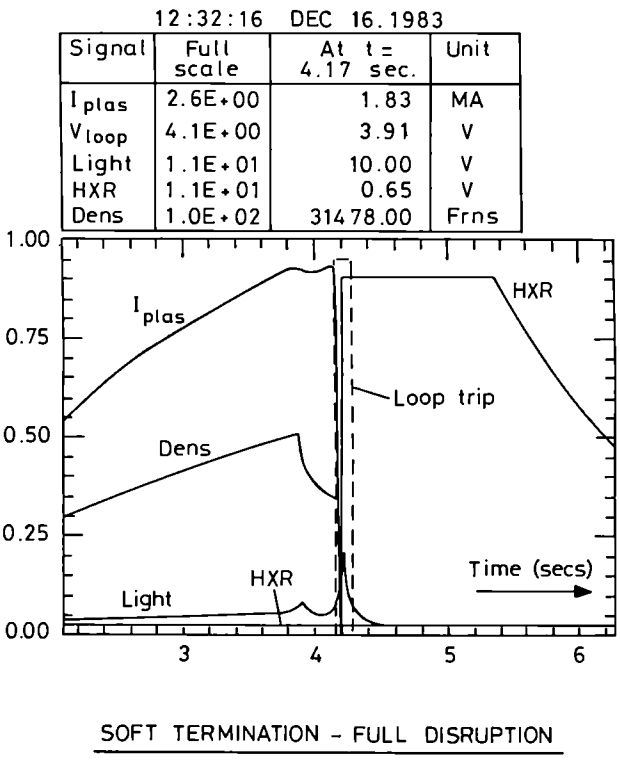

Fig. 77 Example of PFPS correctly identifying an abrupt change in current and simultaneous reversal of loop voltage as a major disruption at t = 4.165s, on Pulse #1349. The response was soft termination (end the pulse in an orderly manner).

conditions and in particular, to identify faults sufficiently early to avoid irreversible conditions, such as disruptions. These will be incorporated into PFPS together with features associated with major new subsystems, such as neutral injection.

Poloidal Field Distribution without Plasma

(P.F. Thomas, F.C. Schüller, H. Niedermeyer*, L. de Kock, G. Tonetti, G. Cordey, M. Brusati, E. Lazzaro)
*EURATOM-IPP Association, Garching, FRG.

There was sustained activity in preparation of operational procedures for the poloidal field (PF) system, including that for PF magnetic field distribution measurements (PF19). The main purpose of these measurements was to test the correctness of the model for the iron magnetic circuit used in the equilibrium and circuit codes. In addition, it was intended to evaluate the effects of eddy currents in the vessel's mechanical structure and coil support rings.

Due to time pressures, this test was undertaken in parallel with the high power test of the poloidal field power supplies and the magnetic diagnostics on the position control system.

The main goals were achieved and it was found that the models predicted JET's electromagnetic behaviour with high accuracy and could be used reliably for any calculation of the poloidal field distribution with a given current distribution. In addition, it provided a useful first test of the CODAS data acquisition system and a practice run of control room procedures.

Operations Related Physics Subjects

Breakdown Conditions

(H. Niedermeyer*, P.R. Thomas, E. Lazzaro)
*EURATOM-IPP Association, Garching, F.R.G.

Numerical studies have been performed with the Blum-code (supplied under contract by the EURATOM-CEA Association) to find the optimum field configuration for start-up. This code is a finite element program which permits computation of both the vacuum magnetic field configurations and MHD-plasma equilibrium configurations, taking into account the presence of the iron transformer and vessel current.

It is commonly believed that a stray field configuration with a hexapole null (i.e. absolute value and gradient of B identically zero) near the centre of the vessel, is favourable for start-up of tokamak discharges. Stray fields with a finite gradient may need high breakdown voltages or lead to a displacement instability at low plasma currents. The calculations performed showed that the technical facilities of JET were capable of fulfilling this condition if an appropriate number of compensation turns (on the PF-coil No. 3), which depends on the absolute value of the primary current, were connected in series with the primary. The number of compensation turns must be chosen so that the remaining stray field at the vessel's centre has the same decay index as the vertical field used to sustain the plasma in equilibrium. In this case, the vertical field system could be used to compensate the stray field, to second order.

In Fig. 78, the vertical field distribution at breakdown (i.e. when the vessel current was a maximum) is shown for various numbers of compensation turns and for various values of premagnetisation currents. Computations show that the plasma elongation was strongly increased, if the plasma current distribution was flat. During start-up, this might be the case due to skin effects. Over-compensation of the stray field tended to increase the elongation further. Both effects together could lead to such a high elongation, that the plasma touched the vessel at top and bottom.

One of the measures taken successfuliy to overcome the initial start-up problems was to choose the optimum number of compensation turns by computation. Unfortunately, time did not permit an experimental investigation of the sensitivity of the breakdown plasmas to stray fields and their gradients.

Another critical breakdown condition was the filling pressure. It was found during 1983 operations, that a

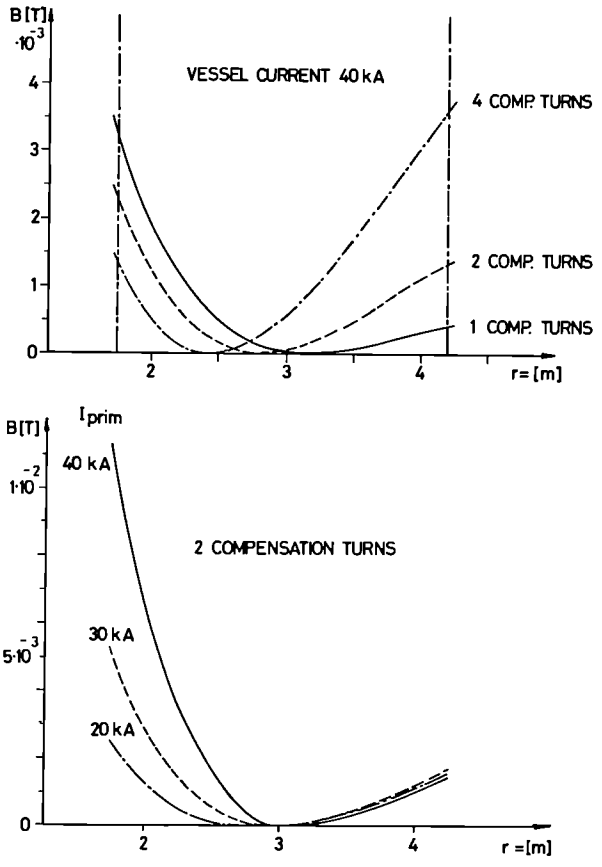

Fig. 78 Computed Hexapole Null Fields. The vertical field in the midplane plotted as a function of radius. All curves for 284 turns in PF-coil No. 1; 54 turns in No. 3; 122 turns in No. 4; vessel current = 2 × primary current.
Top: Primary current 20kA, different number of turns in No. 3, in series with primary.
Bottom: Different primary currents, two turns in No. 3, in series with primary. The vertical field current has been adjusted to get B = 0 at dB/dt = 0.

good rise phase without disruptions could be obtained, if, at t = 0.3 s, the value of $(\beta_p + l_i/2)$ was about 0.5, which could be obtained by a careful choice of filling pressure. Pressure values which were too low gave a hollow T_e profile and a low $(\beta_p + l_i/2)$; high values gave a peaked but low T_e profile with a high value of $(\beta_p + l_i/2)$. The latter discharges developed into highly radiative and resistive plasmas with a reduced or zero current ramp rate. Runaway activity, except at disruption, was always modest because the critical filling pressure for suppression of runaway electrons was even lower than the one giving hollow T_e-profiles. The optimum filling pressure value varied from day-to-day, probably depending on the cleanliness of the wall.

Current Rise Rates

(F.C. Schüller, P.R. Thomas, H. Niedermeyer*)

*EURATOM–IPP Association, Garching, F.R.G.

Unstable skin current profiles might present problems in the rise-phase of JET pulses. The maximum allowable rate of increase of plasma current that could be induced without arcing or production of MHD instabilities (and subsequent disruption) had a substantial impact on the operational capabilities as follows:

- The breakdown and fast-rise power supply is a passive system, so that the available magnetisation flux is directly linked to the fast rise loop voltage and so is limited by the maximum allowable fast-rise current-ramp rate.
- A prolonged slow-rise phase would use up resistive volt-seconds so reducing the available inductive volt-seconds and/or resistive volt-seconds for the flat-top phase.
- A prolonged slow-rise phase would use up the available flat-top time of the toroidal field.

For this reason, JET staff (Schüller, Thomas and Niedermeyer) took part in experiments on ASDEX to investigate the limits of stable current ramp rate. Variable gas injection was used and the consequences of any instabilities initiated were examined. The results broadly confirmed the earlier findings of the Alcator-team which indicated that scaled up to ASDEX-size and magnetic field, non-classical penetration started to become important at $1\,MAs^{-1}$. This limit can be shifted by applying large gas influxes, but at $1.3\,MAs^{-1}$ major disruptions were unavoidable. Scaled to JET-size and magnetic field, a limit of $1\,MAs^{-1}$ was predicted which would mean that a 5 MA discharge could not be reached in less than 4 s.

However, experimental results from JET during the fast-rise phase show that $2–3\,MAs^{-1}$ can be reached; probably because the plasma resistance is still high and because the application of an expanding cross-section scenario during the rise is helpful. Even so, faster ramps during fast-rise were accompanied by unstable behaviour. This meant that, with the lowest possible primary resistance, the premagnetisation flux must be limited. The subsequent slow-rise phase has proved to be stable up to $0.6\,MAs^{-1}$, but faster rates have not been tried.

In view of the low break-down and rise phase voltages that have been used in JET, a conversion to solid-state ohmic supplies looks attractive. Specification of such conversion will be an important activity in 1984.

Simultaneous Ramp of B_T and I_p

(F.C. Schüller, O. Grüber*)

*EURATOM-IPP Association, Garching, F.R.G.

The above difficulties should be alleviated if: the toroidal field could be ramped up in line with the current; economies were made on the available B_T flat-top seconds; the consumption of poloidal volt-seconds was reduced via the rotational transform of the total magnetic field lines; and there was a partial compression of plasma kinetic energy leading to more peaked electron temperature (T_e) and density (n_e) profiles.

Preliminary results of numerical studies carried out under an Article 14 Contract with Euratom-IPP Association, IPP, Garching for these scenario, using the BALOUR-code, show these advantages clearly. In the next operational period, experiments to test these results will be carried out.

The Hugill-diagram

(P.R. Thomas, J. Wesson, F.C. Schüller)

The Hugill-diagram of $1/q_\psi$ versus $\bar{n}R/B_T$ showing the accessible space is commonly used as a representation of the operational possibilities of any ohmically heated tokamak. In Fig. 79, the diagram for JET is shown with the trajectories of a few typical pulses. The following points should be noted:

- During current-rise even with no gas feed, the

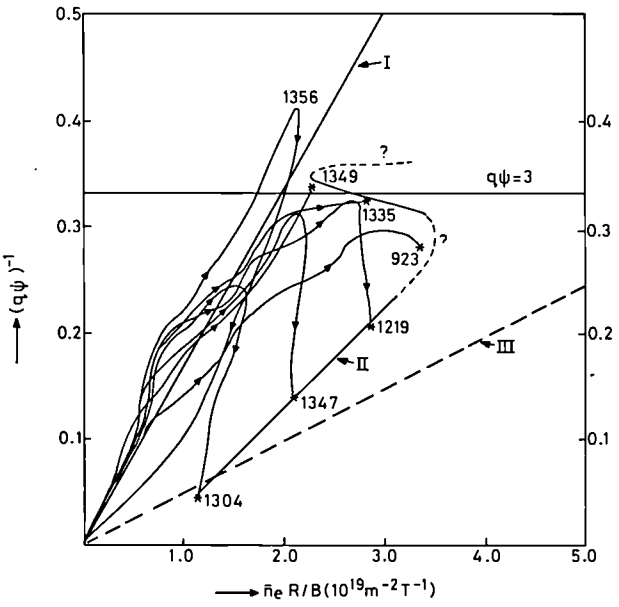

Fig. 79 The Hugill-diagram (of 1/q versus $(\bar{n}R/B_T)$) for JET with trajectories.
Line I : The high density limit beyond which a discharge will disrupt during the decay phase.
Line II : The high density limit at the moment of disruption.
Line III: The high density limit for clean tokamaks ($Z_{eff} < 1.5$) as found in other devices.

density rises proportionally with current. The particle source appears to be limiter outgassing. With gas feed, the density rises more quickly but a slightly less steep line only can be followed otherwise the discharge disrupts or develops into a resistive radiative low-current discharge.

- During the flat-top phase, the density can be increased but if line I is crossed the discharge disrupts, (not immediately but in the decay phase).
- Line II indicates the l/q_ψ and $\bar{n}R/B$-value at the moment of disruption in the decay-phase, at a notably less steep slope than line I.
- The majority of the pulses that disrupt during the flat-top were those which crossed the $q_\psi = 3$ indentation. The few pulses which disrupted at higher q during the flat-top were not sufficient to determine whether a separate high-density limit existed for immediate disruption during flat-top. However, the pronounced skin-effects observed in JET make it plausible that different density limits exist for rise, flat-top and decay phases.
- Line III indicates the density-limit for clean discharges ($Z_{eff} \approx 1$) observed in other tokamaks. The 2 to 3 times lower slope and the fact that in JET, $Z_{eff} \cong 3$, is in agreement with an empirical relationship proposed by the TFR-team:

$$n^{crit} = [2.10^{20}.B/(Rq_aZ_{eff}] \ m^{-3}$$

- Discharges with $q_\psi < 3$ can be created regularly in JET provided that the crossing of the $q_\psi = 3$ line takes place at modest density.

Disruptions

(F.C. Schüller, J. Wesson)

The standard phenomenon of a disruptive energy-quench is also observed in JET. It is characterised by a sudden drop in temperature; a flattening of the current-density profile which leads to an increase of current and a negative voltage-spike; a blow-up of the cross-section towards the inside; and an impurity influx from the limiter.

After the energy-quench three types of further development were observed:

- If the driving voltage was higher or equal to the resistive loop voltage, no subsequent current-quench was observed. These Mini (M) type of disruptions occurred often in the rise phase. The lower or zero current ramp-rate after a M disruption indicated that the impurity content and, therefore, the resistivity increased. Position feedback drove the plasma back to its original position and shape.
- If the driving voltage was lower than the resistive voltage, a current-quench followed the energy-quench. During this current-decay the plasma dissipated its magnetic energy mainly by radiation as was seen from the bolometer signals:

$$P_{rad} \cong 0.9 \ LI.dI/dt$$

- The decay-time was typically 300ms with some scatter caused by various external circuit conditions. This indicated that the temperature during the current-quench was around 50 to 100eV for all disruptions for current levels below 1MA. At such current levels, the current-decay was slow enough that the position feed-back system could force the vertical field down so that the position control was preserved and the plasma remained in contact with the outboard limiter. These were the Controlled (C) type of disruption.
- Plasma currents above 1MA at disruption, led to a current-decay which was too fast to be followed by the positional feedback (even though due to pronounced skin-effects with a notable increase in ℓ_i, the vertical field was requested to drop more slowly than the current, this effect shifted the critical decay-rate which could be followed from $-3MAs^{-1}$ to $-5MAs^{-1}$). At the faster decay rates, position control was lost and the plasma moved inwards to be squeezed against the inboard wall. This Uncontrolled (U) type of current-quench had a much shorter decay-time, so that a typical 2MA disruption led to a decay-rate of $100MAs^{-1}$.

In Fig. 80, a typical example of a U-type disruption is shown. In Fig. 81, a survey of all observed C- and U-type disruptions is given in the I-dI/dt plane. The distinct bending point at $dI/dt = -5MAs^{-1}$ should be noted. In the near future, the voltage capability of the vertical field amplifier will be doubled, which is expected to shift the bending point to $I \simeq 2MA$ and $dI/dt \cong -10MAs^{-1}$.

Particle Balance and Recycling

(A. Tanga, P. Morgan)

The plasma density showed a substantial contribution (typically 50%) deriving from contributions from the limiter (and maybe from the vessel), during the rise of the plasma current. The density was constant during the flat top, in the absence of gas puffing, and decreased during the decay of the plasma current. The virtual recycling coefficient was therefore larger than the value in the rise phase of the discharge, was constant throughout the flat top and fell below one during the decay phase. This quantity and the particle confinement time have been computed making use of the measured plasma density and absolute ionisation rate. The particle confinement time showed a scaling inversely proportional to the plasma density, which is characteristic of a boundary dominated particle transport.

Vertical Instability

(H. Niedermeyer*, P. Noll, J. Wesson)

*EURATOM-IPP Association, Garching, F.R.G.

A version of the Blum-Code has been developed which permitted the computation of equilibria which were asymmetrical about the midplane. With this Code, it was possible to calculate the stabilising or destabilising force of vertically displaced equilibria. Studies are underway to determine this essential parameter for a series of equilibria, which includes magnetic limiter configurations with one and with two stagnation points.

The absolute accuracy of this type of calculation is

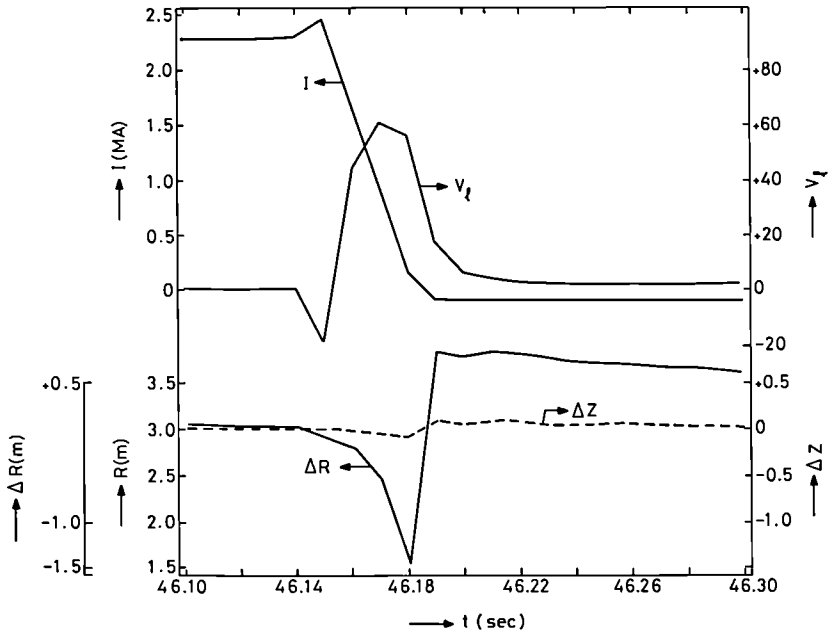

Fig. 80 Uncontrolled (U) type of disruption.

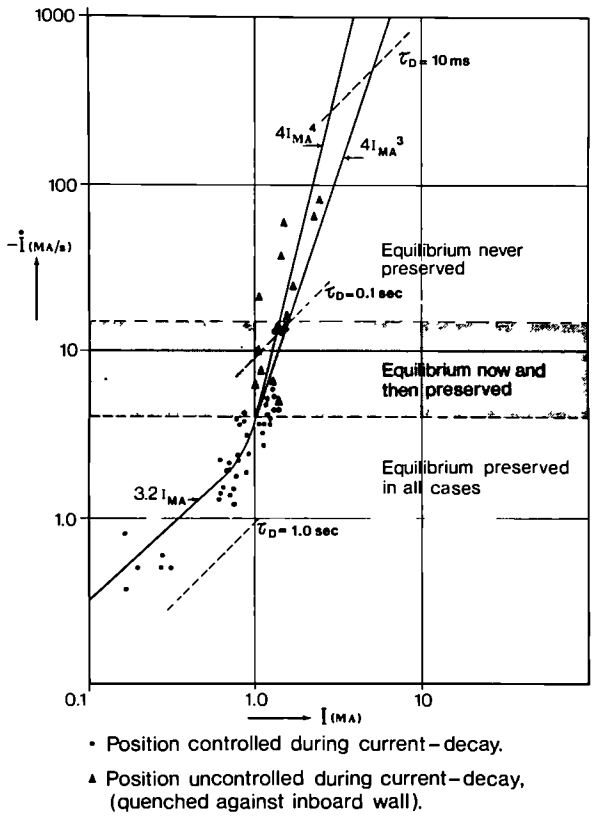

Fig. 81 Survey of all Uncontrolled (U) and Controlled (C) types of discharge in the I v dI/dt plane.

limited and the stability of any configuration is also affected by the incompletely known electromagnetic properties of the surrounding structure and by the performance of the feedback system. Consequently, it is necessary to verify experimentally the calculated properties of the system for vertical instabilities; this is planned for early 1984.

An indication of vertical instability was observed during early operations before the vertical position control was functioning. The typical displacement growth time was around 50 ms with the radial field coils passively connected.

Software Development for Physics Operations

Interpulse Display

(S. Cooper, P.R. Thomas, F.C. Schüller)

As mentioned in the 1982 Annual Report (EUR-JET-A5), a priority reduced raw data set (IPF) containing diagnostic information was generated promptly after each pulse. A suite of codes has been created, commissioned and put into daily use to present this information as screen pictures on the main consoles and synoptic displays. This software includes menus for selecting data channels, sampling rates, processing algorithms, graphics and display stations. Fig. 82 shows an example of a commonly used screen picture.

Control Software

(S. Cooper, A. Hancock, P.R. Thomas)

The user interface programme for PFPS has been created, commissioned and now updated for closed-loop operation. A waveform editor programme, written by this group, has also been adopted and modified by the CODAS Division as the standard tool for editing the reference waveforms controlling the machine subsystems.

Parts of the PDC control software are ready, but others are still under development. A complete package for setting up tokamak discharges is being studied; one

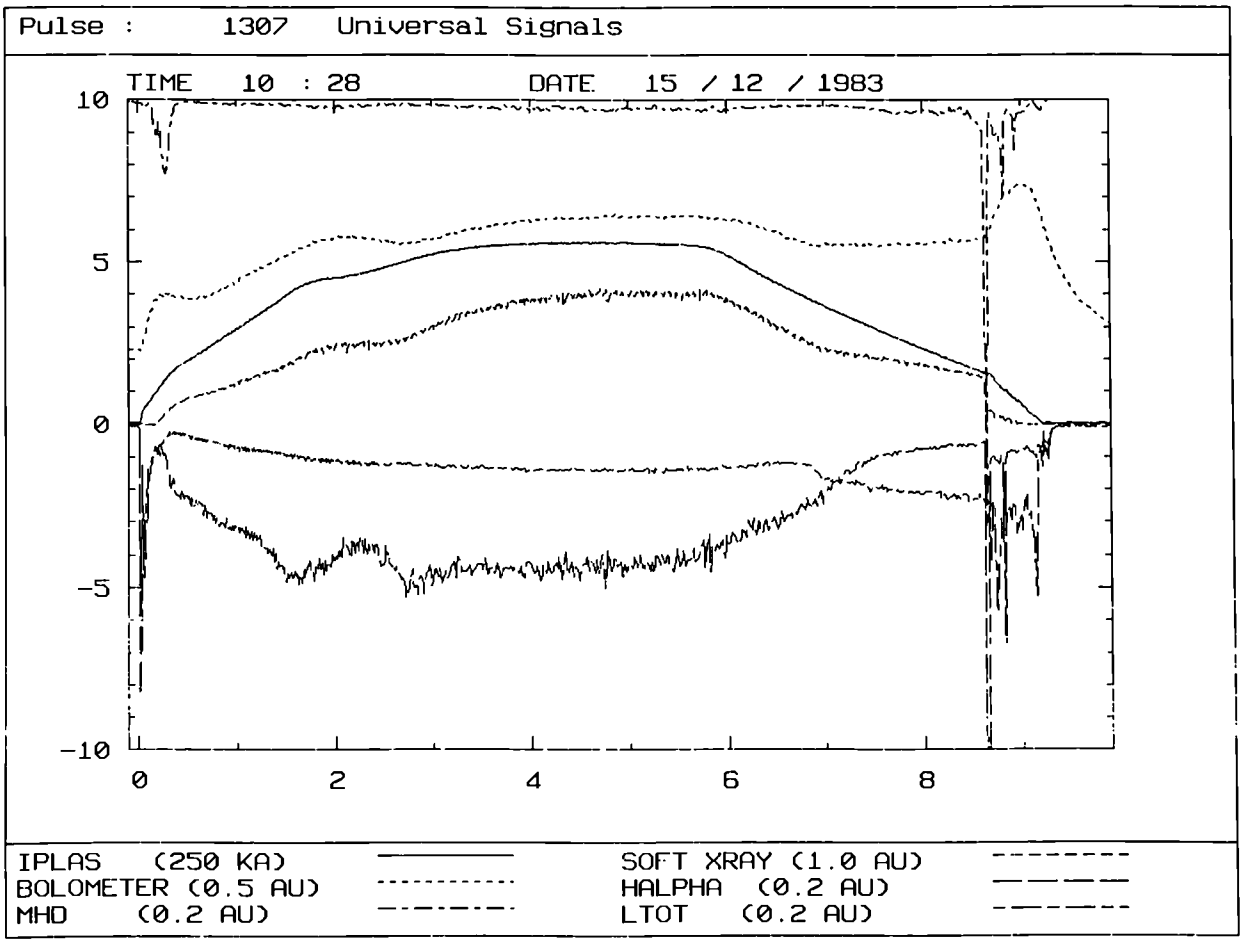

Fig. 82 Typical screen picture output on the main consoles (for Pulse #1307).

important component is the calculation of the excitation voltage waveform of the poloidal field flywheel generator derived from a plasma current waveform via a simplified circuit equation code. This last part will assist the operator considerably and, therefore, has been given a high priority. It will be tested in the next operational period.

A computerised logbook programme will enable the creation of a publicly accessible log-file containing all pre- and post- pulse comments which operators have made. This programme is still under development.

IBM-software

(Miss J. Thompson, P.R. Thomas)

A number of large predictive codes are available as software tools for Physics Operations: the equilibrium code (Blum-Code) now also available in asymmetric version; the beam deposition code NFREYA; the hydrogen retention code PERI; the circuit code and the time dependent coupled transport and equilibrium code SCED. Small interpretative codes are under development for addressing operational issues such as particle balance control using as an input the measurements stored in the JET pulse file (JPF).

Physics Requirements for Possible Future Hardware

During Summer 1983, two Working Groups were established under the supervision of Physics Operations Group, and were required to produce reports on the physics requirements to two possible schemes:

- Density-decay control by means of pumping panels.
- Impurity control by open poloidal divertors (i.e. the so-called "magnetic limiter concept").

Further technical design studies will be necessary if the recommendations of these reports are favourable.

Pumping Panels

(A. Tanga, F.C. Schüller in co-operation with R. Simonini, E.S. Hotston*)

*EURATOM-UKAEA Association, Culham Laboratory

This study was directed at answering two questions:

- geometry: Where to place the panels and of what size?
- material: Which material combines the lowest recycling coefficient with the highest hydrogen-isotope diffusion and the least vulnerability to poisoning?

The first question was addressed by numerical calculation (using a Monte-Carlo method) of the dimensions of the neutral atomic hydrogen cloud surrounding the present-day limiters. The results show that panels with a 'width' in the toroidal direction of 20cm placed next to and underneath the limiters would catch the majority of neutrals originating at the limiter surface. However, it was clear that the final panels would have to be installed in conjunction with new toroidal belt limiters and, therefore, new calculations would be made to determine the optimum belt limiter tile shape for focussing the neutral flux onto the panels.

On material choice, there were doubts about the usefulness of zirconium-alloy which had been used at Princeton (USA). This sintered material required an accurate temperature and hydrogen inventory control to avoid embrittlement; moreover, it seemed to be prone to poisoning. Other materials such as palladium, vanadium and nickel had a higher recycling coefficient but were more robust.

The studies have considered the concept of thin sheaths (~1mm) which are thick enough to retain the hydrogen during a pulse but are thin enough to deplete the hydrogen content by diffusion and surface molecular recombination between pulses. The molecular hydrogen is then pumped out, via the torus, by the main pumps. A small temperature increase between pulses may be necessary, which, in any case, would make tritium recovery in the active phase easier.

Magnetic Limiter

(P. Thomas in co-operation with L. Sonnerup, J. Last, E. Lazzaro, H. Niedermeyer*)

*EURATOM-IPP Association, Garching, F.R.G.

Studies have shown that it would be feasible to operate JET in a "magnetic limiter" or open divertor configuration. The Working Group addressed the possible operational range set by mechanical stresses, modifications to the poloidal busbar system, target plates and scrapers to be placed inside the vacuum vessel, together with other issues such as the vertical instability of the diverted plasma and the relation to active plasma shape control.

A major physics uncertainty was to what extent it is possible to reach the so-called "high density regime" in the target region. It was required that the dimensions of the neutral cloud in front of the targets become smaller than the separatrix area, so that impurity back-flow into the main plasma was prevented by the friction force exerted by the instreaming proton flux. The existence of such a regime depends on the uncertain radial diffusion in the scrape-off layer and on the accessible parameter window of the main plasma.

Radiological Protection and Shielding

Work continues in these areas under contract arrangements with the Euratom-UKAEA Association establishments at Harwell and Winfrith. An extensive system of radiological protection instrumentation with full software facilities and data recording through CODAS was operational from the first JET discharge. Comprehensive documentation is in preparation and a sequence of enhancements is planned for progressive implementation in the period up to 1987.

Shielding calculations continue, making extensive use of the comprehensive numerical model for JET shielding calculations developed by UKAEA, Winfrith under JET contract. The emphasis has shifted from biological shield design and assessment to design and assessment of the radiation hardening of the various diagnostic systems.

Diagnostic Engineering

(A. Ainsworth, M. Barnes, C.J. Caldwell-Nichols, N. Foden, J. Gowman, C.J. Hancock, R. Lobel, P. Millward, B. Oliver, J. Reid, P. Roberts, A. Tiscornia, C. Wilson)

The Diagnostic Engineering Group has been heavily committed during the year. Much of the work was associated with the installation of the seventeen major diagnostic systems which were operational on JET at the year end and, of which, 10 were operational for the first JET discharge. A large amount of preparation work was necessary in the second half of the year for systems planned for installation at the beginning of 1984. Work continues at an increasing pace on the many systems now in construction in the Associations for installation later in 1984 and 1985. Careful preparation of interface specifications, installation procedures and planning has been carried out, in order that subsequent installation proceeds smoothly in accordance with the JET operation schedule. Further details are mentioned in the following Divisional contributions.

Experimental Division 1

(Division Head: P.E. Stott)

Experimental Division 1 is responsible for specification, procurement and operation of about half of the JET diagnostic systems, particularly those associated with electrical measurements, electron temperature measurements, surface and limiter physics and neutron diagnostics. In addition, the Division assists in execution of the programme, in interpretation of results and in making proposals for future experiments, in collaboration with Experimental Division 2, Theory Division, the Physics Operations Group and the Operations and Development Department.

During 1983, the Division was re-organised into three Groups:

(i) Electron Temperature Measurements;

(ii) Plasma Boundary Physics;

(iii) Neutron Measurements.

During the year, considerable efforts were devoted to installation and commissioning of the first diagnostic systems. For the first plasma discharges, Experimental Division 1 operated the magnetic measurements (KC1), the 2mm microwave interferometer (KG2), the neutron (KN1) and hard X-ray monitors (KH1) and the limiter hot-spot monitor (KL1), which all worked satisfactorily, but with many temporary improvisations. During the

August/ September shut-down, full installation and commissioning was completed. In addition, four antennae for the Electron Cyclotron Emission (ECE) diagnostic (KK1) were installed, which produced the first electron temperature (T_e) profiles at the end of November. Installation of the single point Thomson scattering system (KE1) was started during the latter part of 1983 and should be completed early in 1984.

In parallel with this activity on JET, progress was maintained, in collaboration with the respective Associations, on the detailed design and construction of the diagnostics planned for installation in 1984 and 1985, which include the surface physics probes and the neutron diagnostics. The Design Phase of the spatial scan Thomson scattering system (KE2), based on backward scattering from a CO_2 laser, was concluded early in 1983 and an extensive review of the feasibility of this system was undertaken, which resulted in a decision not to proceed. A number of feasibility studies of potential new diagnostics and upgrades of existing ones, were started, including a microwave reflectometer, a 1 mm microwave interferometer, a LIDAR (Light Detection and Ranging) Thomson scattering system and 14 MeV neutron spectrometers.

Electron Temperature Measurement Group

Electron Cyclotron Emission (ECE) Diagnostics

(D.V. Bartlett, D.J. Campbell, A.E. Costley, I. Hurdle, E.A.M. Baker*, A. Hubbard+)
*National Physical Laboratory, London, U.K.
+Imperial College of Science and Technology, University of London, U.K.

Two electron cyclotron emission (ECE) diagnostic systems for JET are under construction. One is a spatial scan system for measuring the spatial dependence of the electron temperature in the poloidal cross-section (KK1), while the other is a fast scan system for measuring the time-dependence of the temperature at fixed positions in the plasma on a fast time-scale (KK2). During the year, substantial developments have taken place in both systems.

Both systems will share an array of ten antennae mounted inside the torus vacuum vessel (Fig. 83) to view the plasma poloidal cross-section along different chords. The ECE radiation is transmitted through crystal quartz vacuum windows and then along oversized aluminium waveguide (S-band) to the Diagnostic Hall. The design of this system has presented considerable problems both in terms of the physics of the propagation of single modes through long oversized waveguides and antenna, and in terms of engineering to meet JET's requirements. Four antennae were installed in the torus during August 1983 and the remainder have been manufactured and will be installed in early 1984. The system was commissioned using two temporary waveguide runs, and the full permanent system of ten waveguides will be fitted in May 1984.

The spatial scan system, which is being developed and constructed by the National Physical Laboratory, UK, consists of five Michelson and six Fabry-Perot interferometers. The spatial dependence of the temperature is deduced using well established procedures. The temperature is determined from the intensity of the emission at the second harmonic of the cyclotron frequency, and the spatial information is obtained from the frequency dependence of the emission.

First plasma parameter measurements were made in November. Measurements were made of the level and frequency spectrum of the emission in the range $100\,GHz < f < 300\,GHz$ ($f_{ce} < f < 4f_{ce}$, for $B = 2.6\,T$), and from the measurements the electron temperature profile in the radial range $2.8\,m < R < 4.2\,m$ was determined. The estimated uncertainties were ± 10% on the

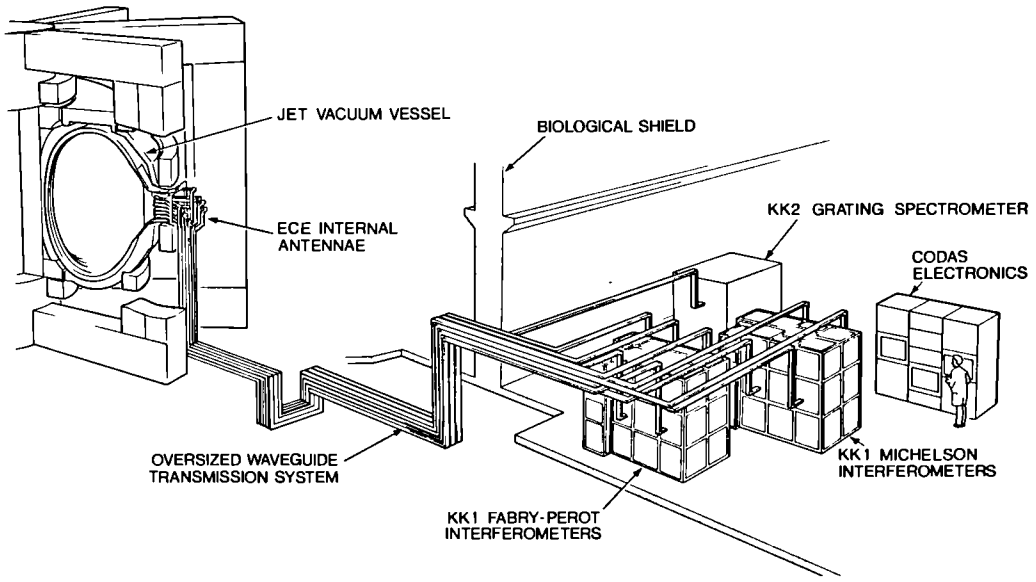

Fig. 83 Array of ten antennae mounted inside the Torus vacuum vessel to view the plasma poloidal cross-section along different chords.

relative level and ± 20% on the absolute level. At any point in the profile, the temperature information was averaged over a volume of dimensions ~ 15 cm along the line of sight, and of radius about 10 cm perpendicular to the line of sight. The time resolution was ~ 15 ms and ~ 30 profiles were obtained per plasma pulse at preset times. The measured profiles have been used both in the optimisation of the plasma performance, and in the first confinement studies on JET. An example of the profiles obtained is shown in Fig. 84. Completion of the installation of the system is planned for May 1984, and it should be fully operational by the Summer.

The fast scan system is being constructed by the Euratom-FOM Association, FOM Institute, The Netherlands. It consists of a 12 channel grating polychromator, liquid helium cooled detectors, and control and data acquisition electronics and software. The grating is a reflection echelon grating and is combined with a mirror in a 'cat's-eye' mount. This is a novel design and gives high efficiency of operation in the frequency range 100 GHZ < f < 600 GHz. With this instrument, it should be possible to measure simultaneously the time dependence of the electron temperature at up to 12 selected positions in the plasma with a time resolution $\lesssim 3\mu s$. The instrument will be particularly suited to the study of localised temperature fluctuations.

The Phase II contract was started early in 1983. Much of the necessary hardware has been constructed and initial assembly has been carried out. Special waveguide tapers have been developed for the entrance and exit slits. The control and data acquisition hardware has been defined and ordered. A numerical model of the grating has been developed to optimise the performance, and control and analysis software is under development. Completion of the construction phase is expected by June 1984 with installation on JET planned to commence in September.

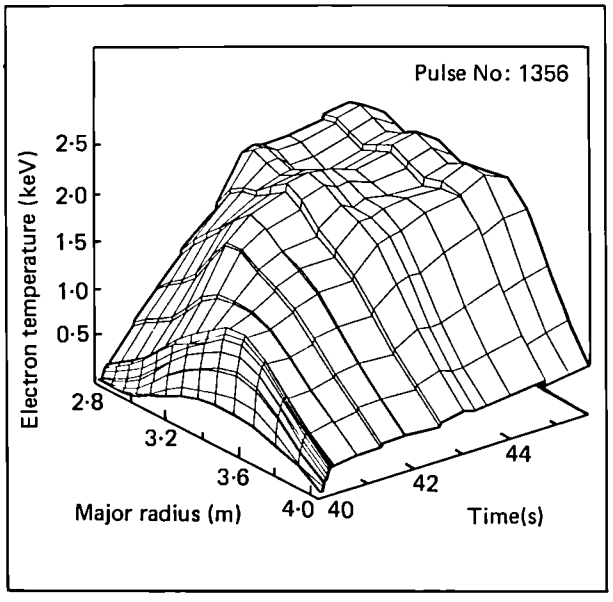

Fig. 84 Electron temperature profiles deduced from electron cyclotron emission measurements (KK1).

Microwave Density Interferometer.

(J. Fessey, C. Gowers, C. Hugenholtz*)
*EURATOM-FOM Association, FOM, Netherlands

As the multichannel interferometer was not planned for the first operation, a single channel 2 mm microwave interferometer had been prepared (KG2) for initial measurements. This interferometer measured the line integral of the density ($\int n_e d\ell$) along a vertical chord at R = 3.14 m. It consists of a 2 mm klystron source, approximately 76 m of oversized (S band) transmission waveguide, a broad-band video detector, and data acquisition and control electronics. All the active components of the system were installed outside the biological protection wall, in the diagnostic hall. Data analysis was carried out on the NORD computers at JET and on the IBM computer at Harwell. The system was linked to the JET Plasma Fault Protection System. The post-detection electronics were developed by the Euratom-FOM Association, FOM Institute, The Netherlands, and FOM also contributed substantially to the development and commissioning of the system at JET.

During 1983, the system was installed on JET and its performance assessed. The attenuation in the transmission system was ~ 20 db greater than first expected, probably due to mode scrambling in the tapers and waveguide run. To overcome this problem, a more sensitive liquid helium cooled indium antimonide detector was employed rather than the ambient temperature crystal diode originally planned. With this change, the system met its originally planned performance specifications (i.e. maximum measurable density ~ $5 \times 10^{19}\,m^{-3}$ with a minimum detectable density change ~ $5 \times 10^{16}\,m^{-3}$, time resolution $\lesssim 10\mu s$). The system was operational on the first day of plasma operation in June, and the line integrated density of an early JET plasma was measured as $1 \times 10^{18}\,m^{-2}$. Since the first day of operation, the system has operated routinely with a high availability of $\gtrsim 95\%$. As in the case of the ECE diagnostic, the results have been used both in the optimisation of the plasma and in the first confinement studies on JET. In the last JET operating period in 1983, line integrated densities up to $7 \times 10^{19}\,m^{-2}$ were measured, suggesting peak densities ~ $4 \times 10^{19}\,m^{-3}$. An example of the results obtained during this period is shown in Fig. 85. An upgrade to a 1 mm interferometer is in preparation, so that peak densities up to ~ $2 \times 10^{20}\,m^{-3}$ can be measured, and should be completed by June 1984.

Thomson Scattering Diagnostics

(B. Brown, A. Costley, M. Gadeberg, C. Gowers,
P. Nielsen, R. Prentice)

The Thomson scattering system on JET (KE1) has the conventional 90° scattering configuration. Light from a powerful ruby laser illuminates the plasma along a vertical chord, and the light, scattered at 90° from a 5 cm length of the beam on the midplane, is collected and spectrally resolved. The electron temperature, T_e, and electron density, n_e, are determined from the spectral width and intensity of the scattered light respectively.

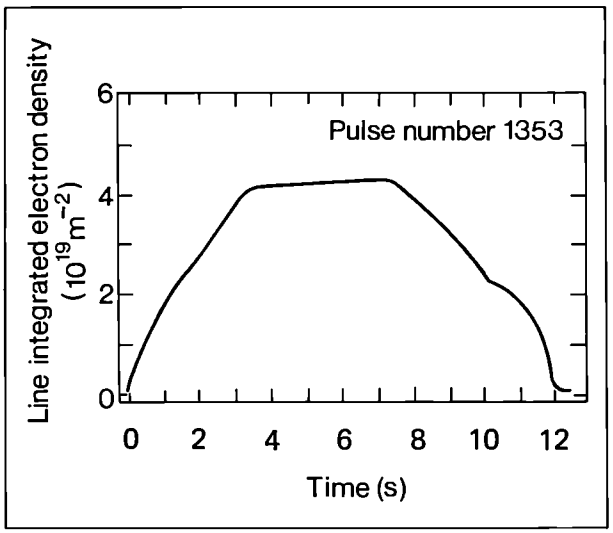

Fig. 85 Line integrated electron density measured with the microwave density interferometer (KG2).

The laser is a low beam divergence (~ 0.5 mrad) ruby laser (λ = 694.3 nm) and can be operated either in a single pulse mode giving one 20 J pulse during each JET discharge, or in a multipulse mode with lower energy at repetition rates up to 1 Hz. The collection system is a double Newtonian telescope arrangement; the dispersion system is a triple prism spectrometer; and the detectors are photomultipliers. Special alignment systems keep the laser beam and the collection system mutually aligned, and up to seven specific locations in the median plane can be probed by moving the input beam, and by appropriately adjusting the collection optics, between plasma pulses. Items sensitive to nuclear radiation, such as the laser and the dispersion and detection systems, are housed behind the radiation shielding in the roof laboratory, so that the system should be compatible with the active phase of JET operation. The system has been designed and constructed by the Risø National Laboratory, Denmark.

Substantial progress was made during 1983. The laser was installed and commissioned in the roof laboratory at JET. Construction of the input optics, collection optics, dispersion systems, detectors, electronics and alignment systems were completed at Risø, and a series of system performance tests were carried out. Subsequently, many of these items have been installed in their final position at JET. The successful installation alongside the torus of the large concrete tower, which supports the collection optics was a significant step forward. The vacuum interface items, principally special window boxes for the vertical ports, and a special flange for the horizontal port, have been designed and constructed and will be installed in January 1984. The control and analysis software has been developed and partly installed on the NORD computers at JET. Commissioning of the system is planned for February–March 1984, with the first plasma measurements possible in late March.

As the Thomson scattering system described above can only explore a limited part of the plasma cross-section, an additional spatial scan system is being considered. This is a LIDAR type system and was recently proposed by researchers at the University of Stuttgart and IPP Garching. According to this technique, an ultrashort laser pulse illuminates the plasma along a vertical chord and the back-scattered radiation (~ 180° scattering) is detected. Spatial information is obained from the time dependence of the scattered radiation, (i.e. the method is based on 'time-of-flight techniques'). This is a novel technique, as yet untried on tokamaks, although the principles have been well established in other areas, such as atmospheric pollution monitoring. It appears to be particularly well suited to the investigation of large plasmas such as in JET.

During 1983, a contract was placed with Euratom-IPP Association, IPP Garching, F.R.G., to carry out a study of the feasibility of applying the technique to JET. The study is being carried out in collaboration with the University of Stuttgart, F.R.G. The target performance is to measure the temperature and density profiles to an accuracy of ± 10% with a spatial resolution ~ 15 cm and at a repetition rate $\gtrsim$ 1 Hz, and the feasibility study should be completed by May 1984.

Plasma Boundary Physics Group

Magnetic Diagnostics

(L. de Kock, A. Stevens, G. Tonetti*, W. Morris+, D. Robinson+, T. Todd+)
*EURATOM-Suisse Association, CRPP, Switzerland. +EURATOM-UKAEA Association, Culham Laboratory, U.K.

The main magnetic diagnostic system consists of sets of 18 poloidal field pick-up coils (i) mounted inside each octant of the vacuum vessel, sets of 14 saddle flux loops on the outside of each octant (ii), and a set of 8 full flux loops completely encircling the torus (iv), which are shown in Fig. 86. In addition, six sets of 5 large flux loops for plasma position control are positioned on two octants (iii). There are also four Rogowski and two pairs of diamagnetic loops mounted on the toroidal field coils. With the exception of the diamagnetic loops, these systems are fully commissioned and operational.

Data acquisition is organised as shown in Fig. 87. The signals from Octants 3 and 7 plus the special set of saddle loops (iii), are exclusively allocated to the plasma control system. The signal conditioning consists mainly of high quality integrators and/or amplifiers with optically isolated outputs to isolate the data acquisition system from the torus. After this stage, the signals can be recorded individually or further processed in analogue circuits to provide, for example, plasma current, horizontal and vertical position, ellipticity or monitoring of selected instabilities. The plasma current signal, its derivative and loop voltage are routed to the plasma fault protection system (PFPS).

During a JET pulse, the signals are digitised by 12-bit

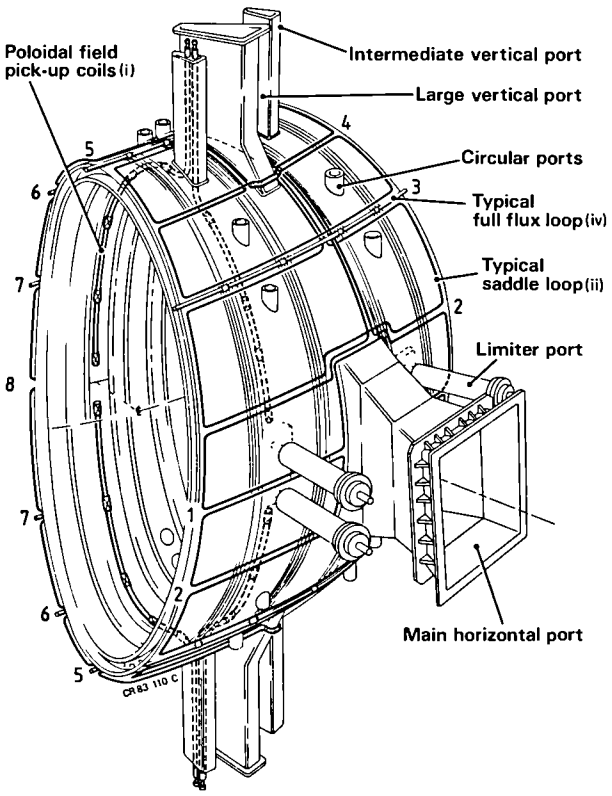

Fig. 86 vacuum vessel octant showing the poloidal field pick-up coils (i), the saddle loops (ii) and the full flux loops (iv).

analogue-to-digital convertors (ADC's) and stored temporarily in CAMAC memories. The CAMAC crate (CODAS cubicle) is interfaced with a NORD 100 computer, through which the user can display the data and set the various sampling sequences. Most of the signals are recorded on 128 channels of 1 kilo-word (kW) memory sampled at ~ 100Hz. Four channels of 8kW memory sampled at ~ 1kHz are used to provide higher resolution of some signals and very fast signals like MHD oscillations and disruptions are recorded on 8 windows of 4kW memory sampled at ~ 10kHz. The starting time of the windows was preset for the experiments described here; but will be triggered by an external event, such as a disruption, in the future.

After the discharge, a reduced number of samples were selected on specific channels and stored in the Intermediate Pulse File (IPF) for a quick processing in between pulses. The experimental control display and the interpretation codes FAST uses these data. Then all data were collected into the JET Pulse File (JPF), which was transferred to the IBM/CRAY storage computer at Harwell. Further interpretation codes and the more detailed data analysis use data from the JPF.

During commissioning of the poloidal field coils, measurements were taken with the coil sets (i), (ii), and (iv). These tests were used to optimise the system and the final results are shown in Fig. 88. The symmetry of the measured fluxes and fields was ± 1%, while the

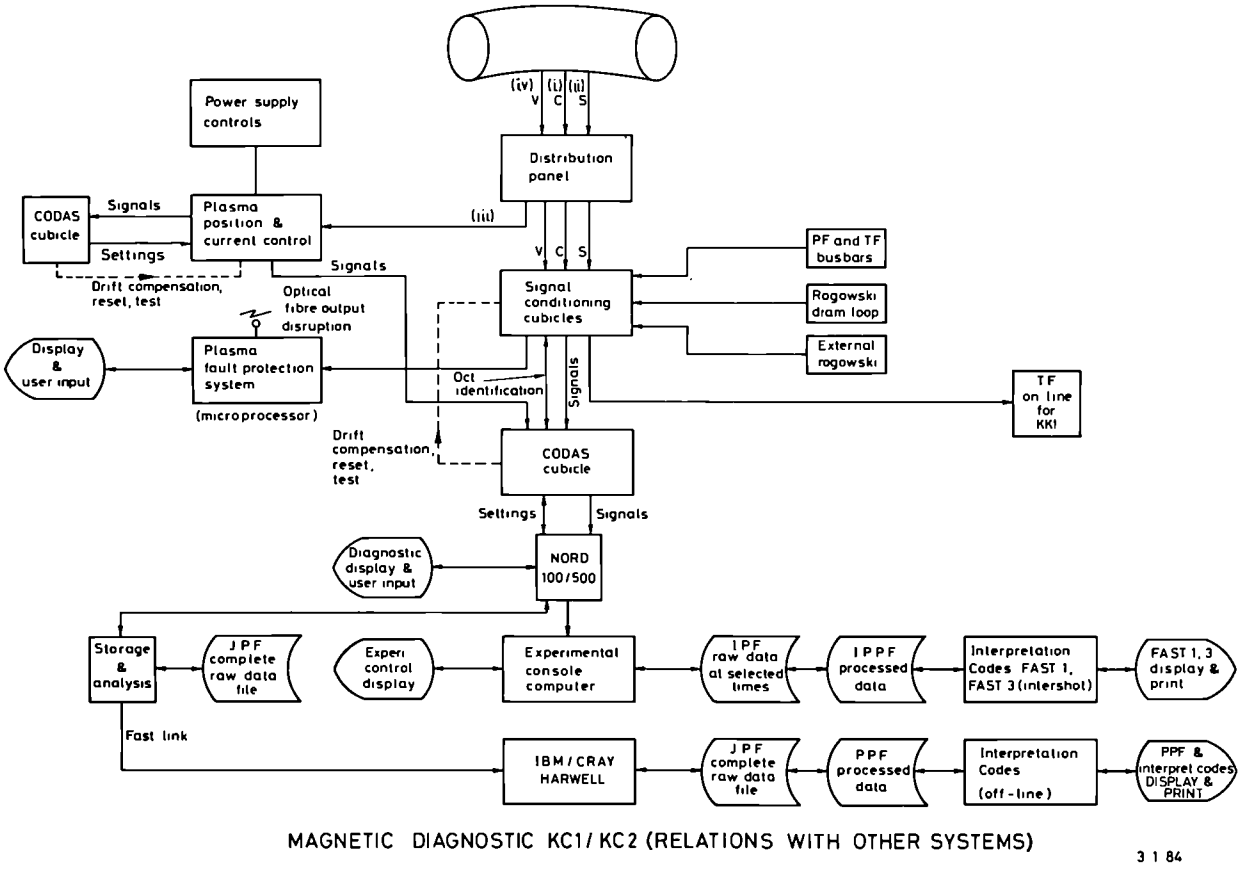

Fig. 87 Data acquisition system used for magnetic diagnostics.

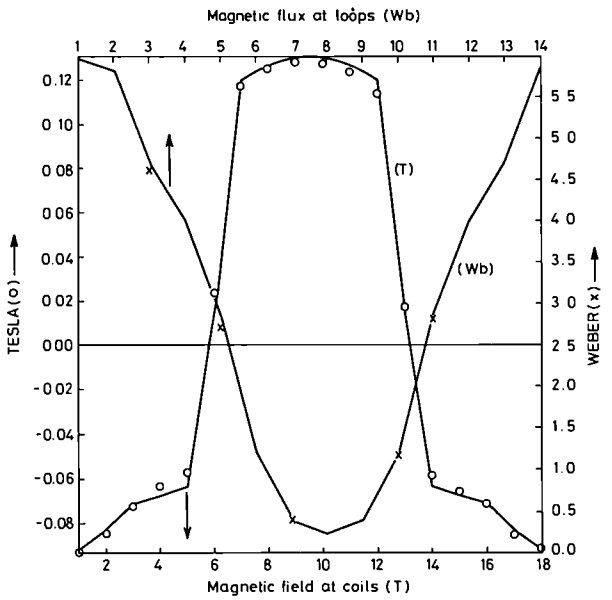

Fig. 88 Comparison of poloidal fields and fluxes as generated by the code INVERS, as measured by pick-up coils and voltage loops during commissioning of the poloidal field system (o, x measurements from 18 pick-up coils and 14 saddle loops).

absolute values agreed well with code predictions.

All sensors showed some unwanted pick-up from the toroidal field. The sampling sequences were set to measure this pick-up so that it could be subtracted from the plasma signals during software processing of the data. In the case of analogue combinations, the toroidal field was substracted on-line in the last summing stages.

As a first stage of software processing, all saddle loop signals were added (after toroidal field correction) and the resulting signal, which should be close to zero, was used as a consistency check. The same was carried out with the poloidal field pick-up coils, where the Rogowski signal was constructed from the measurements with the 18 individual pick-up coils. This resulted in an off-set of several kA, which was very small compared to the normal plasma currents. A preliminary estimate of the accuracy of the signals was obtained by comparing measurements from two different octants on the same discharge, and deviations were $\leqslant 2\%$. Further improvements are being investigated.

In order to study instabilities at various times during the discharge, a number of internal pick-up coils were selected and sampled without integration, which enabled measurement of small fluctuations in the poloidal field ($\lesssim 0.1\%$). The signals generally showed short to long periods of coherent oscillations. The phase and amplitude differences between coils enabled an identification of the dominant instability.

As well as the MHDA signal shown in Fig. 89, seven other coils were used revealing at different times the presence of instabilities with poloidal mode numbers m = 2. 3. 4. and almost invariably with toroidal mode number n = 1. The time window when the coil signals are sampled may be moved through the discharge and this has allowed studies of the current rise and major disruptions. Such a disruption is shown in Fig. 90: the instability grew in amplitude, the rotation with respect to the coils stopped, and rapid loss of energy and termination of the plasma current ensued.

As an example of the performance of the complete system a selection of the signals of JET pulse #1353 is shown in Fig. 89. The explanation of the signal is described in the figure caption.

Plasma Edge and Surface Diagnostics

(J. Hancock, M. Pick, J.A. Tagle, J. Vince, G. McCracken*, S.K. Erents, G. Matthews*)
*EURATOM-UKAEA Association, Culham Laboratory, U.K.

These devices comprised two complementary systems which will allow the introduction of direct reading or collector probes into the edge plasma between the vacuum wall and plasma boundary. Both systems were designed to feed the collector probes directly into an analysis station.

The main system, the Fast Transfer System (FTS) (KY2) will allow probes to be exposed through a horizontal port for one or more plasma pulses and then

Pulse No: 1353

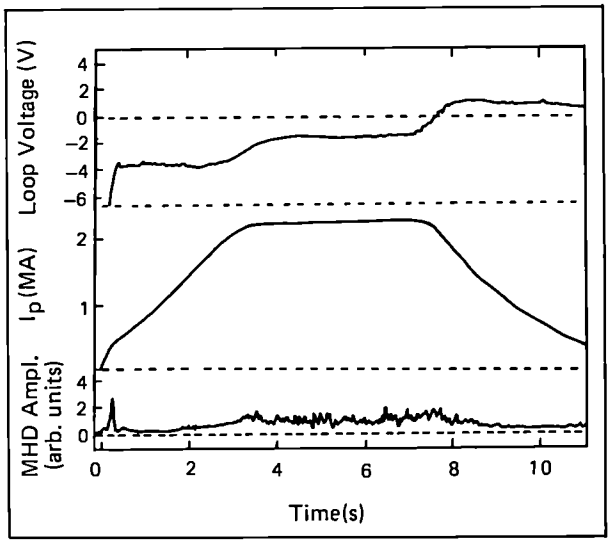

Fig. 89 Selection of signals of JET Pulse #1353, as a function of time.

Top: *Loop voltage from bottom of vessel;*
Centre: *Plasma current obtained from a combination of all poloidal field pick-up coils,*
Bottom: *Amplitude of an m=2, n=1 mode obtained from poloidal field pick-up coils on two opposite octants.*

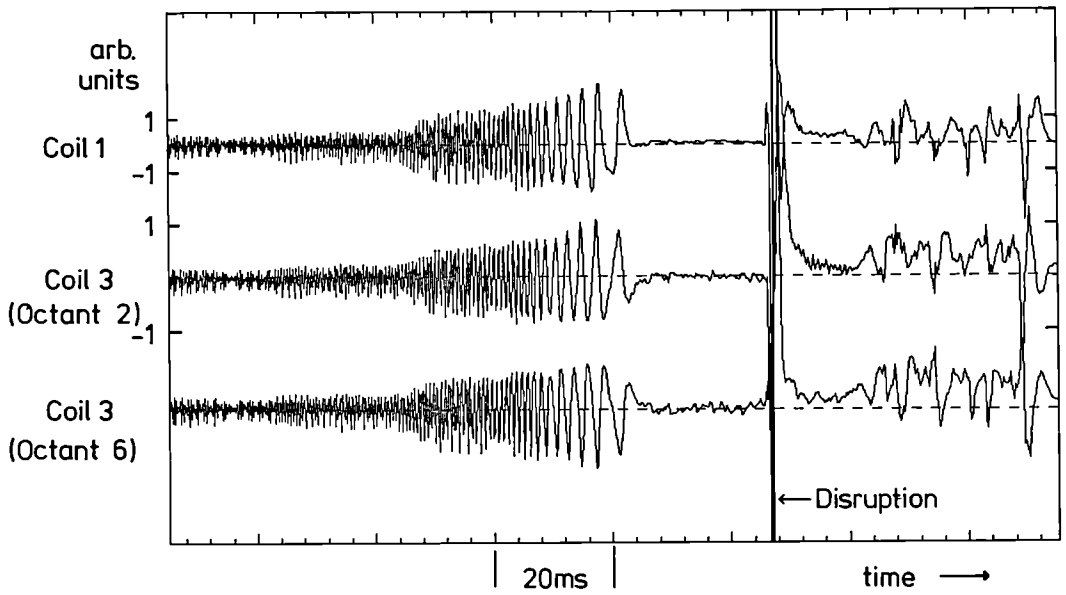

Fig. 90 3 coil signals showing MHD-activity leading to a major disruption. The n=1 toroidal variation may be seen.

removed immediately under ultra high vacuum to the analysis station. The main feature of this system is a carriage which is driven through the tube by means of linear motors. A variety of probes can be mounted on this carriage. The collector probes provide time resolution during a single shot by rotating a cylinder behind a slit. The direct reading probes could be heat flux probes, Langmuir probes or ExB analysers. The design of the FTS, for which the contract was awarded to the Association Euratom-UKAEA, Culham, has been completed and the device is being manufactured, with installation on JET scheduled for September 1984.

The complementary system, the Plasma Boundary Probe System (PBPS) (KY3) allows probes to be exposed through vertical ports in the torus. The basic system is of modular design and can be used in three configurations:

(i) with direct reading probes only;

(ii) with an exchangeable magazine with 5 probes;

(iii) for collector probes that can be analysed in-site using an Auger spectrometer.

The first two versions will be installed in early 1984.

The analysis station is designed to accept collector probes from the FTS and PBPS system and incorporates a number of surface analysis tools, including Rutherford Backscattering Thermal Desorption Spectroscopy, Electron Recoil Detection and Nuclear Reaction Analysis. The analysis station can also accommodate other additional analysis methods. The contract for the manufacture has been signed with the Association Euratom-IPP, Garching, F.R.G., and the design has started, with installation on JET scheduled for early 1985.

In addition to these diagnostics, samples and debris have been collected from the torus during the August – September shutdown. Examples of the debris showed a number of small metallic particles plus fabric from overalls.

Limiter Surface Temperature Measurements
(M. Pick, D. Summers, D. Cowell)

This system is designed to provide real-time information on the plasma-limiter interaction by spectrally imaging the limiters in two wavelength bands, by viewing these through one of the four sapphire windows attached to JET. There will be two types of camera system on JET, one of which is already operational. This utilises charge-coupled-device (CCD) video cameras to image the limiters in a narrow wavelength band in the region of the visible into the near infrared (~ 1100nm). By using optical filters this system provides a thermal image of the limiters in a limited temperature range at any temperature above ~ 500° C. The temperature range is limited by the dynamic range of the combined camera and video recording system of approximately 200:1. Each of the limiters, which are accessible to viewing, can be monitored by two cameras simultaneously operating at two wavelengths. The second camera system, which is still at the conceptual design stage, will operate at slightly larger wavelengths, 3–5 μm, and provide surface temperature data over a wider temperature range.

During the present period, two of the carbon limiters were observed by up to three cameras operating simultaneously. The cameras were equipped with filters at 900, 1000nm and at the H_α wavelength. The latter allowed observation of the hydrogen recycling behaviour in the vicinity of the limiter.

The following observations were made:

- The early discharges in JET were accompanied by numerous arcs on the surface of the limiters. Arcing has now virtually disappeared in more stable discharges but disruptive discharges are still usually associated with its appearance. Fig. 91 shows arcing on the limiter.
- At higher plasma currents (> 1MA), thermal

loading of the limiters was observed with temperatures reaching ~800°C in the hottest regions. The temperature distribution shows two peaks and the distance between them is a direct measurement of the thickness of the energy scrape-off layer. This thickness was found to be of the order of 15 mm in JET. Fig.92 shows a photograph of the thermal load distribution on the limiter.

- Viewing the limiter at the H_a wavelength showed that the hydrogen recycling occurred primarily on the *ion*-side of the limiter. The thermal load on the limiters was also not completely symmetrical. The ion side of the two limiters viewed was usually slightly hotter ($\approx$ 10%) than the electron side. There is no satisfactory explanation for these observations.

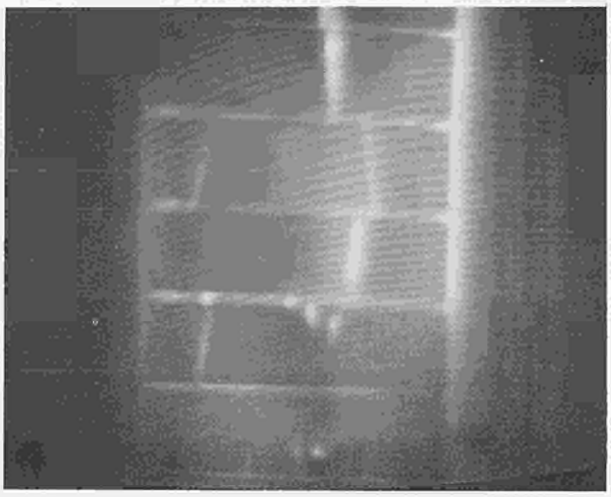

Fig. 91 Arcing on the surface of a carbon limiter.

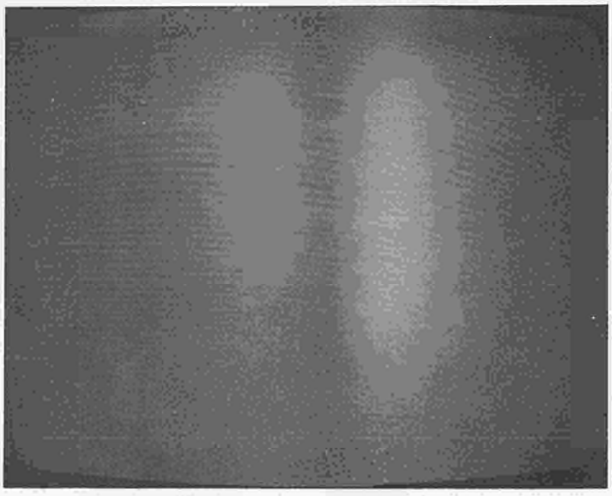

Fig. 92 Photograph of the thermal load distribution of a carbon limiter.

- Although it should be possible to extract the power deposition on the limiters from the temperature distribution, this has been hampered by the appearance of gases (probably hydrocarbons such as methane) which radiate in the infrared near the limiters.

Neutron Measurements

(O.N. Jarvis, J. Källne, G. Sadler, P. Van Belle)

The range of neutron diagnostics needed to study deuterium and tritium plasmas in conditions close to those required for a fusion reactor was described in the 1982 Annual Report. A short summary is provided in Table XII.

The time-resolved neutron yield (KN1) is measured with three pairs of uranium 235 and 238 fission counters mounted on the magnet limbs. These counters are operational although not fully commissioned. Their calibration, using a Cf-252 source of emission strength 2×10^8 neutrons per second, is planned for January 1984. All discharges so far have been in a hydrogen plasma so that the neutron emission was due to the acceleration of electrons to high energies and the production of Bremsstrahlung radiation when they struck the limiters and the vessel bellow protection plates, with consequent photo-neutron generation, primarily from Inconel. A close correlation was observed between the neutron (KN1) and hard X-ray (KH1) measurements.

The observed neutron count rate has been used to provide estimates of the runaway electron current and the total energy deposited during disruptions. The energies of the electrons which give rise to photo-neutrons must lie between 10 and 80 MeV; a reasonable average assumed was 30 MeV. From approximate neutron transport calculations, it was calculated that 1 neutron was detected in a U-235 fission chamber for every 3×10^8 neutrons produced within the torus vacuum vessel. From estimates of the photoneutron production, $\lesssim 0.5 \times 10^{-3}$ photoneutrons were produced for each 30 MeV electron striking one of the carbon limiters (appropriate to steady discharge conditions), whilst $\lesssim 2.5 \times 10^{-3}$ photoneutrons were produced for every 30 MeV electron striking an Inconel limiter or the inner protection plates (approprite to disruptions). In the most serious disruptions to date (pulse #1349), the instantaneous neutron emission reached $10^{15}\,ns^{-1}$ but the total emission integrated over 0.1 s, was only 5×10^{13} neutrons. This corresponded to a total energy deposited on the inner protection plates of $\gtrsim$ 100 kJ, or an initial runaway current of $\gtrsim$ 300 kA. During well-behaved discharges the total neutron yield was typically 10^{10}–10^{11} neutrons, the production being spread uniformly over the 5–10 s discharge; assuming an electron confinement time of 0.5 s, the corresponding runaway electron currents was only 1–10 A.

The neutron activation system (KN2) is well into its construction phase although the detailed interface between the irradiation ends of the pneumatic transport lines and the torus has not been finally agreed. The neutron emission profile system (KN3) has entered the detailed design stage. The 2.5 MeV neutron spectrometer

Table XII

Systems	Short Description	Main Quality	Main Purpose	Expected Installation Date
(a) Time resolved yield monitor (KN1)	Fission counters located on the magnet limbs	Absolute measurement with good time resolution	Time evolution of neutron yield	Operational
(b) Time integrated yield monitor (KN2)	Activation system with a counting station	Interference free absolute measurement	Absolute total yield and power multiplication factor	September 1984
(c) Yield profile measuring systems (KN3)	Multichannel collimator with scintillators and photomultipliers	Spatial resolution and good time resolution	Profile of reaction rate in non circular plasmas, MHD fluctuations	June 1985
(d) 2.4MeV collimator and spectrometers (KM1)	^{3}He ionisation chambers, NE213 scintillator, proton recoil spectrometer etc.	High energy resolution for 2.45MeV neutrons with large dynamic range covering most of D-D plasma conditions	Ion energy spectra and temperatures of D-D plasmas	June 1985
(e) 2.4MeV Time-of-flight system (KM3)	Time of flight			September 1984
(f) Proposed 14MeV collimators and spectrometers	Proton recoil spectrometer, associated particle spectrometer (proton recoil combined with time-of-flight spectrometer) and Si detectors	High energy resolution for 14MeV neutrons with large dynamic range covering most of D-T plasma conditions	Ion energy spectra and temperatures of D-T plasmas	1986

(KM1), to be located in the torus hall, has progressed little due to difficulties in agreeing a support tower design compatible with other requirements. The second spectrometer (KM3), to be located in the roof laboratory, is nearly ready for testing at Studsvik Energiteknik A.B., Sweden. It is expected that all these systems will be commissioned on JET by mid-1985.

Some extensions to these neutron systems are already planned. For example, the radiation counters for the activation system (KN2) can be supplemented by delayed neutron counters. This entails using small quantities of fissile material (e.g. U-238) as the target material to be activated. The method offers high efficiency and a capability for recycling the targets between plasma discharges which cannot normally be achieved with activation foils. The basic neutron spectrometer detectors associated with the KM1 diagnostic can also be supplemented, with a spherical hydrogen filled ion chamber which should provide high efficiency and good energy resolution (2.5% at 2.5MeV). Moreover, nuclear emulsion plates can be used for high efficiency spectrometry with modest energy resolution (4.5% at 2.5MeV) but the need to scan the plates individually means that this technique can only be used sparingly and is most appropriate as a means of calibrating other neutron diagnostic systems.

On computations, two specific activities are being undertaken. Firstly, a contract has been placed with Euratom-FOM Association, FOM, The Netherlands, for "in-vessel" neutron transport calculations to study the variations in response of the KN2 activation detectors as plasma parameters and plasma positions change. Secondly, work at Royal Institute of Technology, Stockholm, Sweden, continues on a code to predict the neutron energy spectra observed with the neutron spectrometers (KM1 and KM3) for plasma–plasma,

beam–plasma and beam–beam interactions. Effects yet to be incorporated in the code include plasma rotation and RF heating and a significant effort will be required to prepare it for general use and to interface with JET interpretation codes.

A Workshop to discuss the options available for neutron spectrometry in D-T operation was held in September. Several viable options were proposed which provided the necessary performance characteristics, although there is a difficult choice between high energy resolution and high efficiency. All the options, require collimated lines-of-sight from a shielded position outside the Torus Hall shielding walls into the plasma, entering the vacuum vessel through one relatively thin window (6mm Inconel) and leaving through an opposite window. A further Workshop should be held towards the end of 1984 to finalise the proposals for constructing these lines-of-sight and to select the most attractive of the spectrometer designs.

Hard X-Ray Monitors

(O.N. Jarvis, J. Källne, G. Sadler, P. Van Belle)

The Bremsstrahlung radiation produced when runaway electrons impact with the eight limiters is monitored with sodium-iodide scintillators coupled to photomultipliers. The system of monitors (KH1) is arranged in two groups of four, one group viewing the carbon limiters in the forward direction for Bremsstrahlung emission and the second group viewing the Inconel limiters from a backward direction. These monitors, which are fully operational, provide a measure of the Bremsstrahlung intensity (total power).

With favourable plasma discharges, the Bremsstrahlung emission is continuous in time and of low intensity, but when the occasional disruption occurs, the signals are of short duration and of sufficient intensity to saturate the linear amplifiers. In order to obtain a measure of the emission during a disruption, whilst also providing a measurable signal for the quiet discharges, it will be necessary to install logarithmic response amplifiers. A further group of three monitors is planned for installation on the North wall of the Torus Hall, using different density scintillators, lead filters and, possibly, pulse-height analysis in order to measure the energy spectrum of the Bremsstrahlung emission, which is directly related to that of the runaway electrons. Some information on the energy spectrum was obtained from the photoneutron signal recorded with neutron yield monitors (KN1), which is always present whenever the hard X-ray signal is of appreciable intensity. This showed that the runaway electrons possessed a component with energy above ~ 10MeV but gave no indication of the upper limit, although theoretically this was unlikely to exceed 80MeV.

Experimental Division 2

(Division Head: W.W. Engelhardt)

Experimental Division 2 is responsible for specification, procurement and operation of about half of the JET diagnostics systems, particularly those associated with spectroscopy, bolometers, interferometry, soft X-ray array and neutral particle analysis. In addition, the Division assists in execution of the programme, in interpretation of the results and in making proposals for future experiments, in collaboration with Experimental Division 1, Theory Division, the Physics Operations Group and the Operations and Development Department. The Division consists of two groups: "Spectroscopy and Impurity Physics" and "Radiation and Particle Analysis". This distinction reflects the focal points of physics investigations being pursued.

Impurities play a major role in tokamaks as they induce radiation and influence the stability of the plasma. Their sources, concentrations, time evolution and transport behaviour are being investigated with classical spectroscopic methods in the spectral range from the X-ray regime to the visible. Integral radiation measurements are being carried out by bolometers and, with coarse spectral resolution, by soft X-ray detectors.

Particle transport is the second extensive field being investigated in the Division. The electron density distribution will be measured by interferometry, the particle sources determined by spectroscopic methods, neutral particle energy distributions analysed and deliberate perturbations of particle densities will be induced by injection of pellets. Spectroscopic Doppler measurements and neutral particle analysis provide insight into the ion energy distribution. The analysis of ion heating and ion energy confinement is another important field which will be investigated.

The Division was established at end of 1982 and built up in 1983 to about half its final size. In order to compensate for the limited JET staff available, several Task Agreements (see following Section) were concluded with Associated Laboratories resulting in fruitful collaboration and in efficient support of the experimental programme on JET.

The main work involved continuing supervision of diagnostics construction in Associated Laboratories. A survey is given in Table XI and details are dealt with in the following sections. During the start-up phase of JET, only limited diagnostics were ready and some were installed only in a provisional way. Examples and preliminary results are given in the following paragraphs. A relatively consistent picture of the impurity situation was obtained with these methods.

Task Agreements

Collaboration with Associated Laboratories is organised by Task Agreements centred around specific fields of research activities. In many cases, these are closely connected to diagnostic instruments built in the Associations, but also based on special expertise. The tasks include installation, commissioning, operation of diagnostics, physics investigations and interpretation of results, in collaboration with the JET team.

The following Agreements were concluded:

- "Bulk Impurity Physics and Impurity Related Diagnostics" (EURATOM-IPP Association, IPP Garching).
  Eight single bolometers and three bolometer arrays were installed and operated by IPP staff. A provisional set of soft X-ray diodes was put into operation as a monitor for internal MHD activity and for electron temperature estimates. The details of this work is dealt with in later sections.
- "Impurity Analysis" (EURATOM-UKAEA Association, Culham Laboratory).
  The work was partly concerned with the construction of an impurity survey VUV spectrometer. Major contributions were made by providing JET with 'visible' spectrometers, analysing spectra and deriving impurity fluxes from the measured line intensities. Detailed results are presented in the following paragraphs.
- "Physics of Neutral Beam Heating Optimisation" (EURATOM-UKAEA Association, Culham Laboratory).
  A comparative literature study on the relative merits of balanced or unbalanced injection in JET was performed. A report concluded that unbalanced injection in co-direction is more promising to obtain efficient heating and good energy confinement. The risk involved with high rotational speed was considered to be tolerable.
  Under the same Agreement, experimental investigations and interpretation of the Doppler broadening of H_α emission were carried out. These measurements will complement the energy analysis of neutral particles escaping from the plasma.
- "Physics of Ion and Electron Energy Transport and Related Diagnostics" (EURATOM-ENEA Association, CREF, Frascati).
  This Agreement consists of two parts, one of which is directly related to the work of the Division. It originated by providing support in the installation of a neutral particle analyser built by Frascati. The operation and physical exploitation is expected in 1984.
- "Spectroscopic Measurements, their Interpretation and Impurity Effects Analysis" (EURATOM-CEA Association, Fontenay-aux-Roses).
  The Task Agreement has been arranged and will be operated in 1984, when the VUV Spectrometers have been delivered to JET.

Progress in Construction and Installation of Diagnostics

Bolometry (KB1)

(G. Magyar, K. Mast*, H. Krause*, A. Bulliard)
*EURATOM-IPP Association, IPP, Garching

This diagnostic is used to make space and time resolved measurements of emissivity and radiation losses from the plasma. Two arrays of bolometers have been installed to view the JET plasma in orthogonal directions through vertical and horizontal ports, and eight individual bolometers, one at each octant. At start-up, a single bolometer was available. In August, the vertical array was installed, together with the remaining seven individual bolometers. By the end of December, accurate measurements of total radiation losses and spatially resolved emissivity profiles were obtained. By January–February 1984, the horizontal array should be installed. The entire system is designed to be operable in the active phase of JET operation.

Multichannel Far-Infrared Interferometer (KG1)

(G. Magyar, J. O'Rourke, G. Braithwaite)
EURATOM-CEA Association, CEA, Fontenay-aux-Roses

This apparatus makes space and time resolved measurements of plasma density, using a DCN laser source at 195μm wavelength. The interferometer components are mounted on a single large C-frame which spans the whole torus, and is mechanically decoupled from it, minimising the effects of vibrations. Corrections for any residual vibrations can be made using a parallel infrared interferometer operating at 3.39μm. During the year, fabrication of major system components were completed, and assembly was started at JET. Operation is expected to start in June 1984. The system is built to be operable in the active phase of JET operation.

X-ray Pulse Height Spectrometer (KH2)

(R. Gill, E. Källne)

This spectrometer will consist of three Si(Li) soft X-ray detectors viewing the JET plasma along three nearly coincident chords in the energy range $E > 1$keV. Each detector will provide an energy spectrum with a different lower cut-off energy over a different energy band, by using Be-foil filters in front of the detectors. The spectrometer will determine impurity species and concentration from resolved line emission and enhancement of the Bremsstrahlung background. The plasma electron temperature will also be obtained from the X-ray energy spectrum in line-free regions.

During the year, a detailed design was started, and manufacture, installation and operation of the system is expected to take place during 1984. Simultaneously, a feasibility study is under way on modifications to make the system operable in the D-D and partly in the D-T phase of JET operation.

A provisional spectrometer using an uncooled mercury-iodide (HgI_2) detector is expected to be operational in mid-1984, which will view the plasma through $\cong 400\mu$m Be-foil windows, providing an accessible energy range of $E > 4$keV, with energy resolution of ~500eV. The provisional system will be suitable for measuring electron temperature and Bremsstrahlung enhancement.

Soft X-ray Diode Arrays (KJ1)

(R. Gill, H. Krause*, J. Bonnerue)
*EURATOM IPP Association, IPP, Garching

The system consists of two soft X-ray imaging cameras using an array of detectors behind a single pinhole. Two cameras will view the same toroidal plasma cross-section in orthogonal directions (one mounted on a vertical port and one on a horizontal port). This system will enable

space and time fluctuation measurements resolved in X-ray emissivity, which can be interpreted to provide information about MHD plasma phenomena and the location of magnetic surfaces.

A special data acquisition and storage system is being built to handle the large volume of data produced during each pulse. An approved detailed design exists for the vertical camera and it will be installed at the end of 1984. The detailed design of the horizontal camera will be available shortly.

The most serious restriction arises from the detectors sensitivity to neutron and gamma radiation. Massive shielding will be required to permit operation in deuterium plasmas with high-power heating. However, this system is not suitable deuterium-tritium plasma operation due to radiation induced signals and detector damage. Detectors less sensitive to this radiation will be sought.

Neutral Particle Analyser Array (KR1)
(S. Corti, J. Bonnerue, L. Lamb)
EURATOM-ENEA Association, ENEA, Frascati
Ion temperatures can be obtained from an analysis of the energy distribution of escaping fast neutral atoms produced by resonant charge exchange between plasma ions and neutral atoms. This system consists of an array of five separate analysers arranged to view different chords in a poloidal plasma section. The array is mounted on a common support and can scan the toroidal direction to view from near to near tangential directions.

The analysers, which have simultaneous energy and mass resolution for hydrogen and deuterium atoms, can be used for energies up to 80keV/nucleon (i.e. 160keV for D). This will allow measurements of both the thermal ion spectrum and the fast ion distribution resulting from neutral injection and ion cyclotron resonance heating. Construction of the system was completed during 1983 and the complete mechanical support with one analyser (the one viewing through the centre of the plasma) will be installed during January–February 1984. This analyser will be operational during mid-1984. This apparatus is not suitable for use in the active phase of JET operation.

Active Phase Spectrometer (KS1)
(G. Magyar, E. Källne)
EURATOM-IPP Association, IPP Garching
A design study is underway on a double crystal spectrometer which could provide an extended spectral range coverage (0.2–2nm) and time resolved information for single plasma discharges. A particular design feature is high precision mechanisms for moving the two crystals to ensure satisfactory resolution for all wavelengths. The two crystals and detectors will be located outside the Torus Hall behind the radiation wall allowing the instrument to be operational during the D-T phase of JET operation. Phase I of procurement is complete and operation on JET is envisaged during 1986.

Spatial Scan X-ray Crystal Spectrometer (KS2)
(G. Magyar, E. Källne)
EURATOM-IPP Association, IPP, Garching
A complementary instrument, based on the same principle but with an additional crystal rotational motion, has been considered to obtain spatial profiles during a single plasma discharge. The complexity of precision motions required for such an instrument has been the object of an extensive design study, completed during the year. To obtain a reliable spatial scan, it was necessary to locate this instrument near the plasma. Thus, the instrument was designed to be closely coupled to a vertical port on JET, and was enclosed by radiation shielding sufficient only for use up to the D-D phase of JET operation. Phase I of procurement has been completed, and operation is expected by the end of 1985.

H_α Monitor System (KS3)
(P. Morgan, J. Martin)
This system has been operational from start-up in June 1983, providing the first evidence of plasma in JET, and since then it has been used to conduct spectroscopic investigations of impurity species, sources, fluxes, effective ion charge (Z_{eff}), and particle confinement times. Further details are given in the following Section.

The design of a 16 channel system is underway, which will follow the temporal evolution of the visible radiation in a poloidal cross-section of the plasma. By suitable signal processing, the emission of H_α line and continuum radiation can be spectrally resolved. Installation and commissioning of this system should begin in September 1984. The H_α system is suitable for use in the active phase of JET operation.

VUV Spatial Scan Spectroscopy (KT1)
(G. Magyar)
EURATOM-CEA Association, CEA, Fontenay-aux-Roses
This spectroscopic system will be used to cover the wavelength range 10–200nm. The spatial scan is obtained by viewing the plasma through a rotating mirror which has a gold-plated face and is used in near grazing incidence. The scan takes 3ms to complete and will be repeated every 20ms. The three mirrors are synchronised to rotate together and can also be stopped at any predetermined position in order to obtain a continuous recording along a fixed chord. Three of these GISMO spectrometers will be installed, two viewing the plasma through a horizontal port, and one vertically from a bottom port. All three will view the same poloidal cross-section.

During the year, the three spectrometers were equipped, tested and calibrated. The detailed design of the two horizontal channels was approved and delivery is due in February 1984. After clarifying the interface problems, detailed design of the vertical channel with its support and platform started in November 1983. The whole system should be operational in late 1984.

VUV Broadband Spectroscopy (KT2)
(G. Magyar, A. Ravestein, N. Peacock[+], N. Hawkes[+], J.L. Martin)
[+]EURATOM-UKAEA Association, Culham Laboratory
Based on a McPherson broadband spectrometer (covering the range 12–170nm)and a microchannel plate detector, the instrument will be used for time-resolved line identification and impurity monitoring studies. The spectrometer beam line has been designed to permit later replacement by other instruments. A high resolution normal incidence spectrometer and a grazing incidence spectrometer, covering the range 2–10nm, are possible future developments. The wavelength range covered is most suited for the relatively low temperature plasmas expected in the early JET operation, before the full additional heating power is applied. The system should be installed on JET in January 1984.

Visible and near UV Spectroscopy (KT3)
(M. Stamp, M. Forrest[+], J. Martin)
[+]EURATOM-UKAEA Association, Culham Laboratory
Since October, a provisional visible/UV spectroscopic instrument has been used on JET. The instrument is a 1m normal incidence grating spectrometer mounted on a transformer limb of JET close to a horizontal port with a sapphire window. Such close coupling, eliminating the need for optical fibre, has extended the accessible spectral range of the presently available instruments down to 200nm. The JET plasma is viewed tangentially: the imaging can be adjusted so that a limiter, part of the inner wall ($R = R_{min}$) or the plasma boundary can be observed. This has enabled metal influxes from the limiter surface and the vacuum vessel to be distinguished.

High Resolution X-ray Crystal Spectroscopy (KX1)
(G. Magyar, E. Källne)
EURATOM-ENEA Association, ENEA, Frascati
The plasma ion temperature can be measured conveniently from the spectral width of selected impurity lines. At the expected high central temperatures, lines from heavy metal impurities must be used. The high resolution X-ray crystal spectrometer is of classical design based on the Rowland circle geometry with a large (24m) radius of curvature. The large radius allows the main part of the instrument to be placed outside the Torus Hall. The diagnostic is interfaced to JET with a large beryllium window. A curved crystal will serve as the analysing element with focussing properties, and a multiwire proportional counter (which combines high efficiency and good spatial resolution) will serve as detector to study H- and He- like metal impurity lines. The crystal and detector will be placed outside the Torus Hall behind the radiation shielding wall, permitting use of the instrument in the D-T phase of JET operation. During the year the detailed design was completed and the spectrometer is under construction, for installation in JET in 1985.

Hydrogen Pellet Injector (KZ1)
(A. Gondhalekar, J. Bonnerue)
EURATOM-IPP Association, IPP, Garching
The hydrogen pellet injector is a new system which is able to make solid hydrogen or deuterium pellets of up to 10^{22} particles, and launch these into the plasma with a velocity of $1600 ms^{-1}$. The injector is of the pneumatic gun type and can launch a single pellet during a JET pulse. By launching pure hydrogen/deuterium or impurity doped pellets, studies can be undertaken of hydrogen/deuterium ion transport, impurity transport, energy transport, plasma density profile modification and control, and plasma fuelling. Phase II of procurement has started and detailed design is in progress. The system is expected to be operational in late 1985. The system is designed for use also in the D-T phase of JET operation.

Diagnostics in the Start-up Phase and First Experimental Results

Optical Spectroscopy
(K. Behringer)
The H_α monitor system (KS3) is now used as a routine diagnostic. In each channel, a lens mounted adjacent to a torus window images a chord through the plasma onto an optical fibre, which runs from the Torus Hall to the Diagnostic Area (a distance of about 100m) and through which radiation in the wavelength range 350–700nm is transmitted. The light emerging from the fibre is treated in one of two ways, as follows:

(i) The first scheme utilises a beam splitter, a pair of interference filters (each centred on a different wavelength and of bandwidth ~ 1nm) and two photomultipliers as detectors. The system is simple and relatively inexpensive, but rapid changes of detected wavelength cannot be made and no information on spectral shapes can be obtained.

(ii) The alternative method uses a grating spectrometer to disperse the radiation prior to detection, and with an optical multi-channel analyser (OMA) as detector, the temporal and spectral evolution of various emission lines can be followed. Three spectrometers have also been used as monochromators, with a photomultiplier at the exit slit permitting the temporal variation of a selected line to be followed. This system permits a high degree of flexibility in rapidly changing from one spectral line to another between plasma pulses.

In either case, each channel was calibrated absolutely, from lens to detector, using a standard tungsten ribbon lamp.

For the initial operation, two channels were available each viewing the plasma vertically at major radius R = 3.11m, monitoring H_α radiation and total light emission. The number of channels has now been increased, so that at the start of October operation, there were six additional vertical channels (one on each octant of JET, and two viewing the plasma along its equatorial plane). The latter monitored the carbon limiter on Octant 4, and the nickel limiter on Octant 6 (which has been withdrawn from plasma contact).

Most of the 8 vertical channels monitored the H_α emission and the continuum radiation at 523.5nm by

means of filters and photomultipliers. Two were connected to spectrometers (a 1 m and a 0.6 m instrument (M1000 amd M600)) used either in photographic mode or as monochromators recording the temporal behaviour of lines emitted by partially stripped ions (mainly carbon and oxygen).

The plasma emission at the carbon limiter was recorded using a 1 m spectrometer and OMA. The channel viewing the nickel limiter utilised a 0.6 m monochromator and a photomultiplier, with a vibrating mirror attachment to record H_α line profiles. The outputs from the photomultipliers were digitised and stored using standard facilities provided by CODAS Division.

From October onwards, emission in the vicinity of the carbon limiter on Octant 8 was studied using a 1 m grating monochromator, mounted on a JET transformer limb (System KT3), in both photoelectric and photographic modes. Such close coupling obviating the need for optical fibres, has extended the accessible range of wavelengths down to 220 nm. This permitted line emission from nickel and molybdenum ions to be studied, which previously had been unobservable due to severe attenuation in the fibres. The data acquisition system of KS3 was used to record and store the data.

Summary of Results from H_α Emission and Continuum Radiation Studies

(P. Morgan)

By measuring the absolute $H_\alpha(\lambda = 656.3\text{nm})$ photon flux arising primarily from hydrogen entering the plasma from the torus wall or limiters, the ionisation rate could be deduced using a collisional-radiative atomic physics model. The flux of hydrogen atoms Φ_H entering the plasma was estimated from the formula:

$$\Phi_H = 2\pi\, L_w\, A_w\, R_{IE} + 4\pi\, L_L\, A_L\, R_{IE}$$

where, L_w and L_L are the radiance of the H_α line at the wall and limiters, R_{IE} is the ratio of ionisation to excitation and A_w and A_L are the surface areas of the vessel walls and limiters, respectively.

At plasma currents $I_p > 500$kA, the flux of hydrogen atoms released by the limiters dominated those emanating from the wall. The ratio of limiter to wall flux increased approximately linearly with plasma current, and was about 10 for currents near 2MA. The total flux of recycled hydrogen atoms increased with increasing plasma density. A relation of the form $\Phi_H \propto \bar{n}_e^2$ was in fair agreement with the data, for $\bar{n}_e > 10^{19}\,m^{-3}$ (where $\bar{n}_e$ is the average electron density)(see Fig. 93).

In the stationary case, the total plasma electron content divided by the incoming hydrogen flux may be defined as a global particle confinement time, τ_p. The variation of τ_p with the average electron density $\bar{n}_e$, is shown in Fig. 94, for which a dependence $\tau_p \propto \bar{n}_e^{-1}$ is reasonable, for $\bar{n}_e > 10^{19}\,m^{-3}$.

A simple explanation is as follows: the particle losses at the plasma boundary are determined by a diffusion coefficient (independent of the plasma parameters) and by the electron density gradient characterised by the ionisation length, which is proportional to $1/\bar{n}_e$. Therefore,

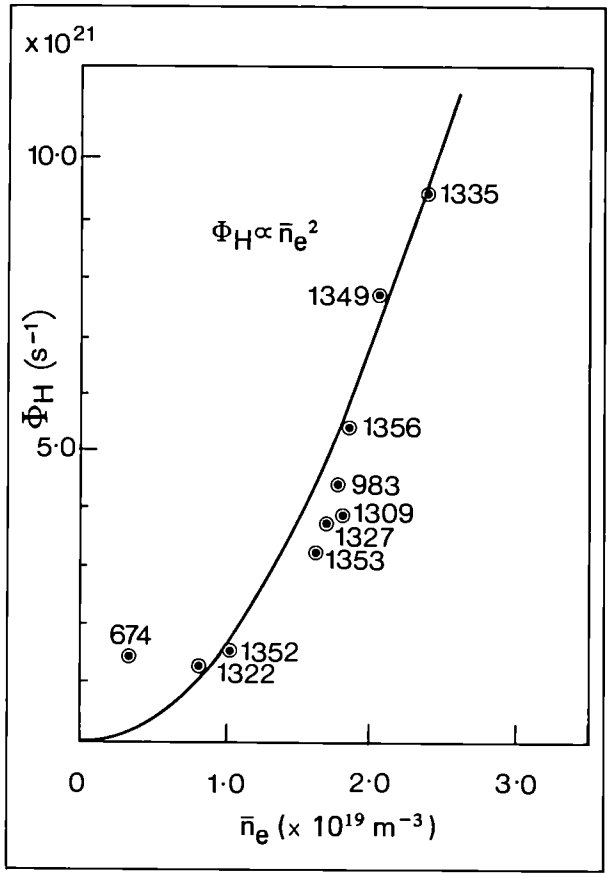

Fig. 93 Total hydrogen flux (ϕ_H) as a function of average electron density ($\bar{n}_e$).

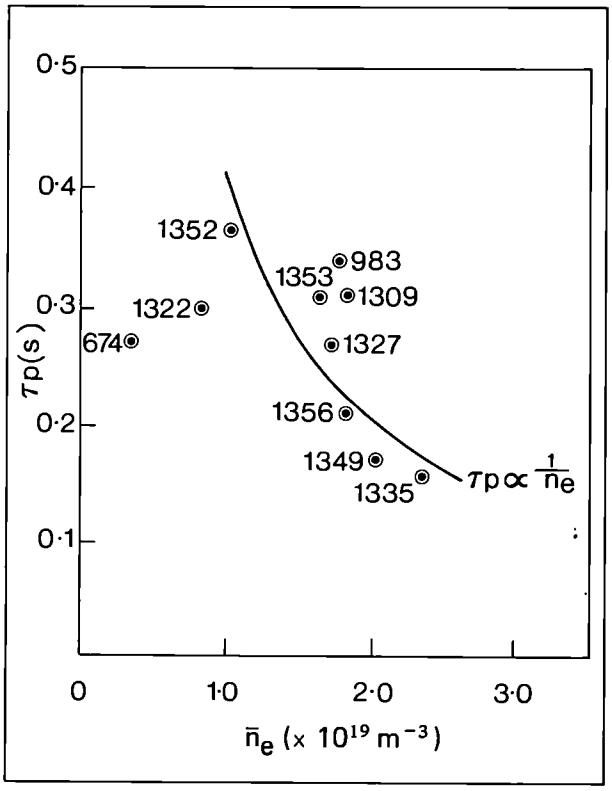

Fig. 94 Hydrogen particle confinement time (τ_p) as a function of average electron density ($\bar{n}_e$).

the losses scale with $\bar{n}_e^2$.

The recycling coefficient, r, is the ratio of the hydrogen flux entering the plasma to the particle flux escaping. The latter is determined by the influx and the time derivative of the electron density. During a plasma discharge, r is approximately 1 throughout the constant current period, being somewhat larger than 1 during current build-up and falling to ~0.9 during current decay. In particular, the decrease could be attributed to a fall in influx from the limiter – the influx from the walls increases during current decay.

A measurement of the effective charge, Z_{eff}, is a useful indicator of the global impurity content of the plasma. The absolute continuum intensity at 523.5 nm was measured by means of a filter-photomultiplier combination, and compared with the intensity calculated for a hydrogen plasma of the same density and temperature. Z_{eff} is the ratio of measured to calculated intensity. During a series of higher-current shots (I > 1 MA), it was seen that the temporal evolution of Z_{eff} during a pulse followed approximately the waveform of the plasma current, albeit with a delay of several 100 ms. In addition, over a number of shots, the value of Z_{eff} at peak current was inversely proportional to the corresponding value of electron density. This is illustrated in Fig. 95.

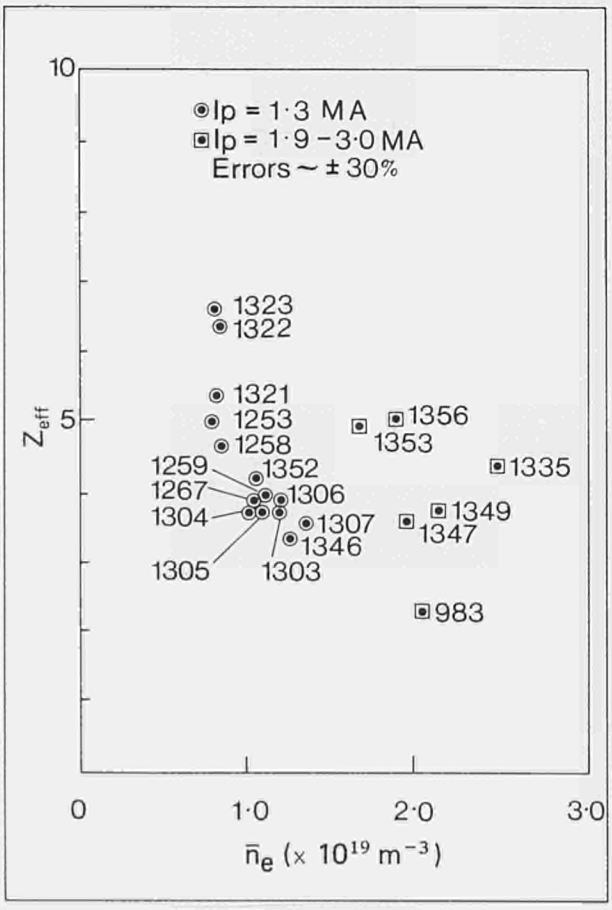

Fig. 95 Variation of Z_{eff} with average electron density ($\bar{n}_e$) for different plasma currents.

Impurity Spectroscopy
(M. Stamp)

During initial JET operation, the M1000 and M600 spectrometers were used photographically and photoelectrically to determine the nature of plasma impurities. As expected, O, C, and Cr were observed, the latter being a major constituent of the vessel walls. With KT3 operating at shorter wavelengths, Ni, Fe, Mo and Ca impurity radiation was also detected. Fig. 96 shows a photographic spectra from KT3, where parts of the carbon limiter and of the walls were imaged on the entrance slit. This photograph suggests that most of the metallic impurities come from the carbon limiter: a fact that is confirmed by the other spectrometers.

In later periods of JET operation, the spectrometers were used mainly to monitor CIII (465 nm), OIV 373.7 nm) and CrI lines, as a measure of impurity influxes. These were checked for correlations with other

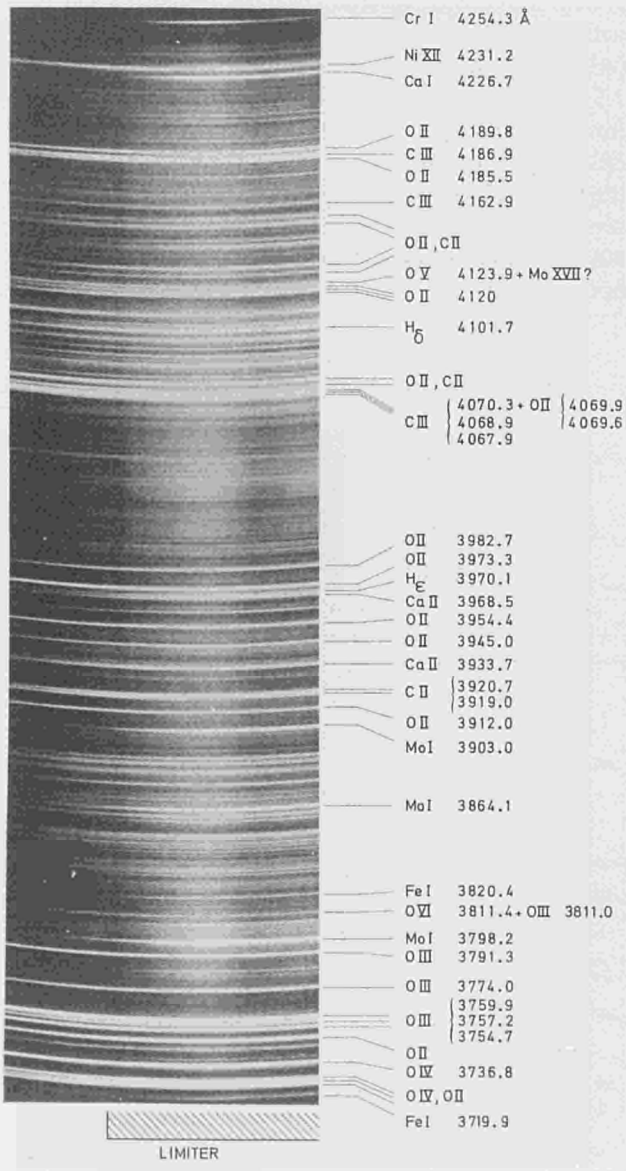

Fig. 96 Photographic spectrum recorded by the torus spectrometer. Parts of the carbon limiter and of the adjacent wall are imaged on the entrance slit.

signals (e.g. limiter viewing camera) and for parameter studies (e.g. impurity influx versus plasma current). A forbidden line of nickel (NiXII, 423.1nm) was also observed, and used to estimate the absolute concentration of nickel in the plasma.

A narrow band interference filter system is presently being constructed for simultaneous measurement of the temporal behaviour of several impurity lines from the same part of the plasma, and will release the M1000 and M600 for other impurity studies.

Spectral Survey from the OMA-Spectrometer

(P. Carolan[+], M. Forrest [+], N. Peacock[+])
+EURATOM-UKAEA Association, Culham Laboratory,

The spectral instrument consists of a 1 metre Czerny-Turner arrangement with a 1200ℓ/mm grating and high quality camera lenses (deployed in a front-to-front configuration), and an Optical Multichannel Analyser (OMA). A zoom lens facility permitted adjustments of the overall system in terms of spectral coverage, resolution and vignetting. With f = 70mm (zoom lens) and f = 130mm (telephoto) combinations, a spectral coverage of about 7.5nm was obtained, with an optimum resolution performance of 0.03nm FWHM. The overall quantum efficiency of the system (i.e. from the collection lens to the OMA output) was measured using calibrated tungsten lamps. There was an abrupt fall-off in sensitivity below 400nm, which was due to losses in the lenses and fibre optics.

The bulk of the emission lines were observed to originate from low ion stages of O, C and the Inconel metal components, Ni, Cr, etc. Some strong lines of Ar, Cl, Ca, etc. were also noted, particularly in the early phase of JET operation before intensive discharge cleaning. These lines could be interpreted in terms of influx of the respective element into the plasma. Thus, the OMA-spectrometer results displayed the time history of the influxes of the individual ion species during the current pulse. These results were particularly graphic when viewing the limiter during disruptions, as the limiters appeared to be the dominant source of these impurities. An example of such a temporal variation is shown in Fig. 97, for the spectral range 422nm to 430nm containing three CI, one CII and a CaI line.

A number of the important impurity multiplets of CII, CIII, OII, CrI, etc., are close to the hydrogen Balmer lines in the OMA spectra. The absolute emissivities of the Balmer lines were measured and calculated. Using these intensities as transfer standards, the volume emissivities and influx rates of the impurities were assessed.

Zeeman splitting of hydrogen (H_α = 656.3nm) and impurity lines, (CII = 657.8nm and 658.3nm and CRI = 425.4nm, 427.4nm and 428.9nm) were observed in the termination phase of the plasma. Tangential viewing optics showed the influence of Zeeman splitting on the line profiles more clearly, as the magnetic field was essentially aligned along the viewing chord. In this case, the central π components of the Zeeman pattern were not observed, which facilitated the detection of the

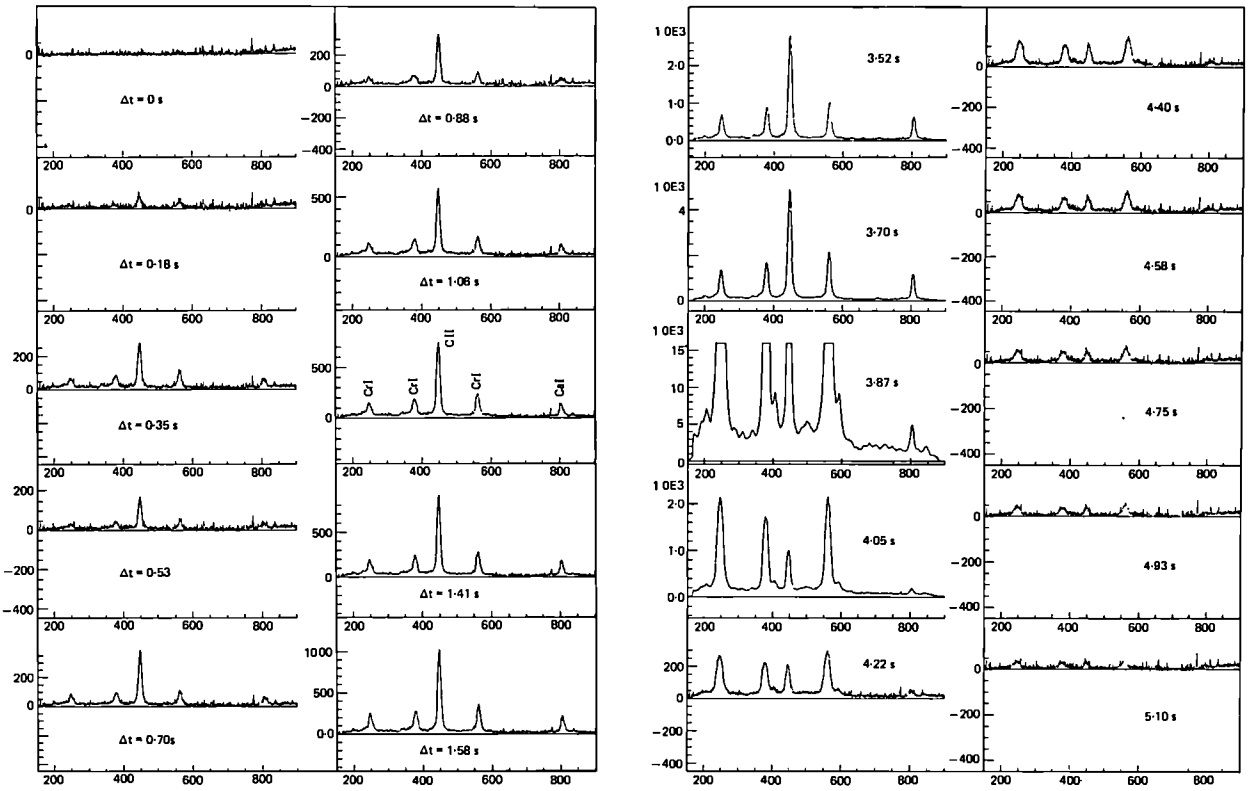

Fig. 97(a) and (b) Part of the OMA spectrum (central wavelength 425nm) versus time of the discharge.

outer σ components. This was important when the instrumental width and Zeeman shifts were comparable.

The locations of the impurities were calculated from the measured spectral splitting and the toroidal field distribution. Since low ionisation states, or neutrals, were restricted to the plasma periphery, this technique afforded a direct measurement of the plasma boundary motion. The observations also highlighted the inportance of Zeeman splitting, at least in tokamak plasmas, for making spectral shift, broadening or absorption measurements (e.g. Doppler, Stark or resonant line absorption effects) in the visible spectrum region.

Several scans from the output of a grating spectrometer (1m Czerny-Turner mount, Rank-Hilger MONOSPEK 1000) are shown in Fig. 98 for Pulse No. 831. These correspond to the pulse termination phase and the instrument detected different spectral regions to encompass (a) the Cr I lines and (b) the H_α and C II lines (exposure time ~50ms). The spectral lines were clearly split, from which the magnetic field strength (i.e. the position of the plasma periphery could be measured. In addition, the measured instrumental functions (FWHM = 0.07 nm) were used to deconvolve the spectra, and the depth of modulation gave the orientation of the field with the viewing direction at the point of intersection between viewing chord and plasma boundary. An example of such a deconvolution (by a "maximum entropy" technique), is shown in Fig. 99, where the π component in the CrI 427.4nm line is almost completely absent (i.e. $\vec{B}$ is parallel to the viewing chord). A summary of the calculated positions of the emitting regions of CrI, C II and H_α as a function of time is shown in Table XIII.

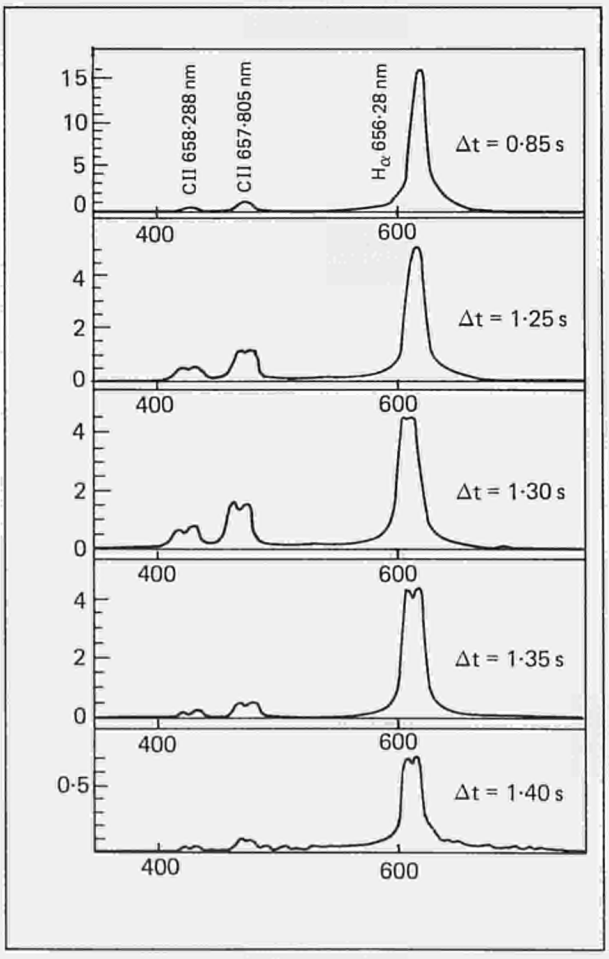

Fig. 98 OMA spectrum around 656nm demonstrating the Zeeman splitting of H_α and CII lines at the end of the pulse.

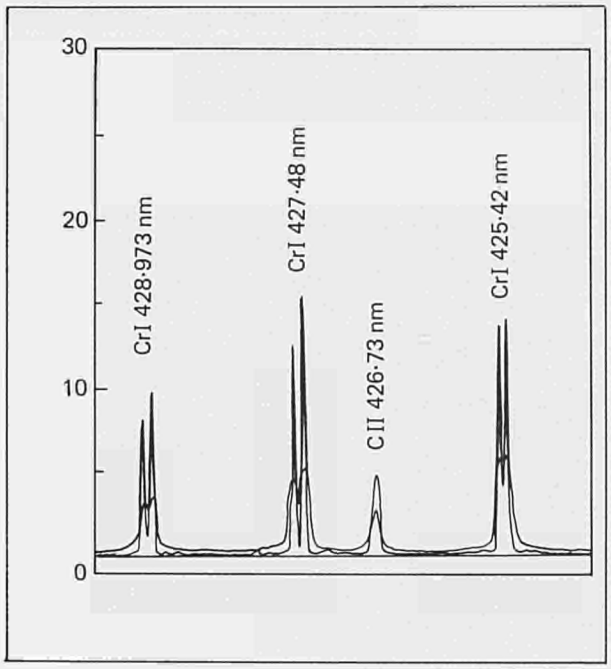

Fig. 99 Deconvolution of spectral line profiles isolating the σ components of Zeeman splitting.

Table XIII

Position of the plasma boundary as a function of time, derived from the magnitude of Zeeman Splitting

Shot No.	Δt (s)	ELMT	λ (nm)	Δλ (nm)	|B| (T)	R (m)
831	1.40	CrI	427.4	0.051	2.99	2.11
	1.40	CrI	428.9	0.044	3.08	
	1.45	CrI	427.4	0.040	2.33	2.72
	1.45	CrI	428.9	0.034	2.38	
838	1.25	CII	658.3	0.060	2.22	2.97
	1.25	CII	653.8	0.042	2.09	
	1.30	CII	658.3	0.066	2.45	2.56
	1.30	CII	657.8	0.012	2.53	
	1.35	CII	658.3	0.072	2.66	2.46
	1.35	CII	657.8	0.053	2.63	
	1.35	HI	656.3	0.044	2.17	2.96
	1.40	HI	656.3	0.035	1.74	3.72

These may be interpreted in terms of a velocity of the plasma, moving to the inner wall.

Scanning Spectrometer

(G. Cottrell, D. Guilhem[+], M. Cox[+])
[+]EURATOM-UKAEA Association, Culham Laboratory

In the present ohmic discharges, the Doppler-broadening of the (Balmer) H_α optical emission has been observed. For the present, analysis has been restricted to interpreting the broad wings of the profile (a result of excited charge-exchange neutrals) in terms of the central ion temperature $T_i(0)$. However, the Doppler-shift technique may also be used to determine any plasma bulk motions (i.e. rotation) by measuring line asymmetry as well as the absolute neutral density profile by using absolutely calibrated measurements. The spectrum was measured using a 0.5 m Czerny-Turner spectrometer with a vibrating mirror to scan the wavelengths of interest.

A typical spectrum is shown in Fig. 100, of an intense but narrow H_α component (centred on λ_0) superimposed on a relatively faint but broad Doppler-broadened wing structure (extending ± 1.5nm from λ_0). The narrow component arose from cold neutrals recycling from the limiter/walls, whereas the broad feature was produced by electron impact excitation of H atoms which populated the hot core of the discharge by charge-exchange cascade. In order to interpret the spectrum, a 1-D Monte-Carlo model of the neutral particle distribution function was used to construct a 'synthetic spectrum' (based on the weighted summation of many 'micro-spectra' along the line of sight). An additional low temperature spectral component was added to the model to describe the emission produced by wall/limiter recycling. From the data in Fig. 100, an edge temperature $T_i(a) \cong 7eV$ was obtained which was close to the expected Franck-Condon energy range of dissociated H_2 molecules. Since few photons were detected in the wings of the line, the synthetic spectrum was fitted to the data using an unbiassed likelihood estimator based on Poisson statistics. From the data in Fig. 100 (solid points), the composite line model (solid line) was fitted and $T_i(0) = 1575 \pm 200eV$ was found, a value close to the electron temperature obtained from the ECE diagnostic under similar discharge conditions.

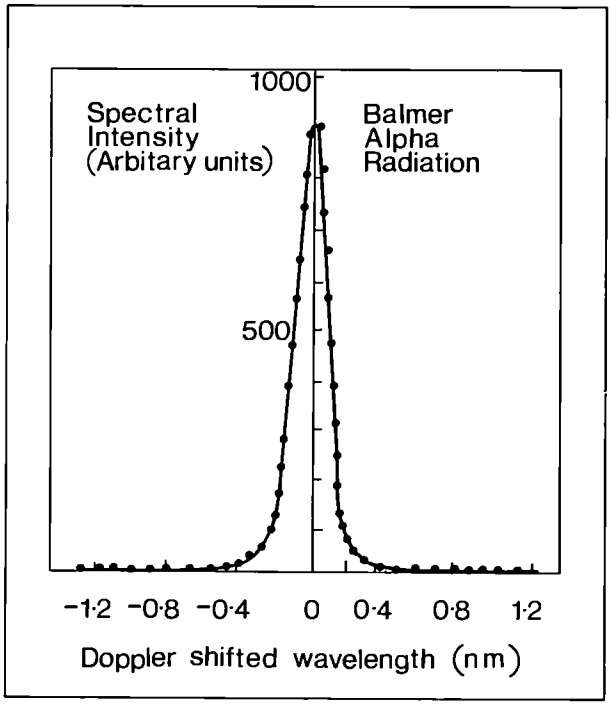

Fig. 100 Line profile of H_α in which the measurements (solid points) have been fitted by a synthetic spectrum. A central ion temperature of 1575eV is derived from the far wings.

Bolometer Diagnostic (KB1)

(K. Mast*, H. Krause*)
*EURATOM-IPP Association, IPP, Garching

Using a provisional electronic system of 15 channels only (two single bolometers and the vertical camera), data were collected from October to December and stored in the JET Pulse File (JPF). Programs for data smoothing and display, the calculation of physical radiation power from the measured data, and for the conversion of measured spatial profiles into local radiation losses (Abel inversion) were developed at JET, making use of sub-programs from JET and from IPP Garching. The plasma elongation was taken into account by introducing elliptical flux surfaces.

Assuming a rectangular emission plasma profile, the first weeks discharges showed radiation losses very close to the ohmic input power. With the installation of the 14 channel vertical bolometer camera in September, the measurement of total radiation losses became insensitive to source geometry assumptions. Fig. 101 shows total radiation losses as a function of ohmic input power for flat top or current peaked discharges in November and

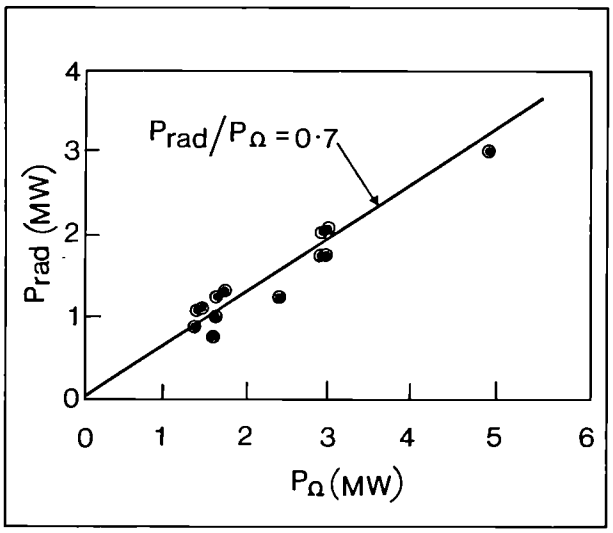

Fig. 101 Total radiation power (P_{rad}) as a function of ohmic input power (P_Ω).

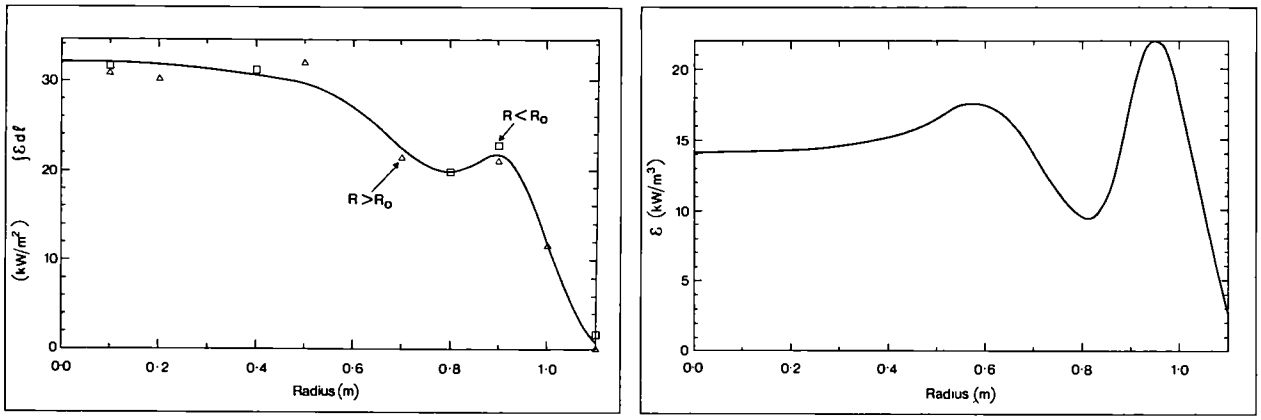

Fig. 102 Radial distribution of total radiation – (a) raw data and (b) Abel-inverted profile.

December. All data were clustered near the 70% level.

Abel inversion of the measured line integrated radiation revealed a variety of emission coefficient profiles from peaked to hollow. Figs. 102a and b show radial profiles and Abel inversions for a 1.2MA discharge. In the discharges with hollow profiles, the central radiation losses were typically 10–30% of the local ohmic heating power, and are indicative of a relatively-clean plasma with metal impurity concentrations of only a few tenths of a percent. Since impurity line radiation does not dominate energy losses on axis, the predominant effect of the metals is to raise the ohmic input by increasing Z_{eff} and to reduce the radial distance in the plasma available for energy confinement. Most heating power is then radiated from half-way between the plasma centre and the limiter radius.

During a major disruption, thermal plasma energy and magnetic energy associated with the plasma current can be deposited on the vacuum vessel walls. For a slow disruption ($\tau \approx 300$ms), Fig. 103 shows the radiative time integrated power detected by the vertical bolometers and the time integrated ohmic power as a function of time, beginning with the onset of the disruption. Therefore, with about 400kJ of thermal plasma energy added about 75% of the available energy is radiated, while the remaining 25% is deposited directly by heat conduction and convection on limiters and walls.

Provisional Soft X-ray Diode Diagnostic (KJ1)
(R. Gill, J. O'Rourke, H. Krause)

In order to study X-ray emission, a set of four silicon (Si) diodes were installed viewing the plasma through a single pin-hole. The aim was to provide preliminary information on the X-ray emission before installation of the multi-detector X-ray cameras.

Three of the four detectors were equipped with beryllium (Be) foils, which gave an energy threshold below which the detectors are insensitive. The different detectors signals were used to construct a coarse X-ray energy spectrum, using foils of thickness 2, 12.7 and 50μm which provided energy cut-offs at 400, 800 and 1300eV.

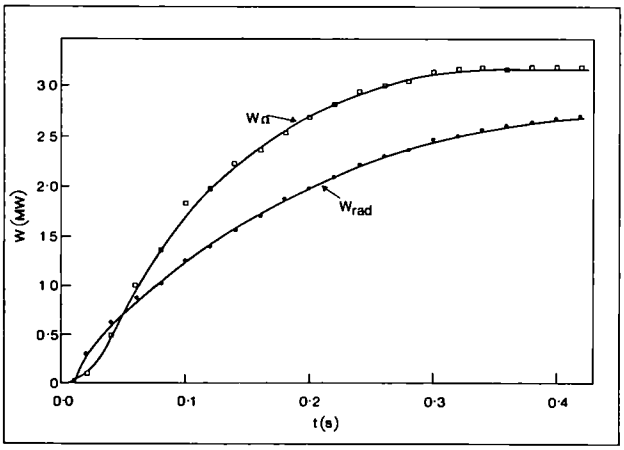

Fig. 103 Integrated ohmic power and integrated radiated power as a function of time after the onset of disruption.

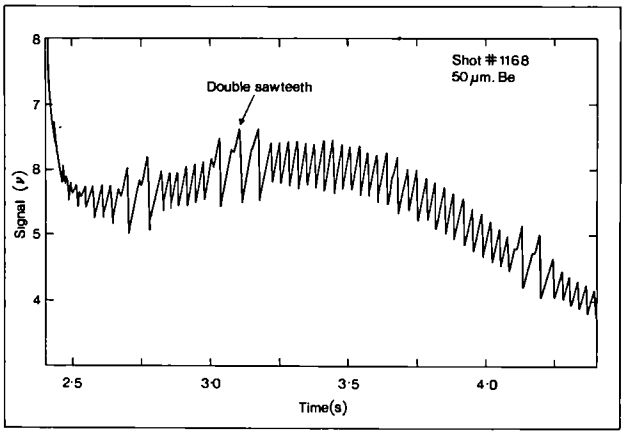

Fig. 104 Soft X-ray signal (50μm Be-foil) showing the sawtooth activity of the plasma.

A principal aim of this diagnostic was to look for MHD effects, particularly sawtooth activity. The presence of sawtooth oscillations indicated that $q < 1$ in the plasma centre, and that the current profile was peaked on axis, as is normal for well contained tokamak discharges. A typical example is shown in Fig. 104.

The diagnostic has also been used to estimate plasma electron temperature (T_e). If the X-ray spectrum is not dominated by impurity line radiation, then the ratio of the signals from two of the detectors can be used to determine T_e. This measurement was of particular value until other diagnostics became available and a typical example is shown in Fig. 105. For comparison, values of T_e derived from electron cyclotron emission, and of T_i from H_α broadening are also presented. The absolute level of X-ray emission measured has also been used to estimate the metal concentration in the plasma.

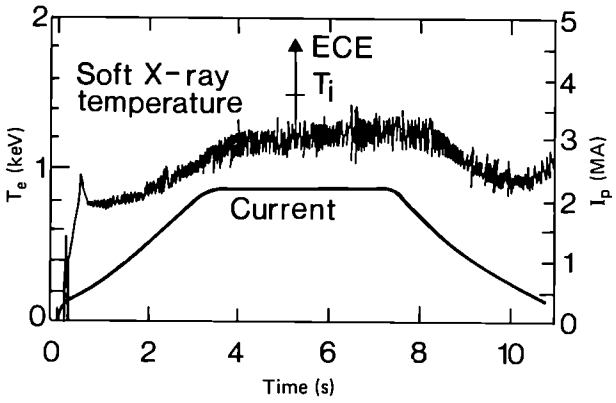

Fig. 105 Soft X-ray temperature (T_e) versus pulse time. ECE results and T_i and H_α broadening are shown for comparison.

Impurity and Radiation Analysis

(K. Behringer)

Method

From the spectroscopic diagnostics, lines of neutrals and low ionisation stages have been used for calculating the influx of the respective impurity species where the light originates. This method is commonly applied to the hydrogen influx derived from the H_α emission, and can be used to evaluate the hydrogen particle confinement time. The basic relation between flux density Γ_I and radiance L_I is given by:

$$\Gamma_I = 4\pi\, r_o\, S_I\, L_I/a\, X_I\, B_I$$

where S_I and X_I are the ionisation and excitation rate coefficients, respectively, B_I is the branching ratio of the transition, r_o/a is the ratio of the radiation shell radius to the plasma minor radius. The coefficients S and X can be calculated, if the electron temperature is known, but the ratio is only a weak function of temperature. For analysis of ionised species lines (OII, CII), a correction must be applied to obtain the neutral influx.

The flux densities and the corresponding hydrogen flux were used to derive values for the release rate of different impurities. The total influx, (i.e. the integral of the flux densities over the plasma surface) was approximated by splitting the total flux (ϕ) into a limiter contribution and a wall contribution:

$$\phi = \Gamma_I(\text{wall})\, A(\text{wall}) + \Gamma_I(\text{limiter})\, A(\text{limiter})$$

where A(wall) and A(limiter) are the areas of the walls and limiters, respectively. The importance of the limiter flux has increased with input power during JET operation. For hydrogen, the situation is now

$$\frac{\phi(\text{limiter})}{\phi(\text{wall})} \sim 10 : \text{while } \frac{A(\text{limiter})}{A(\text{wall})} = \frac{1}{100}$$

The analysis of impurity lines in the visible spectral range suffers from lack of knowledge of the respective atomic rate coefficients. An additional problem may arise as a significant fraction of the respective particles may accumulate in metastable energy levels. Finally, the impurity atoms released at the walls or limiters may leave in excited states, making the interpretation of neutral lines more difficult.

In order to gain some confidence and to explore error limits, many lines of each element were measured and compared with calculations. As an example, Fig. 106 (lower) shows part of the OMA spectrum containing the hydrogen line H_γ and three OII multiplets. One of these multiplets is a quartet system and could be related directly to the ^4S ground state of OII. The other lines originated from doublet configurations and were populated via the

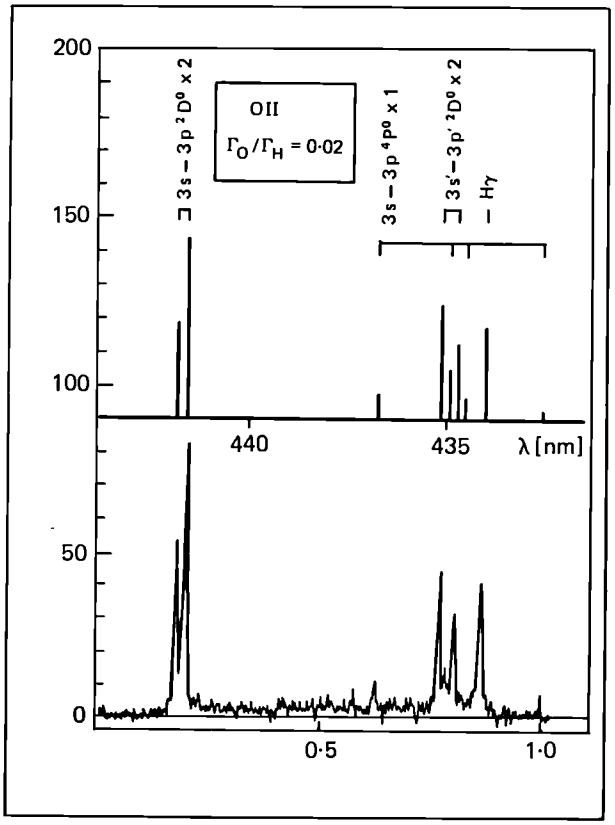

Fig. 106 Measured and calculated intensities of H_γ and three different OII multiplets.

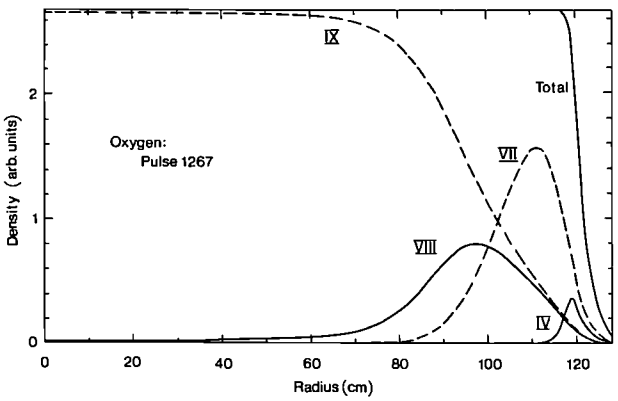

Fig. 107 Radial distribution of oxygen ground states as predicted by the impurity transport code.

metastable ^2P levels. In Fig. 106 (upper), calculated intensities of these lines are presented, assuming the oxygen influx to be 2% of the hydrogen influx. Measured and calculated values agree within a factor of two, which is as good as can be expected from the present model. (Note that the intensities of the doublet lines are x 2).

For impurity densities, the situation is less well known than for the influx, since the usual VUV or X-ray measurements of vacuum ultraviolet highly ionised ions are not yet available. An estimate has been obtained by using influx values and applying plausible particle confinement times. These must always be somewhat less than the hydrogen confinement time (τ_p) and can be assessed by code calculations. The radiated power in the centre of the plasma and the soft X-ray emission are good indicators of heavy impurities. For light impurities, code calculations of the observed lines (CIII, OIV) can be employed to relate these intensities to the respective plasma densities. However, there are appreciable assumptions involved: in particular, the electron density profile at the plasma edge, and the impurity density profiles are needed; and the impurity transport must be known to calculate radiation shell widths and ionisation equilibria. Even so, the result may be checked by means of the measured Z_{eff} value, as derived from visible continuum radiation.

Such a code calculation is given in Fig. 107, which shows the radial distribution of the different ionisation stages of oxygen for Pulse No. 1267. The measured ECE electron temperature profile was used, and the electron density profile was taken from simulation calculations. For impurity transport, a pure diffusion model was adopted with a coefficient of $0.4.m^2 s^{-1}$. In Fig. 107, the shell of OIV is indicated, the highest ionisation stage yet available for analysis. Any conclusion drawn from OIV on the centre oxygen density should have large uncertainties.

It should be noted that, while it is difficult to obtain the oxygen density central value from OIV, a calculation of the oxygen total radiated power is much more reliable, as most originate from low ionisation stages (OIV, OV, OVI).

Results

July Period (up to Pulse No. 308)

Analysis showed that these plasmas were dominated by light impurities. The total influx was difficult to measure, as the horizontal chords were not then available, and it was fortunate that the plasma was limited by the lower vessel wall, rather than the limiters. The results for the oxygen and carbon influxes, as compared to hydrogen, are:

$$\phi_O/\phi_H = 0.04; \phi_C/\phi_H = 0.2$$

from which the following impurity levels were calculated:

$$n_O/n_e = 1–2\%; n_C/n_e \cong 5–10\%$$

resulting in a value of about 3 for Z_{eff}, in reasonable agreement with the measured value of 4. It was not surprising that carbon represented the main impurity in the plasma, since the discharges had been preceded by glow-discharges in methane. The radiated power for O and C was calculated to be about 4MW, and could well explain the measured radiation of 4.5MW. This represents only 50% of the ohmic input power (P_Ω), as compared to 70% in later operation periods. However, 50% of P_Ω is a typical limit for light impurity radiation before edge cooling leads to a shrinking plasma and disruption.

Metal lines (CrI) were observed in July, but metallic impurities did not seem to play an important role in the overall plasma behaviour, which might be due mainly to the low electron temperatures of about 50eV.

October Period (Pulse No. 831)

For this period, the vessel had been intensively cleaned by long baking and discharge cleaning. Consequently, the influx of light impurities, particularly carbon, were considerably reduced. The relation to the hydrogen flux was then

$$\phi_O/\phi_H \cong 0.02; \phi_C/\phi_H \cong 0.02$$

The impurity levels of about 0.5% were estimated for both elements, resulting in 300kW of radiated power. However, the total radiated power was still 2MW, and the bolometer profiles (then available) were centrally peaked, which meant that metal impurities had become important ($T_e(0) \approx 400eV$). In the measured spectra, lines of the inconel components Ni, Cr and Fe were identified. Surprisingly, molybdenum was also found, which should not have been present in the vessel. The full importance of this observation was only realised during the January shut-down period, when the data were analysed more thoroughly and molybdenum was also detected in the post-mortem analysis of the limiter surface. However, even including Mo, the amount of radiated power required very high concentrations of metals of about 1%.

The carbon limiter surfaces had been identified as the major source of metal influx, and were covered with wall material, possibly during discharge cleaning. Disruptions might also be responsible by evaporating metal off the walls. A later analysis of new carbon tiles showed that molybdenum must have been on the limiter surfaces at installation. Most likely, the carbon was contaminated

during outgassing at high temperatures in a furnace containing molybdenum. From spectroscopic investigations, chromium and nickel entered the plasma roughly in the proportion contained in inconel (the actual result is 1/6), and the total flux amounted to 10^{20} particles/s. Compared to this value, CX-sputtering is a small contribution (~10%).

During the October period, arcing on the limiters was a major problem, releasing hydrogen and impurities and finally leading to disruption. A slower current increase during the "fast-rise" seemed to cure the problem and long quiet discharges were obtained. However, when the ECE temperature measurement was available, it was realised that pulses might start out with peaked or hollow temperature profiles depending on the initial gas filling and some other unknown parameters. Hollow profiles often led to bad discharges and disruptions, possibly because they favoured the formation of arcs and impurity release.

November–December Period

In November, long quiet pulses were obtained, the electron temperature rose to 1keV and sawtooth activity was observed regularly on the soft X-ray diodes. Since then, the impurity behaviour has been relatively consistent, allowing trends and parameter dependences to be studied. There may have been some change in the JET performance, when comparing late December pulses to Pulse No. 983, which had the lowest ever value of Z_{eff}, $\cong$ 1.8 (radiated power 63%). It is not clear whether this is due to a series of disruptions after Pulse No. 983, which might have caused more metal being deposited on the limiter surface.

In general, a considerable ohmic input fraction (about 70%) was radiated, for which metallic impurities were almost entirely responsible. The bolometer profiles were rather flat or slightly hollow. An example is shown in Fig. 102 for a plasma current of 1.2MA and $n_e = 1.1.10^{19}\ m^{-3}$. The details of this profile need not be taken too seriously, especially near the plasma axis, where the errors of the Abel inversion become large. However, the general shape can be explained well by metal radiation, assuming corona ionisation equilibrium and using the respective influxes as a measure of the relative contributions of Ni, Cr and Mo. For this purpose, the measured ECE electron temperature profile and a mildly peaked electron density profile were used. From the absolute radiation level a value of $3.5 \times 10^{16}\ m^{-3}$ was derived for the metal density in the plasma (i.e. 0.2% of n_e).

The impurity behaviour as a function of input power P_Ω (or plasma current) and of electron density n_e can be discussed with reference to Figs. 108 and 109, which show the radiated power, Z_{eff}, and the influx of both light and heavy impurities as a function of the above parameters.

The radiated power increased approximately proportionally to the input power. At constant density, this showed that the metal content of the plasma increased accordingly. In addition, Z_{eff} increased, but less steeply. Unlike the case of radiation, there were about equal

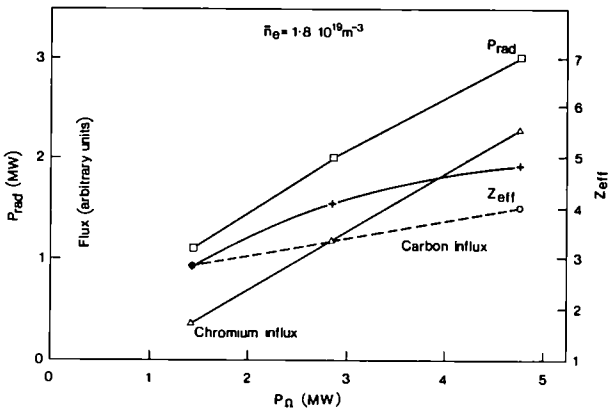

Fig. 108 Radiated power (P_{rad}), Z_{eff} and impurity influx as a function of ohmic input power (P_Ω).

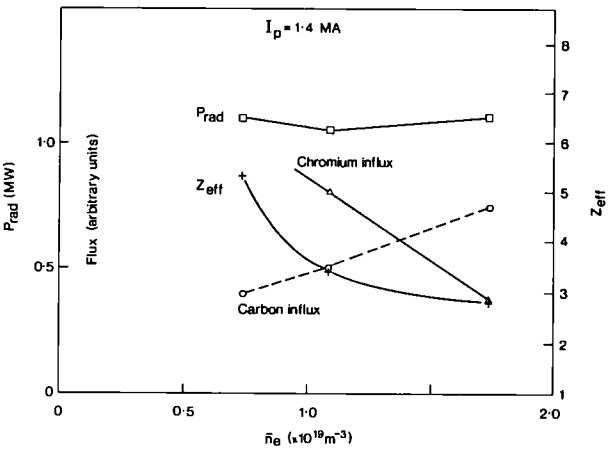

Fig. 109 Radiated power P_{rad}, Z_{eff} and impurity influx as a function of line average electron density ($\bar{n}_e$).

contributions to Z_{eff} from light and heavy impurities, and light impurities were little affected by the increase in ohmic input power. These trends were confirmed by the influxes of chromium and oxygen. The chromium flux was a steep function of P_Ω, probably because the plasma edge became hotter and the sputtering yield increased. Oxygen is usually produced by desorption even by low energy particles. Consequently, this flux was almost independent of P_Ω. It should be pointed out that the respective impurity densities were probably a weaker function of P_Ω, because the impurity confinement decreased with P_Ω, i.e. higher edge temperature.

Fig. 109 shows the impurity fluxes as a function of electron density for a plasma current of 1.4MA. The influx of light elements, i.e. carbon, increases with density because of an increase in the hydrogen flux. The chromium production decreases as a consequence of a cooler edge temperature, overcompensating the higher number of impinging particles. Again, the shielding of the plasma should improve with density and the amount of impurities

in the plasma will probably be nearly constant for carbon and fall strongly for metals, resulting in the plotted decrease of Z_{eff}. The integral radiation is caused by the product of metal and electron densities and remains almost constant, a normal finding for tokamak impurity radiation.

The absolute flux values can be discussed for Pulse No. 1356, at peak current. The total metal influx originating at the carbon limiters was about 10^{20} atoms/s and consisted mainly of nickel, chromium and molybdenum, which entered the plasma in the ratios 7:1:1. Charge-exchange (CX) sputtering was again of minor importance, though the CX flux had probably increased proportionally to the hydrogen flux. Using the hydrogen limiter flux of 5×10^{21} particles/s, a metal release rate of 2% was determined, a value, which represents a reasonable sputtering yield at $T_e > 100$eV for a Ni surface. A plasma edge temperature of this order is also necessary for interpreting the heat load on the limiters and is indicated in the ECE measurements. On the other hand, the metal influx may be barely sufficient to explain the metal content of the plasma of 0.3%. Other sources of metal production can not be excluded. The main source of carbon was again the carbon limiter. The ratio of carbon and hydrogen flux was about 10% and a carbon plasma fraction of about 2% was estimated. The oxygen flux and content were lower than that of carbon and would be about 0.5%. Totalling the contributions of these impurities to Z_{eff}, a value of 4 was obtained. The measured value of Z_{eff} was 4.8, somewhat higher, but consistent within the overall error limits, especially since there were some traces of additional elements in the plasma (e.g. calcium). Finally, it should be emphasised that, even though the plasma is still dominated by impurity radiation, the radiated power from the plasma centre was always much less than the ohmic input power (i.e. ~ 10–30%). This allows reasonable studies of energy transport and energy confinement times.

Theory Division

(Division Head: D.F. Düchs)

Theory Division is responsible for the prediction of JET performance by computer simulation, the interpetation of JET data and the application of analytic plasma theory to gain an understanding of JET physics. In addition, the Division assists in execution of the programme and in making proposals for future experiments, in collaboration with Experimental Divisions 1 and 2, the Physics Operations Group and the Operations and Development Department.

In undertaking these tasks, the Division is divided into three main groups: Analytic Plasma Theory Group; Interpretation Group; and Prediction Group. The first priority of the Interpretation Group has continued to be the development and refinement of data evaluation codes for the first operational phase of JET. The Analytic Plasma Theory Group was expanded at the end of last year and this has permitted increased theoretical activity, particularly in MHD stability, and optimisation of RF and neutral injection heating schemes. A considerable effort was still devoted to originating, monitoring and evaluating contract work with the Associations. The Prediction Group's main efforts were devoted to more refined forecasts of JET (and other tokamaks) behaviour by introducing more elaborate physics models in standard codes, as well as introducing more refined computer codes.

Analytic Plasma Theory Group

The Group was expanded at the end of last year, providing an increased range of theoretical activity, particularly in magnetohydrodynamics (MHD), describing the gross equilibrium and stability of the plasma. The Group's MHD work falls into four categories, as follows:

(i) The early experimental results for the initial operating phase, which had concentrated on plasma position and current control, were analysed. The predicted vertical motion of the plasma column in early discharges, before vertical feedback control was introduced, was compared with observations. Some pulses terminated abruptly in a rapid current decay, the so-called major disruption. The resulting rapid transformation of magnetic energy and subsequent loss were considered.

(ii) JET plasma behaviour has been simulated numerically by evaluating the time-dependent MHD equations. Two codes are being developed: one following 3-D non-linear behaviour on a resistive time-scale and the other calculating the form of the perturbations arising from tearing modes.

(iii) The roles played in disruptions by different processes have been studied. This work includes: modelling the disruption as a loss of non-linear equilibrium; calculations of the effect of impurities and neutral recycling; and computer simulations of disruptions.

(iv) Earlier JET stability calculations have been extended aimed at introducing more realistic assumptions, including the effects of the resistive vacuum vessel and the non-linear consequences of violating the kink stability criterion. An analytic model of the ballooning mode criterion has been used to investigate the β-limit.

Ion cyclotron resonance heating will eventually be the largest source of additional heating for JET. Many heating scenarios involving either harmonic heating of a main plasma constituent, or fundamental heating of a minority species have been studied, to find the optimum in different operational phases. Practical models for the RF energy deposition profile are under development to enable the Prediction Group to simulate plasma performance in the different phases.

Other problems requiring theoretical study have arisen during the year. For example, in certain conditions in TFR, serious damage to the vacuum vessel occurred

due to electrons trapped in regions of minimum magnetic field. To determine whether this could occur in JET, calculations have been started, in which an analytic approximation to the magnetic field in JET was developed, to avoid time-consuming exact computations. Another, but different type of problem undertaken was the excitation of electrostatic instabilities in the NIB neutraliser, where the accelerated ion beam passes through a low density plasma.

In many of the above problems, Association staff have provided valuable assistance. The analytic effort within JET is intentionally limited, on the understanding that the Associations will provide theoretical support. The Analytic Theory Group attempts to foster interest and support by periodic visits, and, where appropriate, Article 14 Contracts are originated for JET specific work.

Further details of this work are described in the following paragraphs.

Analysis of Experimental Results

(J.A. Wesson)

In the earliest JET discharges, the vertical position control system was not operational and the elongated plasma was vertically unstable. A complete analysis of this instability was not possible but it was found that the observed exponential growth rate could be understood in terms of the degree of elongation of the plasma, the resistive diffusion time of the vacuum vessel and the stabilising effect of primary coils.

The stability of the total current in a tokamak depends upon the current/voltage characteristic of the circuit. If a constant voltage is applied, a simple model of the plasma predicts instability. Experimentally, the plasma was stable under such conditions. An explanation of this was proposed based on a recalculation of stability including the effect of the observed sawtooth oscillations. This predicted that sawtooth activity would increase and lead to current stability. A steady current would then be achieved.

The fast current quench of the observed disruptions was analysed. The basic effect was that the inductive magnetic energy of the plasma rapidly collapsed producing intense ohmic heating of the plasma, sometimes up to several hundred megawatts. Calculations of the resistance, temperature and confinement times suggested that the ohmic heating was rapidly transformed into radiation, probably due to impurities introduced by the disruption. Bolometer measurements of the radiation provided support to this suggestion.

JET MHD Simulations

(i) 3-D Code – MASCOT

(M.F. Turner*, J.A. Wesson)

*EURATOM-UKAEA Association, Culham Laboratory

This code is designed to follow the MHD behaviour of JET on the timescale of the experiment, following the 3–D non-linear resistive growth of instabilities in full JET geometry. The code has now been developed to the 3-D stage and test calculations following the growth of tearing modes have been carried out. An example of the resulting magnetic field structure is shown in Fig. 110.

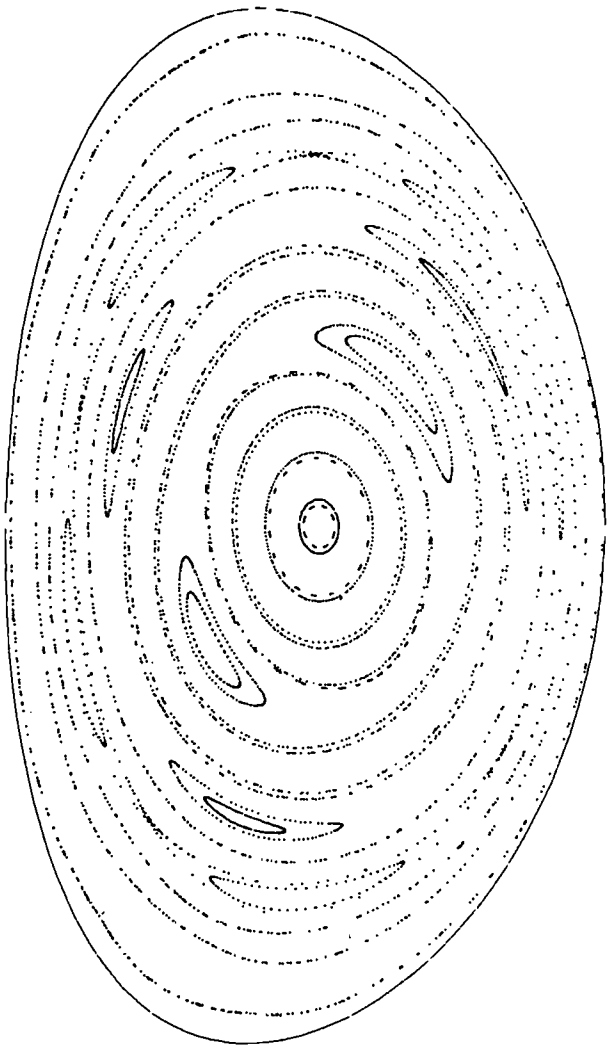

Fig. 110 Magnetic surfaces calculated for JET using the non-linear 3-D MASCOT code.

(ii) Tearing Modes in JET

(M.H. Hughes*, A. Sykes*, J.A. Wesson)

*EURATOM-UKAEA Association, Culham Laboratory

The form of tearing modes outside their magnetic islands is essentially determined by the linearised MHD equations. This structure is being calculated in JET geometry using the Sykes-Wesson tokamak stability code modified to include resistivity. The code is being checked against a simpler 1-D, large aspect-ratio code. When operational, it will be used as a diagnostic tool to study the MHD behaviour in JET.

Disruptions

Tokamak disruptions are a complex phenomenon with several phases. The first phase is the change in parameters to disruptive conditions, usually high current or too high a plasma density for a given current. The second is the growth of MHD instability, which in turn leads to a rapid loss of energy. Finally the plasma current falls to zero.

(i) Conditions for Disruption

(J.A. Wesson)

Attempts have been made to explain the high density limit by the increased impurity radiation from the cool edge region. At sufficiently high density, radiation replaces heat conduction as the dominant loss mechanism near the edge. The increased edge cooling causes a contraction of the current profile. At high currents, this can immediately lead to a strongly unstable configuration. At low currents, a higher impurity or particle density is necessary to contract the current channel to such an unstable state. This prediction seems to be in conflict with the experimental evidence. The cooling of the outer plasma by neutral recycling has also been considered. At sufficiently high density, this effect could produce disruption. The Frascati tokamak, for example, is sometimes run at sufficiently high density to be in this regime.

(ii) Onset of MHD Instability

(F. Romanelli[+], M.F. Turner*, J.A. Wesson)

*EURATOM-UKAEA Association, Culham Laboratory

[+]EURATOM-ENEA Association, Frascati

Further work has been carried out on the catastrophe description of the onset of disruptions. It has been shown that for a sufficiently large magnetic island, free energy becomes available making the island unstable and leading to rapid growth. This occurs in conditions where high current disruptions are observed experimentally. The analytic calculation of catastrophe conditions for magnetic islands is complicated, but nevertheless some progress has been made and the conditions for disruption calculated for a simple model.

(iii) Growth of Instability

(K. Hopcraft*, J.A. Wesson)

*EURATOM-UKAEA Association, Culham Laboratory

Numerical calculations of the disruption have been carried out using a quasi-linear model in which the different m-number tearing modes interact through their effect on the equilibrium current profile. This has produced very similar mode growth and mode interaction to that obtained using the full equations. Therefore, it appears that the quasi-linear effects are more important than the direct mode interactions.

Theoretical Analysis of JET Stability

The simplifying assumptions made in linear stability analysis are often misleading. A number of calculations have been carried out to clarify some of the issues which are important for JET.

(i) Resistive Vacuum Vessel

(T.J. Martin*, M.F.F. Nave, J.A. Wesson)

*EURATOM-UKAEA Association, Culham Laboratory

As expected, it was found that a resistive wall could reduce the growth rate of kink and tearing modes if it was sufficiently close to the plasma and the resistive time constant was sufficiently long. The more important question was whether the real frequency, produced either by motion of the plasma or diamagnetic effects, leads to further stabilisation. The calculations carried out so far show that the effect on kink instabilities is small and indicate a similar result for tearing modes under most conditions.

(ii) Non-linear Kink Modes

(R. Sturgess*, J.A. Wesson)

*EURATOM-UKAEA Association, Culham Laboratory

The assumption that kink instability presents a limit to tokamak operation is an oversimplification. On passing the stability boundary, a helically deformed plasma will appear and under typical conditions this will be limited in amplitude. Calculations of this amplitude are being carried out. Under a wide range of conditions, it appears to be quite small, at about 10% of the plasma radius.

(iii) β-limit for Tokamaks

(A. Sykes*, J.A. Wesson)

*EURATOM-UKAEA Association, Culham Laboratory

Recent computer calculations of linear MHD stability β-limits have led to a need for a greater understanding of the results obtained, particularly the almost linear dependence of β on total current. Using a large aspect ratio model, the predicted β-limit for stability against ballooning modes was approximately proportional to current, reaching a maximum $\beta \cong 16\epsilon\%$ where ϵ is the inverse aspect ratio. When the stability of kink and tearing modes was also included, this limit was reduced to $\beta_m \cong 8\epsilon\%$.

RF Heating Theory

(T. Hellsten)

Many possible heating scenarios exist in which the RF energy can either heat the bulk ions or electrons, or create high energy tails in the distribution function. The absorption mechanisms and their strength can differ over the various parts of the wave spectrum. Existing theory has been used, and new theory and models have been developed to calculate the power deposition and the interaction between RF-waves and the plasma. The objective is to find optimal heating scenarios for the various operation phases and to interpret the experimental results.

At present, three types of codes exist: ray tracing codes developed at EURATOM-IPP Association, IPP Garching and ERM, Brussels; a Fokker-Planck code developed at the University of Wisconsin; and a one-dimensional kinetic code being developed in collaboration with EURATOM-CRPP Association, CRPP, Switzerland (K. Appert, J. Vaclavik and L. Villard).

The ray tracing code can be used to obtain the spatial distribution of heating power. The Fokker-Planck code (operated by W.G.F. Core), which is non-linear two-dimensional in velocity space and zero dimensional in real space, is used to calculate the energy distribution of the heated species. These codes are used to construct models of the power deposition for use in the prediction codes.

The analysis used, in conjunction with ray tracing to evaluate the wave absorption and conversion, makes certain assumptions which may not always be valid. By solving the wave equation, the one-dimensional code studies the physics of the absorption region more exactly. The details of the interaction can result in

enhanced damping, mode conversion or reflection. The simultaneous occurrence of mode conversion and damping makes the problem intractable by analytical methods.

In cases where the wavelength is short and absorption takes place over a few wavelengths, ray tracing methods can describe the power deposition. However, the ray tracing method fails when the wavelength becomes comparable to the plasma dimensions. To study this regime a two dimensional code is being developed in collaboration with EURATOM-Suisse Association, CRPP, in which the full wave equation is solved numerically as a stationary boundary value problem.

Fig. 111 shows the x-component of the electric field (E_x) calculated with the kinetic code for fundamental ion cyclotron resonance heating of deuterium in a hydrogen plasma. The fast magneto-acoustic wave enters from the low field side (i.e. the right hand side). It partly undergoes mode conversion into a kinetic wave, which propagates towards the fundamental ion cyclotron resonance (ω_{CD}) of deuterium and becomes damped by that resonance.

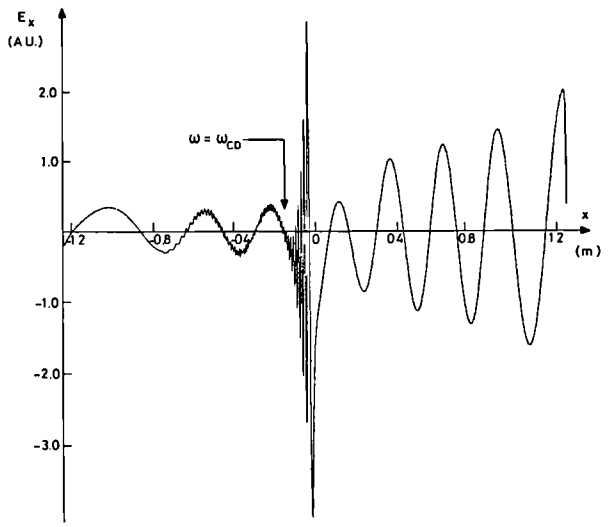

Fig. 111 Variation in the electric field as a wave propagates through cyclotron resonance of deuterium in a hydrogen plasma ($n_D/n_H = 0.05$).

Other JET-Related Theory Problems

(i) Effect of Ripple Trapping of Electrons in JET

(T.E. Stringer)

This analysis was undertaken to answer the question whether the process which produced holes in the TFR vacuum liner could occur in JET. The damage in TFR occurred during low density discharges and was attributed to electrons trapped in the magnetic field ripple resulting from the discrete nature of the toroidal field coils. Runaway electrons can excite a cyclotron instability, which transfers some of their parallel energy into the perpendicular energy of the trapped electrons. These electrons then drift vertically, and strike the wall in localised hot spots. Calculations were made of ripple trapping in the JET magnetic field. Due to the rapid decrease in ripple amplitude with distance from the coils, trapping does not occur near the minor axis, where runaways are normally produced. However, this process could pose dangers in the expanding aperture scenario, when the discharge is initiated in a region of high field ripple.

(ii) An Analytic Model for the Poloidal Field in JET

(T.E. Stringer)

The preceding calculation, and other problems studied, required a simple analytic model for the poloidal field which produced all the features of the exact field. A model was developed based on the moments description originated at ORNL, and already used in JET prediction and interpretation codes. Simple analytic fits to the radial variation of the computed coefficients were found in terms of β and the current profile parameter. Analytic expressions have been found for rotational transform and local shear, and field lines can be followed on a simple computer.

(iii) Electrostatic Instabilities Driven by the Ion Beam in a Neutraliser Chamber

(T.E. Stringer)

This work was triggered by the deviation of the measured beam focusing in the JET neutral injection system from that computed. It predicts that the monenergetic ion beam, traversing the self-produced plasma in the JET neutraliser, excited unstable electron plasma waves.

(iv) Theory of JET Boundary Layer

(W. Feneberg[o])

[o]EURATOM-IPP Association, IPP Garching, FRG.

In this area, problems associated with an ergodic divertor and also the boundary layer of the future toroidal JET belt limiter have been studied. In the ergodic divertor, additional perturbation currents have been introduced to create a boundary layer with decreased confinement time by destroying the magnetic surfaces in a narrow region in front of the limiter. A 3-dimensional program has been developed (in cooperation with P. Martin, IPP Garching) to calculate the density distribution which results from convection along field lines. The code is under test and should give results in 1984.

For toroidal limiter studies, a 2-D code has been prepared to solve numerically equations based on a classical two-fluid model. It has been shown that the classical perpendicular transport resulting from the thermodiffusion coefficient in the electron motion equation depends on the electron temperature gradient along the field lines. This leads to a non-symmetric boundary layer existing on one side only of the limiter. The layer thickness is predicted to be of the same order as that based on the assumption of anomalous diffusion.

(v) MHD Stability Analysis

(R. Gruber*, E. Lazzaro)

*EURATOM-Suisse Association, CRPP, Switzerland

An equilibrium code (JETEQU) (produced by EURATOM-CRPP Association, CRPP Lausanne) has been installed and interfaced with JET data to provide a more flexible

analysis of the current density profiles. A JET version of the ideal MHD stability code ERATO has been adapted to access and interpret the JET experimental data. The information will be used to establish the range of operation in which the plasma is stable against ideal kink and ballooning modes, leading to the determination of optimum or limiting β values.

Interpretation Group

During the first six months, the Group's main efforts were concentrated on developing and installing interpretation codes on the IBM and NORD computers. A substantial effort was also invested in setting up a data display package. Since the beginning of the experimental programme, the Group has been heavily involved in the analysis of the data both during machine operation (intershot analysis) and subsequently (off-line analysis).

In the following reports on the use of the various interpretation codes, examples of the output of each code are given for a typical pulse (Pulse # 1353). During the period June–December, about 200 plasma shots were analysed and preliminary scaling studies are now being undertaken on these data. In addition, a series of related activities on data analysis and other problems are discussed.

Analysis of Experimental Data

(i) Simple Intershot Analysis on the IBM

(J.G. Cordey and R.T. Ross)

The purpose of this program is to present a simple analysis of the data shortly after each pulse. At present, it uses data mainly from the magnetic diagnostic, but, in future, data from other diagnostics will be used. From the magnetic data and the Shafranov integral relations, basic parameters (such as the current and position of the current centre) can be calculated simply and these are shown as a function of time in Figs. 112(a) and (b). The loop voltage on the plasma surface (see Fig. 112(c)) was determined from the time derivative of the magnetic flux at the limiter, which, in turn, was obtained by a Taylor expansion from the measured loop flux close to the limiter. The ohmic input power (see Fig. 112(d)) was then evaluated after the inductive contribution had been subtracted.

The horizontal and vertical separations of the plasma from the vacuum vessel wall were used extensively in the early phases of JET operation to check the plasma position control system. These were obtained from a local expansion of the vacuum field equations about the flux loops at the horizontal and vertical extremities of the vacuum vessel. The time behaviour of these quantities is shown in Fig. 112(e).

(ii) Intershot Analysis on the NORD EC Computer

(J.P. Christiansen, N. Gottardi)

The intershot analysis presents in graphical form a summary of the time behaviour of plasma physics parameters like current, loop voltage on axis or at the plasma surface, safety factor, plasma beta, etc. This analysis is performed concurrently with JET plasma pulse operation. Two intershot analysis programs FAST 1 and FAST 3

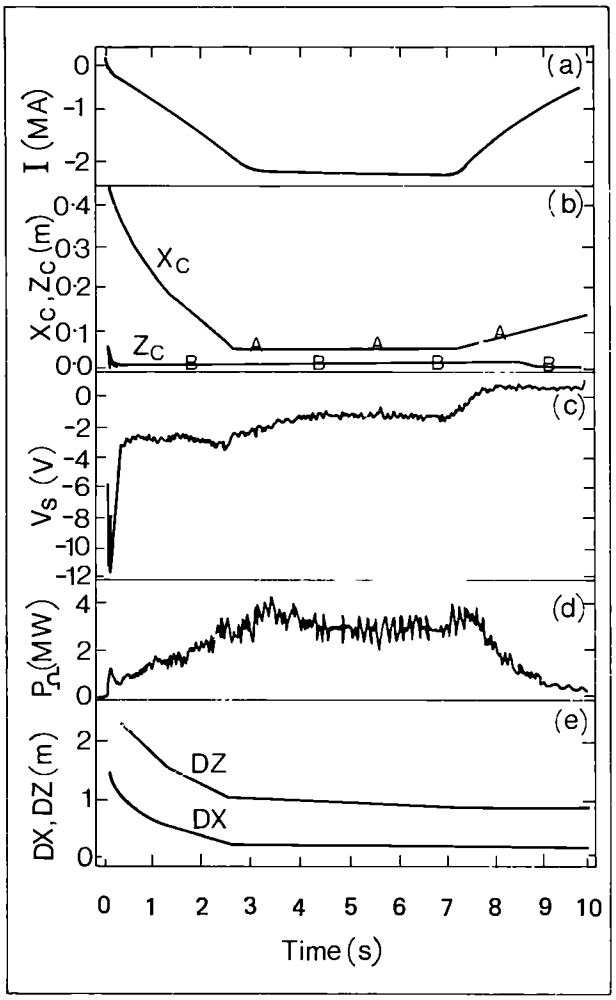

Fig. 112 Time dependence of basic parameters for Pulse #1353
(a) plasma current;
(b) position of plasma current centre, Z_C vertical position, X_C horizontal position measured from R = 2.96 m;
(c) loop voltage on the plasma surface;
(d) Ohmic input power;
(e) distance of plasma extremities from vacuum vessel, DZ distance from top, DX distance from inner vacuum wall.

have been used and one of these programs is activated automatically a few minutes after each JET pulse. The running of the programs has been integrated with the display of raw data from the Immediate Pulse File (IPF). The data from the magnetic diagnostic is used by both programs and FAST 1 requires additional data from the poloidal field system. In order to calculate these parameters, the plasma boundary must be identified. FAST 1 describes the plasma current by a number of current carrying filaments, from which the field is calculated by complex formulae involving the JET iron core and poloidal field coil geometry. FAST 3 models the plasma current by a small D shaped surface with a non-uniform current distribution. This model has been developed in EURATOM-IPP Association, IPP, Garching under an Article 14 Contract (W. Feneberg, K. Lackner and P. Martin). Both programs match the field produced by

the models to the fields measured by the magnetic diagnostic. Fig. 113 shows the JET vessel geometry and the plasma surfaces identified by FAST 3. Fig. 114 indicates the variation of the safety factor at the plasma boundary with time and Fig. 115 shows the time variation of plasma beta and internal inductances.

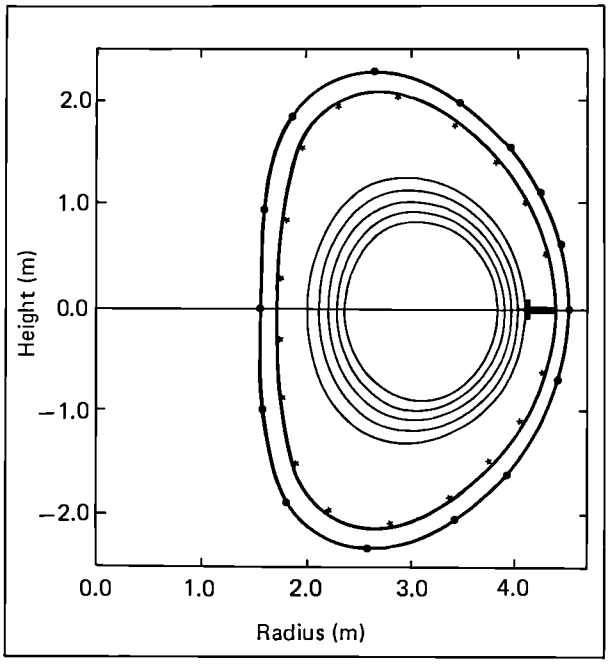

Fig. 113 JET vessel geometry, limiter, pickup coils and flux loops, the plasma boundary and three internal flux surfaces obtained from FAST 3.

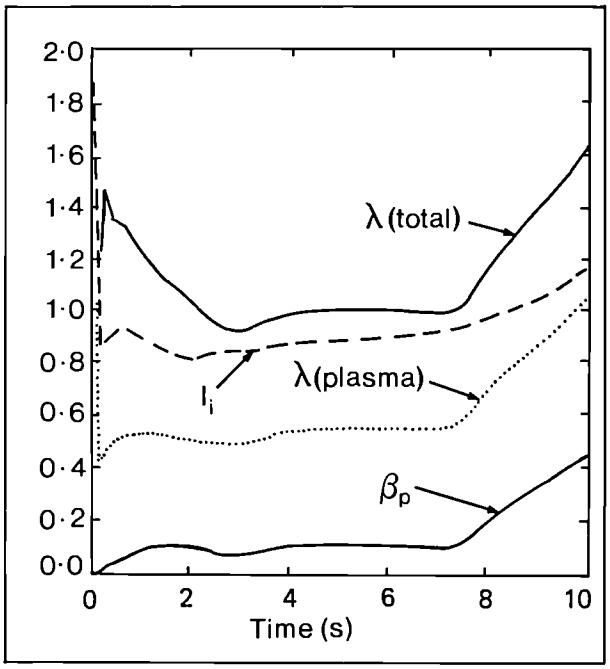

Fig. 115 The poloidal β_J, plasma inductance ℓ_i and Shafranov Lambda (for plasma and plasma plus vacuum) versus time.

(iii) Investigation of Results from Intershot Analysis
(J.P. Christiansen)

The FAST 3 program has been used on the Harwell IBM computer to produce results from the magnetic and interferometer data. A computer program ALICAT can extract, print and display requested parameters as a JET discharge catalogue. Fig. 116 shows the Hugill diagram of 1/q the safety factor plotted against the reduced

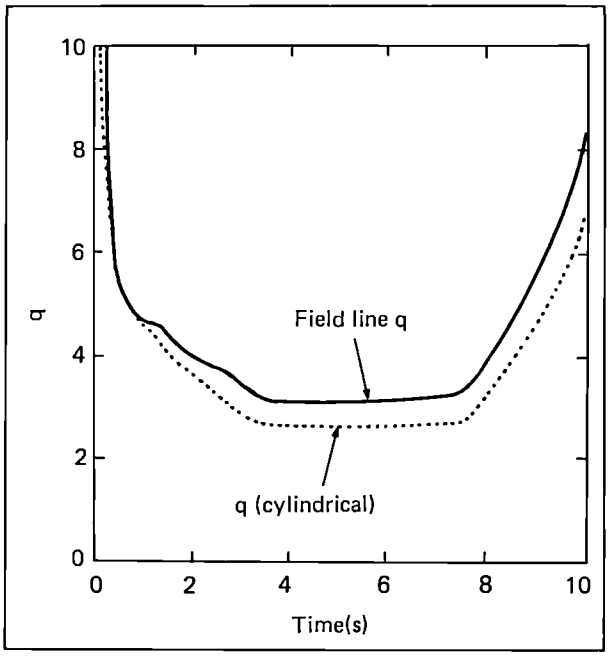

Fig. 114 The field line q and cylindrical q on the plasma boundary versus time for Pulse #1353.

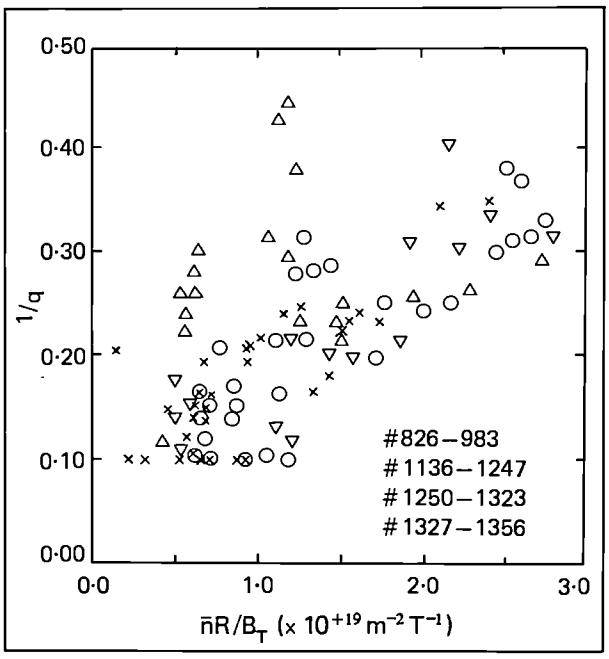

Fig. 116 The Hugill diagram of 1/q versus $\bar{n}R/B_T$ at peak current for the shots from October–December 1983.

density ($\bar{n}R/B_T$). Similar diagrams or catalogues for confinement time scaling studies can be extracted from the data banks.

(iv) Flux Surface Identification Code (IDENTB)

(E. Lazzaro and E. Horlitz)

A subset of the code SCED developed at EURATOM-CEA Association, Fontenay-aux-Roses has been assembled in a form (IDENTB) suitable to follow the evolution in time of plasma equilibria, using the magnetic data. For each time element, the measured values of magnetic flux and field provide the boundary conditions for the MHD equilibrium solver, which as a result of an optimisation procedure gives also the shape of the current density profile and equivalently, the values of β_0 and the internal inductance ℓ_i. Fig. 117 shows the evolution of the equilibria with time for Pulse #1353. The current profile and safety factor as a function of flux are given in Fig. 118 for the last equilibrium shown in Fig. 117.

(v) Generalised Abel Inversion Programme

(N. Gottardi)

A generalised Abel inversion method for calculating the spatial distribution of plasma quantities for peaked or hollow profiles has been developed. The method has been specially designed for irregularly shaped flux surfaces, such as the D-shaped ones expected in JET. The inputs are the line integrated measurements from a particular diagnostic (e.g. bolometer, interferometer, soft X-ray spectrometer, etc.), the viewing geometry of the diagnostic and the flux surfaces delivered by the equilibrium code (IDENTB). The method has been tested on simulated data and will shortly be used on the bolometer data.

An essential condition for a successful Abel inversion

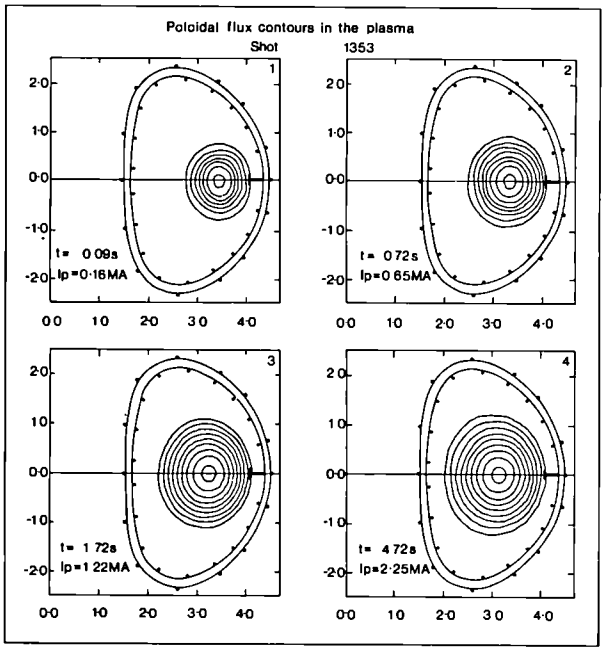

Fig. 117 Evolution of the magnetic flux surfaces during the current rise phase for Pulse #1353. The last equilibrium at t = 44.2 secs is on the current flat top.

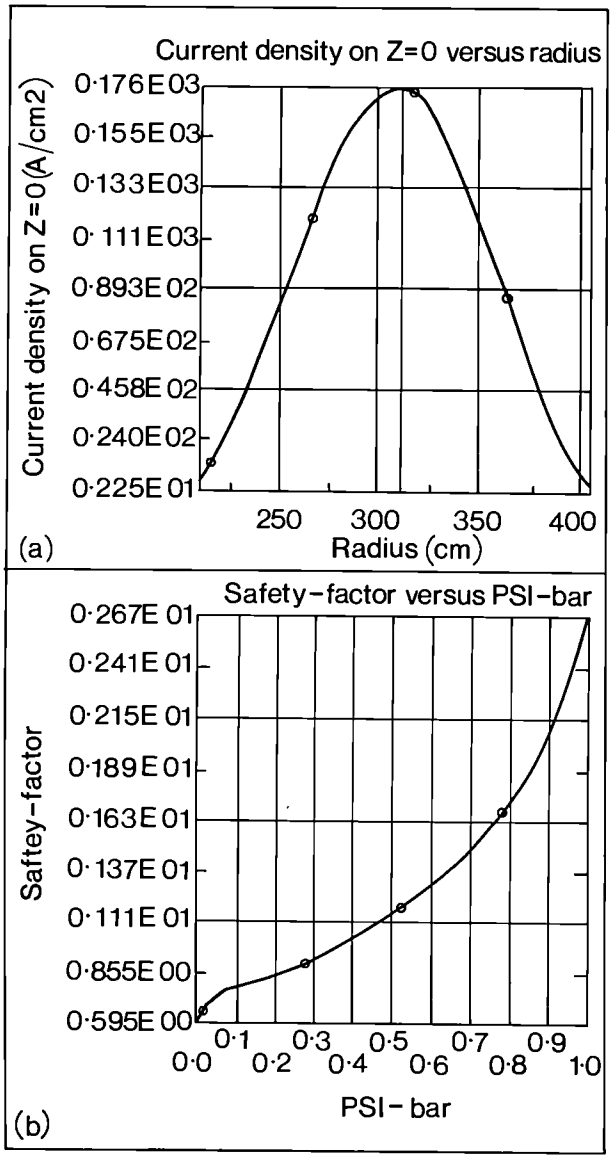

Fig. 118(a) Current density versus major radius on z = 0.
(b) Safety factor versus flux ψ, both for the last equilibrium of Fig. 117.

is that the data are consistent with the geometry of the flux surfaces. As a first test, the evolution of the plasma boundary as viewed by the bolometer camera has been compared with that predicted by the equilibrium code. In Fig. 119, results of a test for a typical shot are shown. In view of the amplitude of the observation cones of the bolometer channels, the result was most satisfactory.

(vi) Confinement Studies using JICS

(M. Brusati, P. Ashman and V. Symons)

The main 1½D off-line transport analysis code, JICS, has been used to assess the energy confinement time of the recent JET Pulses. Due to the limited diagnostics available, the code was operated in a reduced mode. In particular, it has been used to check the consistency of the ECE temperature profiles with those from the plasma resistivity profile (obtained using the current profile calculated from IDENTB). The trapped electrons were found to

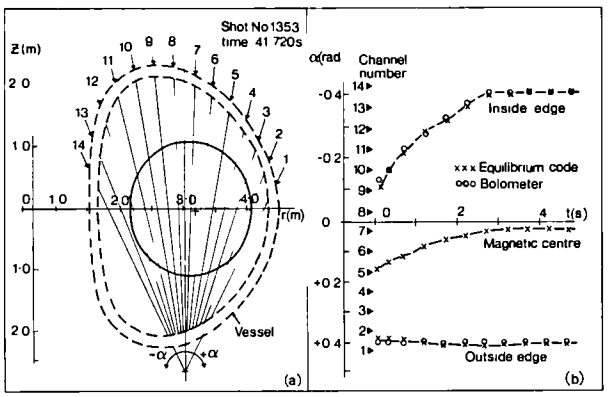

Fig. 119(a) Layout of the bolometer camera.
(b) Time evolution of plasma boundary position as seen by bolometer cameras (designated by 0) and that predicted by the equilibrium code (designated by X).

make a substantial contribution to the resistivity for present parameters, and the effect on the electron temperature is shown in Fig. 120 where the two profiles (omitting or including trapping) are compared with the temperature profile obtained from the ECE measurement.

(vii) Comparison of Iron Core Model with Experimental Results

(E. Lazzaro)

An important test of the reliability of the MHD equilibrium code INVERS (the present JET version of the SCED code developed at EURATOM-CEA Association, Fontenay-aux-Roses, France) was performed during the poloidal field commissioning tests. The vacuum poloidal field configuration of the JET iron core assembly was analysed with INVERS as a pure magnetostatic code, using the actual currents in the poloidal field coils and the axisymmetric currents induced in the vacuum vessel.

The values of magnetic flux and magnetic field measured by the flux loops and the pick-up coils on the vacuum vessel were displayed on the same plot as the values calculated by INVERS. This allowed a thorough check of the consistency of the connections of the various flux loops and the pick-up coils.

Fig. 121 shows the good agreement between the measured and the calculated values of the magnetic flux and field at the position of the flux loops and pick-up coils. At the same time, JET operation with a reduced iron core was also analysed by INVERS, to check the axisymmetric simulation of the iron assembly and the magnetisation curve built into the code. The former appeared to be good but the latter needed some adjustment. In addition, the code INVERS was used to choose the present number of turns in the magnetising and shaping coils which minimised the stray vertical and horizontal fields (B_z and B_r) and their gradients at breakdown (see Fig. 122).

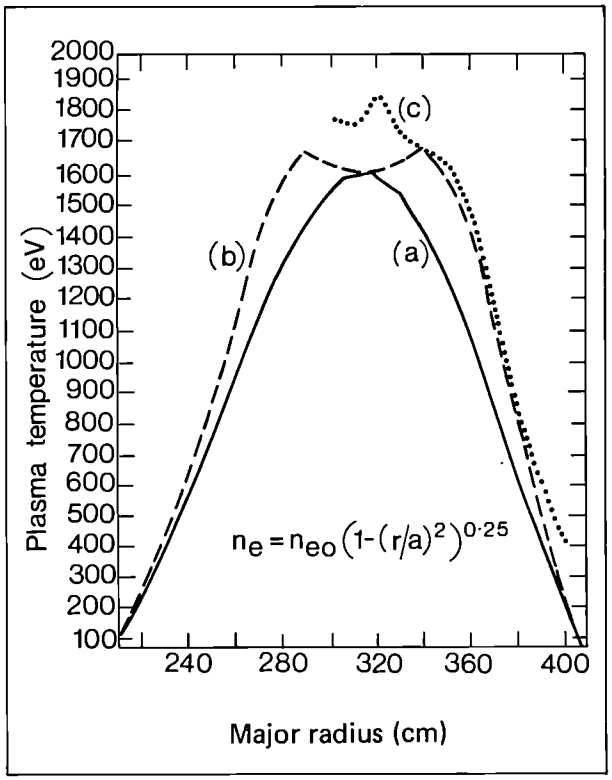

Fig. 120 Electron temperature profiles for Pulse #1353 from:
(a) resistivity profile omitting trapped electron effects;
(b) resistivity profile including trapped electron effects;
(c) ECE measurement.

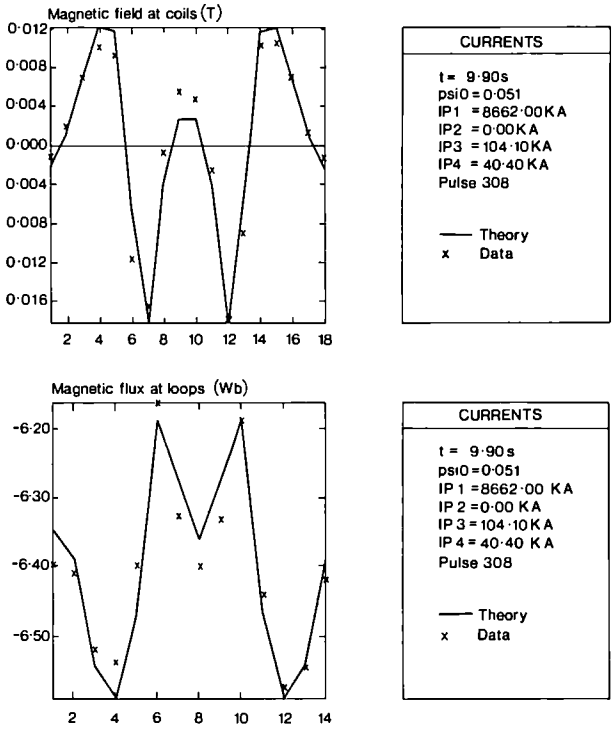

Fig. 121(a) Magnetic field measured at pickup coils versus coil number.
(b) Magnetic flux versus loop number.
In both figures, the continuous lines are the theoretically predicted values from INVERS.

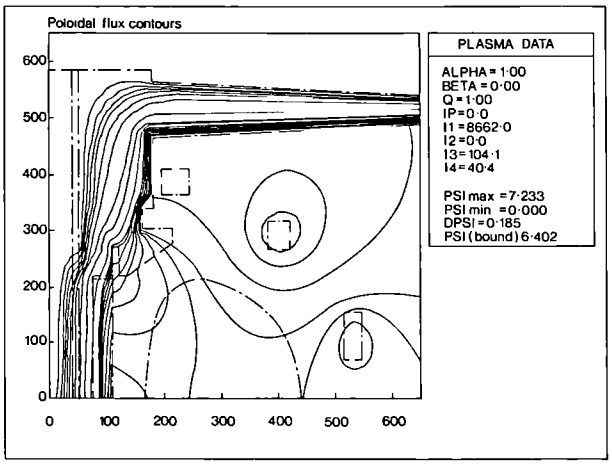

Fig. 122 Vertical cross section through iron core assembly, poloidal field coils, vacuum vessel and flux contours just before breakdown.

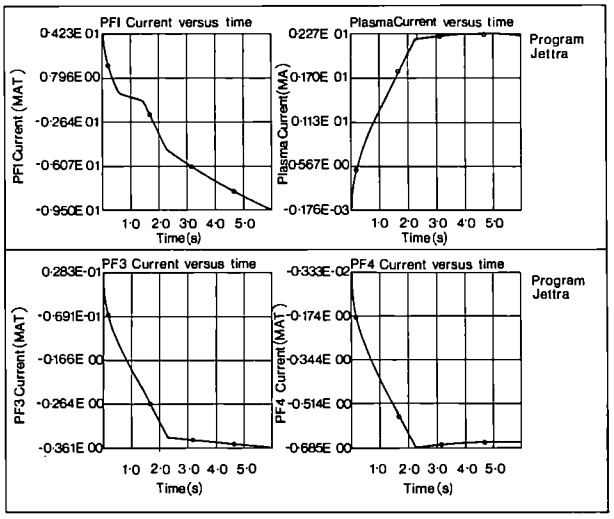

Fig. 123 The predicted currents in the poloidal field conductors PF1, PF3, PF4 and the plasma current versus time.

(viii) Poloidal Field Circuit Model

(E. Lazzaro)

The code JETTRA has been developed to provide a simple zero-dimensional (0-D) simulation of the JET poloidal field (PF) system. The model consisted of a system of active circuits driven by the power supply and vertical field generator and a set of passive circuits representing the vessel and the mechanical structure in which eddy currents were induced. The plasma was described as an inductively coupled circuit with a lumped inductance coefficient obtained from suitable runs of the MHD equilibrium code, and resistive losses (loop voltage) provided either by a simple model or by coupling with a suitable 1-D transport code (e.g. ICARUS). The code was also used to estimate the development of eddy currents in the vessel, during the commissioning phase. Examples of the current waveforms in the various PF coils and in the plasma, obtained with a simple model for the plasma resistance, are shown in Fig. 123 for input parameters of Pulse #1353.

(ix) Data Processing on the IBM

(R.T. Ross and K. Jarrett)

In order to make JET data collected in each pulse available foı display and analysis on the Harwell IBM 3081 and CRAY 1A computers, a system of programs communicating via the Processed Pulse Files (PPF's) has been established. Within a few minutes after each JET pulse, the full JET Pulse File (JPF) is stored on the CODAS computers and simultaneously transmitted via the BT Megalink to be stored on the Harwell IBM.

As soon as the JPF for the current pulse was complete on the IBM, the program JPF Processed Pulse File (PPF) was executed. This program extracted the raw data from various diagnostic systems. Corrections and calibrations were applied and the data written out in a standardised layout (PPF).

The first level PPF was then available for interactive display, and to produce a prescribed set of standard plots for the current shot. For good plasma shots, this file was used as input to the full interpretation codes: IDENTB, JICS and FAST. These codes then produced results in the same standardised PPF layout as the first level results, for subsequent display or further analysis.

Thus, the PPF data files contained those with processed diagnostics data and files with the results of interpretation codes, all stored in the same standardised layout. One programme, PPFDSP, displayed any of the data from any PPF file, either in an interactive mode, or running in batch mode. Similarly the data from any PPF was easily available to any other user program by a simple FORTRAN interface.

A Survey Data Base has been designed and is currently being implemented. This will contain the main characteristics of each plasma shot, such as plasma current, density, loop voltage, confinement times, etc., at a few time points, the data being extracted from the more detailed results stored in the PPF's. Since the IBM system provides the final storage for all the JPF's, an interactive graphical display system working directly from the JPF's has also been provided.

Other Activities

(i) Statistical Analysis of Physical Parameters

(M. Brusati, P. Ashman and V. Symons)

In the analysis of Tokamak data, non-linear combinations of the input data make it difficult and cumbersome to keep track of error propagation. To solve this problem, a technique has been developed which automatically adds perturbations to the input data before the data is processed. This procedure is repeated a large number of times and a random ensemble of values for the dependent variable is obtained, which can be studied statistically.

Fig. 124 shows the probability distribution of the values of β_0 and the energy containment time when a fluctuation of 2% is imposed on the pick-up coils and the flux loops respectively, and the effective charge,

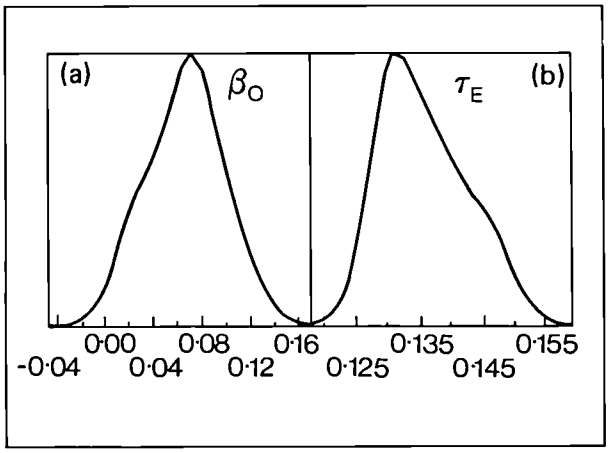

Fig. 124(a) Probability distribution of the plasma β_0 as computed by IDENTB, for a 2% fluctuation of the experimental input data.
(b) Probability distribution of the total containment time, computed by JICS using a resistivity model, for a 30% uncertainty in Z_{eff}. Both refer to Pulse #1353 at 4.5s after breakdown.

Z_{eff}, has a 30% uncertainty. This procedure allows an investigation of both the sensitivity of a statistical fluctuation due to uncertainties in selected input data and "systematic errors" associated with different calculations and numerical techniques.

(ii) Data Analysis on Tokamaks other than JET

(M. Brusati, P. Ashman and V. Symons)

The full suite of codes JICS has been used to analyse data from other operating tokamaks. Results have been obtained on ohmic and neutral injected discharges in DITE and ohmic discharges on FT. Calculations are underway to analyse data from neutral injected discharges in PDX.

The aim of this effort is to test the different physical models and numerical techniques used in JICS in a variety of tokamak operating regimes, and to organise the relevant data in a form suitable for studies on transport, confinement and scaling.

(iii) A Generalised 2-D PDE Solver with Mesh Generator and Grid Adaptor

(M. Brusati, A. Galway and V. Symons)

A code is being developed for solving 2-D systems of partial differential equations with automatic mesh generation and grid adaptation. The equation solver acts on a normalised rectangular computational space. The mesh is generated solving a system of inhomogeneous coupled partial differential equations for the local metric coefficients, with Cartesian boundary conditions. The non-homogeneous terms are given by local exponential series to control the mesh by specifying the degree of attraction to one or more co-ordinate lines and/or points. This approach allows for multiply-connected regions to be specified.

The PDE solver allows for the initial mesh to be updated at a specified frequency by re-locating the same grid points according to the maximum usefulness of both co-ordinate values, due to increments of space, rate of change of the dependent variable chosen for adaptation and of its steepness.

(iv) Numerical Studies on the Generalised Fokker-Planck Equation

(M. Brusati, J.G. Cordey and A. Galway)

Work has started to use the 2-D PDE solver to perform a numerical study of the Fokker- Planck equation:

$$C(f) = R(f) + S(u.v)$$

where f is the fast ion distribution function, C the collision operator, R the radio-frequency diffusion operator and S is the fast ion source function. The main aim of this effort is to investigate the plasma behaviour in JET when both neutral injection and ion cyclotron RF heating are operational.

Prediction Group

During 1983, the activities of the group were concentrated in four major areas:

- Much effort was spent in updating existing codes, installing new codes which had not been previously available to JET and adapting them to JET needs.
- The available plasma models were used extensively for interpretation of JET measurements, especially for checking consistency.
- The models were also applied in studies of possible future JET plasmas, taking into account possible different limiter materials and geometry, heating scenarios, etc.
- Considerable effort was devoted to rewriting and developing software for JET data handling on the Harwell IBM/CRAY system and in preliminary studies for implementation of a JET data bank.

Implementation and Updating of Codes

The following codes, previously not available to the Project, have been incorporated:

(i) BALDUR (Düchs-McKenney version) with Improvements in the AURORA Package for Background Neutrals

(A. Taroni, R. Simonini)

In one version of this code AURORA has been replaced by FRANTIC, a much faster package that proved to be as suitable as AURORA to test cases of interest for JET.

(ii) Preliminary Version of BOTTO (ENEA-Bologna Transport Code)

(A. Taroni)

(iii) BITC, Non-Coronal Impurity Transport Code

(A. van Maanen-Abels)

This code was developed at ENEA Bologna under a NET contract. It takes into account both anomalous and the full neoclassical transport terms, and was restructured extensively at JET to facilitate the data-initialisation and enable a future link-up with existing graphics facilities. Modifications were also needed to permit running of the code on the CRAY-1. A routine was written to read in density and temperature data rather than use analytic initial profiles. This option was used to obtain profiles

from an ICARUS simulation and interpolate to values on the mesh used by BITC. The code can now run in this way both on the CRAY and the IBM, and the IBM version has been sent to Bologna for use by the Italian group. A code similar to BITC for the non-coronal transport of impurities is being developed under contract with EURATOM-IPP Association, IPP, Garching, FRG
(J.G. Cordey, M.L. Watkins).

(iv) A Multiple Pencil Beam (MPB) Code
(P.M. Stubberfield, M.L. Watkins)
This code for the deposition profile for injected neutral beams (developed originally under contract with EURATOM-UKAEA Association, Culham Laboratory) has been implemented as a stand-alone package and comparisons with the previously available code NFREYA showed good agreement for reduced computer time. The multiple pencil beam code was also incorporated into the 1½-D version of the ICARUS transport code.

(v) MESHJET
(A. Taroni, E. Springmann)
This code is a finite element mesh generating package, and has been developed from a pre-existing simpler package, RETE, originated at EURATOM-ENEA Association, Bologna to be used in connection with codes IDENTB and INVERS for the computation of MHD equilibria.

(vi) Neutral Particle Transport
(W.G.F. Core)
Fast efficient packages for routine use in transport codes have been developed for the calculation of neutral particle transport in systems where the influx of primary neutral atoms is due to point sources located on or near the plasma-wall interface. These packages provide an adequate description of neutral gas transport in non-circular tokamak plasmas, and can also be used for the interpretation of neutral particle analyser (NPA) data.

(vii) New Versions of AURORA and FRANTIC
(A. Taroni, E. Springmann)
In the same field of background neutral computations, two new versions of packages AURORA and FRANTIC have been developed. The following features were added to AURORA:

(a) A new model for reflection and desorption after absorption at the wall. Most of the theoretical and experimental information available to date was taken into account.

(b) A new geometry package written and added as an option. This package models flux surfaces and walls as double semi-elliptical tori. This feature was used mainly to assess the validity of the 2-D infinite cylinder approximately for main plasma calculations.

The FRANTIC code has been improved by eliminating the serious drawback of the absence of any model of wall interaction and recycling. In the new model, the H-neutrals diffused by the walls are either backscattered without change in energy, or are re-emitted at 3eV according to the latest data available. Sputtering sources are also computed. Detailed comparisons show that FRANTIC, in the new version, is perhaps the best neutral package now existing at JET for use in transport codes, in that it is both fast and sufficiently accurate, even when plasmas with non-circular cross sections are considered. (FRANTIC is strictly valid only for circular plasmas).

(viii) NIMBUS
(R. Simonini)
The 3D Monte Carlo code NIMBUS developed at EURATOM-ENEA Association, Bologna, has been implemented for the treatment of background neutrals in the plasma boundary layer, taking into account a realistic representation of the JET limiters.

(ix) Additional Heating Codes
(R. Simonini, W.G.F. Core)
A ray tracing code obtained from EURATOM-EB Association, École Militaire, Brussels has been implemented. Also in connection with RF heating, a Fokker-Planck code from University of Wisconsin, USA has been used.

(x) ICARUS
(A. van Maanen-Abels, P.M. Stubberfield, M.L. Watkins)
The program and the data structure of the transport code ICARUS was developed to allow easier operation in a 1-D or 1½-D mode. Additional features have included: a more sophisticated model for the neutral beam penetration (multiple pencil beam model); an extension of the impurity radiation and sputtering package to take account of more recent data; the definition of interfaces for additional anomalous transport models; plasma profile modification due to anomalous penetration of skin currents; effects associated with $q < 1$ and ballooning modes; the definition of interfaces for input information from the JET PPF and for additional diagnostic information such as neutron yields from D-D and D-T interactions; and the improvement of output facilities.

(xi) Review of Atomic Physics Packages
(D.F. Düchs, M.L. Watkins)
A review of all the atomic physics packages available at JET for ionisation, charge exchange, recombination and radiation for both main plasma ions and relevant impurities has been carried out. This was a first step towards the implementation of a well-checked and continuous updated library of routines to be used for JET computations. Fig. 125 shows a typical example of the difference found in the literature and codes with respect to radiating efficiencies. The importance of determining accurately the radiating efficiencies in the edge plasma was realised. In this connection, theoretical studies of various atomic cross-sections have been established under contract with EURATOM-UKAEA Association, Harwell. Particular emphasis has been placed on theoretical determination of the influence of auto-ionising levels on the electron impact ionisation cross-sections for various charge states of nickel and for the theoretical determination of the electron capture cross-section for various atomic species of relevance in the edge region of JET.

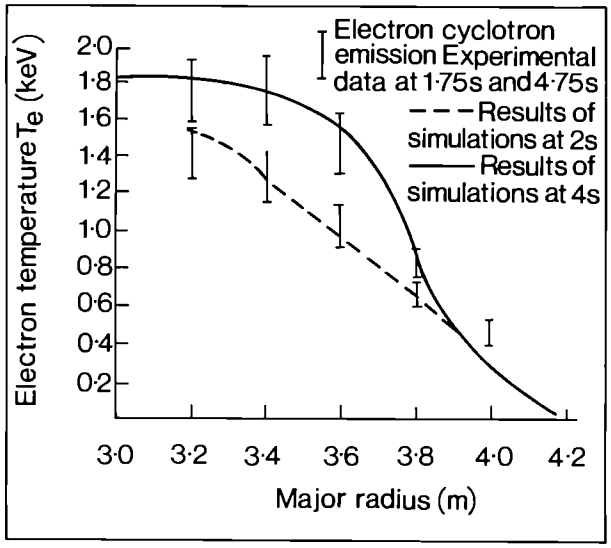

Fig. 125 Radiating efficiency for Nickel as used in ICARUS (---) and BALDUR (___). Above 30eV both codes use the same function.

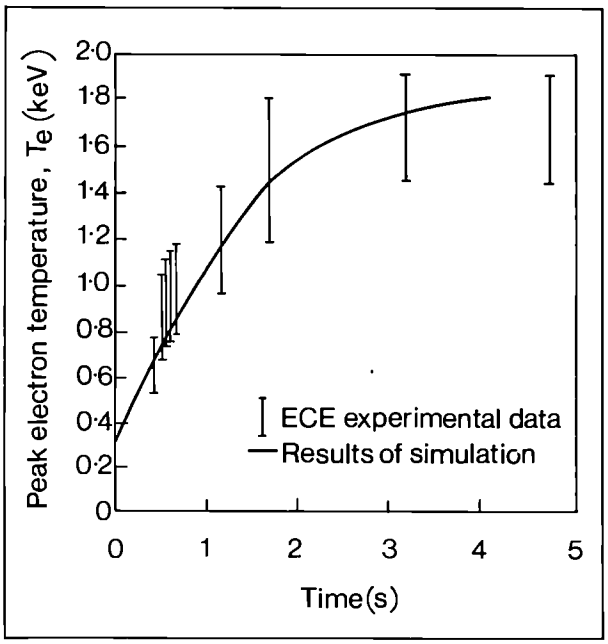

Fig. 127 Electron temperature profile obtained from ECE measurements compared with the results of simulations.

Consistent Simulation of JET Results

Simulation of JET Results

(P.M. Stubberfield, A. Taroni, M.L. Watkins)

Effort has concentrated on the identification of the "best" plasma model for the simulation of JET experimental results taken from all periods of operation, starting in June 1983. The codes now provide a reasonable description of JET ohmic plasmas (see Figs. 126 and 127) and can be used with some confidence to interpolate or predict quantities which cannot be measured.

All available data obtained up to December 1983 have been reproduced, within measurement uncertainties, in a consistent and comprehensive picture of plasma evolution. In particular, the following points were identified as critical to good confinement:

- Anomalous activity in connection with $q \leqslant 1$.
- Inward pinching of impurities and, possibly, the main plasma.
- Radiation from metal impurities, especially nickel.

For the anomalous activity associated with the region $q \leqslant 1$, an empirical model able to reproduce saw-tooth oscillations was used. Computations indicated (as confirmed in JET experiments), a strong dependence of the global confinement time, τ_E, on the safety factor at the plasma boundary, q_a (i.e. $\tau_E \propto q_a^x$, $x \cong 3/4$) (see Fig.128). This can be explained by the extent of the region $q < 1$ and does not necessarily imply a local thermal diffusivity dependent on the safety factor. These results depend only weakly on details of the model.

On the other hand, the present confinement estimates are not sufficiently sensitive to distinguish between popular local transport assumptions, such as the so-called Alcator-Intor, Neo-Alcator and Coppi-Mazzucato thermal diffusion coefficients. This is due to the large extent of the $q < 1$ region on the inside and of the radiation dominated region on the outside. However, the results indicate that the local transport becomes sufficiently important at higher plasma densities, larger plasmas and reduced metal impurity concentration.

Inward pinching of particles is required to reproduce the experimental radiation profiles. With an anomalous inward term of the form, $\Gamma_{in} = D(2r/a^2)n$, good agreement was obtained. Light impurities, even considering non-coronal equilibrium radiation, could only play a major role locally in the edge plasma or, with concentrations of several percent, at the beginning of the discharge.

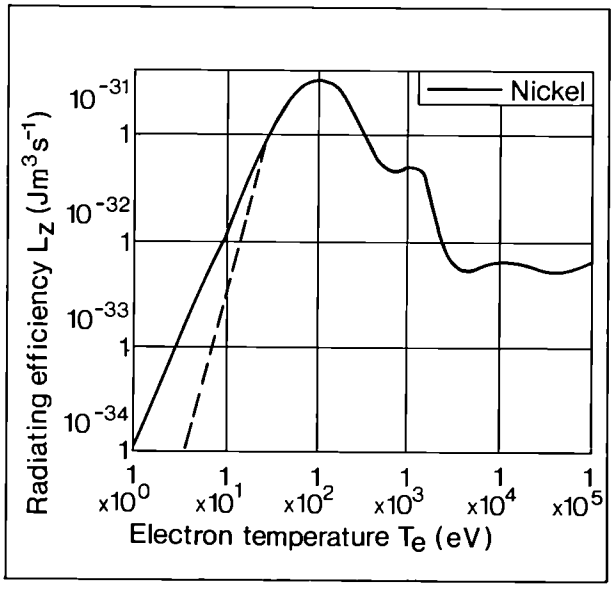

Fig. 126 Peak electron temperature as a function of time obtained from ECE measurements compared with the results of simulations.

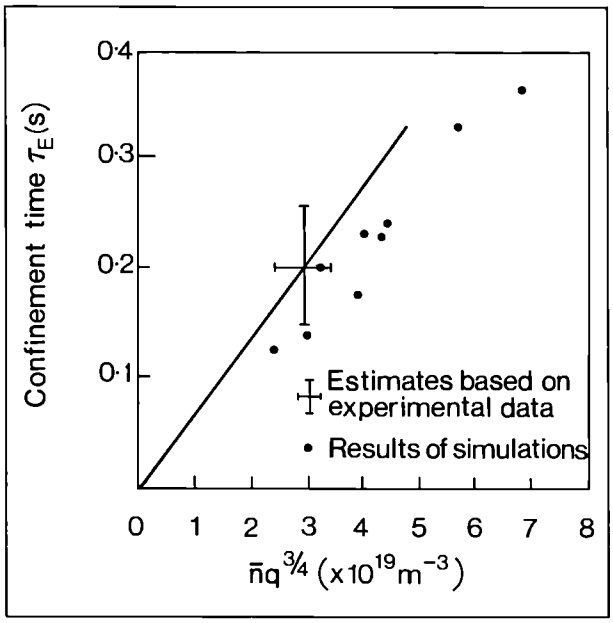

Fig. 128 The energy confinement time (τ_E) versus $\bar{n}q^{3/4}$ (where $\bar{n}$ is the average density and q the safety factor) for estimates based on experimental data compared with the results of simulations.

The simulation of the current-rise phase of the discharge has also been carried out on the basis of semi-empirical modelling.

Prediction of Future JET Performance

(i) Ohmic and Additional Heating Phase Plasmas

(P.M. Stubberfield, A. Taroni, M.L. Watkins)

Work has concentrated mainly on predicting behaviour in the ohmic phase and in successive phases of JET on the basis of "best" transport models.

(ii) Assessing Limiter Materials for JET

(A. van Maanen-Abels, D.F. Düchs, P.M. Stubberfield, M.L. Watkins)

As indicated in the 1982 Annual Report (EUR-JET-A5), a strong dependence on limiter material is exhibited for a transport model with rapid cross-field transport and good impurity confinement. Nickel limiters and wall lead to small aperture plasmas with modest temperatures and global energy confinement times. Beryllium limiters (and wall) lead to full aperture plasmas with low central temperatures and modest global energy confinement times. The calculations indicate the benefits of forming an edge radiating layer of sufficient width (cool plasma mantle); otherwise, the sputtered influx of impurities can lead to unacceptably high impurity concentrations or severe limiter erosion. Acceptable conditions can be achieved, in general, with a controlled influx of low Z material, such as neon, and sometimes with a combination of a low Z limiter and a nickel wall. However, some other models for the particle balance, in particular, can indicate little dependence on the choice or limiter material. This is found for models that lead to a large circulation of impurities in the edge plasma, and for models that lead to insufficient ionisation in the edge plasma, since there is then little protection of the wall from hot charge-exchanged neutrals.

(iii) Influence of Additional Edge Transport

(A. van Maanen-Abels, P.M. Stubberfield, M.L. Watkins)

Removal of power from the edge plasma by additional transport can be beneficial. With the additional transport restricted to the shadow of the limiter, the plasma performance (measured in terms of the central ion temperature and the global energy confinement time) can improve. The magnitude of the additional transport should not be too high ($\sim 10\,m^2\,s^{-1}$ compared with INTOR values $\sim 1\,m^2\,s^{-1}$ in the edge plasma), since at higher values the performance can be reduced due to overcooling of the edge plasma, again leading to little protection of the wall from hot charge-exchanged neutrals.

(iv) Limiter Wall Loading

(R. Simonini, in collaboration with A. Tanga)

Further work has been concerned with the prediction of heat and particle loading upon the walls close to the JET limiter, with the purpose of evaluating whether the installation of pumping panels is worthwhile and feasible. This has been possible using code NIMBUS.

(v) ICRF Heating Scenarios

(W.G.F. Core)

The RF Fokker-Planck code has been used to investigate ICRF heating scenarios and to interpret recent TFR data. The effect of high energy tails of minority plasma ions on bulk plasma temperatures has been calculated.

JET Physics Data Bank Design and Related Software

(i) Data Bank Design

(D.F. Düchs)

A proposal was worked out for the physics data banks created from JET diagnostics. The JET raw data is organised in JET pulse files (JPFs) which are produced on the local NORD computers and then sent to a dedicated disk connected to the Harwell IBM 3081. The JPF raw data are stored permanently for all discharges. From these raw data a "survey bank" is created for all shots with plasma. It contains a selection of characteristic global physics quantities: some as functions of time such as plasma current or loop voltage, some as scalars such as filling pressure or toroidal field.

For selected discharges, a "detailed physics bank" is produced. At the first level, all measured physics quantities are stored, diagnostic by diagnostic. These (usually complex) quantities are further analysed in various "evaluation paths" and the results (e.g. flux surface patterns, MHD mode structures, transport coefficients, etc.,) stored in higher levels of this data bank. This bank contains only data which have been validated by the diagnosticians. Finally there will be a "condensed data bank" in which publishable data are compiled for "typical" shots.

(ii) Assessing Raw Data: VSFORTRAN Version of ISIS

(M.G. Pacco, E. Springmann)

A set of routines, called ISIS (ISAS Interface System), is necessary to access the data. These routines were written

for the NORD-100, which is a 16-bit machine and were converted for use on the 32-bit IBM. Altogether, there are about 50 routines, which need approximately 140K memory. With one exception (the conversion routine from NORD to IBM floating point format), they are all written in VSFORTRAN and should be easily portable to other 32-bit computers. Some additional routines were also written to satisfy the needs of IBM users.

(iii) JET Pulse File Management

(M.G. Pacco, E. Springmann)

During 1983, the JET experiment created 653 raw data files of size between 30K and 756Kbytes (1K = 1024). The number of files created and their size is rapidly increasing and could grow to 50 files of 10Mbytes per operation day.

These JPFs should be stored on private mass store volumes not subjected to the IBM HSM (Hierarchical Storage Manager) migration. This HSM independent JPF management has the advantage of a faster retrieval for a short sequence (only JET files are stored on those private cartridges) and of saving disk space and cost.

After the JPFs have been stored on MSS (Mass Store System) and backed up on magnetic tape, they must be deleted from the dedicated disk in order to leave space for new JPFs. A JPF directory was created to handle the bookkeeping of the JPFs, to automate backup on magnetic tape, deletion from the dedicated disk and retrieval. Entries can be made into the directory while other users are reading (a comment file is available), so that the directory can also be used as a quick reference.

At present, after a JPF has been created, an entry for this file is made in the directory and the file, copied onto MSS. The files are backed up to tape at a later time. The back-up process, as well as the deletion of the JPFs on the dedicated disk, will be automated as soon as the IBM product RACF (Resource Access Control Facility) is available at Harwell. Some utilities to reorganise the directory are available.

(iv) Organisation of JET Data

(M.G. Pacco)

JET processed data will be organised in several data bases. The JET requirements regarding data amount, frequency of updating and method of retrieval have been set up. An evaluation of available commercial data base management systems is still in progress.

JET – Future Plans

Following the successful operation of JET during the period June–December 1983, the JET Council re-affirmed the JET Development Plan, whose main features are full power operation with deuterium by mid-1988, and the start of operations with tritium by mid-1989. The Outline Project Timetable is shown below:

JET PROJECT TIMETABLE

Phase	Plasma	Additional Heating Power at Start and End of each Phase (in MW)	Timing
I	Hydrogen	None	Mid 83 – Late 84
IIA	Hydrogen	NI 5 – 5 RF 3 – 9	Early 85 – End 85
IIB	Hydrogen	NI 10 – 10 RF 3 – 9	End 85 – Early 87
IIIA	Hydrogen/ Deuterium	NI 10 – 10 RF 9 – 15	Early 87 – Mid 88
IIIB	Deuterium	NI 10 – 10	Mid 88 – Mid 89
IV	Deuterium/ Tritium	NI 10 – 10 RF 15 – 15	Mid 89 – Close

Phase I

(Mid 1983–Late 1984)

Phase I, already in operation, is the ohmic heating phase, for which the main aim is to create a clean hydrogen plasma suitable for the additional heating studies of later phases. Important elements of the work are to study the conditions necessary (a) to achieve stable control of plasma position, size and shape; (b) to control the influx of impurities; and (c) to determine the conditions for disruptive-free discharges.

The initial results achieved have been described in Section 2, and these results were much in line with expectation. To achieve them an enormous amount of commissioning work has been necessary, both on the engineering elements of the machine, as well as on diagnostics and interpretation codes. Up to the end of 1983, only about half the full volume of the torus had been used for the discharge. Therefore, the first campaign of 1984 is concentrated on increasing the plasma size, reducing still further the impurity content and increasing the plasma density.

It is then planned to extend the performance of the machine towards the highest possible currents and fields consistent with freedom from hard disruptions. By the end of this phase, the Project aims to have achieved the machine's design limits of a plasma current of 4.8MA with a toroidal field of 3.4T, though at a relatively low density.

Although JET intends to operate primarily with plasmas of D-shaped cross-section, the phase will include some comparative studies of the properties of circular cross-section plasmas and of plasmas with smaller vertical elongation. In particular, the stability and confinement characteristics of such plasmas will be studied.

Another important aspect of this phase will be to study the influence on plasma behaviour of different first-wall materials, in particular, carbon, beryllium and nickel. At present, the machine contains four radiation-cooled graphite limiters and eight water cooled nickel limiters. Tests on the suitability of beryllium as a limiter material will take place during 1984 on the ISX-B tokamak at the Oak Ridge National Laboratory, under a contract from JET. Uncertainties over the use of beryllium in the first wall include the hydrogen inventory, material deterioration under hydrogen ion influence and thermal shock resistance under plasma conditions.

Phase IIA

(Early 1985–End 1985)

It is proposed that in Phase IIA, full-aperture D-shaped hydrogen plasmas should be studied with up to 8MW of additional heating. The heating would come mainly from the first neutral beam injection box, which will be fitted to the machine in 1985. At full power, the box will provide neutral beam power with 5MW at the full energy beam component of protons at 80keV. Co- and counter-injection will be compared by changing the plasma current direction.

There will also be an investigation of RF heating scenarios in this phase. The first two RF antennae (radiation-cooled A_0 antennae) will be installed in late 1984. One of the A_0 antennae will be of monopole design and the other quadrupole. Although the existing design standard is monopole, it has been calculated that the quadrupole design should be superior in reducing the generation of impurities.

When first installed, the antennae will be operated at a low power of about 200kW using the first stage of the amplifier chain only. Coupling will be studied over a wide range of frequencies at this power level. Early in

1985, each antenna will be connected to a 3MW generator unit. Later in the year, up to 3MW of high-grade RF heating (i.e. about 50 per cent of the generator power), will be coupled to the plasma in short pulses of up to 1.0s. Scenarios to be studied during this phase include second harmonic heating of pure hydrogen plasmas and minority heating schemes with small quantities of helium-3 or deuterium.

Phase IIB

(End 1985–Early 1987)

The main aim of this phase will be to continue studies on a full-aperture D-shaped hydrogen plasma, but at substantially higher additional heating powers. The second neutral beam injection box, identical with the first will be installed directly onto the device in mid- to late-1985. The boxes are designed so that they can be installed either with both in co-injection or with one in co- and the other in counter. The two boxes together will provide neutral beam heating at a power of 10MW in the full energy component.

The ICRH power will be increased to 9MW during this phase after installation of six water-cooled A_1 antennae at the beginning of 1986. RF heating studies in this phase could involve deuterium as the majority ion species with helium-3 as a minority. The deuterium/helium-3 fusion reaction should produce small quantities of alpha particles and 14MeV protons for which confinement and perhaps heating effects could be studied. There may also be experiments on controlling the temperature profile by setting the generator for each antenna to the particular frequence required to shape the energy deposition profile.

With this increase in additional heating power to 19MW, an enlarged limiter surface will be desirable. The most promising limiter configuration consists of two belt limiters above and below the equatorial plane. Since the larger surface area of these limiters would lead to low average surface loads, radiation-cooling seems to be feasible perhaps even during full performance. With such a design, it would be possible to leave the final choice of limiter material until the results of earlier tests with various limiter surfaces are known. Since the belt limiters would also serve to protect the antennae, the antennae would require side frames only, and these could be similar in construction to the limiters themselves. A design is being developed in which both the limiters and the antennae frames would be cooled by the same flow of water.

However, if the power density on the belt limiters is higher or more unevenly distributed than the present design values, this radiation-cooling might be insufficient for the maximum heating power of the device. In that case, JET would have to revert to an actively-cooled hypervapotron design for the later phases of the programme. Therefore, it would be essential during 1985 and 1986 to continue the parallel development of a hypervapotron design.

At the end of this phase, both neutral beam injection boxes would be taken out of operation for several months in order to convert them and their power supplies to operate at 160keV.

Phase IIIA

(Early 1987–Mid 1988)

Plasmas in Phase IIIA should be mainly of deuterium. By the end of the phase, the additional heating power should have been raised to its full performance level of 25MW: 15MW of RF and 10MW of neutral beam heating.

The six A_1 antennae should be replaced by ten A_2 around mid-1987. However, for the A_2 to be ready in time, they would have to be similar in design to the A_1. It is intended that each of the A_1 antennae should be refurbished to provide six out of the ten A_2. The principal changes to the A_1 would be to their cooling systems, which would need to be enhanced, and to the shape of the side-protection, whose design would evolve as the character of the scrape-off layer becomes better understood.

The A_2 antennae would be installed initially with the radiation-cooled belt limiters. Hypervapotron belt limiters, if required, would be needed before the end of this phase. To preserve the possibility of manual intervention during their installation, neutron activation in the machine should be carefully monitored and managed.

Phase IIIB

(Mid 1988–Mid 1989)

The main aims of work in this period would be to reach maximum performance with deuterium plasmas and to prepare all systems for active operation with tritium. The tritium systems should be commissioned by the end of 1988.

Parameters of the following order need to be achieved to justify proceeding to the final phase of the programme, in which tritium should be introduced:

peak temperature	$\sim$ 8keV
peak density	$\sim 10^{20}\,m^{-3}$
energy confinement time	$\sim$ 1s.

Phase IV

(Mid 1989–1990)

This phase should be devoted to the study of alpha particle heating in deuterium-tritium plasmas. The objective would be to reach a temperature of 10keV and a plasma density of $1.5 \times 10^{20}\,m^{-3}$ with an equal deuterium-tritium mixture. There would be attempts to achieve core ignition and, if possible, full ignition.

Appendix 1
A Joint Undertaking—Legal Entity

Article 49 of the Euratom Treaty states:
"Joint Undertakings shall be established by Council decision. Each Joint Undertaking shall have legal personality. In each of the Member States it shall enjoy the most extensive legal capacity accorded to legal persons under their respective laws; it may, in particular, acquire or dispose of movable or immovable property and may be a party to legal proceedings.

"Save as otherwise provided in the Treaty or in its own statutes, each Joint Undertaking shall be governed by the rules applying to industrial or commercial undertakings; its statutes may make subsidiary reference to the national laws of the Member States.

"Save where jurisdiction is conferred upon the Court of Justice by this Treaty, disputes in which Joint Undertakings are concerned shall be determined by the appropriate national courts or tribunals".

Article 22.2 of the statutes of the JET Joint Undertaking states:
"Without prejudice to the provisions of the third paragraph of Article 49 of the Euratom Treaty, for the avoidance of doubt the Joint Undertaking shall not be regarded as a company within the meaning of the Companies Act 1948 and 1967 of the United Kingdom".

Appendix 2
The JET Joint Undertaking— Relevant Documents

1. Decisions of the Council of the European Communities.

1.1 Council decision of 30 May 1978 amending decision 76/345/Euratom adopting a research related programme (1976–80) of the European Atomic Energy Community in the field of fusion and plasma physics.
78/470 Euratom

1.2 Council decision of 30 May 1978 on the establishment of the Joint European Torus (JET) Joint Undertaking.
78/471/Euratom

1.3 Council decision of 30 May 1978 on the conferment of advantages on the Joint European Torus (JET) Joint Undertaking.
78/472/Euratom

1.4 Council decision of 3 August 1979 approving amendments to the Statutes of the Joint European Torus (JET) Joint Undertaking (consequent upon the accession of Switzerland to the Joint Undertaking).
79/720/Euratom

1.5 Council decision of 13 March 1980 adopting a research and training programme (1979–83) for the European Atomic Energy Community in the field of controlled thermonuclear fusion.
80/318/Euratom

1.6 Council decision of 19 May 1981 amending decision of 13 March 1981 adopting the research and training programme (1979–83) for the European Atomic Energy Community in the field of controlled thermonuclear fusion.
81/380/Euratom

2. Statutes of the Joint European Torus (JET) Joint Undertaking.

3. Agreement between the participating organisations.

4. The support agreement between the Joint European Torus (JET) Joint Undertaking and the United Kingdom Atomic Energy Authority.

5. Financial regulations of the Joint European Torus (JET) Joint Undertaking.

Appendix 3
The Members and Organisation of JET

Members

3.1 The JET Joint Undertaking has the following Members:

- The European Atomic Energy Community (EURATOM)
- The Belgian State, acting for its own part (Laboratoire de Physique des Plasmas of the École Royale Militaire) and on behalf of the Université Libre de Bruxelles (Service de Chimie-Physique II of the ULB)
- The Commissariat a l'Énergie Atomique, France (CEA)
- The Comitato Nazionale per la Ricerca e per lo Sviluppo dell'Energia Nucleare e delle Energie Alternative, Italy (ENEA)
- The Consiglio Nazionale delle Richerche, Italy (CNR)
- The Hellenic Republic (Greece)*
- The Forsøgsanlaeg Risø, Denmark (Risø)
- The Grand Duchy of Luxembourg (Luxembourg)
- Ireland
- The Kernforschungsanlage Jülich GmbH, Federal Republic of Germany (KFA)
- The Max-Planck-Gesellschaft zur Förderung der Wissenschaften e.V.
  Institut für Plasmaphysik Federal Republic of Germany (IPP)
- The Swedish Energy Research Commission (SERC)
- The Stichting voor Fundamenteel Onderzoek der Materie, the Netherlands (FOM)
- The United Kingdom Atomic Energy Authority (Host Organisation)

*Greece became a Member on 14 June 1983.

Management

3.2 The JET Joint Undertaking is governed by Statutes which were adopted by the Council of the European Communities on 30 May 1978. The organs of the Joint Undertaking are the JET Council and the Director of the Project (Appendix 4). The JET Council is assisted by the JET Executive Committee (Appendix 5) and is advised by the JET Scientific Council (Appendix 6).

JET Council

3.3 Each member of the Joint Undertaking is represented on the JET Council which is required to meet at least twice yearly. The Council is responsible for the management of the Joint Undertaking and is also responsible inter alia for:

- The nomination of the Director and senior staff of the Project with a view to their appointment by the Commission or the Host Organisation as appropriate;
- The approval of the annual budget, including staffing, as well as the Project Development Plan and the Project Cost Estimates;
- Ensuring the collaboration between the Associated Laboratories and the Joint Undertaking in the execution of the Project, including the establishment in due time of rules on the operation and exploitation of JET.

3.4 Three meetings of the JET Council were held during 1983, on 24/25 March, 30 June/1 July, and on 20/21 October. The JET Council appointed Mr. A.W. Plattenteich to be Chairman of the JET Executive Committee in succession to Professor R. Toschi who resigned following his appointment as Chairman of the NET Team. Professor Toschi was warmly thanked by the JET Council for the very important contribution that he made to the Project from the beginning. The Council's main item of business during the period was the discussion of the Project Development Plan and Project Cost Estimates for JET for the next EEC Pluriannual Programme, 1985–89.

JET Executive Committee

3.5 The JET Executive Committee is required to meet at least six times a year. Its functions include:

- Advising the JET Council and the Director of the Project on the status of the Project on the basis of regular reports;
- Commenting and making recommendations to the JET Council on the Project Cost Estimates and the Draft Budget, including the establishment of staff, drawn up by the Director of the Project;
- Approving, in accordance with the rules on the award of contracts established by the JET Council (Annex II, JET Financial Regulations, see Appendix 2), the tendering procedure and the award of contracts;
- Promoting and developing collaboration between the Associated Laboratories and the Joint Undertaking in the execution of the Project.

3.6 The representation of the members in the JET Executive Committee is shown in Appendix 5. The Committee met seven times during the year on 3/4 February, 10/11 March, 19/20 May, 12/12 July, 29/30 September, 18 November, and on 16 December.

JET Scientific Council

3.7 In 1979, in accordance with the JET statutes, the JET Council established a JET Scientific Council and appointed the members, including Professor C.M. Braams as its Chairman, for a four-year term. In October 1982, the JET Council reappointed Professor Braams as Chairman of the JET Scientific Council for a further three years from 1 January 1983. Then in March 1983, the JET Council established a new JET Scientific Council comprising the fourteen existing members together with three new members (see Appendix 6) for a term of two years from 1 January 1983.

3.8 The JET Statutes confer the following functions on the JET Scientific Council:

- Upon the request of the JET Council, to advise on scientific and technical matters, including proposals involving a significant change in the design of JET, its exploitation, and its long-term scientific implications;
- To perform such other tasks as the JET Council may request it to undertake.

3.9 The Scientific Council met three times during 1983 on the following dates: 20 April, 31 May/1 June, 5/6 October. They prepared reports for the JET Council on the Remote Handling of JET, the Revised Project Development plan for JET, and Chances and Risks in the operation of JET. These reports were based on extensive discussions on the diagnostic requirements, impurity control, the experimental programme, remote handling and tritium handling. Working parties comprising members of the Scientific Council, the JET team and experts nominated by the Directors of the Associated Laboratories were established by the Scientific Council to provide specialist assessments of the JET team proposals relating to remote handling and tritium handling.

The Director of the Project

3.10 The Director of the Project is the chief executive of the Joint Undertaking and its legal representative. He is responsible to the JET Council for the execution of the Project Development Plan which specifies the plan for the execution of all elements of the Project, in particular, work to be performed by the Project Team, by third parties and by members of the Joint Undertaking. The Project Development Plan covers the whole term of the Joint Undertaking and is regularly updated. The Director is also required to provide the JET Council, the JET Executive Committee, the JET Scientific Council and other subsidiary bodies with all information necessary for the performance of their functions.

The Host Organisation

3.11 The United Kingdom Atomic Energy Authority, as the Host Organisation for the JET Joint Undertaking, has made available to the Joint Undertaking land, buildings, goods and services required for the implementation of the Project. The details of such support, as well as the procedures for co-operation between the Joint Undertaking and the Host Organisation, are covered by a "Support Agreement" between both parties. The Host Organisation is required to bear the costs of putting the JET site into "standard condition". All standard site conditions as defined in the Annex to the JET Statutes have now been completed by the UKAEA. The Host Organisation also provides such technical, administrative and general services as are required by the Joint Undertaking. In addition to providing staff to the JET team, the Host Organisation provides support staff, at proven costs, to meet the requirements of the JET Project.

Project Team Structure

3.12 With the start of the Operational Phase in mid-1983, a new structure of the Project came into being. The three Departments are now: the Operation and Development Department; the Scientific Department; and the Administration Department.

Operation and Development Department

3.13 The Operation and Development Department is responsible for the operation and maintenance of the tokamak and for developing the necessary engineering equipment to enhance the machine to its full performance. The Department contains six Divisions:

(1) Torus Division;
(2) Power Supply Division;
(3) Neutral Beam Heating Division;
(4) Radio Frequency Heating Division;
(5) Fusion Technology Division;
(6) Control and Data Acquisition Systems Division (CODAS).

Scientific Department

3.14 The Scientific Department is responsible for the definition and execution of the experimental programme, the specification, procurement and operation of the diagnostic equipment and the interpretation of experimental results. The Department contains three Divisions:

(1) Experimental Division 1;
(2) Experimental Division 2;
(3) Theory Division.

Administration Department

3.15 The Administration Department is responsible for providing administrative support and services to the

project in the areas of Contracts, Finance and Personnel.

The JET Directorate

3.16 The three Heads of Department report to the Director of the Project and together with the Director they form the JET Directorate. Various special functions are carried out by the Director's office. The Internal Audit section monitors the Project's financial activities and provides advice on accounting and control procedures, as well as maintaining links with the Court of Auditors. The Project Control Office is responsible for financial planning and for the preparation of the Project Development Plan and Project Cost Estimates. The Secretariat provides secretarial services to the JET Council and to the Executive Committee and also to the JET Project Board. JET's internal management committee.

Appendix 4
Organs of the JET Joint Undertaking

4.1 The JET Council

Members	**Representatives**
The European Atomic Energy Community (EURATOM)	P. Fasella (Vice-Chairman, D. Palumbo)
The Belgian State, acting for its own part (Laboratorie de Physique des Plasmas de l'École Royale Militaire) and on behalf of the Université Libre de Bruxelles (Service de Chimie-Physique II of the ULB)	P.E.M. Vandenplas Mlle. L. Buyse
The Commissariat à l'Énergie Atomique, France (CEA)	J. Teillac (Chairman) J. Horowitz
The Comitato Nazionale per la Ricerca e per lo Sviluppo dell 'Energia, Nucleare e delle Energie Alternative, Italy (ENEA). (Previously known as Comitato Nazionale per l'Energia Nucleare, Italy (CNEN))	B. Brunelli, P. Longo
The Consiglio Nazionale delle Richerche, Italy (CNR)	
The Hellenic Republic (Greece) from June	A. Katsanos
The Forsøgsanlaeg Risø, Denmark (Risø)	H. von Bülow, N.E. Busch
The Grand Duchy of Luxembourg (Luxembourg)	J. Hoffmann, P. Schüller (Jan.–April) N. Didier (May–Oct.) M. Thill (from Nov.)
Ireland	C. Cunningham, J. O'Callaghan (Jan.–Dec.) D. Byrne (from Dec.)
The Kernforshungsanlage Jülich GmbH, Federal Republic of Germany (KFA)	A.W. Plattenteich
The Max-Planck-Gesellschaft zur Förderund der Wissenschaften e.V. – Institut für Plasmaphysik, Federal Republic of Germany (IPP)	K. Pinkau
The Swedish Energy Research Commission (SERC) (Previously known as the National Swedish Board for Energy Source Development)	Mrs. B. Bodlund, G. Holte
The Swiss Confederation	F. Troyon, P. Zinsli
The Stichting voor Fundamenteel Onderzoek der Materie, the Netherlands (FOM)	C.M. Braams, C. le Pair

The United Kingdom Atomic Energy Authority (UKAEA)	A.M. Allen, R.S. Pease
4.2 **The Director of the Project**	H-O. Wüster

Appendix 5
JET Executive Committee

Members	Representatives
The European Atomic Energy Community (EURATOM)	C. Maisonier (Vice Chairman from July) K. Melchinger
The Belgian State, acting for its own part (Laboratoire de Physique des Plasmas of the École Royale Militaire) and oin behalf of the Université Libre de Bruxelles (Service de Chimie-Physique II of the ULB)	R. Vanhaelewyn
The Commissariat à l'Énergie Atomique, France (CEA)	B. Garric, F. Prevot
Comitato Nazionale per la Ricerca a per lo Sviluppo dell 'Energia Nucleare e delle Energie Alternative, Italy (ENEA)	R. Toschi (Chairman to July) R. Andreani
The Consiglio Nazionale delle Ricerche, Italy (CNR)	
The Hellenic Republic (Greece) from June	A. Theofilou
The Forsøgsanlaeg Risø, Denmark (Risø)	I. Rasmussen, V.O. Jensen
The Grand Duchy of Luxembourg (Luxembourg)	R. Becker
Ireland	C. Cunningham, F.G. Burrows
The Kernforschungsanlage Jülich GmbH, Federal Republic of Germany (KFA)	V. Hertling, A. W. Plattenteich (Chairman from July)
The Max-Planck-Gesellschaft zur Förderung der Wissenschaften e.V. – Institut für Plasmaphysik, Federal Republic of Germany (IPP)	G. von Gierke (Vice-Chairman to July)
The Swedish Energy Research Commission (SERC)	G. Holte
The Swiss Confederation	A. Heym, P. Zinsli
The Stichting voor Fundamenteel Onderzoek der Materie, the Netherlands (FOM)	C. Westland, M.F. van Donselaar
The United Kingdom Atomic Energy Authority (UKAEA)	D.M. Levey, W.M. Lomer

Appendix 6
JET Scientific Council

Members nominated by the JET Council

C.M. Braams (Chairman)
EURATOM-FOM Association
FOM-Instituut voor Plasmafysica
"Rijnhuizen"
Postbus 1207 – Edisonbaan 14
NL-343- BE Nieuwegein
The Netherlands

G. Briffod
EURATOM-CEA Association
Département de Recherches sur la Fusion Contrôlée
Centre d'Etudes Nucléaires
Boite Postale 85X
F-38041 Grenoble Cedex
France

F. Engelmann
EURATOM-FOM Association
FOM-Instituut voor Plasmafysica
"Rijnhuizen"
Postbus 1207 – Edisonbaan 14
NL-3430 BE Nieuwegein
The Netherlands

V.O. Jensen
Risø National Laboratory
PO Box 49
DK-4000 ROSKILDE
Denmark

M. Keilhacker
EURATOM-IPP Association
MAX-Planck-Institut für Plasmaphysik
D-8046 Garching bei München
Federal Republic of Germany

A. Messiaen
EURATOM-EB Association
Laboratorie de Physique des Plasmas de
l'École Royale Militaire
Avenue de la Renaissance 30
B-1040 Brussels
Belgium

D.C. Robinson
EURATOM-UKAEA Association
Culham Laboratory
GB-Abingdon, Oxfordshire
OX14 3DB
Great Britain

A. Samain (Secretary)
EURATOM-CEA Association
Département de Recherches sur la Fusion Contrôlée
Centre d'Études Nucléaires
Boite Postale No. 6
F-02260 Fontenay-aux-Roses
France

S. Schlüter
EURATOM-IPP Association
Max-Planck-Institut für Plasmaphysik
D-8046 Garching bei München
Federal Republic of Germany

S. Segre
EURATOM-CNEN Association
ENEN Centro di Frascati
Casella Postale 65
I-00044 Frascati/Roma
Italy

D.R. Sweetman
EURATOM-UKAEA Association
Culham Laboratory
GB-Abingdon, Oxfordshire
OX14 3DB

F. Troyon
EURATOM-SUISSE Association
Centre de Recherches en Physique des Plasmas
Ecole Polytechnique Fédérale
21 Avenue des Bains
CH-1007 Lausanne
Switzerland

F. Valckx
EURATOM-CEA Association
Départment de Recherches sur la Fusion Contrôlée
Centre d'Études Nucleaires
Boite Postale No. 6
F-92260 Fontenay-aux-Roses
France

F. Waelbroeck
EURATOM-KFA Association
Kernforschungsanlage Jülich GmbH
Institut für Plasmaphysik
Postfach 1913
D-5170 Jülich 1
Federal Republic of Germany

A. Wilhelmsson
EURATOM-NE Association
(CTH) Institute for Electromagnetic Field Theory
and Plasmaphysics
Chalmers University of Technology
Fack
S-412.96 Göteborg 5
Sweden

G. Wolf
EURATOM-KFA Association
Kernforschungsanlage Jülich GmbH
Institut für Plasmaphysik
Postfach 1913
D-5170 Jülich 1
Federal Republic of Germany

Appendix 7
Articles, Reports and Conference Papers published, 1983

1. **Overmoded millimeter waveguide transmission system for the JET ECE diagnostic.**
Baker, E.A.M., Bartlett, D.V., Campbell, D.J., Costley, A.E., Daly, D.J., Dellis, A., de Kock, L.C.J.M., Fessey, J.
8th Int. Conf. on Infrared and Millimeter Waves, Miami, USA, September 1983.

2. **First electron cyclotron emission measurements from JET.**
Baker, E.A.M., Bartlett, D.V., Campbell, D.J., Costley, A.E., Kiff, M., Neill, G.
8th Int. Conf. on Infrared and Millimeter Waves, Miami, USA, September 1983.

3. **Installation, commissioning and operation of the JET integrated power supply system.**
Bertolini, E.
10th Symposium on Fusion Eng., Philadelphia, USA, December 1983.

4. **Architecture of the control and data acquisition system of the JET experiment.**
Bombi, F.
10th Symposium on Fusion Eng., Philadelphia, USA, December 1983.

5. **Wall conditioning in JET.**
Dietz, K.J.
IXth Int. Vacuum Congress, Madrid, Spain, September 1983.

6. **Is additional edge transport in tokamaks beneficial?**
Düchs, D.F., Noll, P., Watkins, M.L.
11th Eur. Conf. on Controlled Plasma Physics, Aachen, FRG, September 1983.

7. **Construction and commissioning of JET.**
Duesing, G.
IXth Int. Vacuum Congress, Madrid, Spain, September 1983.

8. **Fabrication, installation and testing of the JET ohmic heating circuit.**
Eriksson, T.
10th Symposium on Fusion Eng., Philadelphia, USA, December 1983.

9. **Design, manufacture and testing of saturable inductors for JET ohmic heating subsystem.**
Eriksson, T., Papp, K., Stella, A., Tiez, P.
8th Int. Conf. on Magnet Technology, Grenoble, France, September 1983.

10. **JET plasma electron density measurements from 2mm wave interferometry.**
Fessey, J., Gowers, C., Hugenholtz, C.
8th Int. Conf. on Infrared and Millimeter Waves, Miami, USA, September 1983.

11. **Empirical determination of the parameters of ignition and reactor tokamaks.**
Gill, R.D.
XIth Eur. Conf. on Controlled Fusion and Plasma Physics, Aachen, FRG, September 1983.

12. **Design, erection and commissioning of the JET flywheel-generator-covertor system.**
Huart, M.
10th Symposium on Fusion Eng., Philadelphia, USA, December 1983.

13. **Design, manufacture and performance of the JET toroidal field coils.**
Huguet, M., Pöhlchen, R., Booth, J.
10th Symposium on Fusion Eng., Philadelphia, USA, December 1983.

14. **Design studies on the JET ICRF antenna.**
Lallia, P.P., Jacquinot, J., Rebut, P.H.
5th Conf. on Radio Frequency Plasma Heating, Madison, Wisconsin, USA, February 1983.

15. **Coupling and termination technique for flexible concentric multipass cryotransferlines.**
Mayaux, C., Obert, W., Gerth, D., Schippl, K.D.
ICMC/CEC Congress, Colarado Springs, USA, May 1983.

16. **The use of optical fibre in a high-radiation environment to monitor H_α light from the JET tokamak.**
Morgan, P.D., Magyar, G.
Photon '83 Int. Conf. on Optical Fibres and their Applications, Paris, France, May 1983.

17. **Charge-changing collisions in the JET neutral injection bending magnets.**
Nielsen, B.R., Goede, A.P.H., Hemsworth, R.S., Thompson, E.
Low Energy Ion Beams Conf., Loughborough, UK, March 1983.

18. **The Joint European Torus (JET).**
Smart, D.L.
5th Topical Mtg. on the Technology of Fusion Energy, Knoxville, USA, April 1983.

19. **Fokker-Planck calculations for JET ICRF heating scenarios.**
Scharer, J., Jacquinot, J., Lallia, P.P., Blackfield, D.
Amer. Phys. Soc. 25th Ann. Plasma Physics Mtg., Boston, USA, October 1983.

20. **Neutral beam injectors for fusion research.**
Thompson, E.
Int. Ion Engineering Congress, Kyoto, Japan, September 1983.

21. **Impurity control studies for JET.**
Watkins, M.L., van Maanen-Abels, A.E.P.M.
Symposium on Energy Removal and Particle Control in Toroidal Fusion Devices, Princeton, USA, July 1983.

22. **Tokamak transport calculations for JET with different limiter materials.**
Watkins, M.L., van Maanen-Abels, A.E.P.M.
11th Euro. Conf. on Controlled Fusion and Plasma Physics, Aachen, FRG, September 1983.

23. **Impurity control studies for JET.**
Watkins, M.L., van Maanen-Abels, A.E.P.M., Düchs, D.F.
Symposium on Energy Removal and Particle Control in Toroidal Fusion Devices, Princeton, USA, September 1983.

24. **Tokamak disruptions.**
Wesson, J., Sykes, A., Turner, M.
Sherwood Conference, Arlington, Maryland, USA, 21–23 March 1983.

25. **The JET project and the European fusion research programme.**
Wüster, H-O.
Lecture to the British Nuclear Energy Society and the Institution of Nuclear Engineers, London, UK, November 1983.